THE CHEMISTRY OF COMPLEX ION ANTI-TUMOUR AGENTS

A thesis submitted in partial fulfillment of
the requirements for the degree of
Doctor of Philosophy in Chemistry
in the University of Canterbury, Christchurch, New Zealand.

by

Sian E. Miller

1991

Dedicated to the memory of
John Derrick Miller
21st February 1934 - 3rd June 1987

For 'though it cannot hope to be useful or informative on all matters, it does make the reassuring claim that where it is inaccurate, it is at least definitively inaccurate. In cases of major discrepancy, it is always reality that's got it wrong.

Douglas N. Adams (b. 1952)
The Hitch-Hikers Guide to the Galaxy

Creativity in science could be described as the act of putting two and two together to make five.

Arthur Koestler (b. 1905, d. 1983)
The Art of Creation

ABSTRACT

Reported here is a study of the solution chemistry of the anti-cancer drug *cis*-dichlorodiammineplatinum(II), *cis*-$[PtCl_2(NH_3)_2]$. In view of uncertainties in literature values of rate constants and in reaction conditions for the reactions of *cis*-$[PtCl_2(NH_3)_2]$, the kinetics of the first acid hydrolysis step of *cis*-$[PtCl_2(NH_3)_2]$ are reinvestigated in $HClO_4$ media, as well as the kinetics of the second hydrolysis step. All the kinetic investigations in this thesis are made using a DMS100 UV - visible spectrophotometer, using the changes in absorbance to monitor reactions.

The nature and rate constants for the hydrolysis of *cis*-$[PtCl_2(NH_3)_2]$ and the anation kinetics of the products under a variety of pH and ionic strength conditions are investigated, such as the kinetics of the base hydrolysis of *cis*-$[PtCl_2(NH_3)_2]$ and its rates of hydrolysis over a wide pH range. The kinetics of the reactions of some of these hydrolysis products with a variety of ligands, some physiologically relevant and some not, such as chloride ions, sodium hydrogen malonate, glycine and *ortho*-phenylenediamine, are also investigated. In order to model the situation *in vivo* as closely as possible, a technique involving the combination of the UV - visible spectrophotometer with a pH-stat is used extensively. This enables the pH to be kept constant while a reaction in progress is being monitored. The likely distribution of platinum(II) species present in blood plasma and inside a cell is thus calculated as a result of these investigations.

A possible role for metal ions in accelerating both the acid and base hydrolyses of *cis*-$[PtCl_2(NH_3)_2]$ is investigated, although metal ions found *in vivo* are found to have no effect. The crystal structure of the product of the reaction between *cis*-$[PtCl_2(NH_3)_2]$ and $HgCl_2$ is reported. The effect of mixtures of aqueous and non-aqueous solvents on the rate of hydrolysis of *cis*-$[PtCl_2(NH_3)_2]$ was investigated as well as the kinetics of the first acid hydrolysis step of *cis*-$[PtBr_2(NH_3)_2]$ and the bromide anation of *cis*-$[PtBr(NH_3)_2(OH_2)]^+$.

As a result of this experimental work, attempts were made to extrapolate the results of these kinetic investigations, all carried out under stringent reaction conditions, to the possible reactions of *cis*-$[PtCl_2(NH_3)_2]$ *in vivo*.

ACKNOWLEDGEMENTS

During the course of this work there have been many people whose assistance I have greatly appreciated. First and foremost I would like to thank my supervisor Dr D.A. House for his tremendous enthusiasm and for making the project highly entertaining as well as interesting. Thanks also go to Dr W.T. Robinson and Huo Wen for doing the only crystal structure in this thesis. I would also like to thank the Chemistry Department, in particular Dr C.G. Freeman, for the award of a teaching fellowship for three years.

Gratitude also goes to Mr B.A. Reid and Mr R.S. Thompson for their time and expertise on the technical side of things during the course of this work. Much appreciated too were the efforts of the staff of the Physical Sciences Library, in particular Ms J.C. Bray, for dealing with frequent, heavy and sometimes unorthodox or puzzling interloan requests.

For valuable and expensive support and pep-talks from Auckland I would like to thank Joanne Hawkins and Shirley Ng, and thanks also to Roger Meads, Brett Cameron and Dr Maurice Judd for assistance and amusement. Finally I would like to thank my mother, David and Gordon for all their patience, help and support over the years of my Ph.D. work.

CONTENTS

LIST OF FIGURES

LIST OF TABLES

CHAPTER 1

INTRODUCTION.

The use of chemotherapy in the treatment of cancer has evolved mainly over the last forty or fifty years. Prior to 1969, out of 150 000 compounds tested by the United States National Cancer Institute for anti-cancer activity, less than twenty were inorganic in nature [1].

Serious interest in the biological uses of platinum group metals was first raised in 1965 when Rosenberg and his co-workers reported the first definitive observation of the biological activity of platinum compounds [2]. In 1965, during their study on the effects of electric fields on growth processes in the bacteria *Escherichia coli*, a curious phenomenon was observed. When current was passed via platinum electrodes immersed in a nutrient medium known as C medium (composed of 2 g l^{-1} NH_4Cl; 6 g l^{-1} Na_2HPO_4; 3 g l^{-1} KH_2PO_4; 3 g l^{-1} NaCl; 0.01 g l^{-1} $MgCl_2$; 0.026 g l^{-1} Na_2SO_4) [1], containing the bacteria, long, filamentous bacterial rods, up to 300 times their normal length were formed [2]. That is, cell division had been inhibited but cell growth was not affected.

Subsequent experiments established that the current itself did not cause the filamentous growth but did cause approximately 10 ppm of platinum to dissolve electrolytically into the C medium from the platinum electrodes [3]. The species formed during the electrolysis was identified as $[PtCl_6]^{2-}$, which is present in part as the ammonium salt in C medium. The ammonium hexachloroplatinate compound can, at high concentrations, inhibit cell division itself but aged solutions were found to be far more efficient at producing filaments although only if exposed to visible light. This gives rise to a photochemical reaction, where the $[PtCl_6]^{2-}$ became the more active agent $[PtCl_5(NH_3)]^-$, which however inhibited neither growth nor cell division but readily converted to the neutral species $[PtCl_4(NH_3)_2]$ in C medium [4].

The compound, $[PtCl_4(NH_3)_2]$, exists in two isomeric forms, *cis*-$[PtCl_4(NH_3)_2]$ and *trans*-$[PtCl_4(NH_3)_2]$. Testing of the synthesised *cis* and *trans* isomers showed that the *cis* species was biologically active while the *trans* isomer had little effect on cell growth processes. The corresponding platinum(II) species *cis*- and *trans*-$[PtCl_2(NH_3)_2]$ were tested and again only the *cis* isomer caused bacterial filamentation. The species *cis*-$[PtCl_2(NH_3)_2]$ is also likely to be formed in small quantities during the reduction of

cis-$[PtCl_4(NH_3)_2]$ [1]. Filamentous growth in bacteria may be indicative of the ability of an agent to react with DNA, leading to a selective inhibition of DNA synthesis, with no accompanying effect on other biosynthetic pathways such as RNA or protein synthesis. A variety of agents such as UV- and X-irradiation and cytotoxic alkylating agents can also elicit this response as a result of their common ability to damage DNA [5].

Further bacterial effects of platinum compounds were later discovered by Reslova *et al.* [6]. They investigated lysogenic strains of *E. coli*, that is, *E. coli* which had previously been infected by viruses, from which genetic material had been incorporated into the bacterial cell, become repressed and not normally detectable. This lysogenic bacteria can be induced to develop partial or complete viruses by the platinum compounds, leading to destruction (lysis) of the cell. Other agents such as UV- and X-rays and chemicals, including nitrogen mustard and other known anti-tumour agents are also known to have this effect [7].

Since the platinum complexes in Figure 1.1 were active in inhibiting cell division in bacteria, it was suggested that they be tested as anti-tumour agents. This suggestion was reinforced by the fact that other anti-tumour agents, for example, alkylating agents and actinomycin D, also caused elongation and lysis in lysogenic bacteria [1]. Four compounds were tested initially: *cis*-$[PtCl_4(NH_3)_2]$, *cis*-$[PtCl_2(NH_3)_2]$, $[PtCl_2(NH_2CH_2CH_2NH_2)]$ and $[PtCl_4(NH_2CH_2CH_2NH_2)]$. All were found to be effective in inhibiting tumour growth [8]. Further testing showed *cis*-$[PtCl_2(NH_3)_2]$ to be the most potent of the original four compounds [9]. The complex *cis*-$[PtCl_2(NH_3)_2]$, *cis*-dichlorodiammineplatinum(II), cisplatin or *cis*-DDP as it will be referred to in this thesis, was not a new or unknown compound. It had first been synthesised in 1845 and was known as Peyrone's Chloride [10,11]. The molecular structural differences between the *cis* and *trans* complex had been solved by Werner in 1890 [12] and the crystal structure of the *cis* isomer has been determined by Milburn *et al.* (Figure 1.2) [13]. However it was Rosenberg and associates' work that had shown its significant biological actions.

Further screening for the anti-tumour activity of *cis*-$[PtCl_2(NH_3)_2]$ was provided by the National Cancer Institute of America, which led to its selection for pre-clinical evaluation, and phase 1 clinical trials commenced in 1971 [14]. Despite evidence of a broad range of toxic effects, marked activity against advanced testicular cancer and ovarian cancer was observed [15]. The dose-limiting side-effect was kidney damage with nausea and vomiting extensive and intense. Due to the toxicity of the treatment, doubts were expressed in 1973 as to whether *cis*-DDP would ever be used in cancer therapy [16]. However, in 1977 Cvitkovic *et al.* discovered that using D-mannitol, an osmotic diuretic agent, while hydrating the patient prior to, during and after the administration of *cis*-DDP substantially decreased kidney toxicity [17]. This allowed the drug dosage to be increased by 300%. A further advance was made when it was

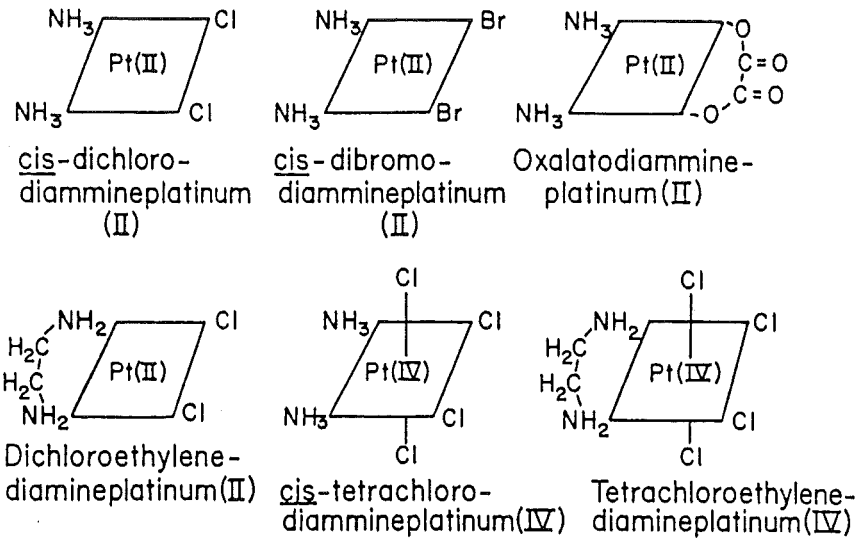

Figure 1.1. First Platinum Compounds Tested for Anti-Tumour Activity.

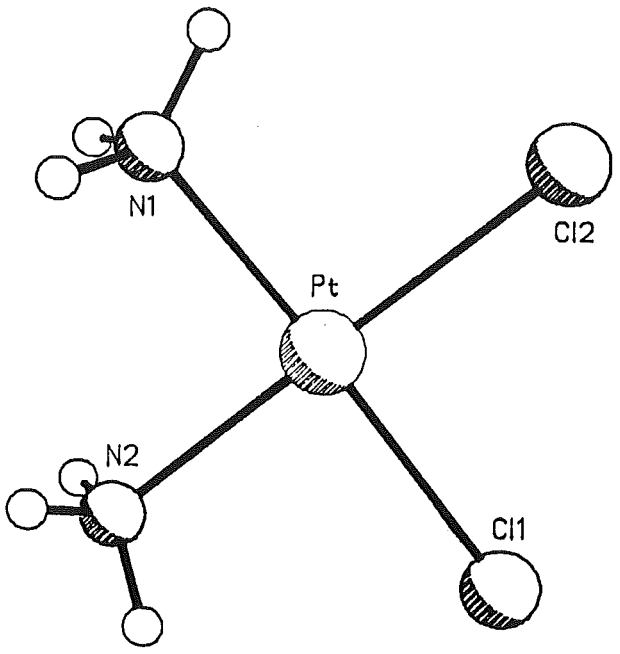

Figure 1.2. The Crystal Structure of *cis*-$[PtCl_2(NH_3)_2]$.

found that administration of the drug as a slow infusion over six to eight hours also relieved kidney toxicity without loss of anti-cancer action [18].

Studies were conducted at this time showing that *cis*-DDP would act either additively or cooperatively with a number of other anticancer drugs, giving a substantial improvement in the effectiveness of the treatment [19]. Further studies tested a variety of combinations of *cis*-DDP with other known anti-tumour agents, with substantial success obtained in the treatment of testicular and ovarian cancers [18,20]. In 1978 marketing approval was obtained in the U.S.A. for the sale of *cis*-DDP under the tradename Platinol, followed closely by approval in the U.K. in 1979 and Japan in 1984 [16,21].

The treatment for testicular tumours today involves all patients receiving at least two litres of fluid orally (saline solution, dextrose and vinblastine) during the 24 hours preceeding the commencement of intravenous fluids. Bleomycin (a naturally occurring antibiotic and a chemotherapeutic agent which can induce strand breaks in DNA [22]), hydrocortisone and *D*-mannitol are then administered followed by 100 mg m^{-2} of *cis*-DDP over 30 to 60 minutes. Further hydration with saline and dextrose solutions is then carried out for 24 hours after *cis*-DDP administration. The use of conventional hydration protocols provides adequate protection against nephrotoxicity at *cis*-DDP levels up to 100 mg m^{-2} [23]. For gynaecological tumours, hydration 24 hours prior to *cis*-DDP administration uses saline and and dextrose solutions but no vinblastine. Adriamycin (another antibiotic and chemotherapeutic agent [22]), cyclophosphamide and mannitol are then given intravenously followed by 50 mg m^{-2} of *cis*-DDP. Post-administration treatment is the same. Patients receive on average four to five courses of chemotherapy, once every three weeks [24].

Three years ago *cis*-DDP was the leading and most widely used anti-cancer drug with 30 000 patients cured each year in the U.S.A. [25]. As well as testicular and ovarian, other types of human cancers sensitive to *cis*-DDP are head and neck, bladder, lung and cervical cancers [14,26]. About ten years ago, testicular cancer was usually fatal [27], but now complete remissions are obtained for testicular cancers in more than 85% of all treated patients [28], with up to 100% remission rates when post-treatment surgery is used to remove residual disease [20] or if the cancer is recognised early [29]. In reality, if a given cancer does not return within some specified time, usually about five years, the patient is considered cured [27,30].

Soon after the first reports about the biological activity of *cis*-DDP, extensive investigations were initiated in the search for analogs with similar activities and improved properties as drugs. The synthesis of a large number of platinum(II) and platinum(IV) analogs for anti-tumour testing has revealed a great deal of general information on the structure - activity relationships of the platinum complexes [31,32,33,34,35]. The most important structural requirements for the anticancer activity of platinum compounds include the following.

- The complexes should be electrically neutral although the active form may be charged after undergoing ligand exchanges *in vivo*. The suggestion has been made that neutrality is necessary for transport of the compound across biological membranes to the site of action [6]. In addition, charged species have been found to be quite toxic [36].

- Two *cis* monodentate (or one bidentate) anionic leaving groups are required.

- The *cis* leaving groups, usually anions, should consist of groups that have intermediate binding strength to platinum(II), or for other reasons are easily leaving (for example, through enzymatic action). That is, they must be neither too reactive (compound reacts immediately with blood constituents and never gets to the tumour cells) nor too stable (compound gets to the tumour cells but does nothing once it's there) [6]. Platinum complexes which exhibit good anti-tumour activity generally possess ligands of intermediate bond strength as leaving groups, such as chloride [37].

- The amine ligands, either monodentate or bidentate, should be in the *cis* orientation, be relatively inert and should have at least one N-H group, that is, possess a hydrogen bond donor function. All compounds with both amine ligands lacking such a property were found to be inactive [28,38]. It has been suggested that hydrogen bonds between the amines and polar groups of DNA may play a role in the interaction of the drug with DNA [31,39,40]. The activity appears to be maximised when the amine ligands are NH_3 or primary amines [41].

- Most of the platinum complexes which have been found to possess anti-tumour activity have had platinum in the +2 oxidation state [35,42]. However, Tobe *et al.* found that the oxidation state of the platinum was not critical for anti-tumour activity [43]. Rosenberg *et al.* showed that the anti-tumour activities of *cis*-$[PtCl_4(NH_3)_2]$ and $[PtCl_4(NH_2CH_2CH_2NH_2)]$ were not markedly different from those of the well-known platinum(II) analogues [8].

- The two chloride leaving groups of the *cis*-DDP are spaced with atomic centres 3.4 Å apart on the molecule [13]. This is an interesting number as the spacing between the steps of the Watson-Crick DNA ladder is also 3.4 Å.

It should be noted here that *trans* compounds are more chemically reactive than *cis* compounds, the *trans*-DDP aquating four times faster and ammonating approximately 30 times faster than the *cis* isomer [36,44]. This means that *trans* compounds are likely to react faster and with a wider variety of body constituents than the *cis* isomers.

There is considerable evidence, mainly from biochemical studies, that DNA is the principal target of *cis*-DDP *in vivo* and that the interactions of *cis*-DDP with DNA impair its function as a template for further DNA replication [5]. The evidence includes:

- Induction of filamentous growth in bacteria
- Induction of lysis in lysogenic bacteria
- Preferential inhibition of DNA synthesis as opposed to RNA and protein synthesis
- Inactivation of viruses and bacteriophages
- Different sensitivity of DNA repair proficient and deficient bacteria and cells
- Correlation between the disease response of *cis*-DDP treated patients and the formation of certain platinum adducts in leucocyte DNA of peripheral blood cells [45].

Cancer is essentially a problem of abnormal growth. The cancer cells differ in two fundamental respects from their normal progenitors. Firstly, the genetic control of life span is lost which results in immortality. Secondly, cancer cells are more or less unresponsive to feedback mechanisms from neighbouring cells, and as a consequence, cell division is no longer modulated by contact inhibition which gives cancer cells the potential of uncontrolled proliferation [46]. The specific action of *cis*-DDP on tumour cells is thought to be caused both by the faster division of the cells compared with normal cells and by the fact that damage induced by *cis*-DDP is repaired faster in normal cells than in tumour cells [47].

Deoxyribonucleic acid (DNA) is a macromolecule composed of covalently linked building blocks, each of which consists of a nitrogenous base, a 2'-deoxy-D-ribose and phosphoric acid, that is, a deoxyribose sugar-phosphate backbone and four nucleotide bases. The components are joined as shown in Figure 1.3 for two DNA strands. The nitrogenous bases are usually the purine heterocycles guanine (G) and adenosine (A), and the pyrimidine heterocycles cytosine (C) and thymine (T). There are different conformational forms of DNA - these are known as A-, B-, D- or Z-DNA, although B-DNA is the most common form. In B-DNA, the GC and AT base pairs are stacked in a right-handed double helix and are hydrogen-bonded to one another. This hydrogen bonding between complementary bases of two opposite strands (G=C, A=T) and base stacking are considered the major forces for duplex formation (Figure 1.4) [48]. Because each base pair contains one two-ringed purine (A or G) and one single-ringed pyrimidine (T or C), the width of each base pair is similar, contributing to the smooth, cylindrical shape of the double helix. The base pairs are rotated by 36° with respect to each adjacent pair, so that there are ten pairs per helical turn, each separated by 3.4 Å [49].

DNA offers a wide variety of potential metal binding sites to platinum(II) owing to its size and chemical complexity [50]. Because platinum is a class B or 'soft' metal, it is expected that platinum compounds show a higher affinity for the nitrogen donor sites, that is, for the nucleobases rather than the phosphate deoxyribose moiety. Platinum -

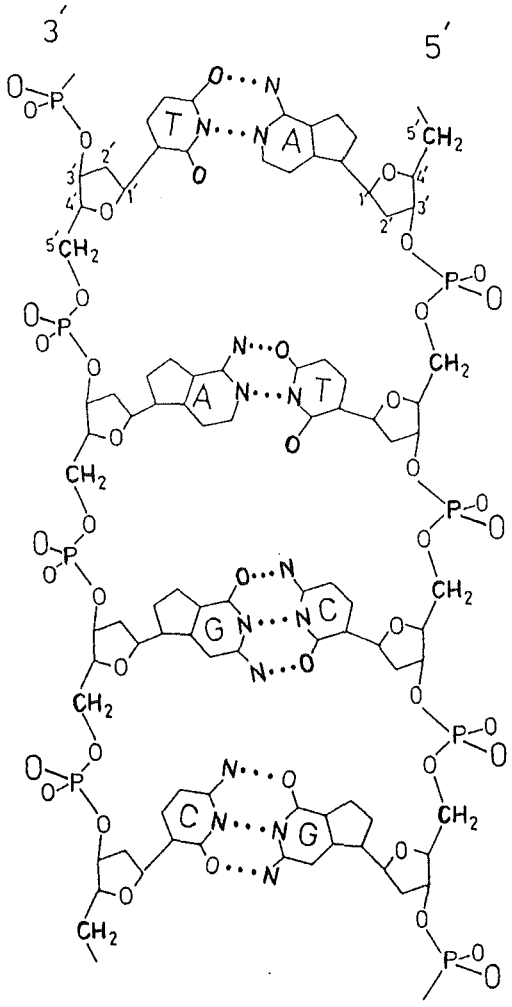

Figure 1.3. Unrolled DNA Double Helix with Watson-Crick Base Pairs.

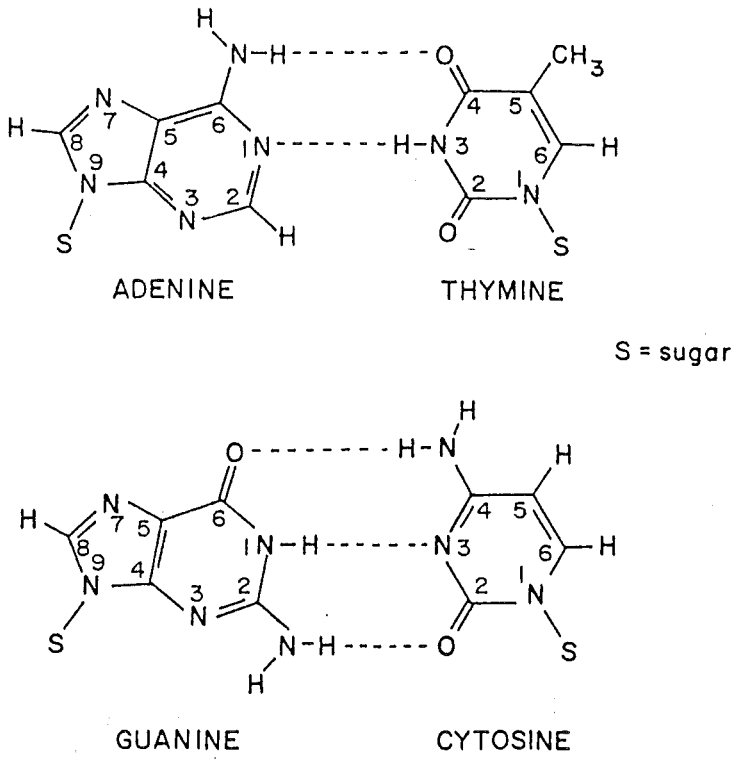

Figure 1.4. Schematic of Watson-Crick G-C and A-T Base Pairs, showing the Atom-Numbering Schemes.

phosphate interactions do occur in certain cases [51,52], but under physiological conditions, phosphate's role for coordination is thought to be secondary, possibly important for hydrogen bonding [28]. Metal binding to a nucleobase is influenced by a variety of factors such as basicity of the donor, steric fitting, interligand interactions and state of the metal, for example, charge or hydrolysis state [53,54].

The relative biological activities of different *cis*-DDP-DNA adducts have thus far been difficult to determine since most studies have been performed on DNA containing all possible *cis*-DDP adducts. However from *in vitro* studies, a number of binding patterns of *cis*-DDP to DNA have been established and quantified [55,56,57,58,59,60,61,62]. The DNA of living cells appears to form essentially the same adducts [63], but reaction with proteins occurs as well. The various adducts at low levels of platinum binding are listed as follows [48].

- Bifunctional binding to the N(7) positions of two adjacent guanine bases of one strand (50 to 60% of total platinum bound).
- Bifunctional binding to an adenine and guanine nucleobase on the same strand (20 to 30%).
- Monofunctional binding to a single guanine base (time dependent).
- Bifunctional binding to two guanines of two different DNA strands (< 1%).

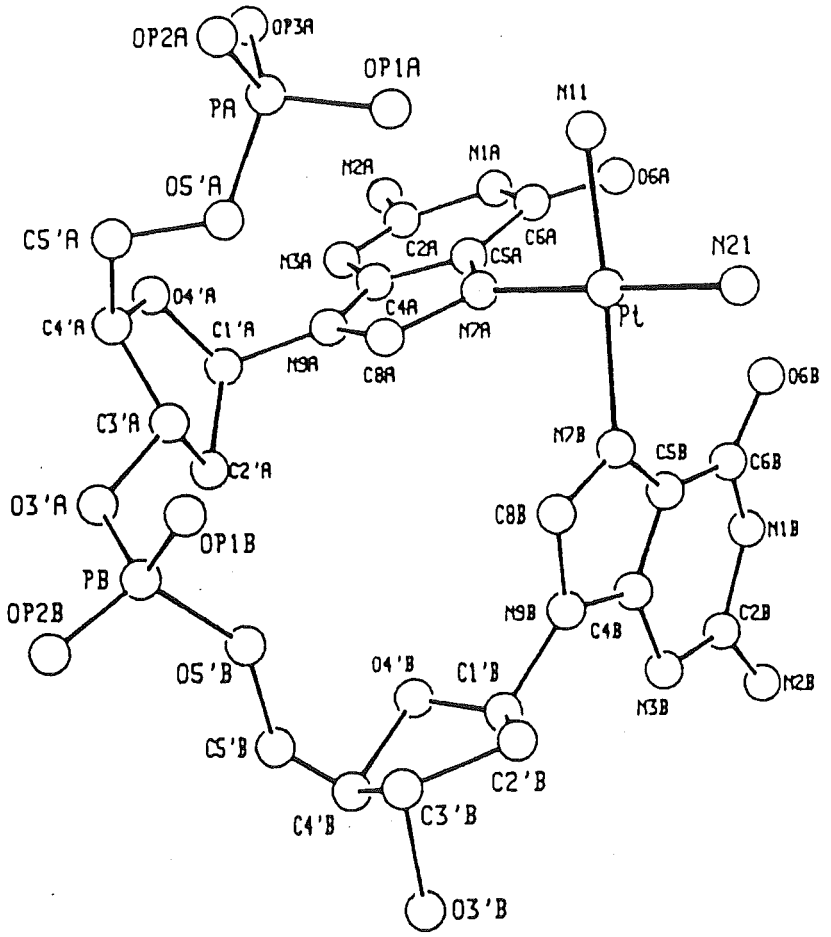

Figure 1.5. Structure of the Major Adduct of *cis*-DDP with DNA, *cis*-$[Pt(NH_3)_2\{d(pGpG)\}]$ [64]

- Bifunctional binding to two guanines separated by a third nucleobase N ($\sim$ 10%).
- DNA-protein cross-linking ($<$ 1%).

These adducts account for more than 90% of the bound platinum. It seems likely that only the two major adducts formed by *cis*-DDP, *cis*-$[Pt(NH_3)_2\{d(pGpG)\}]$ and *cis*-$[Pt(NH_3)_2\{d(pApG)\}]$, will be important in inhibiting DNA replication. The structure of the most prevalent adduct, *cis*-$[Pt(NH_3)_2\{d(pGpG)\}]$, determined using X-ray crystallography [64,65], is depicted in Figure 1.5. The distribution of the various adducts, plus minor and yet unidentified adducts, depends to some extent on reaction conditions (for example, platinum concentration, time of incubation, ionic strength). There is evidence that at higher platination levels, duplex unwinding takes place [66], which almost certainly renders additional binding sites available to platination.

It is suggested by structural and spectroscopic studies of the d(pGpG) adduct of *cis*-DDP, as well as by molecular mechanics calculations, that hydrogen bonding between a proton of an NH_3 group and a phosphate oxygen may be significant [48].

However, hard chemical evidence for the existence of N(7)-O(6) chelate formation with guanine by *cis*-DDP is lacking at the present time [67]. One aspect that makes such a proposition particularly attractive is the involvement of the O(6) site of guanine. In the field of carcinogenesis by alkylating agents it is suggested that alkylation at the O(6) site is the most relevant in causing mutation in body cells. This is considered to be a necessary step in the transformation of the normal cell into a cancer cell. When this lesion is not repaired prior to DNA replication, this leads to a mispairing of guanine with thymine instead of the correct pairing with cytosine. Further replication leads to the replacement of the original GC pair by an AT pair, a base substitution mutation. If the cancer cell becomes so because of its inability to repair the O(6) guanine lesion caused by a carcinogen, then it may also be unable to repair the *cis*-DDP-induced damage [68]. However, the normal cells have intact repair mechanisms and can repair the damage prior to DNA replication and thus survive. This postulate allows an explanation of the selective destruction of cancer cells by the platinum drugs. Both molecular mechanics modelling and NMR studies [69,70,71] of short oligonucleotide fragments reveal that the *trans* isomer cannot form such a closed ring chelate involving the N(7)-O(6) positions of guanine and this may account for the difference between the biological effectiveness of the *cis* and *trans* isomers. Other adducts with DNA formed by *trans*-DDP are more efficiently removed in the cell [26].

As proposed for other DNA binding drugs [72], the mechanism of action of these drugs may be more subtle than just causing a gross inhibition of DNA synthesis and subsequent cell death. There are at least a few observations pointing in this direction, for example, curious alterations in cell nucleus structure at *cis*-DDP concentrations not affecting DNA synthesis, have been observed [48,73]. However, irrespective of the questions concerning the actual origin of cytotoxicity and antitumour activity, the present knowledge strongly supports the idea that initial drug binding to DNA is important and probably responsible for the biological effects [48].

It has long been a matter of interest to what extent *cis*-DDP itself or some of its hydrolysis products are responsible for particular biological effects *in vivo*. Modelling the interactions of *cis*-DDP with DNA is complicated by questions concerning the biologically active metal species. The issues are further complicated by the unknown nature of the distribution of *cis*-DDP and its hydrolysis products inside and outside the cell, and the likelihood that no thermodynamic equilibrium is reached under physiological conditions. Moreover, very little is known about the transport properties of the various species across the cell membrane, and there is the fact that pH gradients exist both within a cell and in an organism as a whole [74].

In the earliest biological experiments, an initial insensitivity to *cis*-DDP, lasting about two hours was noted [75,76]. It was suggested that *cis*-DDP may not itself be the active species but is rather converted over a period of time to the actual active form

of the drug. Examination of the aqueous chemistry of *cis*-DDP provides an explanation for this behaviour. In water the labile chloride ions are displaced by solvent molecules in a stepwise manner as shown in Equations 1.1 and 1.2.

$$cis\text{-}[PtCl_2(NH_3)_2] \underset{k_{-1}}{\overset{k_1}{\rightleftharpoons}} cis\text{-}[PtCl(NH_3)_2(OH_2)]^+ + Cl^- \qquad (1.1)$$

$$cis\text{-}[PtCl(NH_3)_2(OH_2)]^+ \underset{k_{-2}}{\overset{k_2}{\rightleftharpoons}} cis\text{-}[Pt(NH_3)_2(OH_2)_2]^{2+} + Cl^- \qquad (1.2)$$

The rate constants k_1 and k_2 had been measured as 2.5×10^{-5} and 3.3×10^{-5} s^{-1} respectively [77,78], and this suggested that the rate-determining step in the reaction with DNA was aquation.

In addition to the solvolyses shown in Equations 1.1 and 1.2, three acid-base equilibria, Equations 1.3 to 1.5, are possible.

$$cis\text{-}[PtCl(NH_3)_2(OH_2)]^+ \rightleftharpoons cis\text{-}[PtCl(OH)(NH_3)_2] + H^+ \qquad (1.3)$$

$$cis\text{-}[Pt(NH_3)_2(OH_2)_2]^{2+} \rightleftharpoons cis\text{-}[Pt(OH)(NH_3)_2(OH_2)]^+ + H^+ \qquad (1.4)$$

$$cis\text{-}[Pt(OH)(NH_3)_2(OH_2)]^+ \rightleftharpoons cis\text{-}[Pt(OH)_2(NH_3)_2] + H^+ \qquad (1.5)$$

Assuming that the NH_3 ligands are inert, this leads to six monomeric species in equilibrium, the distribution of which depends on pH and chloride ion concentration. In addition to these mononuclear species, μ-hydroxo complexes containing one [48], two, three or even four bridges [79,80,81,82,83,84,85,86] have been shown to form in solution [87,88,89,90] and have been isolated respectively. However, the formation of μ-hydroxo compounds under biological conditions is generally considered unlikely [48].

Thus it is commonly thought that in blood plasma (pH = 7.4 [91]) where the chloride ion concentration is high ($\sim$ 103 mM), the predominant species is the neutral dichloro complex *cis*-DDP, which can passively diffuse across cell membranes. Inside the cell, the chloride ion concentration drops to about 4 mM [30,48,92], allowing the various hydrolysis products to form. According to calculations by Martin [93], the aquated species amounts to about 33% of the total present inside the cell, yet is present in only a few percent in body fluids. Since water is a much better leaving group than chloride [94,95], and hydroxo groups are inert to substitution in platinum compounds [95], the aquo species are those most likely to react with DNA. These positively charged platinum complexes may be electrostatically attracted to the negatively charged DNA helix [26].

The hydrolysis of *cis*-DDP is a well studied reaction [33,96,97,98,99,100,101,102,103] [104,105,106,107,108,109,110,111,112,78,113], yet there are questions to be resolved before it can be said for certain that these studies on *cis*-DDP and other biologically active

molecules are useful and relevant. A major area of question is whether the reaction should be investigated under physiological conditions where there is some doubt as to the reaction products, or should it be investigated using stringent reaction conditions where the nature of the products can be controlled. In the latter case it is possible that the data obtained will be specific but unrelated to the biological situation [41]. However, it was thought, for the work presented in this thesis, that it would be easier and more useful to extrapolate the data obtained from controlled, specific reactions to the biological situations than it would be to attempt to interpret unspecific data with a variety of unknown parameters as under 'physiological conditions'. Hence abiological conditions have been used extensively in the work presented here.

The investigations presented here commenced with measurement of the rate constants for the forward and reverse directions of the first step of the hydrolysis of *cis*-DDP in acid media (Equation 1.1). As mentioned above, the hydrolysis of *cis*-DDP is well studied yet uncertainties exist about some of the literature data. Table 1.1 shows a wide variety in values for the literature rate constants for the forward direction (k_1), obtained in a variety of media. Many of these hydrolysis studies were made in water which can be a problem. Unless stringent controls are adopted, water will have a natural pH of less than 7 due to dissolved carbon dioxide. This means that the concentrations of H^+ and OH^- are ill-defined and the buffering capacity is unknown. Dissolution of *cis*-DDP in water does not change the pH. Coordinated NH_3 groups have the potential to act as proton donors, but the extent of this in most coordination complexes is small and strong proton acceptors are required. Nevertheless, there are some complexes where hydrolysis proceeds via the OH^- present at pH = 3 [114], for example, $[Co(picdien)Cl]^+$. As the hydrolysis of *cis*-DDP proceeds (Equation 1.1), the pH will drop (Equation 1.3). In this situation the products are the *cis*-$[PtCl(NH_3)_2(OH_2)]^+$ and the *cis*-$[PtCl(OH)(NH_3)_2]$ in an ill-defined ratio since, prior to the work presented in this thesis, the pKa for Equation 1.3 was unknown. It was found in the course of this work to be difficult to obtain reliable rate constants for this reaction in water using spectrophotometry as the absorbance versus time data are wavelength dependent due to the changing ratio of secondary products as the reaction proceeds, a phenomenon noted by others [115].

Some studies [108,109] overcame these problems by using acidic media,but unfortunately in these titrations, nitric acid, HNO_3, was the acid used. Nitrate ions are known to interfere in other hydrolysis reactions [90,117] and its innocence in the reaction system of *cis*-DDP was doubtful. Initially it was thought that the values of k_1 reported in the literature were valid but that the value for k_2 was wrong and should be redetermined. However, an examination of the literature values shown in Table 1.1 shows inconsistencies and uncertainties. It can be seen that the rate constants k_1 obtained in the presence of HNO_3 [108,109,116] are significantly higher than those obtained in

Table 1.1. Summary of literature rate constants (k_1) for the first hydrolysis step of *cis*-$[PtCl_2(NH_3)_2]$ [a]

Temperature (°C)	[K]	$10^5 \times k_1$ (s^{-1})
0.0	[273.2]	0.095 [b]
23.0	[296.2]	2.38 [c]
25.0	[298.2]	2.5 [d], 2.6 [e], 2.3 [f], 2.8 [b], 2.35 [g], 2.5 [h], 2.47 [i], 2.85 [j], (2.58 ± 0.2 mean), 3.67 [k l], 3.8 [m n], 3.16 [m o]
28.0	[301.2]	4.57 [j]
30.0	[303.2]	6.63 [j], 5.08 [b], 3.5 [p]
34.0	[307.2]	7.16 [j]
35.0	[308.2]	7.58 [j], 7.6 [d], 10.4 [m o]
37.0	[310.2]	11.7 [i], 11.0 [e], 11.6 [q], 4.94 [r], 11.0 [s]
40.0	[313.2]	16.5 [j], 18.5 [t], 21.2 [t], 15.8 [t], 19.6 [m o]
45.0	[318.2]	33.0 [m o]
45.3	[318.5]	33.0 [m u]
50.0	[323.2]	36 [e], 35 [h]

[a] In H_2O, (pH = 4 to 7) with and without added salts and buffers.
[b] Reference [98]
[c] Reference [110]
[d] Reference [78]
[e] Reference [99]
[f] Reference [112]
[g] Reference [100]
[h] Reference [113]
[i] Reference [106]
[j] Reference [102]
[k] Ambient temperature
[l] Reference [107]
[m] In 0.01 *M* HNO_3 (data are underlined)
[n] Reference [108]
[o] Reference [109]
[p] References [104] and [105]
[q] Reference [97]
[r] Reference [101]
[s] Reference [111]
[t] Reference [103]
[u] Reference [116]

water alone or in water/$NaNO_3$ media [78,110,111,112], as shown in Table 1.1.

Other studies used buffers, which can also cause problems. These will control the product ratio, but if the hydroxo/aquo equilibrium constant is unknown, the product ratio, while now constant, still cannot be calculated. Use of buffer systems may also mean the introduction of spurious or catalytic counter ions in the buffer medium. Platinum(II) systems are known to be very susceptible to nucleophilic attack and phosphate [90,102,103,115], acetate, citrate, TRIS or other buffer counter ions could easily influence the solvolysis reaction. Nor are these reagents particularly close to the biological regime. It was thus decided for the work presented in this thesis to systematically study the reactions of *cis*-DDP and its various hydrolysis products in media where the products could be predicted with some certainty.

In view of these uncertainties it was felt to be worthwhile to investigate not only the kinetics of the second hydrolysis step of *cis*-DDP but also to reinvestigate the kinetics of the first step, in $HClO_4$ media using UV-visible spectrophotometry, using the changes in absorbance of *cis*-DDP to monitor the reaction. A natural progression from this was to investigate the nature and rate constants for the hydrolysis products of *cis*-DDP and the anation kinetics of these products, under a variety of pH and ionic strength conditions and the rate constants of the reactions of these species with a variety of ligands, some physiologically relevant and some not. In order to model the biological situation as closely as possible, a technique involving the combination of a UV-visible spectrophotometer with a pH-stat was used extensively. This enables pH to be kept constant while a reaction in progress is being monitored. The possible role of metal ions accelerating the hydrolysis reactions of *cis*-DDP was also investigated.

Thus, this thesis describes investigations of the solution chemistry of the anticancer drug *cis*-$[PtCl_2(NH_3)_2]$, or *cis*-DDP, and its various hydrolysis products, with a view to extrapolating the results to the physiological system *in vivo*, in order to contribute to present knowledge of the behaviour of *cis*-DDP in solution and *in vivo*.

CHAPTER 2

THE KINETICS OF FORMATION AND ANATION OF THE *cis*-DIAMMINE(AQUA)CHLOROPLATINUM(II) CATION IN ACIDIC AQUEOUS SOLUTION.

2.1 Introduction.

The kinetics of the first hydrolysis step of *cis*-DDP (Equation 1.1) have been investigated in acidic media in both the forward and reverse directions using UV spectroscopy to monitor the reactions, to give values for the rate constants k_1 and k_{-1} plus activation parameters for each and a value for the equilibrium constant K_1 at 25 °C.

The rate of loss of the first chloro ligand from *cis*-DDP (k_1) to give an equilibrium mixture of *cis*-DDP, *cis*-$[PtCl(NH_3)_2(OH_2)]^+$ and Cl^- has been measured spectrophotometrically in a variety of $HClO_4/NaClO_4$ media over a 22 K temperature range. The absorbance versus time data were analysed in terms of first-order kinetics and the effect of acid strength and ionic strength on the reaction evaluated.

In order to measure k_{-1}, the species *cis*-$[PtCl(NH_3)_2(OH_2)]^+$ was generated using anion exchange chromatography to remove the released chloride ion. Known amounts of chloride ion (as NaCl in $HClO_4$) were added to the *cis*-$[PtCl(NH_3)_2(OH_2)]^+$ solution, giving rise to a rapid reaction which was followed spectrophotometrically.

2.2 Experimental.

2.2.1 Measurement of k_1.

Measurement of the rate of loss of the first chloride ligand from *cis*-DDP was carried out in 0.1 *M* $HClO_4$, 1.0 *M* $HClO_4$ and in 0.1 *M* $HClO_4$ plus 0.9 *M* $NaClO_4$. In order to carry out the measurements, 3.0 ml of the appropriate solution were allowed to reach thermal equilibrium in 1.00 cm quartz spectrophotometer cells, sitting in a temperature controlled (± 0.1 °C), heated cell-block, in the cell compartment of a Varian DMS100 UV-visible spectrophotometer.

Preliminary experimental work determined that the reaction could be followed between 345 and 220 nm, in the UV region, with the best wavelengths to collect absorbance data at being 304, 260 and 236 nm, as these were the positions of maximum

change in absorbance with time. This initial work also determined the time intervals at which data should be collected.

To the thermally equilibrated electrolyte solution in the spectrophotometer sample cell, a small amount ($\sim$ 3 mg) of solid *cis*-DDP was added. Solubility was generally rapid and the concentration of *cis*-DDP of approximately 3×10^{-3} M gave an initial absorbance reading of 0.2 to 0.4. As soon as the *cis*-DDP had dissolved, absorbance versus time data were collected at the above wavelengths, at appropriate time intervals (dependent on the temperature of the reaction system). Reactions were monitored for six to eight half-lives and constant 'infinity' data were usually obtained.

The absorbance versus time data obtained for every $HClO_4/NaClO_4$ solution at each temperature were analysed in terms of a first-order rate law for each wavelength to give values for k_1 (Table 2.1). The values obtained for k_1 were found to be constant within experimental error over more than four half-lives and were wavelength independent. Activation parameters associated with k_1 were computer calculated from the variation of the rate constant with temperature [118] (Table 2.7).

2.2.2 Measurement of k_{-1}.

The first step was the preparation of the solution of *cis*-$[PtCl(NH_3)_2(OH_2)]^+$ in 0.1 M $HClO_4$ which was essentially free of the chloride ions lost initially. A solution of *cis*-DDP (50 mg) in 0.1 M $HClO_4$ (50 ml) was allowed to aquate for six to eight half-lives, either overnight at room temperature or two hours at 40 °C and then several hours at room temperature.

Samples of the resulting equilibrium system (10 ml) were passed slowly (0.5 ml per minute) through a short ($\sim$ 4 cm long by 0.5 cm wide) column of Amberlite IRA-400 ion exchange resin in the perchlorate form, that had been pre-washed with 0.1 M $HClO_4$ at room temperature. On passing the *cis*-$[PtCl(NH_3)_2(OH_2)]^+$ solution through the column, the first 4 ml of effluent was discarded as this was most likely to contain 0.1 M $HClO_4$ only. An approximate total of 8 ml of 'clean' solution were collected, the last portions obtained by addition of a small volume of 0.1 M $HClO_4$ to the column once the sample had passed through. Preliminary experiments carried out using 0.002 M HCl in 0.1 M $HClO_4$, showed that this anion exchange technique removed more than 95% of the ionic chloride ions present.

Solutions of NaCl (0.25, 0.35, 0.40, 0.50, 0.60, 0.75 and 0.90 M) in $HClO_4$ of sufficient concentration to give a final ionic strength of 1.0 M were prepared. In all cases, the initial chloride ion concentration was greater than ten times that of the platinum concentration. Equal volumes of the chosen $NaCl/HClO_4$ solution (1 ml) and the *cis*-$[PtCl(NH_3)_2(OH_2)]^+$ solution (1 ml) were placed respectively in one arm each of a Y-shaped rapid mixing device [119], which was then thermally equilibrated in a water bath at a chosen constant temperature. The sample 1.00 cm spectrophotometer

cell was then mounted on top of the mixing device and the system was inverted, rapidly mixing the two solutions.

The rapid absorbance changes resulting from the subsequent reaction were monitored between 345 and 220 nm using UV spectroscopy, with absorbance data collected at 305, 260 and 235 nm. Due to the speed of these reactions, the sample and reference cells were held in a water-cooled jacketed cell holder inside the cell compartment of the spectrophotometer. This cell holder had water pumped through it from a water bath, which was kept at a low, constant temperature by the combined use of a heater unit and a refrigeration unit.

The absorbance versus time data obtained for every $NaCl/HClO_4$ solution at each temperature were analysed in terms of a first-order rate law, for each wavelength, to give k_{obs} (s^{-1}) (Table 2.4). Values of k_{-1} (M^{-1} s^{-1}) were obtained by using the expression

$$k_{-1} = k_{obs}[Cl^-]^{-1} \tag{2.1}$$

The activation parameters associated with k_{-1} (Table 2.4) were computer calculated from the variation of the rate constant with temperature, as with k_1 [118].

2.3 Results and Discussion.

The hydrolysis of *cis*-DDP is a well studied reaction. The rate of hydrolysis in water has been measured using conductivity [33,96,97,98,99], high-performance liquid chromatography (HPLC) [104,105,106,107], spectrophotometry [100,101,102,103], chloride ion titration [108,109], chloride ion specific electrode [111], $^{36}Cl^-$ ion exchange [78,112], or hydrogen ion titration [78,112,113]. The latter technique can be used as, during the course of the reaction, the pH decreases [99] due to the reaction shown in Equation 1.3. Acidic media would prevent the formation of any hydroxo species (by reversal of Equation 1.3), but these conditions were used only when the reaction was followed using chloride release titration [108,109]. Unfortunately in these titrations, nitric acid, HNO_3, was the acid used. The problems with this acid have already been outlined in Chapter 1, as have the problems associated with the use of water and with the use of buffers as reaction media.

Thus it was decided to systematically study the rate of hydrolysis of *cis*-DDP in media where the products could be predicted with some certainty. The acid hydrolysis of *cis*-DDP was investigated using $HClO_4/NaClO_4$ media as the background electrolyte since these are both UV transparent and the perchlorate ion has only weak nucleophilic properties towards *cis*-DDP [90]. By investigating this reaction in acidic conditions, it can confidently be assumed that the influence of *cis*-$[PtCl(OH)(NH_3)_2]$ on the reaction rate can be reduced to zero and only the *cis*-$[PtCl(NH_3)_2(OH_2)]^+$ and chloride ions will be produced.

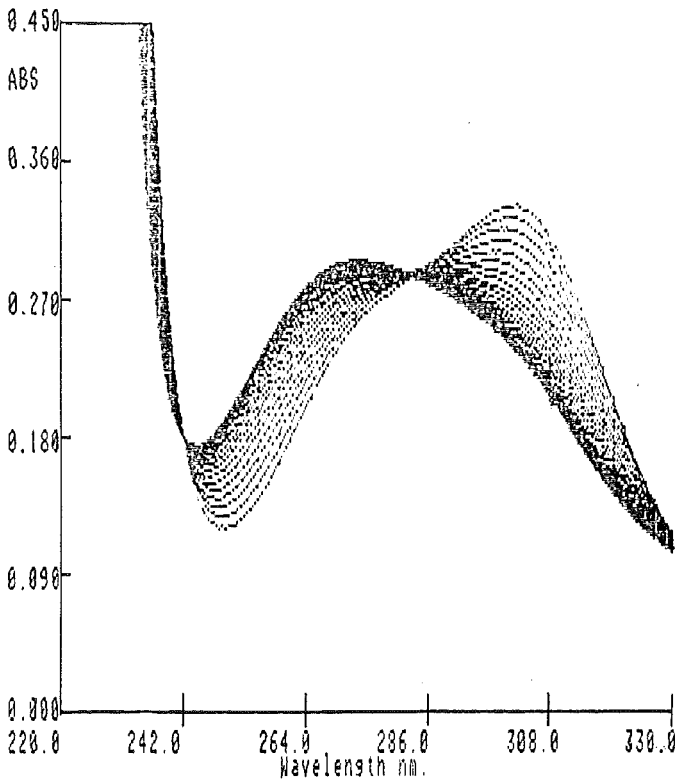

Figure 2.1. Spectrophotometric scans for the acid hydrolysis of *cis*-$[PtCl_2(NH_3)_2]$ (0.1 M $HClO_4$; 43 °C; 5 minute intervals)

The absorption spectra of *cis*-DDP dissolved in $HClO_4$ (0.1 to 1.0 M) change slowly with time at 25 °C. The *cis*-DDP has an absorption maximum at 304 nm ($\epsilon = 125$ M^{-1} cm^{-1}) (obtained from Figure 2.1) which decreases as the reaction proceeds and a minimum at 246 nm ($\epsilon = 44$ M^{-1} cm^{-1}) which increases as the reaction proceeds. Two isosbestic points are formed and maintained at 282 ± 2 nm ($\epsilon = 103$ M^{-1} cm^{-1}) and 242 ± 2 nm ($\epsilon = 61$ M^{-1} cm^{-1}) (Figure 2.1). The same isosbestic points are developed in the reverse reaction when chloride ions are added to the *cis*-$[PtCl(NH_3)_2(OH_2)]^+$ (Figure 2.2). The maintenance of an isosbestic point in the absorption spectral profile of a reacting compound gives no information on the number of species being produced. A single compound producing a single compound will maintain an isosbestic point, but so will a single compound producing two compounds in a constant ratio. The presence of a well-maintained isosbestic point indicates that a reaction sequence A → B → C is unlikely.

The absorbances of *cis*-DDP and *cis*-$[PtCl(NH_3)_2(OH_2)]^+$ at 304, 260 and 236 nm for the acid hydrolysis reaction, are sufficiently different to enable accurate rate constants, k_1, to be calculated according to the first-order rate law [120,121].

$$kt = \ln\left(\frac{A_\infty - A_0}{A_t - A_0}\right) \tag{2.2}$$

where k is the rate constant k_1, A_0 is the absorbance at time $t = 0$, A_∞ is the absorbance

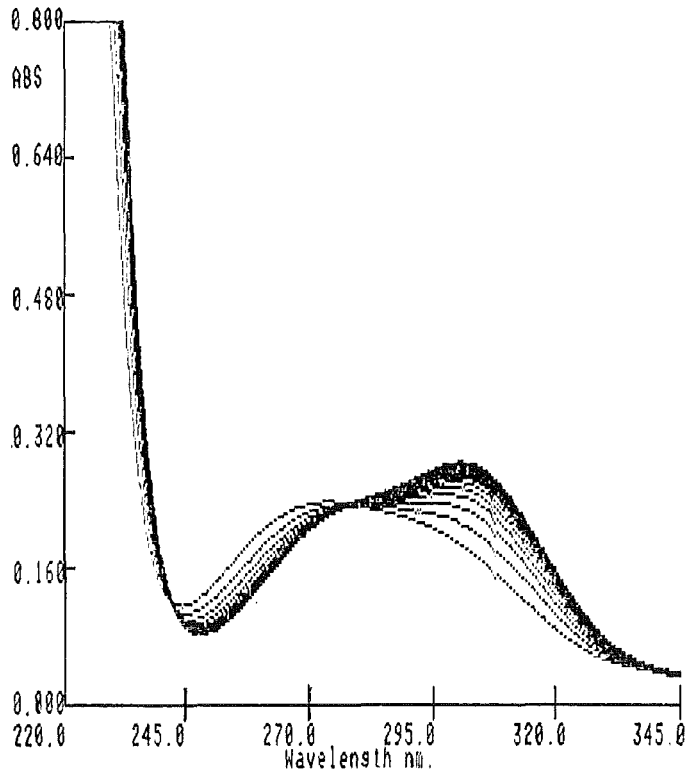

Figure 2.2. Spectrophotometric scans for the anation of *cis*-$[PtCl(NH_3)_2(OH_2)]^+$ by chloride ions (0.03 *M* Cl^-; $\mu = 0.1$ *M*, $HClO_4$, NaCl; 30 °C; 3 minute intervals)

at time t ='infinity' and A_t is the absorbance at time = t. The values for k_1 obtained in this way over the 22 K temperature range are listed in Table 2.1.

It must be noted that the acid hydrolysis reaction of *cis*-DDP (Equation 1.1) is in fact reversible and proceeding to equilibrium so simple first order kinetics are not strictly applicable to this A $\rightleftharpoons$ B + C system [98,110,111,121], but most investigators have ignored the contribution from the reverse reaction [109]. The data presented here shows that the equilibrium (Equation 1.1) is substantially (greater than 90%) to the *cis*-$[PtCl(NH_3)_2(OH_2)]^+$ species at the *cis*-DDP concentrations used (Table 2.2). See Appendix B for method of calculation of the equlibrium concentrations of the platinum(II) species.

Inspection of the data shows that k_1 is independent of hydrogen ion concentration and ionic strength in the measured range (0.1 to 1.0 *M*). The hydrogen ion independence is normal for complexes of this type with strongly acidic leaving groups [122]. The ionic strength independence is is agreement with the Debye-Hückel theory for a reactant with zero charge [120,121], where it is anticipated that for a reaction involving only neutral molecules, the ionic strength effects would be small except at high ionic concentrations.

A comparison of the data obtained in $HClO_4/NaClO_4$ media with those in Table 1.1 shows that the k_1 values obtained in acidic conditions are approximately two to three

Table 2.1. Spectrophotometrically determined first-order rate constants (k_1) for the first step in the acid hydrolysis of *cis*-$[PtCl_2(NH_3)_2]$. [a]

0.1 *M* $HClO_4$			1.0 *M* $HClO_4$			0.1 *M* $HClO_4$ + 0.9 *M* $NaClO_4$		
$10^4 \times k_1$ (s^{-1})			$10^4 \times k_1$ (s^{-1})			$10^4 \times k_1$ (s^{-1})		
obs.	T(°C)	calc. [b]	obs.	T(°C)	calc. [b]	obs.	T(°C)	calc. [b]
1.19±0.15	(29.9)	1.24	1.25±0.08	(30.1)	1.12	1.74±0.29	(30.5)	1.51
1.82±0.09	(34.1)	1.88	1.64±0.06	(33.9)	1.70	2.03±0.19	(34.8)	2.34
2.20±0.67	(34.9)	2.03	1.74±0.15	(35.0)	1.91			
2.47±0.04	(36.7)	2.41	2.29±0.21	(37.2)	2.41	2.74±0.12	(36.9)	2.87
3.21±0.20	(39.9)	3.27	3.33±0.90	(40.1)	3.28	3.38±0.27	(40.1)	3.93
4.43±0.04	(43.0)	4.35	4.48±0.75	(42.9)	4.37	4.60±0.11	(42.9)	5.14
5.21±0.30	(44.9)	5.17	5.47±0.26	(44.7)	5.25	6.45±0.17	(45.0)	6.26
9.54±0.63	(50.1)	8.22	8.81±0.09	(49.8)	8.71	11.2±0.37	(50.2)	10.1
11.2±0.79	(52.5)	10.5	12.0±0.34	(53.2)	12.1	13.8±0.11	(53.1)	13.1

[a] Data are the mean plus or minus the standard deviation from greater than 15 values at three wavelengths (304, 260 and 236 nm).

[b] Calculated from the activation parameters cited in Table 2.7.

Table 2.2. Equilibrium concentrations (m*M*) for the first acid hydrolysis reaction of *cis*-$[PtCl_2(NH_3)_2]$ (Equation 1.1) in aqueous $HClO_4$ (μ = 1.0 *M*) at 25.0 °C using $K_1 = 1.01 \times 10^{-2}$.

Initial concentration (m*M*)	Equlibrium concentrations (m*M*)	
cis-$[PtCl_2(NH_3)_2]$	*cis*-$[PtCl_2(NH_3)_2]$	*cis*-$[PtCl(NH_3)_2(OH_2)]^+ = Cl^-$
100	73	27
10	4	6
1.6	0.2	1.4
1.0	0.1	0.9

Table 2.3. Spectrophotometrically determined rate constants (k_1) for the first hydrolysis step of *cis*-$[PtCl_2(NH_3)_2]$ in a variety of acidic media.

Temperature (°C)	[K]	Solvent	$10^4 \times k_1$ (s^{-1})
37.2	[310.4]	0.1 *M* HTF	2.20±0.14
37.5	[310.7]	0.1 *M* HAc	2.46±0.07
38.1	[311.3]	0.1 *M* HTS	2.42±0.06
37.6	[310.8]	0.1 *M* HNO_3	3.27±0.02
37.8	[311.0]	0.05 *M* H_2SO_4	2.69±0.06
37.5	[310.7]	0.01 *M* HNO_3	3.24±0.01
37.1	[310.3]	0.05 *M* Tartaric Acid	2.75±0.59
37.3	[310.5]	0.05 *M* Malonic Acid	2.46±0.37
37.2	[310.4]	0.05 *M* $H_2C_2O_4$	2.80±0.08
36.7	[309.9]	0.1 *M* $HClO_4$	2.47±0.05
37.2	[310.4]	1.0 *M* $HClO_4$	2.29±0.24
36.9	[310.1]	0.1 *M* $HClO_4$ + 0.9 *M* $NaClO_4$	2.74±0.15

times greater than those previously obtained in water (pH = 4 to 7), indicating that the *cis*-$[PtCl(OH)(NH_3)_2]$ species has been eliminated from the reaction system used here. It was thought initially from the literature that the H^+ or NO_3^- ions may have been having an acceleratory effect on the reaction rate (Table 1.1).

The rate constant, k_1, in 0.1 *M* HNO_3 was measured ($10^4 k_1 = 3.3 \pm 0.4\ s^{-1}$ at 37.6 °C) (Table 2.3) and found to be slightly higher than that determined in 0.1 *M* $HClO_4$ ($10^4 k_1 = 2.47 \pm 0.04\ s^{-1}$ at 36.7 °C). However, comparison is difficult since it is thought that the product of the reaction in HNO_3 is not the *cis*-$[PtCl(NH_3)_2(OH_2)]^+$ species, as nitrate is known to coordinate to platinum(II) aquo complexes [90]. Comparison of rate data at ~ 37.5°C in 0.1 *M* trifluoroacetic acid, 0.1 *M* acetic acid, 0.05 *M* H_2SO_4 and in 0.05 *M* oxalic, malonic and tartaric acids also shows that the rate constants are very similar to the data in 0.1 *M* $HClO_4$ (Table 2.3), but once more, comparison does not give much useful information as again, the final product in all cases is not the *cis*-$[PtCl(NH_3)_2(OH_2)]^+$ species. These preliminary data show that the effect of nitrate ions should be investigated further in future work.

The variation of k_1 with temperature allows calculation of the activation parameters associated with the forward reaction (Equation 1.1). The activation parameters associated with previous studies of this reaction are summarised in Table 2.7. Since several of these studies used only a very narrow temperature range, it is difficult to make comparisons between the earlier data, and the data presented here. However, the values of $\Delta H^{\neq}$ and $\Delta S^{\neq}$ obtained from this work do not agree too badly with those values obtained in water.

An increase in temperature leads to an increase in reaction velocity and hence in rate constants. Arrhenius first pointed out that the variation of rate constants with temperature can be represented by Equation 2.3, an equation similar to that used for

equilibrium constants, namely the Arrhenius Equation

$$k = \mathrm{PZ}\exp\left(\frac{-\mathrm{E_a}}{\mathrm{RT}}\right) \tag{2.3}$$

where k is a general rate constant, $\mathrm{E_a}$ is the energy of activation, R is the gas constant, T is the absolute temperature, Z is the collision rate between reactant molecules and P is the probability factor which is inserted to allow for the disparity between calculated and observed values of k [123]. The logarithmic form of this equation is

$$\ln k = \ln \mathrm{PZ} - \frac{\mathrm{E_a}}{(\mathrm{RT})} \tag{2.4}$$

This equation shows a linear relationship between $\ln k$ and $1/\mathrm{T}$, the slope being $-\mathrm{E_a}/\mathrm{R}$ and the intercept on the $\ln k$ (y) axis is $\ln \mathrm{PZ}$.

If there is a range of known rate constants, each at a known temperature, the activation energy $\mathrm{E_a}$ and PZ may be determined directly. Additionally, the enthalpy of activation, $\Delta\mathrm{H}^{\neq}$, and the entropy of activation, $\Delta\mathrm{S}^{\neq}$, may be calculated from the values of $\mathrm{E_a}$ and PZ [123]. If Equation 2.4 is integrated between the limits $k = k_1$ at $\mathrm{T} = \mathrm{T_1}$, and $k = k_2$ at $\mathrm{T} = \mathrm{T_2}$ then

$$\ln\left(\frac{k_2}{k_1}\right) = \frac{\mathrm{E_a}}{\mathrm{R}}\left(\frac{\mathrm{T_2} - \mathrm{T_1}}{\mathrm{T_1T_2}}\right) \tag{2.5}$$

that is, as soon as two values of k are available at two different temperatures, $\mathrm{E_a}$ may be evaluated; or, when $\mathrm{E_a}$ and a value of k at some one temperature are known, k at another temperature may be calculated, which is how we obtain calculated values for k_1 (and k_{-1}) at 25.0 °C.

An alternative approach to reaction kinetics is transition-state theory. This postulates that molecules, before undergoing reaction, must form an activated complex in equilibrium with the reactants, and that the rate of any reaction is controlled by the concentration of the complex present at any instant. The activated complex is assumed to be endowed with certain properties of an ordinary molecule and to possess some, although temporary, stability. On the basis of these ideas it was shown [124] that a rate constant k could be given by

$$k = \frac{\mathrm{RT}}{\mathrm{Nh}}\exp\left(\frac{-\Delta\mathrm{G}^{\neq}}{\mathrm{RT}}\right) \tag{2.6}$$

where N is Avogadro's number, h is Planck's constant and $\Delta\mathrm{G}^{\neq}$ is the free energy of activation. Since the activated complex is in equilibrium with the reactants, thermodynamics can be used and we can write

$$\Delta\mathrm{G}^{\neq} = \Delta\mathrm{H}^{\neq} - \mathrm{T}\Delta\mathrm{S}^{\neq} \tag{2.7}$$

Equation 2.6 can thus be written as

$$k = \frac{RT}{Nh} \exp\left(\frac{\Delta S^{\neq}}{R}\right) \exp\left(\frac{-\Delta H^{\neq}}{RT}\right) \tag{2.8}$$

since $\Delta H^{\neq}$, the enthalpy of activation can be taken as being identical to E_a. Equation 2.8 is of the same form as Equation 2.3 if $\Delta H^{\neq}$ is approximated to E_a, hence

$$PZ \simeq \frac{RT}{Nh} \exp\left(\frac{\Delta S^{\neq}}{R}\right) \tag{2.9}$$

For a reaction in solution [121,123]

$$E_a = \Delta H^{\neq} + RT \tag{2.10}$$

since for such a reaction the energy of activation, E_a, is greater than $\Delta H^{\neq}$[125]. Hence from the rate constants over a range of temperatures, the activation energy E_a, $\ln PZ$, the rate constant k_1 at 25.0 °C, the enthalpy of activation $\Delta H^{\neq}$ and the entropy of activation $\Delta S^{\neq}$ can be calculated (Table 2.7). The entropy of activation is a measure of the total entropy changes taking place in the reactants and the solvent on formation of the activated complex and, as such, its sign and magnitude are determined chiefly by the charge of the activated complex relative to the charge of the reactants. For reactions between oppositely charged ions, the activated complex will have a lower charge than the reactants and, as a consequence, will be less solvated (that is, less 'ordered'). Since the formation of the activated complex is accompanied by an increase in 'disorder', the $\Delta S^{\neq}$ value will be positive. For a reaction between ions of like charge, $\Delta S^{\neq}$ will be negative.

For the determination of k_{-1} (reverse of Equation 1.1), the *cis*-$[PtCl(NH_3)_2(OH_2)]^+$ species was isolated in chloride ion free 0.1 *M* $HClO_4$ using anion exchange chromatography. This technique has seldom been used in previous studies to obtain the *cis*-$[PtCl(NH_3)_2(OH_2)]^+$ species [78]. Methods used most commonly have been to incubate the *cis*-DDP with a stoichiometric amount of $AgNO_3$ solution [126], or with $NaNO_3$ solution [127], leaving *cis*-DDP to aquate on standing in D_2O at pH = 3 [103], or even by dissolving *cis*-DDP in solutions containing varying amounts of NaCl and incubating overnight, the resultant solution containing 8 to 60% of the *cis*-$[PtCl(NH_3)_2(OH_2)]^+$ species [128]. However the anion exchange method is preferred here as an almost chloride ion free solution can be obtained, hence we know accurately the concentration of chloride required to produce a second-order rate constant, without the interference of the extraneous chloride ion.

Addition of controlled amounts of excess chloride ions to the chloride ion free solutions of *cis*-$[PtCl(NH_3)_2(OH_2)]^+$ produces varying amounts of *cis*-DDP, the extent of the reaction depending on the chloride ion concentration used. Due to the speed of this reaction, only a restricted range of chloride ion concentrations could be used. In all cases, the initial chloride ion concentration was greater than ten times that of

the initial platinum(II) species concentration, so that pseudo-first-order kinetics could be obtained for k_{-1}. The pseudo-first-order rate constants (k_{obs}, s^{-1}) obtained for a range of chloride ion concentrations are listed in Table 2.4. These rate constants were then used to obtain values for the second order rate constants (k_{-1}, M^{-1} s^{-1}) using Equation 2.1

Reactions which are not truly first order, but which show first-order kinetics under special conditions are called pseudo-first-order reactions [129]. The pseudo-first-order rate nature of a reaction is explainable by the fact that the concentration of one of the reactants is present in such excess that its concentration practically remains constant during the course of the reaction [120,124]. Under these conditions, the second-order rate equation for the reaction becomes that of a first-order reaction. It is evident however that the new rate constant, k_{obs}, for this reaction is not independent of the concentration, as is the case with first-order rate constants, but may vary with the concentration of the reagent present in excess, in this case Cl^-, as the latter is changed appreciably. When this is the case, the true rate constant k_{-1} (M^{-1} s^{-1}) can be obtained from k_{obs} (s^{-1}) by dividing the latter by the concentration of the reagent present in excess, that is, $[Cl^-]$, and Equation 2.1 is obtained [124].

The validity of using this expression for this reaction can be justified because of the constancy of the k_{-1} values obtained using this method over a range of chloride ion concentrations, the plots of k_{obs} versus chloride ion concentration are linear and pass through the origin at $[Cl^-] = 0$ (see Figure 2.3), and the plots of $\ln k_{-1}$ (where k_{-1} is obtained over a chloride ion concentration range of 0.025 to 0.9 M) versus 1/T are linear and give sensible values for the activation parameters (Table 2.4). The data for k_{-1} are in agreement with those previously obtained (indirectly) in water (Tables 2.5 and 2.6). A value for $k_{-1} = 6.7 \times 10^{-3}$ M^{-1} s^{-1} was reported in the literature [130] at 25 °C but at an unspecified ionic strength. However, this value is in good agreement with the value of $k_{-1} = 6.3 \times 10^{-3}$ M^{-1} s^{-1} at 25 °C and $\mu = 1.0$ M obtained in this work.

The equilibrium constant K_1 for Equation 1.1, is obtained from the expression

$$K_1 = \frac{k_1}{k_{-1}} \tag{2.11}$$

This expression is valid for a simple, one-step reaction such as we have here. Combining the temperature dependence expressions for $k_{-1} = 2.104 \times 10^{11} \exp\left(\frac{-77.21 \times 10^3}{RT}\right)$ and $k_1 = 4.413 \times 10^{10} \exp\left(\frac{-84.73 \times 10^3}{RT}\right)$ (both at $\mu = 1.0$ M, $HClO_4$) in Equation 2.11 gives the temperature dependence of the equilibrium constant K_1 in the form

$$-\ln K_1 = \frac{7.52 \times 10^3}{RT} + 1.562 \tag{2.12}$$

The temperature dependence expressions for k_1 and k_{-1} are from the Arrhenius Equation (Equation 2.3) and from the computer calculations done to determine activation

Table 2.4. Spectrophotometrically determined chloride ion anation rate constants (k_{-1}) for *cis*-$[PtCl(NH_3)_2(OH_2)]^+$ (Equation 1.1) at $\mu = 1.0\ M$ ($HClO_4$). [a] [b]

Temperature (°C)	[K]	$[Cl^-]_i$ [c] (M)	$10^4 \times k_{obs}$ [d] (s^{-1})	$10^3 \times k_{-1}$ [e] ($M^{-1}\ s^{-1}$)	$10^3 \times k_{-1}$ (mean) ($M^{-1}\ s^{-1}$)	$10^3 \times k_{-1}$ (calc.) [f] ($M^{-1}\ s^{-1}$)
10.0	[283.2]	0.25	3.48±0.52	1.39±0.21	1.22±0.11	1.20
		0.35	4.07±0.39	1.17±0.11		
		0.40	5.36±0.93	1.34±0.23		
		0.50	5.96±0.81	1.19±0.16		
		0.60	7.39±0.86	1.23±0.14		
		0.75	8.04±1.49	1.07±0.20		
		0.90	10.33±1.26	1.15±0.14		
15.0	[288.2]	0.25	4.57±0.52	1.83±0.21	2.11±0.22	2.12
		0.35	6.91±0.77	1.97±0.22		
		0.45	9.51±0.83	2.11±0.81		
		0.60	13.47±1.93	2.24±0.32		
		0.75	15.50±0.94	2.07±0.12		
		0.90	22.30±1.50	2.47±0.16		
20.0	[293.2]	0.10	3.63±0.44	3.63±0.44	3.54±0.34	3.68
		0.90	31.2 ±2.3	3.46±0.25		
25.0	[293.2]	0.05	3.88±0.27	6.76±0.54	6.31±0.32	6.26
		0.125	7.63±0.40	6.34±0.33		
		0.15	9.36±0.50	6.24±0.33		
		0.20	12.6 ±0.8	6.30±0.40		
		0.25	14.7 ±1.2	5.88±0.48		
30.0	[303.2]	0.05	5.44±0.34	10.9±0.7	10.5±0.4	10.5
		0.10	10.6±0.20	10.6±0.2		
		0.125	12.6±0.70	10.1±0.6		

[a] The concentration of *cis*-$[PtCl(NH_3)_2(OH_2)]^+ \simeq 1.6 \times 10^{-3}\ M$.
[b] Ionic strength adjusted to 1.0 M using NaCl and $HClO_4$.
[c] Initial Cl^- concentration $\geq 10 \times$ [Pt]
[d] Spectrophotometrically determined pseudo-first-order rate constant. Mean of data calculated at $\lambda = 260$ and 305 nm.
[e] Calculated using Equation 2.1
[f] Calculated from the activation parameters $E_a = 77.2\ kJ\ mol^{-1}$, $\Delta S^{\neq} = -36.3\ J\ K^{-1}\ mol^{-1}$

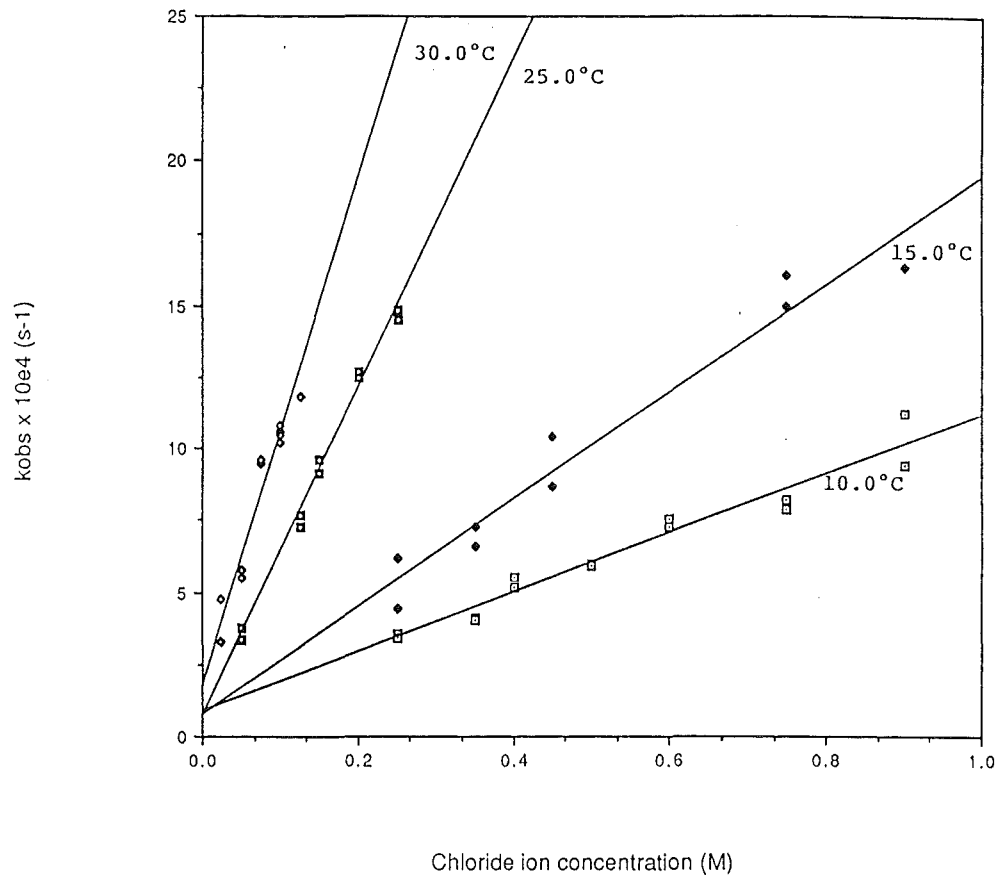

Figure 2.3. Plots of k_{obs} versus $[Cl^-]$ for the chloride anation *cis*-$[PtCl(NH_3)_2(OH_2)]^+$ (k_{-1}) (reverse of Equation 1.1).

Table 2.5. Summary of data for the equilibrium constants (K_1) associated with the first hydrolysis step of *cis*-$[PtCl_2(NH_3)_2]$ (Equation 1.1) in water.

Added electrolyte	Temperature (°C)	$10^5 \times k_1$ (s^{-1})	$10^3 \times k_{-1}$ ($M^{-1}\ s^{-1}$)	$10^3 \times K_1$	Reference
None	0	0.095	0.23	4.1	[98]
	25	2.8	7.3	3.7	[98]
	30	5.08	13.5	3.8	[98]
0.2 *M* KNO_3	25	2.58	6.4	4.05	[108]
0.318 *M* KNO_3	25	2.58	7.1	3.63	[112]
	35	7.59	17.3	4.37	[112]
0.318 *M* Na_2SO_4	25	2.5	7.6	3.3	[78]
0.318 *M* Na_2SO_4	35	7.6	19.5	3.9	[78]
$\mu = 0.3$ *M*	50	39	120	3.3	[100]

Table 2.6. Forward (k_1) and reverse (k_{-1}) rate constants and equilibrium constants (K_1) for the first step of the acid hydrolysis of *cis*-$[PtCl_2(NH_3)_2]$ in $HClO_4$ ($\mu = 1.0\ M$).

Temperature T (°C)	[K]	$10^5 \times k_1$ [a] (s^{-1})	$10^3 \times k_{-1}$ [b] ($M^{-1}\ s^{-1}$)	$10^3 \times K_1$ [c] [d]
10.0	[283.2]	1.03	1.20	8.58
15.0	[288.2]	1.94	2.12	9.15
20.0	[293.2]	3.54	3.68	9.62
25.0	[298.2]	6.32	6.26	10.1
30.0	[303.2]	11.1	10.5	10.6
35.0	[308.2]	19.2	17.4	11.3
40.0	[313.2]	32.6	28.1	11.6
45.0	[318.2]	54.3	44.8	12.1
50.0	[323.2]	89.2	70.3	12.7

[a]Calculated from the expression (1.0 M $HClO_4$) $k_1 = 4.413 \times 10^{10} \exp\left(\frac{-84.73\times10^3}{RT}\right)$ (Tables 2.1 and 2.7)

[b]Calculated from the expression $k_{-1} = 2.104 \times 10^{11} \exp\left(\frac{-77.21\times10^3}{RT}\right)$ (Table 2.4)

[c]Calculated from Equation 2.11 which is equivalent to Equation 2.12.

[d]The variation of K_1 with temperature indicates that the forward reaction is endothermic and from [c], $\Delta H^{\ddagger}_{298.2} = 7.52$ kJ mol^{-1} (*cf.* $\Delta H^{\ddagger}_{298.2} = 14.2$ kJ mol^{-1} in water [112]). Other thermodynamic parameters associated with the forward reaction are $\Delta G^{\ddagger}_{298.2} = 11.4$ kJ mol^{-1} and $\Delta S^{\ddagger}_{298.2} = -13$ J K^{-1} mol^{-1}.

parameters for k_1 and k_{-1}, the activation energies E_a and values for PZ for both k_1 and k_{-1} were obtained, and these values inserted into Equation 2.6 for each of k_1 and k_{-1} (Table 2.6).

The van't Hoff equation (Equation 2.13) provides a way of measuring the enthalpy of a reaction without using a calorimeter, where m = 298.2 K.

$$\ln K = \frac{\Delta H^{\ominus}_m}{RT} \tag{2.13}$$

From plots of $\ln K_1$ versus 1/T, the reaction enthalpy can be determined since the slope of this graph will be $-\Delta H^{\ominus}_m/R$ [120]. Thus $\Delta H^{\ddagger}_{298.2}$ for the endothermic forward reaction is calculated to be 7.52 kJ mol^{-1} ($\Delta H^{\ominus}_m$ is greater than zero for an endothermic reaction). The equilibrium constant K_1 gets larger as the temperature increases therefore the equilibrium shifts towards the reaction products, since for an endothermic reaction, a rise in temperature favours the products [120]. This variation of K_1 with temperature (Table 2.6) is small and rather more precisely established than has been possible from previous studies (Table 2.5).

Other thermodynamic parameters associated with the forward reaction were calculated. From the general expression

$$\Delta G^{\ominus}_m = -RT \ln K \tag{2.14}$$

where m = 298.2 K and $K = K_1$, $\Delta G^{\ddagger}_{298.2} = 11.4$ kJ mol^{-1}, and for the reverse

reaction, $\Delta G^{\ominus}_{298.2} = -11.4$ kJ mol^{-1} (calculated using the expression $K_1' = 1/K_1$). This negative value for $\Delta G^{\ominus}_{298.2}$ for the reverse reaction means that the overall reaction has a natural tendency to move spontaneously from products to reactants, that is, the reaction of *cis*-$[PtCl(NH_3)_2(OH_2)]^+$ plus chloride ions (k_{-1}) is the spontaneous reaction, not the forward reaction (k_1). This is reinforced by the fact that $\Delta H^{\ominus}_{298.2} = -7.52$ kJ mol^{-1} for the reverse anation reaction shows that this reaction is exothermic and exothermic reactions are usually the spontaneous reactions [131], although there are exceptions to this. Using the expression

$$\Delta G^{\ominus}_m = \Delta H^{\ominus}_m - T\Delta S^{\ominus}_m \tag{2.15}$$

for the forward reaction, a value of $\Delta S^{\ominus}_{298.2} = -13$ J K^{-1} mol^{-1} was obtained, and for the reverse reaction, $\Delta S^{\ominus}_{298.2} = 13$ J K^{-1} mol^{-1}. Since the forward reaction is endothermic, the principal driving force is the increasing entropy of the system, because the entropy of the surroundings decreases as enthalpy is sucked into the system. The effect of the unfavourable change in their entropy is reduced if the temperature is raised and so the reaction can proceed more strongly towards the products [120].

2.4 Conclusions.

Determination of the rate constant k_1 was carried out in $HClO_4/NaClO_4$ media, where the acidic conditions removed any influence of the *cis*-$[PtCl(OH)(NH_3)_2]$ species on the rate constants. The use of perchlorate electrolytes to remove any acceleratory or binding effects that electrolytes such as nitrate ion might have also removes uncertainties inherent in previous literature values of k_1. The rate constant k_{-1} was obtained from solutions of *cis*-$[PtCl(NH_3)_2(OH_2)]^+$ free of background chloride ions and was found to agree with a value obtained recently in the literature [130]. Calculation of the equilibrium constant K_1 was thus possible and at 25 °C, the value of $K_1 = 1.01 \times 10^{-2}$ is larger than values reported in the literature (Table 2.5).

Knowledge of the equilibrium constant K_1 meant that the equilibrium hydrolysis product concentrations ($\mu = 1.0$ M, $HClO_4$) for various initial *cis*-DDP concentrations, in the absence of added chloride ion could be calculated at any temperature (Table 2.2). The method of calculation of these equilibrium concentrations of platinum(II) species is given in Appendix B.

Table 2.7. Summary of the kinetic parameters obtained at 25°C for the first hydrolysis step of *cis*-$[PtCl_2(NH_3)_2]$.

Solvent	$10^5 \times k_1$ (s^{-1})	$\Delta H^{\neq}$ (kJ mol^{-1})	$\Delta S^{\neq}$ (J K^{-1} mol^{-1})	$\Delta V^{\neq}$ (cm^3 mol^{-1})	Reference
H_2O	2.8	83	-58		[102]
H_2O	2.8	90	-25		[98]
H_2O	2.6	81.5	-58		[99]
H_2O	2.5	82.3	-59		[112]
0.001 *M* HNO_3				-9.5±1.2 [a]	[116]
0.01 *M* HNO_3	3.2	91	-25		[109]
0.1 *M* $HClO_4$	7.56	73.7±3	-76.5±5		this work
0.1 *M* $HClO_4$ + 0.9 *M* $NaClO_4$	8.51	76.2±3	-67.3±6		this work
1.0 *M* $HClO_4$	6.32	82.3±1.9	-49.4±4		this work

[a] At 43.5 °C.

CHAPTER 3

THE KINETICS OF CHLORIDE ANATION OF THE *cis*-DIAMMINEDI(AQUA)PLATINUM(II) CATION AND OF THE BASE HYDROLYSIS OF *cis*-DICHLORODIAMMINEPLATINUM(II) AND *cis*-DIAMMINE(CHLORO)HYDROXOPLATINUM(II).

3.1 Introduction.

In Chapter 2 the results of the investigation of the first step of the acid hydrolysis reaction of *cis*-DDP (Equation 1.1) in both directions to give the rate constants k_1 and k_{-1} and hence the equilibrium constant K_1, were presented. The second step of this hydrolysis reaction (Equation 1.2) thus came under scrutiny, in order to determine the rate constants for the forward, k_2, and reverse, k_{-2}, directions of this step, and the equilibrium constant K_2 for this process.

Thus described in this chapter are the quantitative numerical data for the rate and equilibrium processes associated with Equation 1.2. However, in order to gain entry into this area to investigate these processes, the overall rate constant (k^{12}_{OH}) for the base hydrolysis of *cis*-DDP (Equations 3.2 and 3.3) also had to be measured, and rate data for this process are also presented. Also described in this Chapter is the rate of loss of the chloro ligand from *cis*-$[PtCl(OH)(NH_3)_2]$, (k^2_{OH}, s^{-1}) to give *cis*-$[Pt(OH)_2(NH_3)_2]$ (Equation 3.3).

3.2 Experimental.

3.2.1 Base Hydrolysis Kinetics - Determination of k^{12}_{OH}.

Standard solutions of sodium hydroxide (0.1 M) were prepared from VOLUCON ampoules. More concentrated solutions were prepared from weighed amounts of solid sodium hydroxide pellets. All solutions were adjusted to the appropriate ionic strength using weighed amounts of $NaClO_4.H_2O$ or NaCl. Three ml of the appropriate sodium hydroxide solution were allowed to reach thermal equilibrium in the 1.00 cm spectrophotometer cell and placed in the temperature controlled (± 0.1 °C) cell compartment of the spectrophotometer. Small samples (~ 3 mg) of solid *cis*-DDP were added and

after dissolution, repeat scan or repeat fixed wavelength data collection modes were started between 345 and 220 nm, with absorbance data collected at 304, 260 and 236 nm. The reaction was monitored until no further change in absorbance with time was observed (approximately six to eight half-lives). First order rate constants (k^{12}_{OH}) were calculated from the absorbance versus time data as in Chapter 2 (Equation 2.2; Tables 3.1 and 3.2), and hence activation parameters were computer calculated using Equations 2.3 to 2.10 (Table 3.4).

3.2.2 Determination of k^2_{OH}.

A sample of *cis*-DDP (50 mg) was allowed to hydrolyse in 0.01 *M* NaOH (45 ml) for approximately eight half-lives (about 48 hours at room temperature). To this solution was added 5 ml of 0.2 *M* $HClO_4$, and the now acid solution ($[H^+]$ = 0.011 *M*) was allowed to anate at room temperature for a further 48 hours, to give approximately 98% *cis*-$[PtCl(NH_3)_2(OH_2)]^+$ and 2% *cis*-$[Pt(NH_3)_2(OH_2)_2]^{2+}$. Samples of this solution (2.0 ml) and 1.0 ml of 0.3 *M* NaOH solution were thermally equilibrated at the appropriate temperature in a temperature controlled water-bath. On mixing in the 1.00 cm spectrophotometer cell the *cis*-$[PtCl(OH)(NH_3)_2]$ species was generated (λ_{max} = 267 nm) in 0.1 *M* NaOH and the subsequent chloride release kinetics were monitored spectrophotometrically at 304, 255 and 250 nm (Figure 3.2). The resulting absorbance versus time data were used to obtain the k^2_{OH} data reported in Table 3.3.

3.2.3 Determination of k_{-2}.

Stock solutions of *cis*-$[Pt(OH)_2(NH_3)_2]$ (3.33×10^{-3} *M*) were prepared by allowing *cis*-DDP (50 mg) to hydrolyse for more than six half-lives at room temperature in 0.01 *M* NaOH (50 ml). One ml samples of each of *cis*-$[Pt(OH)_2(NH_3)_2]$ and $NaCl/HClO_4$ solution (μ = 2.0 *M*) were placed respectively in the seperate arms of the glass Y-shaped rapid mixing device [119], and the arms were immersed in the temperature controlled water bath. A dry 1.00 cm quartz spectrophotometer cell was mounted on top of the mixing device and on inversion, the two solutions were rapidly mixed.

The cell was placed in the temperature controlled cell compartment of the spectrophotometer, the mixing device was removed from the cell, and repeat fixed wavelength data for the subsequent reaction were recorded. The wavelengths chosen to monitor the reaction (240 and 280 nm) correspond to the isosbestic points measured for k_{-1} (Chapter 2). Rate constants from reactions with half-lives as short as 42 seconds could be determined using this procedure. The temperature of the cell compartment was controlled using a water-cooled, jacketed cell-holder with the temperature of the water kept low and constant by the simultaneous use of a refrigeration unit and a heater unit in the water tank, as in Chapter 2.

The initial chloride concentrations chosen were always greater than ten times that of

the concentration of the *cis*-$[Pt(NH_3)_2(OH_2)_2]^{2+}$ and pseudo-first-order rate constants (k_{obs}, s^{-1}) were calculated using the absorbance versus time data at each wavelength and temperature (Table 3.9). The second-order anation rate constants (k_{-2}, $M^{-1}\ s^{-1}$, Equation 1.2, Table 3.9) were calculated using Equation 3.1 as plots of k_{obs} versus the chloride ion concentration were linear and passed through the origin (Figure 3.7).

$$k_{-2} = k_{obs}[Cl^-]^{-1} \tag{3.1}$$

3.2.4 Determination of K_2.

Stock solutions of *cis*-$[Pt(OH)_2(NH_3)_2]$ (3.2, 1.3 and 0.53 mM) were prepared by hydrolysis of the appropriate amount of *cis*-DDP in 0.01 M NaOH. Samples (2.0 ml) were acidified with 1.0 ml of 1.5 M $HClO_4$ and the mixture allowed to anate at room temperature for 48 hours and then for three hours at 25°C, before recording the UV absorption spectrum.

Knowledge of the molar absorptivity coefficients (ϵ) of the *cis*-$[Pt(NH_3)_2(OH_2)_2]^{2+}$ and *cis*-$[PtCl(NH_3)_2(OH_2)]^+$ species (Table 3.6) at any wavelength (Figure 3.6) allowed the calculation of K_2 (Table 3.7).

3.3 Results and Discussion.

Previous studies on the base hydrolysis of *cis*-DDP have shown that *cis*-DDP hydrolyses in base to give *cis*-$[Pt(OH)_2(NH_3)_2]$ and two chloride ions [98,100,108,113]. However, speculation has arisen as to how the reaction proceeds. A two-step process was favoured by some studies - Grinberg and Korableva thought that the reaction was a two step process and that Equation 3.2 was the slow step and Equation 3.3 was much faster [113]. They based this assumption on the observation that the alkaline hydrolysis of *cis*-DDP involved essentially the simultaneous replacement of both coordinated chlorides. However, since simultaneous replacement was scarcely possible, they interpreted this as meaning that the rate of replacement of the second chloride in *cis*-DDP (Equation 3.3) had to be considerably greater than that of the first (Equation 3.2). Thus the first step was said to be the slowest and therefore rate-determining.

$$cis\text{-}[PtCl_2(NH_3)_2] + OH^- \xrightarrow{k^1_{OH}} cis\text{-}[PtCl(OH)(NH_3)_2] + Cl^- \tag{3.2}$$

$$cis\text{-}[PtCl(OH)(NH_3)_2] + OH^- \xrightarrow{k^2_{OH}} cis\text{-}[Pt(OH)_2(NH_3)_2] + Cl^- \tag{3.3}$$

The rate constant for the overall process (k^{12}_{OH}, s^{-1}) had been measured previously prior to this investigation and the literature values were $k^{12}_{OH} = 2.35 \times 10^{-5}\ s^{-1}$ [132] or $k^{12}_{OH} = 1.3 \times 10^{-5}\ s^{-1}$ [113] both at 25°C. A value for k^2_{OH} has also been determined, $k^2_{OH} = 2.2 \times 10^{-5}\ s^{-1}$ at 25°C [108]. Comparison of these literature values

Table 3.1. Spectrophotometrically determined rate constants (k_{OH}^{12}, s^{-1}) for the hydrolysis of *cis*-$[PtCl_2(NH_3)_2]$ in NaOH solution ($[OH^-]$ variation).[a]

Temperature		$[OH^-]$ variation, $\mu = 1.0\ M$ ($NaClO_4$)					
(°C)	[K]	$[OH^-] = 0.01\ M$		$[OH^-] = 0.1\ M$		$[OH^-] = 1.0\ M$	
		obs.	calc. [b]	obs.	calc. [b]	obs.	calc. [b]
25.0	[298.2]		0.233		0.155		0.337
35.3	[308.5]	0.691	0.720	0.554	0.535	0.991	0.995
45.1	[318.3]	2.18	1.93	1.64	1.69	2.63	2.61
55.2	[328.4]	4.97	5.13	5.02	4.84	6.74	6.77
$\Delta H^{\neq}$(kJ mol^{-1})		80.7 ± 7.3		90.3 ± 7.0		78.6 ± 0.6	
$\Delta S^{\neq}$(J K^{-1} mol^{-1})		-63.1 ± 14		-34.3 ± 14		-66.9 ± 1.2	

Temperature		$[OH^-]$ variation, $\mu = 0.1\ M$ ($NaClO_4$)				$[OH^-]$ variation, $\mu = 0.01\ M$	
(°C)	[K]	$[OH^-] = 0.01\ M$		$[OH^-] = 0.1\ M$		$[OH^-] = 0.01\ M$	
		obs.	calc. [b]	obs.	calc. [b]	obs.	calc. [b]
25.0	[298.2]		0.164		0.329		0.145
35.4	[308.6]	0.578	0.578	0.908	0.884	0.560	0.560
37.3	[310.5]	0.792	0.713	1.14	1.03	0.848	0.719
40.1	[313.3]	0.959	1.00	1.25	1.38	0.846	0.941
43.0	[316.2]	1.38	1.39	1.79	1.70	1.44	1.42
45.3	[318.5]	1.95	1.77	2.60	2.10	1.66	1.84
50.0	[323.2]	2.74	3.04	3.50	3.16	3.56	3.06
55.3	[328.5]	4.47	5.08	5.79	4.87	6.26	5.74
60.0	[333.2]	9.94	8.28	5.99	6.90	9.90	9.68
$\Delta H^{\neq}$(kJ mol^{-1})		90.0 ± 4.1		69.5 ± 8.8		96.5 ± 4.8	
$\Delta S^{\neq}$(J K^{-1} mol^{-1})		-34.6 ± 8.2		-97.5 ± 18		-13.8 ± 10	

[a] k_{OH}^{12} (obs.) data plus or minus 10%.
[b] Calculated from the cited activation parameters.

of k_{OH}^{12} and k_{OH}^{2} shows that they are very similar and hence suggests that the two steps (Equations 3.2 and 3.3) have similar rates. If the rate of the second step (Equation 3.3) were rapid as suggested by Grinberg and Korableva [113], there would be an efficient chloride release pathway for the second chloride ion in the pH regime where *cis*-$[PtCl(OH)(NH_3)_2]$ could be generated, for example, in blood plasma (pH = 7.4 [91]), so the rate of this step could have considerable importance.

The overall rate of base hydrolysis of *cis*-DDP (k_{OH}^{12}) was also measured quantitatively in the presence of chloride ions in order to determine the effect, if any, of the chloride ions on the reaction. The rate was measured in basic solution (0.01 *M* NaOH) with ionic strength controlled by the addition NaCl (0.09 - 0.99 *M*, μ = 0.1 and 1.0 *M*). The values of k_{OH}^{12} obtained (Tables 3.1 and 3.2) showed that the presence of chloride ions did not effect the rate or extent of base hydrolysis of *cis*-DDP at all, a result which gives rise to some speculation as to how *cis*-DDP behaves *in vivo*.

The pH of blood plasma is maintained at about 7.4 [91]. At this pH at least some of the administered *cis*-DDP in the blood stream would be reacting via the base

Table 3.2. Spectrophotometrically determined rate constants (k_{OH}^{12}, s^{-1}) for the hydrolysis of *cis*-$[PtCl_2(NH_3)_2]$ in NaOH solution (ionic strength (μ) variation).[a]

Temperature		Ionic strength variation ($NaClO_4$), $[OH^-] = 0.01\ M$					
(°C)	[K]	$\mu = 0.01\ M$		$\mu = 0.1\ M$		$\mu = 1.0\ M$	
		obs.	calc. [b]	obs.	calc. [b]	obs.	calc. [b]
25.0	[298.2]		0.145		0.164		0.233
35.3	[308.5]	0.560	0.560	0.578 (0.577) [c]	0.578	0.691 (0.631) [c]	0.720
45.2	[318.4]	1.66	1.84	1.95 (1.49) [c]	1.77	2.18 (1.64) [c]	1.93
55.1	[328.3]	6.26	5.74	4.47 (4.80) [c]	5.08	4.97 (4.88) [c]	5.13
$\Delta H^{\neq}$ ($kJ\ mol^{-1}$)		96.5 ± 4.8		90.0 ± 4.1		80.7 ± 7.3	
$\Delta S^{\neq}$ ($J\ K^{-1}\ mol^{-1}$)		-13.8 ± 10		-34.6 ± 8.2		-63.1 ± 14	

Temperature		Ionic strength variation ($NaClO_4$), $[OH^-] = 0.1\ M$			
(°C)	[K]	$\mu = 0.1\ M$		$\mu = 1.0\ M$	
		obs.	calc. [b]	obs.	calc. [b]
25.0	[298.2]		0.329		0.155
35.4	[308.6]	0.908	0.884	0.554	0.535
45.2	[318.4]	2.60	2.10	1.64	1.69
55.3	[328.5]	5.79	4.87	5.02	4.84
$\Delta H^{\neq}$ ($kJ\ mol^{-1}$)		69.5 ± 8.8		90.3 ± 7.0	
$\Delta S^{\neq}$ ($J\ K^{-1}\ mol^{-1}$)		-97.5 ± 18		-34.3 ± 14	

[a] k_{OH}^{12} (obs.) data plus or minus 10%.
[b] Calculated from the cited activation parameters.
[c] NaCl used to control the ionic strength.

hydrolysis pathway, and from these results it can be seen that a chloride ion concentration of around 103 mM, as is said to be the concentration present in blood plasma [48,92,97], would play no part in the base hydrolysis. That is, as well as inside the cell as is commonly thought, the hydrolysis reaction of *cis*-DDP could occur outside the cell in the blood plasma. The pH and chloride ion concentrations are such that, in blood plasma, the final products would be a mixture of *cis*-$[Pt(OH)(NH_3)_2(OH_2)]^+$, *cis*-$[PtCl(OH)(NH_3)_2]$ and *cis*-$[Pt(OH)_2(NH_3)_2]$. Both the *cis*-$[Pt(OH)_2(NH_3)_2]$ and *cis*-$[PtCl(OH)(NH_3)_2]$ are relatively inert to substitution but since both are neutral in charge, they should therefore be capable passage through the cell wall with the same ease as *cis*-DDP. However, the *cis*-$[Pt(OH)(NH_3)_2(OH_2)]^+$ or *cis*-$[PtCl(NH_3)_2(OH_2)]^+$ ions would be the active reagents for attack by polar groups in the DNA target molecule. The rapid protolytic equilibria between the *cis*-$[PtCl(OH)(NH_3)_2]$ and the *cis*-$[PtCl(NH_3)_2(OH_2)]^+$ would allow facile transport of platinum(II) species to suitable DNA sites. Additionally, since the *cis*-$[Pt(OH)_2(NH_3)_2]$ species is thought to be the toxic or nausea-initiating substance [97] (the monomeric, dimeric and trimeric hydroxo species are all toxic, but the dimeric species especially so [33]) then this may account for the rapid nausea felt by patients when *cis*-DDP is administered.

The UV absorption spectrum of *cis*-DDP dissolved in an aqueous NaOH solution (0.1 to 1.0 M) changes slowly and smoothly with time, with an isosbestic point at 276 nm (Figure 3.1). It was observed that this isosbestic point drifted slightly as the hydrolysis proceeded, and this suggests that the reaction is biphasic (Equations 3.2 and 3.3) but with the two steps having similar rate constants. If this is the case, reactions 3.2 and 3.3 will have similar isosbestic points.

From absorbance versus time data, collected at 304, 260 and 236 nm, first-order rate constants (k^{12}_{OH}, s^{-1}) were calculated according to Equation 2.2. Analysis of the data at these three different wavelengths gave the same first-order rate constants with there being no evidence for consecutive reactions, which is in agreement with the results from the chloride release titration data of Grinberg and Korableva [113]. The values for k^{12}_{OH} obtained using Equation 2.2, over a 35 K temperature range, are shown in Tables 3.1 and 3.2. The overall hydrolysis rate constant, k^{12}_{OH}, is almost independent of the concentration of hydroxide ions, the ionic strength and the background chloride ion concentration in the range 0.01 to 1.0 M NaOH.

The direct measurement of k^2_{OH} was made using *cis*-$[PtCl(OH)(NH_3)_2]$ generated from *cis*-$[PtCl(NH_3)_2(OH_2)]^+$, using the method outlined. The chloride release reaction can be monitored spectrophotometrically and the development of a sharp isosbestic point at 274 nm (close to but not identical with the isosbestic point generated in the base hydrolysis of *cis*-DDP) was observed (Figure 3.2). Using the first-order rate law (Equation 2.2), values for the rate constant k^2_{OH} were calculated over a 35 K temperature range at all three wavelengths, and are shown in Table 3.3. These values of k^2_{OH} are

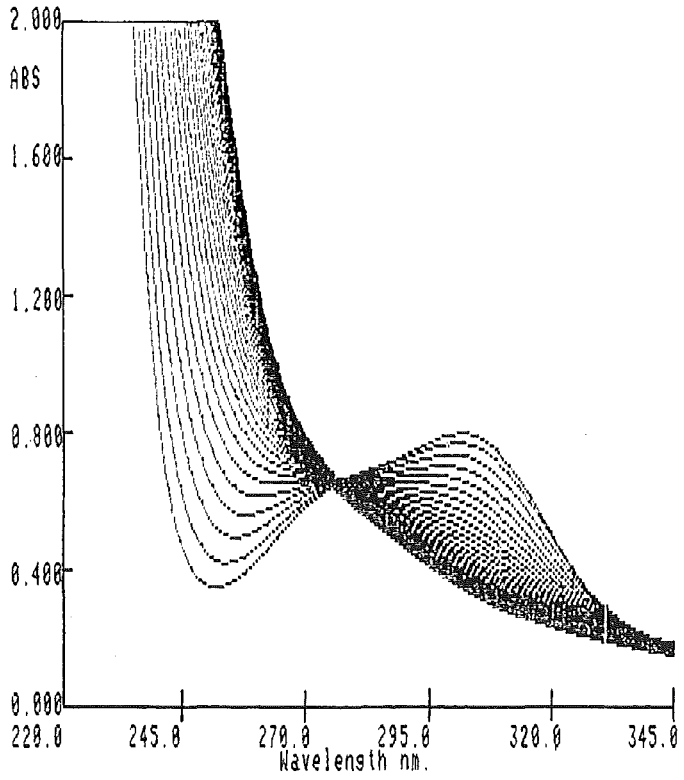

Figure 3.1. Spectrophotometric scans for the base hydrolysis of *cis*-$[PtCl_2(NH_3)_2]$ in 0.01 *M* NaOH at 60.0 °C (2 minute intervals). The absorbance at 300 nm decreases with time and the rather broad cross-over area is centred at 276 nm.

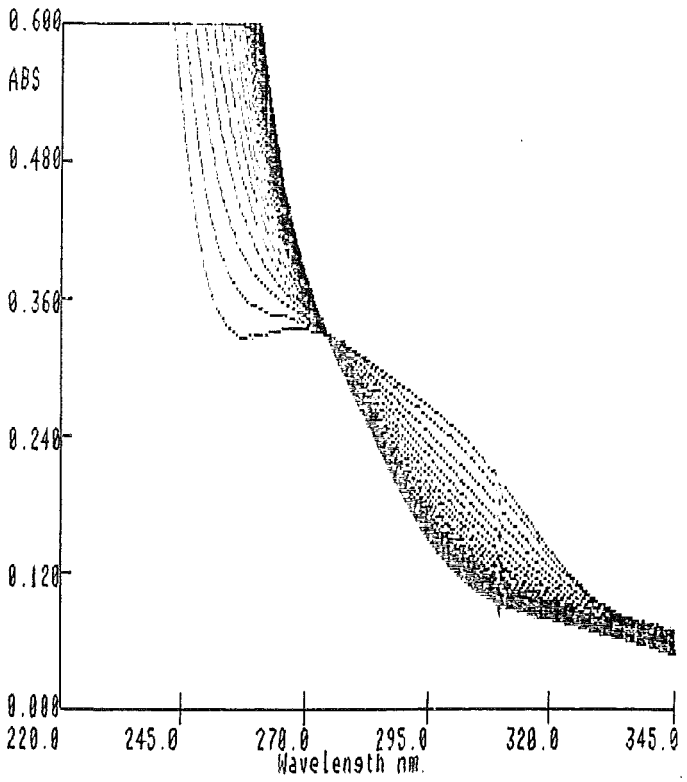

Figure 3.2. Spectrophotometric scans for the hydrolysis of *cis*-$[PtCl(OH)(NH_3)_2]$ in 0.1 *M* NaOH at 60.1°C (3 minute intervals). The absorbance at 300 nm decreases with time.

slightly smaller than those obtained for k_{OH}^{12} but the activation parameters are similar (Table 3.4). Although k_{OH}^{12} and k_{OH}^{2} are comparable in magnitude (Table 3.5), the reaction pathway depicted in Figure 3.3 is still a potential hydrolysis route in regions of high pH as k_{OH}^{12} and, by inference, k_{OH}^{2} are not inhibited by the presence of background chloride ions.

The rate of base hydrolysis of *cis*-DDP is independent of the hydroxide ion concentration, and is much slower than the rate of acid hydrolysis. For platinum(II) complexes, there is generally poor correlation between the basicity and general nucleophilic character of reagents and their rates of substitution in the platinum(II) complexes. The hydroxide ion, which is such a powerful reagent for organic halides and for cobalt(III) ammines is comparatively ineffective towards platinum(II) complexes [133]. However, there is close agreement between the activation parameters for acid hydrolysis (Table 2.7) and base hydrolysis (Figure 3.4, Table 3.4), which suggests that water is the attacking nucleophile in both situations, an idea also put forward by Grinberg *et al.* [113]. It is postulated that the observation that base hydrolysis is about three times slower than acid hydrolysis at all temperatures could be due to the stabilisation of the transition state of the reaction, according to Figure 3.5.

Water and hydroxide ions have much the same nucleophilicity (the degree of attraction of a group towards a positively charged centre), that is, both water and hydroxide

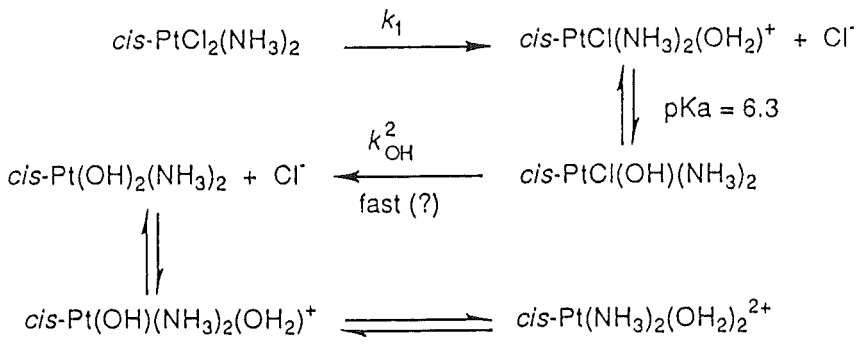

Figure 3.3. Potential hydrolysis route of *cis*-$[PtCl_2(NH_3)_2]$ in regions of high pH.

Table 3.3. Spectrophotometrically determined rate constants (k^2_{OH}) for the hydrolysis reaction of *cis*-$[PtCl(OH)(NH_3)_2]$ (Equation 3.3) ($\mu = 0.1$ *M*, NaOH).

Temperature		$10^5 \times k^2_{OH}$ (s^{-1})	
(°C)	[K]	obs.	calc. [a]
25.0	[298.2]		1.43
35.2	[308.4]	4.27 ± 0.01	4.37
39.8	[313.0]	7.54 ± 0.12	7.06
45.1	[318.3]	11.3 ± 0.02	12.1
50.1	[323.3]	20.7 ± 0.81	19.7
54.9	[328.1]	30.3 ± 0.08	31.0
60.2	[333.4]	52.0 ± 0.06	50.6

[a]Calculated from the activation parameters: $E_a = 86.8 \pm 5.2$ kJ mol^{-1}, lg PZ = 10.3595, $\Delta S^{\neq} = -55 \pm 10$ J K^{-1} mol^{-1}

Table 3.4. Activation parameters for the base hydrolysis of *cis*-$[PtCl_2(NH_3)_2]$ at 298.2 K.[a]

μ	10^4 k^{12}_{OH}(calc.)	E_a	$\Delta H^{\neq}$	$\Delta S^{\neq}$
(*M*)	(s^{-1})	(kJ mol^{-1})	(kJ mol^{-1})	(J K^{-1} mol^{-1})
0.01	0.145	99.4±4.8	97.0±4.8	-12±10
0.10 [b]	0.190	86.8±3.8	84.4±3.8	-52±8
1.0 [c]	0.216	86.0±5.1	83.5±5.1	-54±10
0.10 [d]	0.143	86.8±5.2	84.3±5.2	-55±10

[a]k^{12}_{OH} independent of $[OH^-]$ and $[Cl^-]$ in the range 0.01 to 1.0 *M*.
[b]All data at $\mu = 0.1$ *M* ($NaClO_4$) combined.
[c]All data at $\mu = 1.0$ *M* ($NaClO_4$) combined.
[d]k^2_{OH} data (Table 3.3).

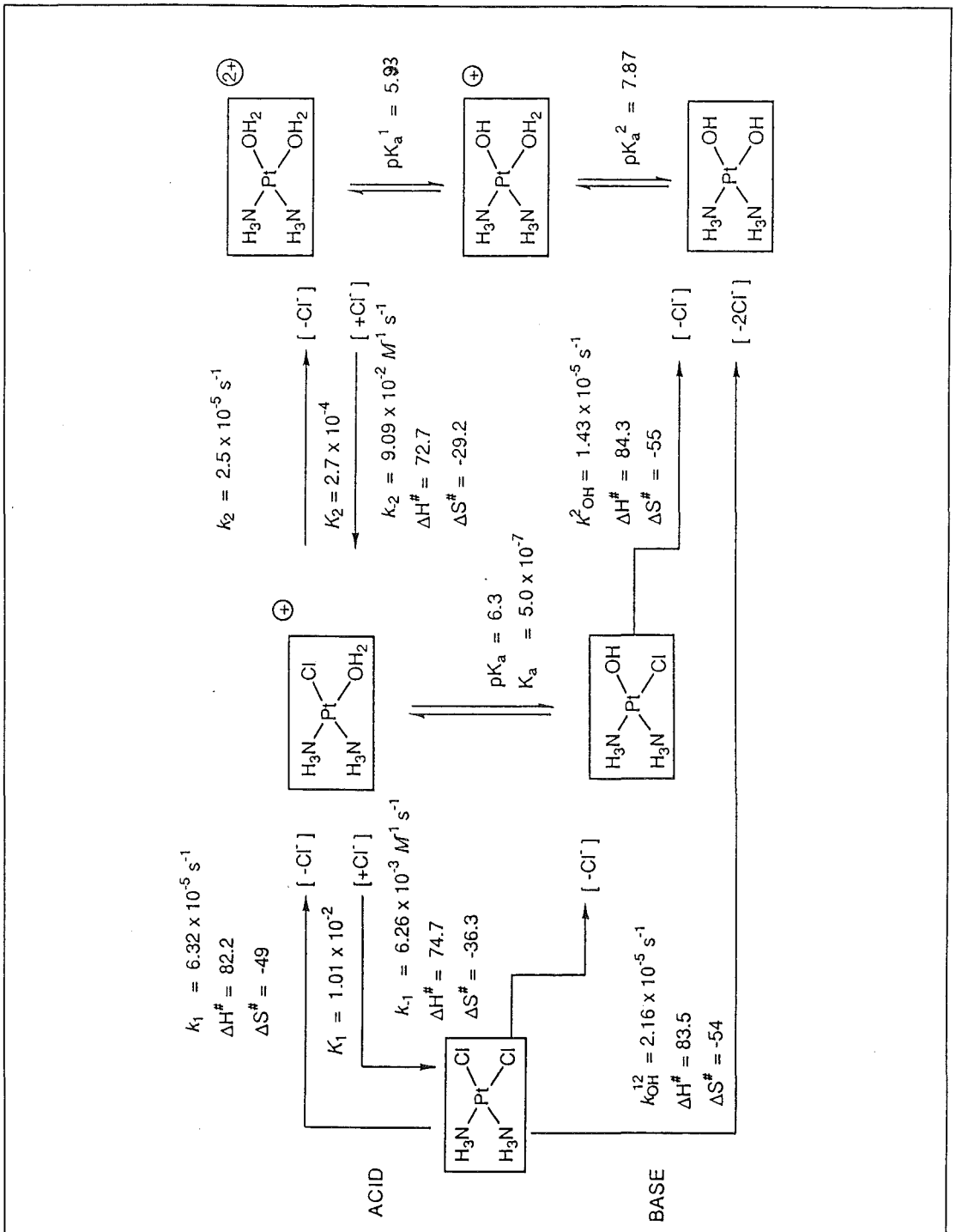

Figure 3.4. Rate and equilibrium constants for *cis*-$[PtCl_2(NH_3)_2]$ and its hydrolysis products in acidic and basic conditions at 25°C.

Table 3.5. Relative chloride release labilities for *cis*-$[PtCl_2(NH_3)_2]$ and its hydrolysis products.[a]

Complex	Chloride release rate constant (25 °C)	Rate ratio relative to *cis*-$[PtCl_2(NH_3)_2]$ in base
cis-$[PtCl_2(NH_3)_2]$	$k_{OH}^{12} = 2.41 \times 10^{-5}$ s^{-1}	1.0
cis-$[PtCl_2(NH_3)_2]$	$k_1 = 6.32 \times 10^{-5}$ s^{-1}	2.6
cis-$[PtCl(NH_3)_2(OH_2)]^+$	$k_2 = 2.5 \times 10^{-5}$ s^{-1}[b]	1.03
cis-$[PtCl(OH)(NH_3)_2]$	$k_{OH}^{2} = 1.43 \times 10^{-5}$ s^{-1}	0.6

[a]Such a comparison should be treated with caution as these rate ratios will only be valid if the activation parameters associated with the chloride release rate constants are similar. If they are not, the relative order of reactivity could easily change with temperature.

[b]The extent to which this complex will aquate is highly chloride ion dependent (see Table 3.8).

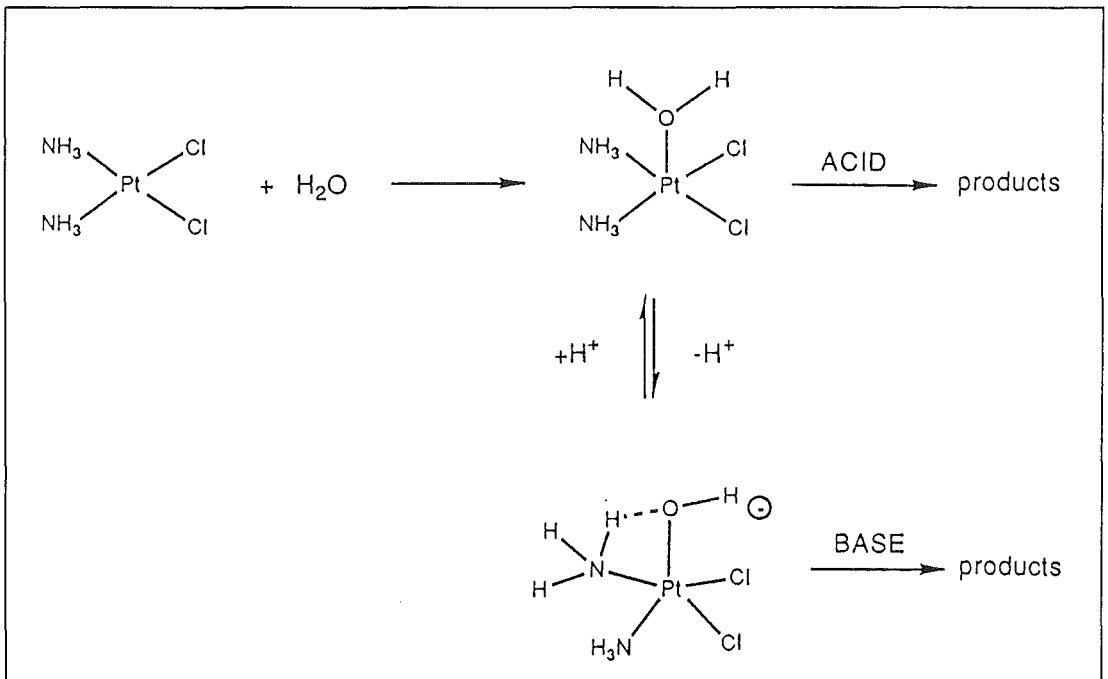

Figure 3.5. Possible stabilisation of the transition state in the base hydrolysis of *cis*-$[PtCl_2(NH_3)_2]$.

ions are relatively poor nucleophiles towards platinum(II) [134]. This is thought to show how important π-bonding is in the stabilisation of the five-coordinate transition state as shown in Figure 3.5. The hydroxide ion cannot accomodate d-orbital electrons from the platinum. In fact, the interaction of the filled p-orbitals of the hydroxide ion and the filled d-orbitals of the metal is expected to be one of repulsion, which may account for the low reactivity of the hydroxide ions towards platinum(II) [133]. Another trend is to relate reactivity with the degree of softness or 'polarizability' of the nucleophile [135]. A 'soft' acid has a large size, small charge and has valence electrons which are easily distorted or removed (that is, it is easily polarized); similarly a 'soft' base is one which is easily polarized. According to the principle of Hard and Soft Acids and Bases [136], hard acids prefer to coordinate to hard bases and soft acids prefer to coordinate with soft bases. It is to be expected then that platinum(II), a soft acid, should react rapidly with soft bases. However, the hydroxide ion is defined as a 'hard' nucleophile and would therefore be more effective towards a 'hard' substrate, therefore reaction between the two is not expected to be rapid. The polarizability of the nucleophile makes a large contribution to its reactivity towards the class (b) metal of the platinum(II) complexes.

The base hydrolysis of *cis*-DDP to give *cis*-$[Pt(OH)_2(NH_3)_2]$ and two free chloride ions as products is an irreversible reaction and this gives access to the reaction chemistry of the *cis*-$[Pt(NH_3)_2(OH_2)_2]^{2+}$ species as it is rapidly generated on acidification of the *cis*-$[Pt(OH)_2(NH_3)_2]$. Subsequently, the *cis*-$[Pt(NH_3)_2(OH_2)_2]^{2+}$ anates slowly (complete in hours at room temperature) with the background chloride ions present to give an equilibrium mixture of *cis*-$[PtCl(NH_3)_2(OH_2)]^+$ and *cis*-$[Pt(NH_3)_2(OH_2)_2]^{2+}$ plus chloride ions. The composition of this equilibrium mixture can be determined spectrophotometrically to give K_2 (Equation 1.2). The UV absorption spectra of *cis*-DDP, *cis*-$[PtCl(NH_3)_2(OH_2)]^+$ and *cis*-$[Pt(NH_3)_2(OH_2)_2]^{2+}$ in 1.0 M $HClO_4$ are shown in Figure 3.6.

The molar absorptivity coefficients of these three species were determined using UV spectroscopy, from weighed samples of *cis*-DDP, from using chromatographic techniques to isolate *cis*-$[PtCl(NH_3)_2(OH_2)]^+$ (Chapter 2) and from using base hydrolysis of *cis*-DDP followed by acidification to generate *cis*-$[Pt(NH_3)_2(OH_2)_2]^{2+}$. Internal constraints are enforced on the system by the positions and intensities of the isosbestic points generated in the acid hydrolysis and anation reactions of *cis*-DDPand its hydrolysis products. The data represented by Figure 3.6 are given in Table 3.6.

In order to obtain the equilibrium constant K_2, the UV absorption spectra of the equilibrium mixtures of *cis*-$[PtCl(NH_3)_2(OH_2)]^+$, *cis*-$[Pt(NH_3)_2(OH_2)_2]^{2+}$ and chloride ions generated above, had to be analysed. The starting point is Beer's Law

$$A = \epsilon c l \tag{3.4}$$

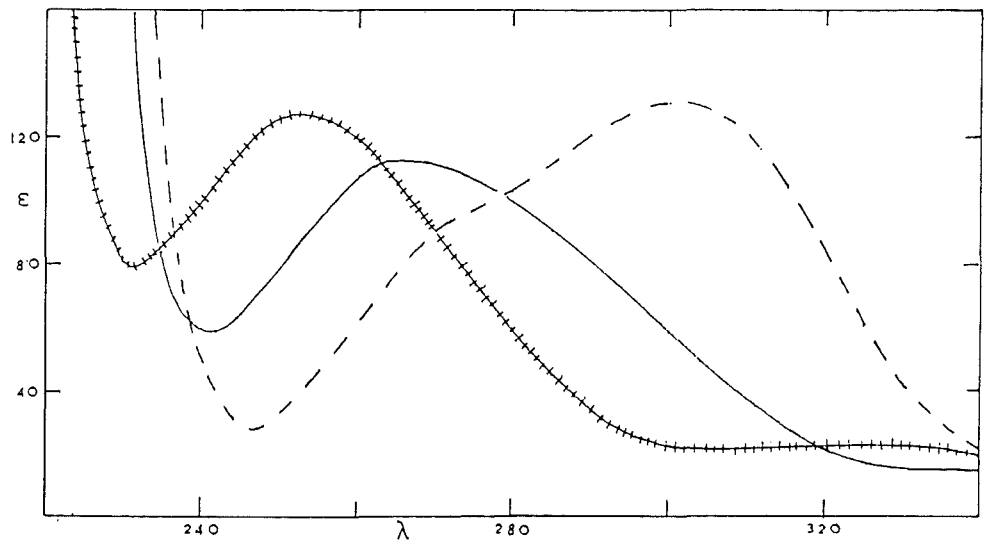

Figure 3.6. The UV absorption spectra (340 – 220 nm) of the species *cis*-$[PtCl_2(NH_3)_2]$ (– – –), *cis*-$[PtCl(NH_3)_2(OH_2)]^+$ (——) and *cis*-$[Pt(NH_3)_2(OH_2)_2]^{2+}$ (+++) in $HClO_4$ solution.

Table 3.6. Molar absorptivity coefficients (ϵ) for *cis*-$[PtCl_2(NH_3)_2]$ and its hydrolysis products in aqueous solution at room temperature. [a]

Complex	Solvent	λ_{max} (ϵ, M^{-1} cm^{-1})	λ_{min} (ϵ, M^{-1} cm^{-1})
cis-$[PtCl_2(NH_3)_2]$ [b] [c]	0.9% NaCl	301(131)	246(27)
cis-$[PtCl(NH_3)_2(OH_2)]^+$	1 *M* $HClO_4$	263(113)	242(59)
cis-$[Pt(NH_3)_2(OH_2)_2]^{2+}$	1 *M* $HClO_4$	253(128)	231(79)
	pH = 2 [d]	~ 255(~ 145)	
cis-$[PtCl(OH)(NH_3)_2]$	0.1 *M* NaOH	267(150)	257(146)
cis-$[Pt(OH)_2(NH_3)_2]$	0.1 *M* NaOH[e]	320(27),304(34),295(45),270(100),245(490)	

[a]Isosbestic points associated with Equation 1.1 are 280(103) and 240(61) nm and those associated with Equation 1.2 are 267(111) and 235(84) nm at μ = 1.0 *M* (NaCl, $HClO_4$).
[b]Reference [137].
[c]There is a marked shoulder at about 280 nm in the UV spectrum of this complex (Figure 3.6).
[d]Extrapolated from Figure 1 of Reference [138].
[e]This complex has only a continuous absorbance, increasing with wavelength in the 350 to 230 nm region (Figure 3.1).

where A is the absorbance, ϵ is the molar absorptivity, c is the concentration and l is the path length of the cell (1.00 cm in this case). For an equilibrium mixture such as we have here, the absorbance obtained will be due to a combination of the species present in solution, that is

$$A_e(\lambda) = \epsilon_{DA}(\lambda)c_{DA} + \epsilon_{CA}(\lambda)c_{CA} \tag{3.5}$$

where $A_e(\lambda)$ is the absorbance of the equilibrium mixture at any wavelength (λ), $\epsilon_{DA}(\lambda)$ and $\epsilon_{CA}(\lambda)$ are the molar absorptivities of the *cis*-$[Pt(NH_3)_2(OH_2)_2]^{2+}$ and *cis*-$[PtCl(NH_3)_2(OH_2)]^{+}$ species respectively, at that wavelength. The equilibrium concentrations of the *cis*-$[Pt(NH_3)_2(OH_2)_2]^{2+}$ and *cis*-$[PtCl(NH_3)_2(OH_2)]^{+}$ species are represented respectively by c_{DA} and c_{CA}. Equation 3.5 combined with Equations 3.6 and 3.7

$$[Pt]_t = c_{DA} + c_{CA} \tag{3.6}$$

$$[Cl^-]_e = 2[Pt]_t - c_{CA} \tag{3.7}$$

are sufficient to calculate K_2 at any wavelength as

$$K_2 = \frac{c_{DA}[Cl^-]_e}{c_{CA}} \tag{3.8}$$

and the $A_e(\lambda)$, $\epsilon_{DA}(\lambda)$, $\epsilon_{CA}(\lambda)$ and $[Pt]_t$ are known. This method becomes unreliable in regions where $\epsilon_{DA}(\lambda) \sim \epsilon_{CA}(\lambda)$, that is, close to isosbestic points.

Pairs of $A_e(\lambda)$ data are required to calculate K_2, where $\epsilon_{DA}(\lambda)$ is approximately equal to $\epsilon_{CA}(\lambda)$ (Figure 3.6). Using Equation 3.5 as a basis, a pair of simultaneous equations is obtained.

$$A_e(\lambda 1) = \epsilon_{DA}(\lambda 1)c_{DA} + \epsilon_{CA}(\lambda 1)c_{CA} \tag{3.9}$$

$$A_e(\lambda 2) = \epsilon_{DA}(\lambda 2)c_{DA} + \epsilon_{CA}(\lambda 2)c_{CA} \tag{3.10}$$

Using the constraint that $\epsilon_{CA}(\lambda 1) = \epsilon_{CA}(\lambda 2)$, these simultaneous equations rearrange to give

$$A_e(\lambda 1) - A_e(\lambda 2) = [\epsilon_{DA}(\lambda 1) - \epsilon_{DA}(\lambda 2)]\, c_{DA} \tag{3.11}$$

or

$$c_{DA} = \frac{A_e(\lambda 1) - A_e(\lambda 2)}{\epsilon_{DA}(\lambda 1) - \epsilon_{DA}(\lambda 2)} \tag{3.12}$$

and since $A_e(\lambda 1)$, $A_e(\lambda 2)$, $\epsilon_{DA}(\lambda 1)$ and $\epsilon_{DA}(\lambda 2)$ are all known, c_{DA} can be calculated. Since $[Pt]_t$ is also known, Equation 3.6 can be used to calculate c_{CA} and then Equation 3.7 to calculate $[Cl^-]_e$. Thus values for c_{DA}, c_{CA} and $[Cl^-]_e$ can be inserted into

Table 3.7. Estimates of k_2, k_{-2} and K_2, the rate and equilibrium constants associated with the second step of the acid hydrolysis of *cis*-$[PtCl_2(NH_3)_2]$ (Equation 1.2) at 25.0 °C.

Solvent	k_{-2} (M^{-1} s^{-1})	k_2 (s^{-1})	K_2	Reference
H_2O		3.3×10^{-5}	4×10^{-5}	[78]
H_2O			1.11×10^{-4}	[112]
H_2O		2.5×10^{-5}		[139]
1.0 M $HClO_4$	9.1×10^{-2}	2.5×10^{-5}	2.7×10^{-4}	this research
?	8.9×10^{-2}			[130]

Table 3.8. Equilibrium concentrations (mM) of *cis*-$[PtCl(OH)(NH_3)_2]$, *cis*-$[Pt(NH_3)_2(OH_2)_2]^{2+}$ and Cl^- in aqueous $HClO_4$ at 25 °C using $K_2 = 2.7 \times 10^{-4}$.

Initial concentration (mM)	Equlibrium concentrations (mM)		
cis-$[PtCl(NH_3)_2(OH_2)]^+$	*cis*-$[PtCl(NH_3)_2(OH_2)]^+$		*cis*-$[Pt(NH_3)_2(OH_2)_2]^{2+}$ = Cl^-
100	95	(95) [a]	5
10	8.5	(85)	1.5
1	0.6	(60)	0.4
0.1	0.022	(22)	0.078
0.01	0.0003	(3)	0.0097

[a] Numbers in parentheses are the percentage of *cis*-$[PtCl(NH_3)_2(OH_2)]^+$ 'undissociated' at equilibrium.

Equation 3.8 to yield a value for K_2. This procedure using simultaneous equations is less reliant on the instrument zero.

Previous estimates of K_2 obtained in water [78,112] are similar to the values obtained for K_2, k_{-2} and k_2 from this work (Table 3.7). A value of $K_2 = 2.7 \times 10^{-4}$ ($\mu = 1.0$ M) for the equilibrium constant associated with Equation 1.2 puts considerable restraint on the extent to which the reaction proceeds. The data in Table 3.8 shows that a solution of 1.0×10^{-3} M *cis*-$[PtCl(NH_3)_2(OH_2)]^+$ will aquate only to the extent of about 40% completion before equilibrium is reached. In the presence of additional chloride ions, the extent of reaction will be even smaller. Accurate spectrophotometric measurement of k_2 could not be made despite being able to produce chloride ion free solutions of *cis*-$[PtCl(NH_3)_2(OH_2)]^+$ (Chapter 2) because of the small spectrophotometric changes associated with the incomplete chloride release in the reaction.

In principle, the spectrophotometric changes with time or the change in free chloride ion concentration with time data for the acidified *cis*-$[Pt(OH)_2(NH_3)_2]$ plus two free chloride ions, could be analysed using second-order equations for the reaction system [121], to give the anation rate constant (k_{-2}). It was preferred however, that k_{-2} be determined under pseudo-first-order conditions, by deliberate addition of extra chloride ions (the concentration of which was always greater than ten times that of the initial platinum(II) species concentration) on acidification of *cis*-$[Pt(OH)_2(NH_3)_2]$. Under these conditions the subsequent reaction proceeded in two steps (the reverse of

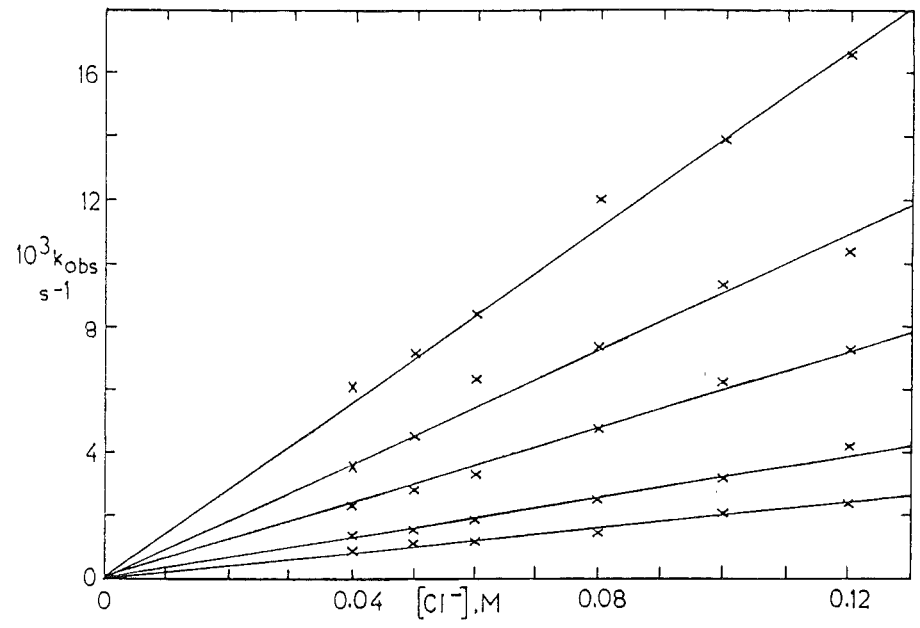

Figure 3.7. Plots of k_{obs} versus $[Cl^-]$ for the chloride anation reaction of *cis*-$[Pt(NH_3)_2(OH_2)_2]^{2+}$ (k_{-2}) (Equation 1.2), at temperatures (reading upwards) 10.5, 14.9, 19.7, 25.0 and 30.0 °C.

Equations 1.1 and 1.2) with *cis*-$[PtCl_2(NH_3)_2]$ being the final product at high chloride ion concentrations.

The rate constants of the first step of the reversal (k_{-2} in Equation 1.2) was determined spectrophotometrically by monitoring the reaction at the isosbestic points at 240 and 280 nm for the second step of the anation (the isosbestic points of the k_{-1} reaction, Figure 2.2). By monitoring the reaction at these points, any contribution to the absorbance data from the second reaction (k_{-1}) is removed. Values for k_{obs} (s^{-1}) (Table 3.9) were calculated from the absorbance versus time data at these wavelengths over a 20 K temperature range, and plots of k_{obs} versus $[Cl^-]$ were linear (Figure 3.7). From values of k_{obs}, using Equation 2.1, values of k_{-2} (M^{-1} s^{-1}) were calculated (Table 3.9). While this work was in progress, a value of $k_{-2} = 8.9 \times 10^{-2}$ M^{-1} s^{-1} at 25 °C was reported in the literature [130] but the ionic strength was unspecified. This literature value is in good agreement with the value of $k_{-2} = 9.1 \times 10^{-1}$ M^{-1} s^{-1} at 25 °C and $\mu = 1.0$ M, obtained from the work presented here.

Knowledge of values of K_2 and k_{-2} at the same temperature and ionic strength conditions means that an estimate of k_2, the rate constant associated with the forward reaction of Equation 1.2, can be made. Substitution of the known values of K_2 and k_{-2} into Equation 2.11 gives a value of $k_2 = 2.5 \times 10^{-5}$ s^{-1} at 25 °C, $\mu = 1.0$ M. This value agrees with one value of k_2 in the literature [139] and is the same order of magnitude as another reported value [78] (Table 3.7). In comparison with the value of $k_1 = 6.3 \times 10^{-5}$ s^{-1} at 25 °C (Chapter 2), it can be seen that k_2 is approximately

Table 3.9. Spectrophotometrically determined chloride anation rate constants (k_{-2}) for the anation reaction of *cis*-$[Pt(NH_3)_2(OH_2)_2]^{2+}$ (Equation 1.2) at $\mu = 1.0$ M ($HClO_4$).[a b c]

$[Cl^-]_i$ [d]	10.5 °C [283.7 K]		14.9 °C [288.1 K]		19.7 °C [293.0 K]	
	$10^3 \times k_{obs}$	$10^2 \times k_{-2}$ [e]	$10^3 \times k_{obs}$	$10^2 \times k_{-2}$ [e]	$10^3 \times k_{obs}$	$10^2 \times k_{-2}$ [e]
(M)	(s^{-1})	(M^{-1} s^{-1})	(s^{-1})	(M^{-1} s^{-1})	(s^{-1})	(M^{-1} s^{-1})
0.04	0.871±0.13	2.18±0.31	1.37±0.13	3.43±0.33	2.28±0.29	5.70±0.72
0.05	1.07±0.08	2.14±0.16	1.45±0.31	2.90±0.62	2.78±0.22	5.56±0.44
0.06	1.11±0.16	1.85±0.23	1.82±0.21	3.03±0.35	3.28±0.56	5.47±0.94
0.08	1.43±0.16	1.79±0.20	2.50±0.64	3.13±0.80	4.73±0.91	5.91±1.14
0.10	2.08±0.34	2.08±0.34	3.13±0.72	3.13±0.72	6.19±0.89	6.19±0.89
	Mean	2.00±0.16	Mean	3.18±0.23	Mean	5.82±0.29
	Calc. [f]	2.03	Calc. [f]	3.25	Calc. [f]	5.40

$[Cl^-]_i$ [d]	25.0 °C [298.2 K]		30.0 °C [303.2 K]	
	$10^3 \times k_{obs}$	$10^2 \times k_{-2}$ [e]	$10^3 \times k_{obs}$	$10^2 \times k_{-2}$ [e]
	(s^{-1})	(M^{-1} s^{-1})	(s^{-1})	(M^{-1} s^{-1})
0.04	3.57±0.45	8.93±1.15	6.14±0.46	15.4±1.15
0.05	4.50±0.30	9.00±0.60	7.17±1.02	14.3±2.04
0.06	6.34±0.22	10.6±0.37	8.46±1.19	14.1±1.99
0.08	7.33±0.91	9.16±1.14	12.1±1.78	15.1±2.22
0.10	9.34±1.32	9.34±1.32	13.9±0.89	13.9±0.89
	Mean	9.28±0.70	Mean	14.4±0.60
	Calc. [f]	9.09	Calc. [f]	14.3

[a] Reaction monitored at 240 and 280 nm as these are the isosbestic points for the k_{-1} reaction.
[b] The concentration of the *cis*-$[Pt(NH_3)_2(OH_2)_2]^{2+}$ is $\sim 1.6 \times 10^{-3}$ M.
[c] Ionic strength adjusted to 1.0 M using NaCl and $HClO_4$.
[d] Initial $[Cl^-]10\times \geq$ [Pt] initial.
[e] Calculated from Equation 3.1
[f] Calculated from the activation parameters: $E_a = 72.75 \pm 1.2$ kJ mol^{-1}, $\Delta S^{\neq} = -29.2 \pm 2.4$ J K^{-1} mol^{-1} and $\log PZ = 11.7034$, *i.e.* $k_{-2} = 5.051 \times 10^{11} \exp\left(-72.7 \times 10^3/RT\right)$.

Table 3.10. Rate data for the loss of the first chloro ligand in the acid hydrolysis of some chloroammineplatinum(II) complexes at 25 °C.

Complex	Solvent	$10^5 \times k$ (s^{-1})	Reference
$PtCl_4^{2-}$	H_2O	3.9	[36]
$PtCl_3(NH_3)^-$ [a]	H_2O	5.6	[36]
cis-$[PtCl_2(NH_3)_2]$	H_2O	2.5	[36]
	1 *M* $HClO_4$	6.3	Chapter 2
trans-$[PtCl_2(NH_3)_2]$	H_2O	9.8	[36]
$PtCl(NH_3)_3^+$	H_2O	2.6	[36]
cis-$[PtCl(NH_3)_2(OH_2)]^+$	1 *M* $HClO_4$	2.5	This Chapter
$PtCl_2(en)$	H_2O	3.4	[140]
$PtCl(en)(OH_2)^+$	H_2O	4.4	[140]

[a] Replacement of *cis* chloro ligand.

two and a half times smaller than k_1, the rate constant associated with the forward reaction of Equation 1.1.

The variation of acid hydrolysis rate with charge is quite marked with cobalt(III) and chromium(III) complexes, for example, the rate constants for the loss of the first chloro ligand from $cis-[CoCl(en)_2(NH_3)]^{2+}$ and $cis-[CoCl_2(en)_2]^+$ are, respectively, 6.7×10^{-6} s^{-1} and 2.5×10^{-4} s^{-1}, at 25 °C and pH = 1 [37]. However this is not the case for platinum(II) complexes (Table 3.10), where the rate constants for some platinum(II) complexes having different charges are shown. In this series of complexes, the charges on the reactant platinum(II) complexes go from -2 to +1 and yet the rate constants change by only a factor of about three, which is quite a small effect. The breaking of a Pt–Cl bond should become more difficult as the charge on the complex becomes more positive, however, the formation of a new bond should become more favourable. The small effect of charge of the complex on the reaction rate suggests that both bond making and bond breaking are important, as is characteristic in an Ia process [134]. Thus, this lack of variation between rate constant and charge is used as evidence for an associative mechanism operating in the aquation reactions of platinum(II) systems [36,37,125].

3.4 Conclusions.

The rate and equilibrium data for the *cis*-$[PtCl_2(NH_3)_2]$ system and its hydrolysis products are summarised in Figure 3.4. This reaction scheme would be complete if the equilibrium constant K_3 for the reaction of *cis*-$[PtCl(OH)(NH_3)_2]$ to give *cis*-$[Pt(OH)(NH_3)_2(OH_2)]^+$ plus chloride ions was known. Later on in this thesis this question is addressed (Chapter 5).

An important feature to note from this work is that although the rate constants k_1

(Chapter 2) and k_2 have similar values (same order of magnitude), the acid hydrolysis of *cis*-DDP is unlikely to proceed beyond *cis*-$[PtCl(NH_3)_2(OH_2)]^+$. The presence of released background chloride ions and a small value of K_2 means that appreciable amounts of the *cis*-$[Pt(NH_3)_2(OH_2)_2]^{2+}$ species cannot be formed. In the absence of background chloride ions, the acid hydrolysis of 1×10^{-3} *M* *cis*-$[PtCl(NH_3)_2(OH_2)]^+$ will only proceed to about 40% completion (Table 3.8).

The situation is quite different for the base hydrolysis of *cis*-DDP since there is no competing equilibrium, so complete chloride release occurs even in the presence of excess chloride ions, and *cis*-$[Pt(OH)_2(NH_3)_2]$ is the stable end product.

At this stage the hydrolysis product responsible for the antitumour activity of *cis*-DDP *in vivo* cannot conclusively be identified. The most abundant hydrolysis product *in vivo* may not be the most reactive and there is also the possibility of 'substrate milking' of the equilibrium systems shown in Figure 3.4 to complicate things further. This 'substrate milking' could drive the reaction to completion via an hydrolysis product present in only very small concentrations.

Base hydrolysis of *cis*-DDP in blood plasma, which has a pH of 7.4 [91], could be a real possibility. The equilibrium end products would then be approximately 50% *cis*-$[Pt(OH)_2(NH_3)_2]$ and 50% *cis*-$[PtCl(OH)(NH_3)_2]$. Therefore, currently accepted mechanisms of action of *cis*-DDP *in vivo*, where *cis*-DDP remains unchanged in blood plasma due to high chloride ion concentration preventing hydrolysis, could well be invalid if the pH is high enough to allow base hydrolysis to occur. Experiments designed to probe these aspects of the hydrolysis reaction are described in Chapter 4.

CHAPTER 4

HYDROLYSIS KINETICS AT PHYSIOLOGICAL pH.

4.1 Introduction.

The hydrolysis kinetics of *cis*-DDP have been measured in both acidic (Equations 1.1 and 1.2 and Chapter 2) and basic media (Equations 3.2 and 3.3, Chapter 3), that is, at both extremes of the pH scale.

In acidic solution an equilibrium is established (Equation 1.1), but because of the small equilibrium constant, K_2, associated with Equation 1.2, the reaction does not proceed further to Equation 1.2 to produce significant amounts of *cis*-$[Pt(NH_3)_2(OH_2)_2]^{2+}$. Another important feature is that the extent of acid hydrolysis in Equations 1.1 and 1.2 is dependent on the amount of chloride ion present. In basic solution however, irreversible hydrolysis occurs (Equations 3.2 and 3.3) and both chloro ligands are lost. Base hydrolysis also proceeds to completion independent of the chloride ion concentration present (Chapter 3).

However, what happens in between these two extremes of pH, and when, was unknown so it was decided to investigate the pH - rate profile of *cis*-DDP in between the extremes, that is, in the pH range 4 to 9. Initially buffers were looked at as a means of controlling pH but due to interactions of the buffers with the platinum(II) hydrolysis products, the use of a pH-stat in combination with the UV - visible spectrophotometer was considered to be a more useful technique.

4.2 Experimental.

4.2.1 Measurements of Rate Constants at Constant pH.

A total of 50 mg of solid *cis*-DDP was dissolved in approximately 5 ml of dimethylformamide (DMF) solvent, and this solution was added to 70 ml of 0.2 *M* $NaClO_4$ ($NaClO_4$; NaCl, μ = 0.2 *M* when studies on the effect of chloride ions on rate were carried out). The $NaClO_4$ solution was placed in the temperature controlled (45.0 ± 0.1 °C) reaction vessel of the Radiometer pH-stat (TTTlc) (coupled to a Radiometer Titrigraph (SBR2)), a double walled glass vessel thermostatically controlled by circulating water from a water bath containing a pump/heater unit and a refrigeration unit, and

the solution was peristaltically pumped (100 ml per minute) through a 2.00 cm quartz, flow-through spectrophotometer cell in the cell compartment of the Varian spectrophotometer. The glass (G202c) and calomel (TS-1) electrodes were standardised with 0.01 *M* disodium tetraborate ('borax'), $Na_2B_4O_7.10H_2O$ (at T = 45 °C, the pH of 0.01 *M* borax solution is 9.038).

The electrodes were placed in the reactant solution and the pH adjusted to just above the set pH by the addition of dilute acid or base. As the hydrolysis proceeded, above pH = 5, the pH dropped and when the set pH was reached, the pH-stat system was activated by the automatic addition of 0.05 *M* NaOH solution from a syringe through a stainless steel needle. When constant pH was satisfactorily maintained, the repeat scan/fixed wavelength modes of the spectrophotometer were activated to monitor the absorbance changes with time associated with the subsequent reactions. The experimental set-up used is shown schematically in Figure 4.1.

The concentrations of the solutions used were such that 6.66 ml of 0.05 *M* NaOH was required if two moles of hydroxide ions were used per mole of platinum(II). Thus, the proportion of NaOH uptake and the rate of change in absorbance with time were measured simultaneously. Preliminary control experiments showed that the system behaved identically if the DMF was not present.

When each kinetic run was completed, 0.877 g of solid NaCl was added to the reaction solution to give a chloride ion concentration of 0.2 *M*. The solid NaCl dissolved quickly in the solution as the reaction vessel contained a magnetic flea and was positioned on top of a magnetic stirrer. The repeat scan function of the spectrophotometer was then reactivated and the absorbance changes associated with the subsequent reaction were recorded. Constant pH was maintained by the periodic, manual addition of 0.1 *M* $HClO_4$. Under these conditions, any aquo ligands coordinated to the platinum(II) were rapidly replaced by the chloride ions. The results are summarised in Table 4.1.

4.2.2 Use of the pH-stat.

The chart recorder is set up first with the pen returned to the zero line on the chart paper. The cable to the automatic titrator (which operates the syringe containing the NaOH solution) itself is uncoupled and then the chart recorder is switched off. Preparation of the reaction vessel first involves standardisation of the pH meter of the pH-stat using the 0.01 *M* borax solution at the temperature that the reaction will be carried out at. After standardisation, the electrodes and reaction vessel are washed with distilled water.

The required volume of solution is placed in the reaction vessel and left to equilibrate at the desired temperature. The magnetic flea and electrodes are then placed in the reaction vessel and the magnetic stirrer switched on. The pH meter of the pH-stat is

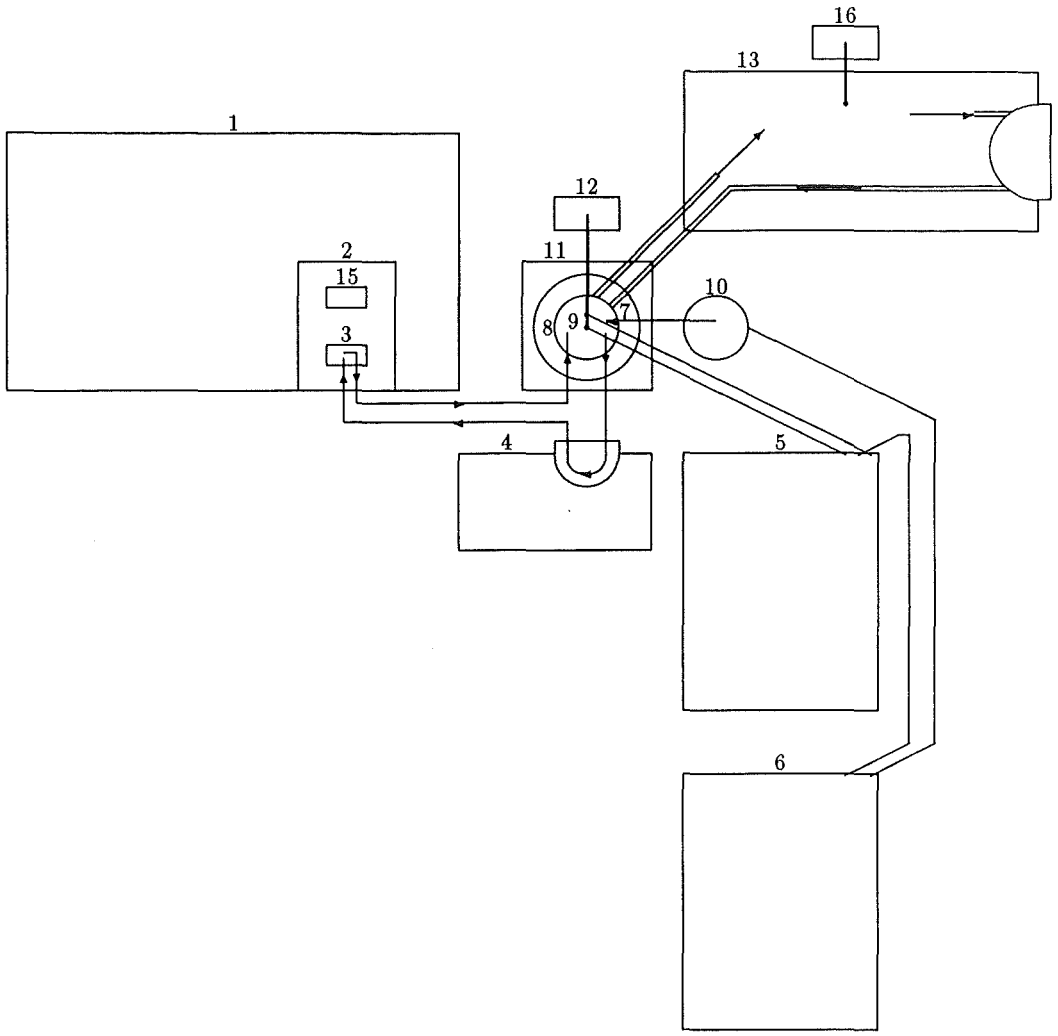

Key	
1	Varian DMS 100 spectrophotometer.
2	Cell compartment.
3	2.00 cm quartz flow-through sample cell.
4	Peristaltic pump.
5	pH-stat.
6	pH-stat chart recorder.
7	Needle (from syringe via plastic tubing).
8	Jacketed glass reaction vessel.
9	Calomel and glass electrodes.
10	Stand holding syringe containing 0.05 *M* NaOH reservoir.
11	Magnetic stirrer.
12	Retort stand holding electrodes.
13	Water bath at 45 °C.
14	Temperature control pump.
15	2.00 cm quartz reference cell.
16	Retort stand holding thermometer.
	All lines shown with arrows are plastic tubing through which the solution flows.
	Double lines are water tubing.
	Single lines are electrical wiring.

Figure 4.1. Equipment layout for the spectrophotometer – pH-stat combination.

switched to 'read'. The syringe, tubing and needle are filled with the NaOH solution using the three-way tap and burette drive. All air bubbles in the system should be eliminated. The three-way tap is then closed to allow the NaOH solution into the needle. Some NaOH solution is added to the reaction vessel manually until the set pH is reached. The cable from the chart recorder to the automatic titrator's burette drive is then reconnected.

On the pH meter, the proportional band is switched to the left-hand side approximately 0.2 units and the pH meter is switched to 'upscale'. The reagent is then added to the reaction vessel. At the first 'click' of the pH-stat, the chart-recorder is switched on and then the repeat scan mode of the spectrophotometer is activated for the simultaneous recording of UV spectra. The pH-stat should be clicking steadily with hydroxide ion addition occurring regularly. As the reaction slows, the amount of NaOH added at each click is decreased by increasing the proportional band switch.

4.2.3 Use of Buffers to Control pH.

Buffer solutions of concentration 0.1 M were prepared, using the buffers MES (pH = 6.2), HEPES (pH = 8.0, 7.4, 7.2), BICINE (pH = 8.0, 7.4) and TRIS (pH = 6.4, 6.9, 7.4, 7.9 and 8.4). The ionic strength (μ = 0.1 M) was controlled by the addition of either $NaClO_4$ or NaCl or, in the case of HEPES, varying amounts of both (but μ = 0.1 M). For TRIS, the final concentration of buffer was 0.05 M with $HClO_4$ or HCl added to obtain the desired pH, and the ionic strength was uncontrolled.

Approximately 2.5 to 3 ml of buffer solution was placed in 1.00 cm quartz sample and reference cells and left to thermally equilibrate in the jacketed, heated cell-holder inside the cell compartment of the spectrophotometer. A small amount of solid *cis*-DDP ($\sim$ 3 mg) was added to the sample cell and, on dissolution, the repeat scan mode of the spectrophotometer was activated to monitor the subsequent reaction.

In order to check whether the buffer had coordinated to the hydrolysis products, on completion of a kinetic run, the contents of the sample cell were acidified with approximately one ml of 6 M HCl. The spectral changes due to the subsequent reaction were also monitored using the repeat scan mode of the spectrophotometer.

4.3 Results and Discussion.

The generally accepted model for the interaction of *cis*-DDP with the target DNA molecule *in vivo*, is based on rate constant, equilibrium constant and hydrolysis data obtained in the pH region 0 to 6.5 (Chapter 2) [30,78,98,99,100,101,102,103,104,105,106] [107,108,109,110,111,112,113,116]. This mechanism is dominated also by the chloride ion dependent equilibria inherent in Equations 1.1 and 1.2.

The model is as follows [30]. The *cis*-DDP, stabilised in saline solution, enters

the blood stream while high hydration therapy is proceeding (Chapter 1) [23,24]. The relatively high chloride ion concentration in blood plasma ($\sim$ 103 mM [48,92,97]) prevents loss of the chloride ligands in hydrolysis and the neutral *cis*-DDP molecule passes through the cell wall. Once inside the cell, hydrolysis proceeds according to Equation 1.1 since the background chloride ion concentration inside the cell is only $\sim$ 4 mM [97]. The species *cis*-$[PtCl(NH_3)_2(OH_2)]^+$ is thought to be the most likely labile complex for donor groups in the DNA target molecule, but many workers investigating these systems have used *cis*-$[Pt(NH_3)_2(OH_2)_2]^{2+}$ as the labile platinum(II) species [103,111,128,139,141,142,143,144,145,146]. However, there is also recent evidence for direct attack on the *cis*-DDP itself by guanosine 5'-monophosphate (GMP) [147] although such changes had been observed previously and interpreted differently [111].

Fewer studies had been made on the base hydrolysis of *cis*-DDP at pH greater than 9. Under these conditions both chloride ligands are irreversibly lost (Chapter 3, Equations 3.2 and 3.3) [98,100,108,113], and the rate was found to be independent of the background chloride ion concentration, the hydroxide ion concentration or the ionic strength (Chapter 3). If base hydrolysis of *cis*-DDP occurred at the physiological pH of 7.4 (the pH of blood plasma [91]), then the entirely different mechanism for the *cis*-DDP – DNA interaction proposed in Chapter 3 could occur. Evidence for this alternative model requires measurements of the rates and extent of hydrolysis in the pH region 4.5 to 8.5, both in the presence and absence of added chloride ions. This sort of work had not been attempted prior to this thesis, and was not a trivial exercise as there were a number of complicating features.

The use of buffers is the conventional technique for controlling pH in the region 6.5 to 8.0 [91], but many buffers contain nitrogen, sulphur or oxygen groups and these are potential donor atoms for the platinum(II) centre. If the buffer compounds are acting as nucleophiles [90], they could be markedly affecting the reaction kinetics [102,103] and the buffer substrate will be coordinated to the platinum(II) at the end of the reaction.

From the work with buffers it was found that reversing the hydrolysis reaction carried out in the buffers with 6 M HCl, all the buffers used, especially TRIS, had some sort of interaction with the platinum(II) hydrolysis products present. In retrospect it is thought that the addition of NaCl to the system to anate any *cis*-$[PtCl(NH_3)_2(OH_2)]^+$ or *cis*-$[Pt(NH_3)_2(OH_2)_2]^{2+}$ species present back to the *cis*-$[PtCl_2(NH_3)_2]$ would have been preferable. As *cis*-$[PtCl(NH_3)_2(OH_2)]^+$ is removed from the equilibrium system to give *cis*-$[PtCl_2(NH_3)_2]$, the equilibrium shifts from the *cis*-$[PtCl(OH)(NH_3)_2]$ to the *cis*-$[PtCl(NH_3)_2(OH_2)]^+$ to give more of the *cis*-$[PtCl(NH_3)_2(OH_2)]^+$. Also present could be the species platinum(II)Cl-Nu where Nu is the buffer nucleophile species present.

Using such a high hydrogen ion concentration as was used here leads to uncertainties in what could be happening. For example, any stable hydroxo species of platinum(II)

would be protonated and could thus react with the chloride ions present, but also the platinum(II)Cl-Nu species, if present, could be broken apart. However, from this work there was enough evidence to suggest that the buffer nucleophiles did bind to some platinum(II) hydrolysis products. In the case of TRIS, addition of 6 *M* HCl showed that the TRIS was binding to the platinum(II) species as the reversed reaction did not completely give *cis*-DDP as a final product.

The reverse reactions in HEPES and MES buffers gave an initial spectrum showing some *cis*-DDP present initially but the subsequent repeat scan spectra showed a slow accumulation of *cis*-DDP, indicating that something, most likely the platinum(II)Cl-Nu species, was slowly releasing an aquo species, most likely *cis*-$[PtCl(NH_3)_2(OH_2)]^+$, which was then reacting with the chloride ions present to give the *cis*-DDP. The forward reaction that took place in the BICINE buffer system was not reversed as this was not thought to be worthwhile since the forward reaction had a very untidy set of repeat scan UV spectra associated with it. Thus the results indicated that the buffer systems tried were interacting with the platinum(II) products (Equation 4.1).

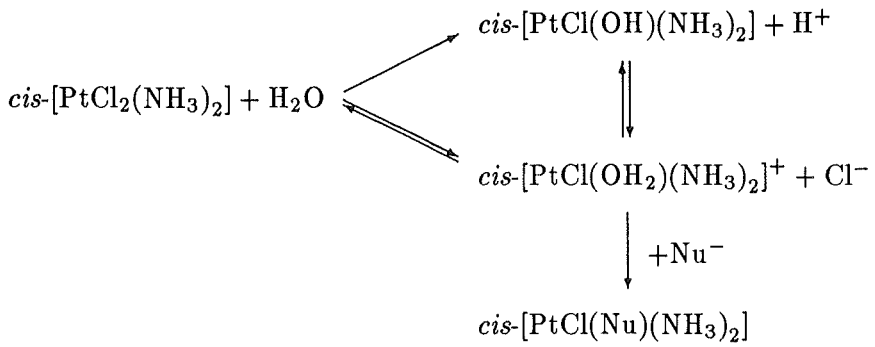

(4.1)

A method of controlling the pH of a reaction proceeding with a pH change, that does not involve the use of buffers is to use a pH-stat [148,149]. For reactions proceeding with consumption of hydroxide ions it is an excellent technique because the hydroxide ion is the only nucleophile present apart from the electrolytes added to control the ionic strength of the system. Thus the pH-stat measures hydroxide ion uptake with time. However, there are disadvantages to using a pH-stat. Firstly, the set pH must be greater than the pK_a for the hydroxo/aquo equilibrium of the product [118,150]. If the set pH is close to the pK_a of the coordinated water molecule (for example, $pK_a = 5.93$ [151]), the hydroxide ion uptake will cease due to the acid - base properties of the coordinated hydroxide ion. Secondly, the conversion of pH to hydroxide ion concentration is subject to the inclusion of non-specific parameters, for example, Na^+ corrections [118], and finally, the only measureable parameter is the rate of hydroxide ion uptake and consequently the nature of the products can be misinterpreted. This latter disadvantage can be overcome to a considerable extent by simultaneously recording the changes in absorption spectra while maintaining a constant pH [152,153]. Thus this combination

of techniques gives both the absorption changes and the extent of hydroxide ion uptake with time, at the same time, under non-buffered, constant pH conditions and was the method employed for this work.

Another problem was one of product identification. The hydrolysis products of *cis*-DDP are known to form $[Pt(NH_3)_2(OH)]_2^{2+}$, the dimer [79] and $[Pt(NH_3)_2(OH)]_3^{3+}$, the trimer [81,83]. Suggestions have been made that these oligomers are responsible for the toxic properties of *cis*-DDP [154,155]. The absorption spectra of these oligomers have been reported [88,89] but the data are not in agreement, possibly due to a typographical error in the literature, and definitive spectral information is not readily available (apart from ^{195}Pt NMR data [87,97,156]). Some values for the molar absorptivities for these hydroxo species of *cis*-DDP have been reported. For *cis*-$[Pt(OH)_2(NH_3)_2]$, $\epsilon_{330} \approx 25\ M^{-1}\ cm^{-1}$ (Chapter 3); for *cis*-$[Pt(OH)(NH_3)_2(OH_2)]^+$, $\epsilon_{330} \approx 48\ M^{-1}\ cm^{-1}$ [88]; for *cis*-$[Pt(OH)(NH_3)_2]_2^{2+}$, $\epsilon_{330} \approx 75\ M^{-1}\ cm^{-1}$ [89] and for *cis*-$[Pt(OH)(NH_3)_2]_3^{3+}$, $\epsilon_{330} \approx 150\ M^{-1}\ cm^{-1}$ [89] or $14\ M^{-1}\ cm^{-1}$ [88] (possible typographical error here).

However, polymers of this type are more likely to be formed in concentrated solution as the rate of formation is proportional to the square of the monomer concentration [97]. From the work presented here, no evidence was found to show that species with high molar absorptivity coefficients (ϵ_{330}) were present in these studies using the pH-stat and spectrophotometer, and the product formed from *cis*-DDP in alkali (*cis*-$[Pt(OH)_2(NH_3)_2]$ in 0.01 M NaOH Chapter 3) passed quantitatively through a cation exchange column in the Na^+ form, as expected for an uncharged species.

Spectral changes reported for *cis*-$[Pt(NH_3)_2(OH_2)_2]^{2+}$ in the region pH = 4 to 5, in the presence of buffers have previously been attributed to formation of the dimer *cis*-$[Pt(OH)(NH_3)_2]_2^{2+}$. However, the observed rate constants were independent of pH and any changes in rate with change in the buffer medium were attributed to ionic strength differences [89], as the reaction of *cis*-$[Pt(NH_3)_2(OH_2)_2]^{2+}$ plus buffer nucleophile was not considered to be a kinetically important event [90]. Therefore the belief that the observed spectral changes are entirely due to dimer or trimer formation lacks conviction. An interesting observation that has been made is that the dimer and trimer are unstable, lasting only a few hours at room temperature in the presence of chloride ion concentrations of 0.15 to 0.4 M, producing *cis*-$[PtCl_2(NH_3)_2]$ and *cis*-$[PtCl(NH_3)_2(OH_2)]^+$ [87]. From the investigations presented here, there was no evidence for the production of oligomers of the *cis*-$[Pt(OH)_2(NH_3)_2]$ species under the experimental conditions used.

The hydrolysis of *cis*-DDP at constant, unbuffered pH proceeded with hydroxide ion uptake which increased as the fixed pH was increased. At pH = 4, there was virtually no uptake of hydroxide ions and the spectrophotometric scans and observed rate constants indicated that the reaction was normal acid hydrolysis (Chapter 2). As the fixed pH was increased, the amount of hydroxide ions consumed also increased

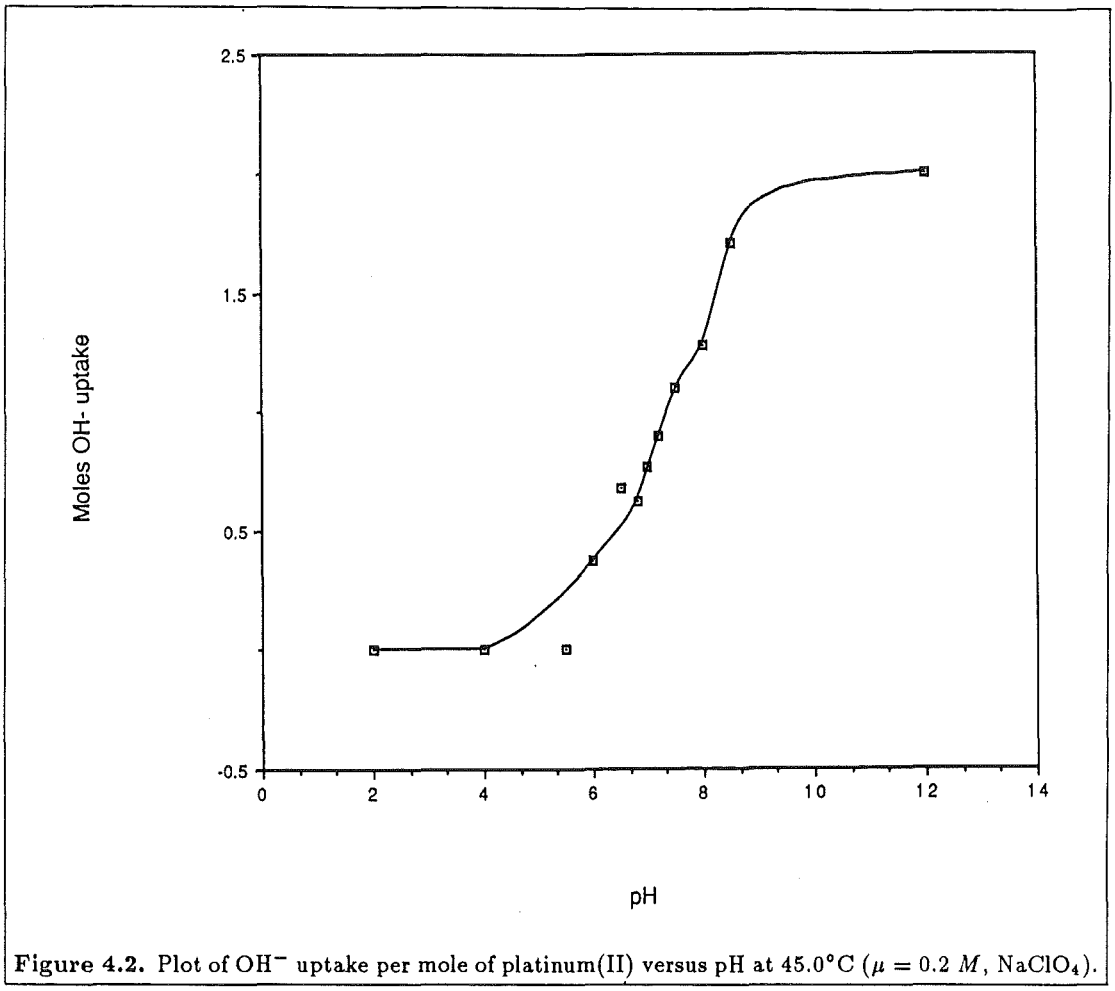

Figure 4.2. Plot of OH^- uptake per mole of platinum(II) versus pH at 45.0°C (μ = 0.2 M, $NaClO_4$).

(Table 4.1, Figure 4.2) and there was a gradual decrease in the rate of hydrolysis (Figure 4.3), an observation which is consistent with going from predominantly acid hydrolysis (Chapter 2) to predominantly base hydrolysis (Chapter 3). At pH = 6.55, 0.5 moles of hydroxide ions were consumed, corresponding to the equilibrium system shown in Equation 4.2.

$$\textit{cis}\text{-}[PtCl_2(NH_3)_2] + H_2O \rightleftharpoons \begin{array}{l} \textit{cis}\text{-}[PtCl(OH)(NH_3)_2] + H^+ \\ \Updownarrow \; pK_a = 6.85 \; [151] \\ \textit{cis}\text{-}[PtCl(NH_3)_2(OH_2)]^+ + Cl^- \end{array} \qquad (4.2)$$

At pH = 8.0, 1.5 moles of hydroxide ions were consumed as the new equilibrium system (Equation 4.3) was established.

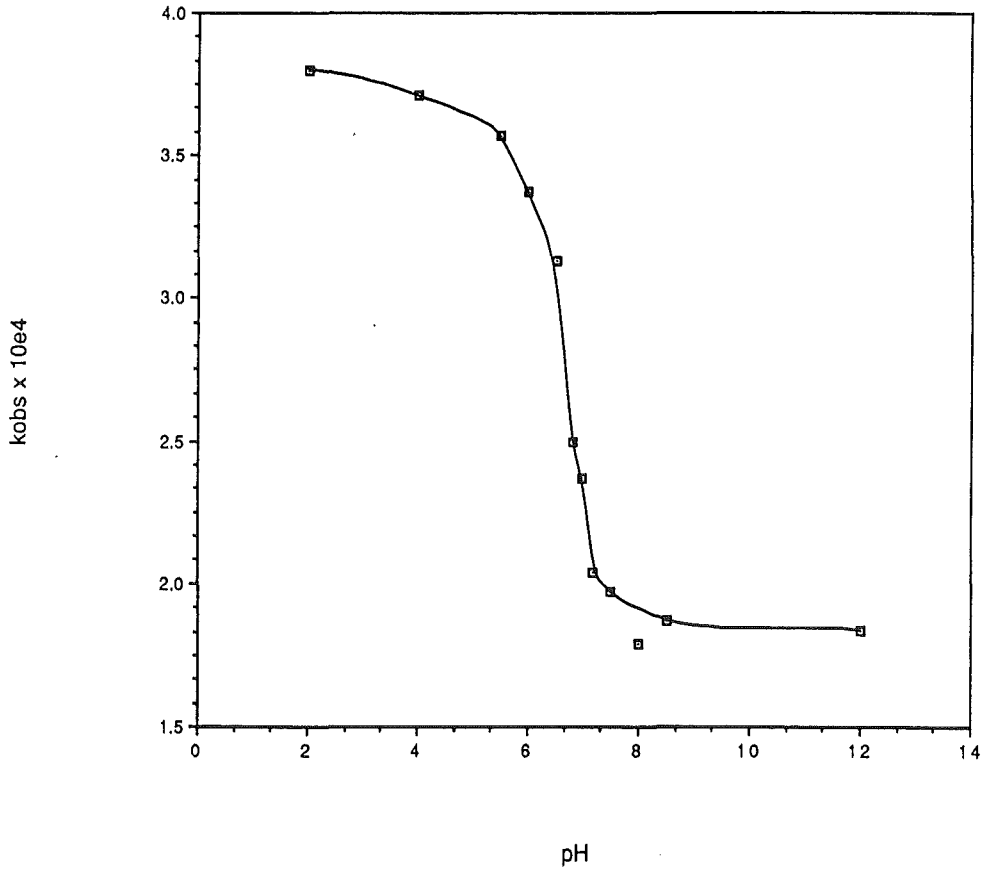

Figure 4.3. Plot of k_{obs} versus pH at 45.0°C ($\mu = 0.2\ M$, $NaClO_4$).

Table 4.1. Spectrophotometrically determined rate data and chloride ion uptake data for the hydrolysis reactions of *cis*-$[PtCl_2(NH_3)_2]$ at various fixed pH in unbuffered media (μ = 0.2 *M*, $NaClO_4$; T = 45.0 °C).

Set pH	$[OH^-]$ uptake (mole/mole Pt(II))	$10^4 \times k_{obs}$ [a] (s^{-1})	Isosbestic points (nm)	Chloride ion uptake [b] $10^4 \times k_{Cl}$ (s^{-1})	Isosbestic points (nm) [c]
2.00	0.00	3.80±0.35	282	[d]	[d]
4.0	0.00	3.71±0.25	283	83.5±4	[d]
5.5	0.00	3.57±0.44	277 then 289	68.2±6	281 then 289
6.0	0.37	3.37±0.33	277 then 285	45.5±3	277 then 287
6.5	0.68	3.13±0.17	274 then 284	15.9±2	274 then 284
6.8	0.62	2.50±0.19	272 then 280	12.9±0.6	273 then 285
7.0	0.77	2.37±0.11	271 then 279	10.9±0.7	272 then 285
7.2	0.90	2.04±0.25	277	9.43±0.5	273
7.5	1.10	1.97±0.15	276	7.67±0.4	271
8.0	1.28	1.79±0.16	276	5.48±0.4	270
8.5	1.71	1.87±0.25	276	4.06±0.4	273
12.0	2.0	1.84	276	no reaction	

[a] Observed first-order rate constants for the overall forward reaction.
[b] The final $[Cl^-]$ = 0.2 *M* and k_{Cl} is proportional to the total *cis*-$[PtCl(NH_3)_2(OH_2)]^+$ or *cis*-$[Pt(OH)(NH_3)_2(OH_2)]^+$ concentration.
[c] For the chloride ion anation reaction.
[d] The reaction was too fast to obtain these accurately.

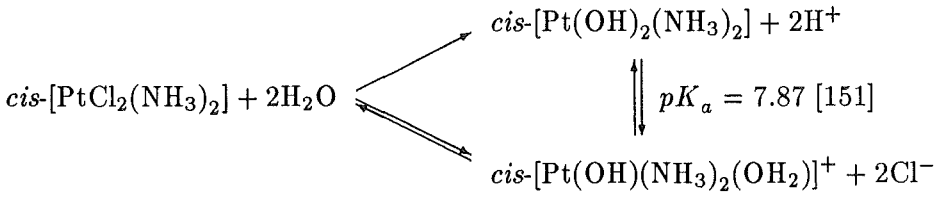

(4.3)

At any pH greater than 9, complete base hydrolysis took place and two moles of hydroxide ions were consumed per mole of *cis*-DDP (Equations 3.2 and 3.3). Once the hydrolysis reaction was complete, the extent of chloride uptake at any fixed pH depended on the amount of *cis*-$[PtCl(NH_3)_2(OH_2)]^+$ or *cis*-$[Pt(OH)(NH_3)_2(OH_2)]^+$ present. As a result the pattern observed was the reverse of the hydroxide ion uptake, although the amount of acid uptake was not quantitatively established. At any pH greater than 8, no chloride ion uptake was observed but rapid and extensive chloride anation took place at pH 4 to 5. Between the two extremes, the pH increased as chloride ion uptake proceeded (the reverse of Equations 4.2 and 4.3) and the reaction stopped prematurely unless constant pH was maintained by the manual addition of acid.

The reaction was predominantly acid hydrolysis and hence monophasic at approximately pH = 5 and below. As the forward reaction at fixed pH in the range 4 to 8.5 proceeded, the spectrophotometric changes indicated that, as the pH increased, the originally monophasic reaction became biphasic, that is, there were two first order

reactions occurring and this was noticeable mainly between pH = 5 to 7. At pH = 7.2 and above, the reaction then reverted again to a monophasic system as the reaction occurring then was predominantly base hydrolysis. As the set pH was changed (increased) under biphasic conditions, the positions of the isosbestic points for the two reactions also changed (Table 4.1). Where the forward reaction was biphasic, the addition of chloride ions to the system also resulted in a biphasic system with the generated isosbestic points mirroring the hydrolysis reaction.

Hydrolysis of *cis*-DDP gave *cis*-$[PtCl(OH)(NH_3)_2]$ and *cis*-$[PtCl(NH_3)_2(OH_2)]^+$ in a fixed ratio and with a fixed isosbestic point at set pH values of 5.5 to 7.2. The ratio obtained depends on the K_a for the *cis*-$[PtCl(NH_3)_2(OH_2)]^+$ – *cis*-$[PtCl(OH)(NH_3)_2]$ equilibrium (pK_a = 6.85 at 25 °C [151]) and the set pH. The position of the isosbestic point for the reaction also depends on this ratio. The *cis*-$[PtCl(NH_3)_2(OH_2)]^+$ does not hydrolyse spontaneously due to the unfavourable chloride ion dependent equilibrium (Chapter 3) but the *cis*-$[PtCl(OH)(NH_3)_2]$ can hydrolyse independent of the chloride ion concentration present, at a rate about five times slower than that of the first hydrolysis step (Chapter 3). Reduction of the *cis*-$[PtCl(OH)(NH_3)_2]$ concentration by hydrolysis to *cis*-$[Pt(OH)(NH_3)_2(OH_2)]^+$ results in a reduction in the concentration of the *cis*-$[PtCl(NH_3)_2(OH_2)]^+$ as the equilibrium ratio must be maintained at a value determined by the set pH.

Eventually, an equilibrium is established with the *cis*-$[Pt(OH)(NH_3)_2(OH_2)]^+$ and the released chloride ion and further chloride ion release from *cis*-$[PtCl(OH)(NH_3)_2]$ ceases. It is this second step (chloride ion release from *cis*-$[PtCl(OH)(NH_3)_2]$) that maintains the second isosbestic point. Thus the final solution contains a mixture of *cis*-$[PtCl(NH_3)_2(OH_2)]^+$, *cis*-$[PtCl(OH)(NH_3)_2]$, *cis*-$[Pt(OH)(NH_3)_2(OH_2)]^+$ and Cl^- ions with the concentration of the *cis*-$[PtCl(NH_3)_2(OH_2)]^+$ becoming smaller as the set pH is increased. Addition of chloride ions to this system results in the anation of any platinum(II) aquo species present, reversing the hydrolysis step and producing a final mixture of *cis*-$[PtCl_2(NH_3)_2]$ and *cis*-$[PtCl(OH)(NH_3)_2]$.

The *cis*-$[Pt(OH)(NH_3)_2(OH_2)]^+$ – *cis*-$[Pt(OH)_2(NH_3)_2]$ equilibrium became dominant when the set pH was further increased to the range 7.2 to 8.5 (pK_a = 7.87 at 5 °C [151]) and the rate of reaction slowed down. In this region, the rate is controlled by chloride ion release from the *cis*-$[PtCl(OH)(NH_3)_2]$, which is the slowest step, to give an equilibrium mixture of *cis*-$[PtCl(OH)(NH_3)_2]$, *cis*-$[Pt(OH)(NH_3)_2(OH_2)]^+$ and *cis*-$[Pt(OH)_2(NH_3)_2]$, with the proportion of *cis*-$[Pt(OH)_2(NH_3)_2]$ increasing with the increasing set pH. Addition of chloride ions to this system again resulted in the anation of any platinum(II) aquo species present and as these were dominated by the *cis*-$[Pt(OH)(NH_3)_2(OH_2)]^+$, the final mixture contained *cis*-$[PtCl(OH)(NH_3)_2]$ and *cis*-$[Pt(OH)_2(NH_3)_2]$. The amount of *cis*-$[Pt(OH)(NH_3)_2(OH_2)]^+$ in the final mixture decreased as the set pH was increased further, and hence the extent of chloride ion

Table 4.2. Spectrophotometrically determined rate data and chloride ion uptake data for the hydrolysis reaction of *cis*-$[PtCl_2(NH_3)_2]$ at pH = 7.4 with variable chloride ion concentration (μ = 0.2 *M*, $NaClO_4$, NaCl; T = 45 °C, $[cis\text{-}[PtCl_2(NH_3)_2]]$ = 2.2 m*M*).

$[Cl^-]_i$ (*M*)	OH^- uptake (mole/mole Pt(II))		$10^4 \times k_{obs}$ [a] (s^{-1})		Cl^- uptake [b] $10^4 \times k_{Cl}$ (s^{-1})	
	obs.	calc. [c]	obs.	calc. [d]	obs.	calc. [e]
0.00	1.10	1.08	1.97±0.15	1.97	7.95±0.4	7.95
0.010	0.68	1.00	2.12±0.10	2.15	7.47±0.4	7.65
0.025	0.71	0.90	2.48±0.12	2.43	6.16±0.4	7.20
0.050	0.75	0.72	2.61±0.19	2.90	7.04±1	6.44
0.075	0.38	0.53	3.32±0.59	3.34	5.86±1	5.68
0.100	0.35	0.35	4.23±0.88	3.80	4.93±0.3	4.93

[a] First-order rate constants for the overall forward reaction.
[b] Final $[Cl^-]$ = 0.2 *M*. The rate is proportional to the amount of *cis*-$[PtCl(NH_3)_2(OH_2)]^+$ at equilibrium after the completion of the forward reaction.
[c] Calculated from the linear relationship: mole OH^- uptake/mole Pt(II) = 1.08 - 7.3$[Cl^-]_i$ (T = 45.0 °C, pH = 7.4, μ = 0.2 *M*).
[d] Calculated from the linear relationship: $10^4 \times k_{obs} = 18.3[Cl^-]_i + 1.97$ (T = 45.0 °C, pH = 7.4, μ = 0.2 *M*).
[e] Calculated from the linear relationship: $10^4 \times k_{Cl} = 7.95 - 30.2[Cl^-]_i$ (T = 45.0 °C, pH = 7.4, $[Cl^-]$ = 0.2 *M*, μ = 0.2 to 0.3 *M*).

uptake also decreased.

A series of kinetic runs were performed using combination of the pH-stat and the spectrophotometer at pH = 7.4 with the temperature kept at 45.0 °C for all the runs, the concentration of the *cis*-DDP being 2.2 × 10^{-3} *M*. Varying amounts of chloride ions were present, with the ionic strength μ = 0.2 *M* (NaCl, $NaClO_4$). The results are presented in Table 4.2. When the chloride ion concentration was zero, at pH = 7.4, the hydrolysis reaction was found to be monophasic (as before) and an equilibrium mixture of *cis*-$[PtCl(OH)(NH_3)_2]$ and *cis*-$[Pt(OH)(NH_3)_2(OH_2)]^+$ was produced in an approximately 60 : 40 ratio, the pK_a for this equilibrium being 6.85 [151]. One mole of hydroxide ions was consumed per mole of *cis*-DDP.

The increase in k_{obs} with increasing chloride ion concentration could be due to the fact that the system was proceeding to equilibrium and thus simple first order kinetics were not strictly applicable to Equation 1.1. As the chloride ion concentration increased, the amount of hydroxide ions taken up decreased and the extent of reaction decreased but the ratio of *cis*-$[PtCl(NH_3)_2(OH_2)]^+$ to *cis*-$[PtCl(OH)(NH_3)_2]$ remained constant as the pH was constant throughout. At the end of the hydrolysis reaction, enough solid NaCl was added to the reactant solution in order to make it 0.2 *M* in NaCl. The amount added depended on what the original concentration of NaCl had been. The rate of this reverse reaction, k_{Cl}, in the presence of an excess amount of chloride ions was also measured and was found to be pseudo-first-order and to decrease with the increase in initial chloride ion concentration, because the amount of *cis*-$[PtCl(NH_3)_2(OH_2)]^+$

present at equilibrium had thus decreased.

The observed number of moles of hydroxide ions taken up per mole of *cis*-DDP was calculated from traces from the chart recorder of the pH-stat. The amount of solid *cis*-DDP used in the reactant solution was 50 mg or 1.67×10^{-4} moles. For every one mole of platinum(II), two moles of chloride ions from the *cis*-DDP are released in a complete reaction, therefore there were 3.33×10^{-4} moles of chloride ions released for this reaction. For a complete reaction, the volume of 0.05 *M* NaOH required was calculated by dividing 3.33×10^{-4} moles by 0.05 *M* to give 6.66 ml. The capacity of the syringe delivering the NaOH solution to the reaction vessel was 3.5 ml, therefore 100 on the chart recorder paper corresponded to approximately 3.5 ml.

The following example shows the procedure used to calculate the number of moles of hydroxide ions consumed. At pH = 7.4, T = 45 °C and $\mu = 0.2$ *M* (0.025 *M* NaCl and 0.175 *M* $NaClO_4$), the infinity of the hydrolysis reaction occurred at $\infty = 71$ on the chart paper. The number of ml of NaOH used was calculated from $71/100 \times 3.5$ ml = 2.485 ml used. Therefore, the number of moles of hydroxide ions consumed $n_{OH^-} = 2.485/3.5 = 0.71$ moles. This calculation was done for all the infinity values of hydroxide ion uptake for all the kinetic runs. The results are presented in Table 4.2.

Plotting the values calculated in this manner, for the observed number of moles of hydroxide ions consumed versus the initial chloride ion concentration, gave a reasonably straight line from which was obtained the following linear relationship

$$\frac{\text{moles } OH^- \text{uptake}}{\text{moles Pt(II)}} = 1.08 - 7.3[Cl^-]_i \tag{4.4}$$

where 1.08 is the intercept of the line of best fit with the y-axis and -7.3 is the slope of this line. It should be noted that Equation 4.4 is in the form of

$$y = mx + c \tag{4.5}$$

the general equation for a straight line [157]. Using Equation 4.4, values for the number of moles of hydroxide ions consumed were calculated (Table 4.2).

When the initial chloride ion concentration is 0.1 *M* (or 100 m*M*) at pH = 7.4 (the approximate chloride ion concentration and pH of blood plasma [48,91,92,97]) and the temperature T = 45.0 °C, the final equilibrium ratio of products is approximately 50% *cis*-$[PtCl_2(NH_3)_2]$, 30% *cis*-$[PtCl(OH)(NH_3)_2]$ and 20% *cis*-$[PtCl(NH_3)_2(OH_2)]^+$. This result was obtained from the self-consistency of the following features:- the final absorption spectra of the hydrolysis reactions, the uptake of 0.37 moles of hydroxide ions per mole of *cis*-DDP, the rates of chloride anation, the final absorption spectra of the anation reactions, and the pK_a value of 6.85 [151] for the *cis*-$[PtCl(NH_3)_2(OH_2)]^+$ – *cis*-$[PtCl(OH)(NH_3)_2]$ equilibrium. It is estimated that this equilibrium mixture would be produced in approximately six hours at 37 °C under the same conditions of pH and initial chloride ion concentration as above. If the initial *cis*-DDP concentration

was reduced, the proportion of *cis*-$[PtCl_2(NH_3)_2]$ still present at equilibrium would increase.

Hydrolysis schemes for the reaction of *cis*-DDP *in vivo* are frequently reported in the literature, but there is usually no real emphasis on the relative importance of any platinum(II) species in particular [28,67,158,159,160,161,162]. However, LeRoy *et al.* did attempt to analyse their hydrolysis scheme in terms of the equilibrium data known at the time [159]. At pH = 7.5 and T = 37 °C, with a chloride ion concentration of 0.1 M and an initial *cis*-DDP concentration of 1×10^{-6} M, they concluded that the predominant species were the *cis*-$[PtCl_2(NH_3)_2]$ at greater than 83%, the *cis*-$[PtCl(NH_3)_2(OH_2)]^+$ at approximately 4% and the *cis*-$[PtCl(OH)(NH_3)_2]$ at approximately 12%. The *cis*-$[Pt(OH)_2(NH_3)_2]$, *cis*-$[Pt(NH_3)_2(OH_2)_2]^{2+}$ and the *cis*-$[Pt(OH)(NH_3)_2(OH_2)]^+$ account for approximately 1% total.

Using more recent values from this thesis for the equilibrium constants (at 25 °C, $K_1 = 1.01 \times 10^{-2}$ M (Chapter 2), $K_2 = 2.7 \times 10^{-4}$ M (Chapter 3) and $pK_3 = 6.85$, $pK_4 = 5.93$ and $pK_5 = 7.87$ [151]), it is calculated that the predominant species are the *cis*-$[PtCl_2(NH_3)_2]$ at 63%, the *cis*-$[PtCl(NH_3)_2(OH_2)]^+$ at 7% and the *cis*-$[PtCl(OH)(NH_3)_2]$ at 30%, where the pH = 7.5, T = 35 °C, the initial chloride ion concentration is 0.1 M and the initial *cis*-DDP concentration is 1×10^{-3} M (an approximate model for the blood plasma environment). See Appendix C for details of how these equilibrium concentrations of platinum(II) species were calculated.

The intracellular chloride ion concentration drops to approximately 4 mM and LeRoy *et al.* [159] calculated, using the same pH, that the distribution of products shifted to give *cis*-$[PtCl_2(NH_3)_2]$ at approximately 31%, *cis*-$[PtCl(NH_3)_2(OH_2)]^+$ at approximately 28% and *cis*-$[PtCl(OH)(NH_3)_2]$ at approximately 32%. Present at approximately 7% is the *cis*-$[Pt(OH)(NH_3)_2(OH_2)]^+$ species while the *cis*-$[Pt(NH_3)_2(OH_2)_2]^{2+}$ and *cis*-$[Pt(OH)_2(NH_3)_2]$ are about 1% each. Different conclusions were reached by Roos [162], who suggested that in blood plasma at equilibrium, the *cis*-$[PtCl_2(NH_3)_2]$ was present at 89%, the 'first hydrolysis products' at 11% and the 'fully hydrolysed products' are present as 0.09% of the total. Also according to Roos, inside the cell the *cis*-$[Pt(NH_3)_2(OH_2)_2]^{2+}$ species was present at 47% and the *cis*-$[PtCl(NH_3)_2(OH_2)]^+$ at 34%.

Martin has also estimated the distribution of platinum(II)species present in blood plasma and inside a cell [93]. In blood plasma he estimated that the *cis*-$[PtCl_2(NH_3)_2]$ was present at about 65 to 70%, the *cis*-$[Pt(OH)_2(NH_3)_2]$ at approximately 2 to 5%, the *cis*-$[PtCl(OH)(NH_3)_2]$ at about 30%, the *cis*-$[PtCl(NH_3)_2(OH_2)]^+$ at 2 to 5% and that there was no *cis*-$[Pt(OH)(NH_3)_2(OH_2)]^+$ or *cis*-$[Pt(NH_3)_2(OH_2)_2]^{2+}$ present at all. This distribution of platinum(II) species present in blood plasma is in general agreement with that calculated in Appendix C of this thesis. For the situation inside a cell, Martin estimated that the *cis*-$[PtCl_2(NH_3)_2]$ was present at approximately 5%,

the *cis*-$[PtCl(NH_3)_2(OH_2)]^+$ at about 3%, the *cis*-$[Pt(OH)_2(NH_3)_2]$ at 30 to 35%, the *cis*-$[PtCl(OH)(NH_3)_2]$ at about 35%, the *cis*-$[Pt(OH)(NH_3)_2(OH_2)]^+$ at about 20% and the *cis*-$[Pt(NH_3)_2(OH_2)_2]^{2+}$ at about 1%. There is not such good agreement between Martin's estimates of the distribution of platinum(II) species in the intracellular environment with that obtained by LeRoy *et al.* [159]. However, Martin's statement that about 33% of the platinum(II) complexes contain good water leaving groups at the intracellular chloride ion concentration (4 mM) is in agreement with LeRoy's calculations. Differences in the percentages of each specific species present are most likely due to different assumptions made in the calculations or different estimates for the pK_a values.

Calculated on the basis of the work presented in Chapters 2, 3 and 4 of this thesis, the distribution of products is in reasonable agreement with the calculations of LeRoy *et al.*. It is thus suggested that the *cis*-$[Pt(NH_3)_2(OH_2)_2]^{2+}$ is one of the least likely platinum(II) species to be attacked by donor atoms on the DNA at physiological pH. There are many studies which have used the *cis*-$[Pt(NH_3)_2(OH_2)_2]^{2+}$ plus various nucleophiles as models for the *cis*-DDP/DNA interactions [40,141,143,144,151,163,164,165,166,167]. While it seems they may provide an order of nucleophilic ability, they probably have little relevance to processes which take place inside replicating cancer cells.

The observations made previously in this discussion that buffer nucleophiles readily interact with the hydrolysis products of *cis*-DDP makes designing models for the transport of platinum(II) species in biological systems, for example, in blood plasma, extremely difficult. If *cis*-DDP were to hydrolyse in the blood stream at the physiological pH of 7.4 via Equations 3.2 and 3.3, then the most likely nucleophiles for the *cis*-$[Pt(OH)(NH_3)_2(OH_2)]^+$ or the *cis*-$[PtCl(NH_3)_2(OH_2)]^+$ species would be blood serum albumin or other plasma proteins. This is equivalent to the situation with the buffer nucleophiles. If the anating ligands are neutral, the resulting complex will remain charged and will effectively be wasted since transport of charged platinum(II) species across the cell membrane is less likely than transport of neutral platinum(II) complexes. The most likely neutral species would be the unreacted *cis*-$[PtCl_2(NH_3)_2]$ and the *cis*-$[PtCl(OH)(NH_3)_2]$ although there could also be traces of *cis*-$[Pt(OH)_2(NH_3)_2]$ present. This speculative model of what could occur in blood plasma and inside the cell is shown in Figure 4.4.

4.4 Conclusions.

The results obtained here for the hydrolysis of *cis*-DDP in 0.1 M NaCl solution at pH = 7.4 suggested that Rosenberg's model for the transport of *cis*-DDP *in vivo* [30] may need modification. At physiological pH and chloride ion concentrations ($\sim$ 104 mM) hydrolysis of the *cis*-DDP was measureable (with a half-life of approximately one hour at 37 °C) and if no platinum(II) species were removed, an equilibrium sys-

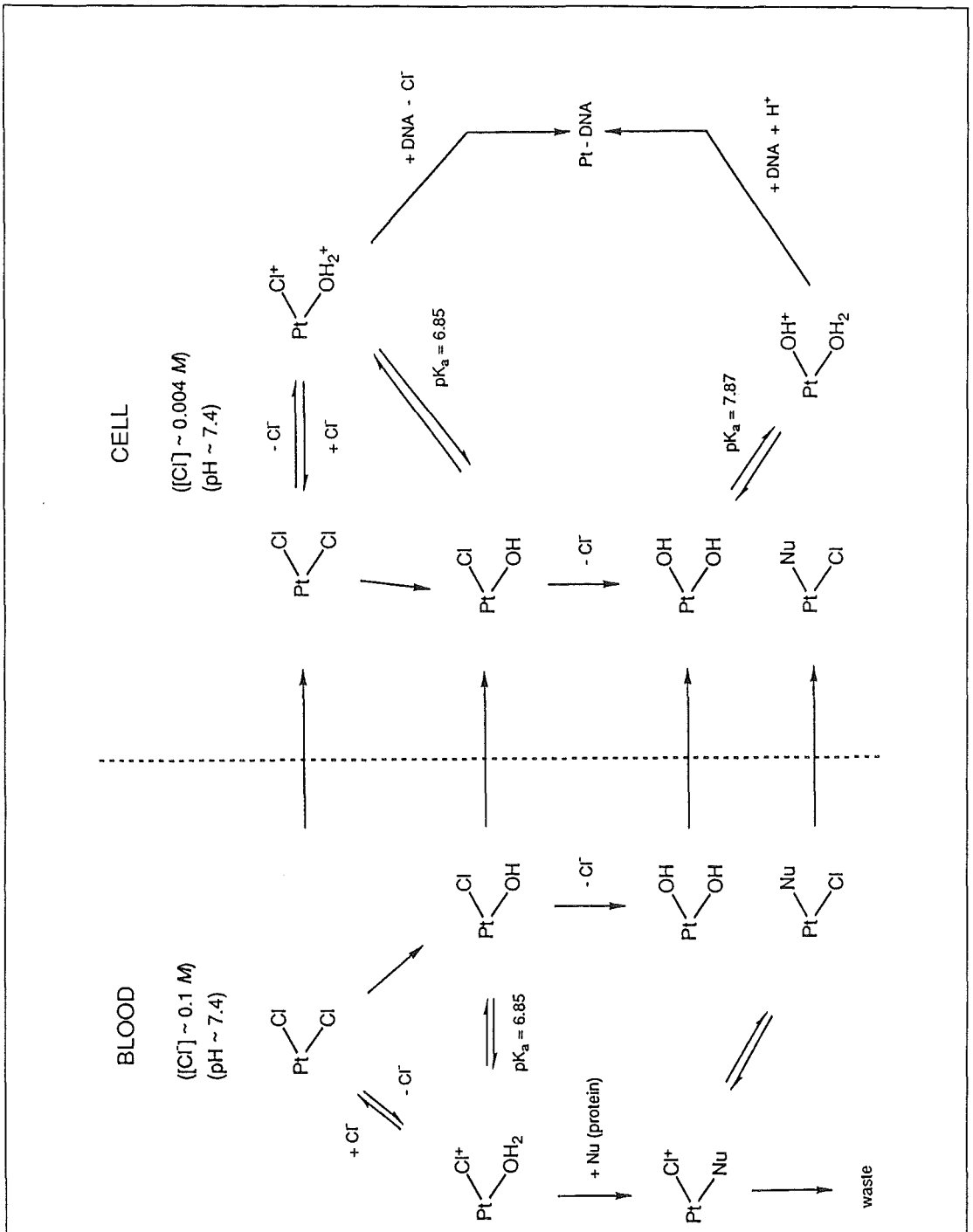

Figure 4.4. A speculative model of the reactions of *cis*-$[PtCl_2(NH_3)_2]$ under physiological conditions in blood plasma and inside a cell.

tem of *cis*-$[PtCl_2(NH_3)_2]$, *cis*-$[PtCl(NH_3)_2(OH_2)]^+$ and *cis*-$[PtCl(OH)(NH_3)_2]$ was produced in about six hours (at 37 °C). Thus there would be two neutral species, the *cis*-$[PtCl_2(NH_3)_2]$ and the *cis*-$[PtCl(OH)(NH_3)_2]$ available for transport through the cell membrane. If transfer through the cell wall was rapid relative to the rate of hydrolysis then Rosenberg's model would be valid, but if cell wall transfer was slow then both the *cis*-$[PtCl_2(NH_3)_2]$ and the *cis*-$[PtCl(OH)(NH_3)_2]$ would be available. Another possibility is that the *cis*-$[PtCl(NH_3)_2(OH_2)]^+$ in the blood stream could be removed from the system by binding to plasma protein before transfer across the cell wall (via conversion to the *cis*-$[PtCl(OH)(NH_3)_2]$). This process would also upset the rapidly interconverting *cis*-$[PtCl(NH_3)_2(OH_2)]^+$ – *cis*-$[PtCl(OH)(NH_3)_2]$ equilibrium concentrations.

Within the cell itself, where the chloride ion concentration drops to approximately 4 mM, almost complete hydrolysis of the *cis*-DDP takes place with a half-life of approximately two hours at 37 °C and pH = 7.4 to give a 50 : 50 *cis*-$[PtCl(NH_3)_2(OH_2)]^+$ – *cis*-$[PtCl(OH)(NH_3)_2]$ equilibrium mixture, assuming that there is no loss of any platinum(II) species. Removal of platinum(II) species can however occur via binding of DNA to the *cis*-$[PtCl(NH_3)_2(OH_2)]^+$ [146]. Thus so far, while understanding of the hydrolysis behaviour of *cis*-DDP in solutions that attempt to model the physiological situation is somewhat clearer, complete knowledge of the behaviour of *cis*-DDP *in vivo* is still some way off.

CHAPTER 5

THE ANATION KINETICS OF *cis*-$[PtX(NH_3)_2(OH_2)]^+$ ($X = Cl^-, OH^-$) WITH CHLORIDE IONS, GLYCINE AND MONOHYDROGEN MALONATE.

5.1 Introduction.

So far, the kinetics of hydrolysis and anation of *cis*-DDP and its hydrolysis products under acid, base and physiological pH conditions have been studied (Chapters 2 to 4). From this work, the species *cis*-$[PtX(NH_3)_2(OH_2)]^+$, where X = Cl^- or OH^-, have been emphasised as the most likely platinum(II)-containing species available to bind DNA under physiological conditions.

For these *cis*-$[PtX(NH_3)_2(OH_2)]^+$ species it was therefore of interest to establish some reactivity patterns. Thus, in this Chapter, the hydrolysis of *cis*-$[PtCl(OH)(NH_3)_2]$ and the anation of *cis*-$[Pt(OH)(NH_3)_2(OH_2)]^+$ with chloride ions at pH = 7.4 are described, as well as the chloride ion anation of *cis*-$[Pt(OH)(NH_3)_2(OH_2)]^+$ at pH = 7.8 (the pH at which the greatest concentration of *cis*-$[Pt(OH)(NH_3)_2(OH_2)]^+$ is present). As a result, a complete hydrolysis reaction profile for *cis*-DDP under a variety of pH conditions can be postulated.

The kinetics of the species *cis*-$[PtCl(NH_3)_2(OH_2)]^+$ with glycine and sodium hydrogen malonate are also reported in this Chapter.

5.2 Experimental.

5.2.1 The Hydrolysis of *cis*-$[PtCl(OH)(NH_3)_2]$ and the Chloride Ion Anation of *cis*-$[Pt(OH)(NH_3)_2(OH_2)]^+$ at pH = 7.4.

A solution of 2.38×10^{-3} *M* *cis*-$[PtCl(NH_3)_2(OH_2)]^+$ was first prepared by allowing 0.1786 g of *cis*-DDP to hydrolyse in 1.0 *M* $NaClO_4$ (245 ml) plus 0.1 *M* $HClO_4$ (5 ml) at 50 °C for three to four hours and then left overnight at room temperature. For each kinetic run, 70 ml of this solution were placed in the temperature controlled reaction vessel of the pH-stat and peristaltically pumped (at a rate of 100 ml per minute) through a 2.00 cm quartz, flow-through cell in the spectrophotometer. Glass and calomel electrodes were placed in the solution in the reaction vessel and the pH

was maintained at 7.4 by the manual addition of 0.1 *M* NaOH plus 1.0 *M* $NaClO_4$ (to maintain the ionic strength of the solution) as the reaction proceeded (Chapter 4, Experimental section shows the experimental set-up for the combination of the spectrophotometer and pH-stat (Figure 4.1), the method of calibration of the pH-stat and the electrodes and the method of temperature control). For this experimental work, the automatic titration of NaOH solution and the chart recorder were not made use of. The pH-stat was essentially used as a pH meter.

As the reaction proceeded, absorbance versus time data were collected using the spectrophotometer at 300, 282 and 255 nm. At the end of the reaction (after six to eight half-lives), the reactant solution was made 0.2 *M* in NaCl by the addition of solid NaCl. The rate of the subsequent chloride ion uptake (k_{obs}, s^{-1}) was also monitored spectrophotometrically with absorbance versus time data collected at the same three wavelengths as the forward reaction, and the pH was maintained at 7.4 by the manual addition of 0.1 *M* $HClO_4$ plus 1.0 *M* $NaClO_4$.

First order rate constants (k_3, s^{-1}) for the forward reaction (Equation 5.5) were calculated from the absorbance versus time data using Equation 2.2 and the values obtained for k_3 are reported in Table 5.1. Values for the rate constants k_{-3} (M^{-1} s^{-1}) (Equation 5.5) were calculated from the expression

$$k_{-3} = 5k_{obs} \tag{5.1}$$

which derives from

$$k_{-3} = \frac{k_{obs}}{[Cl^-]} \tag{5.2}$$

where the chloride ion concentration is always 0.2 *M*, and these values are reported in Table 5.1. Values for the equilibrium constant, K_3, for Equation 5.5 were obtained from the expression

$$K_3 = \frac{k_3}{k_{-3}} \tag{5.3}$$

and are reported in Table 5.2.

5.2.2 Chloride Ion Anation of *cis*-$[Pt(OH)(NH_3)_2(OH_2)]^+$ at pH = 7.8.

Using the combination of the pH-stat and the spectrophotometer, 1.67×10^{-3} *M* solutions of *cis*-$[Pt(OH)_2(NH_3)_2]$ (75 ml) (Chapters 3 and 4) were titrated with $HClO_4$ (1.0 and 0.1 *M*) to a fixed pH in the range pH = 2 to 10. The results showed that the maximum amount of *cis*-$[Pt(OH)(NH_3)_2(OH_2)]^+$ was formed at pH = 7.8. This result is in agreement with the measured pK_a of 7.87 for the *cis*-$[Pt(OH)(NH_3)_2(OH_2)]^+$ – *cis*-$[Pt(OH)_2(NH_3)_2]$ equilibrium [151].

The 75 ml of 2.22×10^{-3} *M* *cis*-$[Pt(OH)_2(NH_3)_2]$ in 0.01 *M* NaOH solutions plus NaCl (0.05 to 0.4 *M*) were adjusted to pH = 7.8 with 1.0 or 0.1 *M* $HClO_4$, in the reaction vessel of the pH-stat, and peristaltically pumped through the 2.00 cm cell as in the previous section with the pH-stat again used as a pH meter. The absorbance changes due to the subsequent reaction were monitored at 300, 285 and 255 nm and were found to be chloride ion and temperature dependent. A constant pH of 7.8 was maintained throughout the reaction by manual addition of 0.1 *M* $HClO_4$. Values of k_{-3} (M^{-1} s^{-1}; Equation 5.5) were calculated using Equation 5.2 and are presented in Table 5.3.

5.2.3 The Reaction of *cis*-$[PtCl(NH_3)_2(OH_2)]^+$ with Glycine.

A solution of *cis*-$[PtCl(NH_3)_2(OH_2)]^+$ of the same volume and concentration as that used in the hydrolysis of *cis*-$[PtCl(OH)(NH_3)_2]$ (see above) was used in the reaction vessel of the pH-stat and the pH-stat used in the same manner as above. However, solid glycine, sufficient to give concentrations of 0.01, 0.05 or 0.1 *M*, was added to the *cis*-$[PtCl(NH_3)_2(OH_2)]^+$solution in the reaction vessel prior to immersion of the glass and calomel electrodes. The pH of the reactant solution was adjusted to 7.4 by the addition of 0.1 *M* NaOH in 1.0 *M* $NaClO_4$ but very little further pH adjustment was required during the subsequent reaction due to the self-buffering nature of the glycine.

The spectral changes were monitored between 360 and 235 nm (Figure 5.5), with absorbance versus time data collected at 304 and 245 nm. From plots of the pseudo-first-order rate constants (k_{obs}, s^{-1}) versus the glycine concentration (Figure 5.6, Table 5.6), second-order rate constants, k_{Nu}, were obtained from the slopes of the plots, and from the intercepts, values for $k_0 = k^2_{OH}$ (s^{-1}) (Equation 5.4, Table 5.6) were also obtained, since, for this reaction

$$k_{obs} = k_0 + k_{Nu}[Nu] \tag{5.4}$$

where in this case, [Nu] = [glycine] [125].

5.2.4 The Reaction of *cis*-$[PtCl(NH_3)_2(OH_2)]^+$ with Sodium Hydrogen Malonate.

A stock solution of 2.38×10^{-3} *M* *cis*-$[PtCl(NH_3)_2(OH_2)]^+$ was prepared by allowing 25 mg of *cis*-DDP to hydrolyse in 1.0 *M* $NaClO_4$ (24.8 ml) plus 0.1 *M* $HClO_4$ (10.2 ml) at 50 °C for three to four hours and then left overnight at room temperature. A solution of 0.1 *M* NaHmal (μ = 1.0 *M*) was prepared from equal volumes of 0.2 *M* malonic acid and 0.2 *M* NaOH, both in 0.9 *M* $NaClO_4$. Solutions of 0.05 *M* and 0.01 *M* NaHmal (μ = 1.0 *M*) were similarly prepared.

A 2.0 ml sample of the *cis*-$[PtCl(NH_3)_2(OH_2)]^+$ solution was placed in one of the separate test tubes attached to the arms of the glass Y-shaped rapid mixing device and

a 1.0 ml sample of the chosen NaHmal solution was placed in the other (Chapter 2). The arms of the mixing device were then immersed in a temperature controlled water bath and a dry 1.00 cm quartz spectrophotometer cell mounted in the vertical position. On inversion, the solutions were rapidly mixed, the cell was placed in the temperature controlled cell compartment of the spectrophotometer, the mixing device removed and the repeat fixed wavelength mode of the spectrophotometer was activated.

The two consecutive reactions were monitored separately. The first reaction (k_{obs}, s^{-1}) was followed at 245 nm for ten to twenty lots of five minute cycles (Figure 5.2), the number of cycles depending on the temperature. Values of k_{obs} were calculated and the results are presented in Table 5.5. Values for the second-order rate constants (k_{Hmal}, $M^{-1}\ s^{-1}$) were calculated from the slopes of plots of k_{obs} versus NaHmal concentration (Figure 5.3) using Equation 5.4. A possible interpretation of what the intercepts of these plots with the y-axis mean will be given later in this Chapter.

The second reaction was followed at 290 nm and only this second reaction developed an isosbestic point, at 267 nm (Figure 5.4). The rate constants for this reaction (k_{cycl}, s^{-1}) were independent of the concentrations of the NaHmal solutions used (Table 5.5).

5.3 Results and Discussion.

A complete hydrolysis reaction profile for *cis*-DDP under a variety of pH conditions was assembled (Figure 5.1). Rate and equilibrium constants had been established (Chapters 2, 3 and 4; [151]) for all the interconversions except for Equation 5.5

$$cis\text{-}[PtCl(OH)(NH_3)_2] + H_2O \underset{k_{-3}}{\overset{k_3}{\rightleftharpoons}} cis\text{-}[Pt(OH)(NH_3)_2(OH_2)]^+ + Cl^- \quad (5.5)$$

with $K_3 = k_3/k_{-3}$ (Equation 5.3), which is similar to Equation 1.1, with $K_1 = k_1/k_{-1}$ (Equation 2.11; Chapter 2) except that chloride ion has been substituted for hydroxide ion.

The kinetics of both the forward and reverse directions (k_3 and k_{-3}, respectively) of Equation 5.5 have been measured at pH = 7.4 using the *cis*-$[PtCl(NH_3)_2(OH_2)]^+$ as a source of starting material (Chapters 2 and 3). Both the *cis*-$[PtCl(NH_3)_2(OH_2)]^+$ and the *cis*-$[PtCl(OH)(NH_3)_2]$ are available at this pH for hydrolysis (the pK_a for the *cis*-$[PtCl(NH_3)_2(OH_2)]^+$ – *cis*-$[PtCl(OH)(NH_3)_2]$ equilibrium system is 6.85 [151]) but only the *cis*-$[PtCl(OH)(NH_3)_2]$ reacts to any extent (Chapters 2, 3 and 4). As the reaction shown in Equation 5.5 proceeds, the equilibrium between *cis*-$[PtCl(NH_3)_2(OH_2)]^+$ and *cis*-$[PtCl(OH)(NH_3)_2]$ shifts to provide more of the *cis*-$[PtCl(OH)(NH_3)_2]$ and thus eventually, *cis*-$[Pt(OH)(NH_3)_2(OH_2)]^+$ is the major product. Constant pH for this reaction was maintained by the manual addition of NaOH solution. Since the pK_a for the *cis*-$[Pt(OH)_2(NH_3)_2]$ – *cis*-$[Pt(OH)(NH_3)_2(OH_2)]^+$ equilibrium is 7.87 [151], some

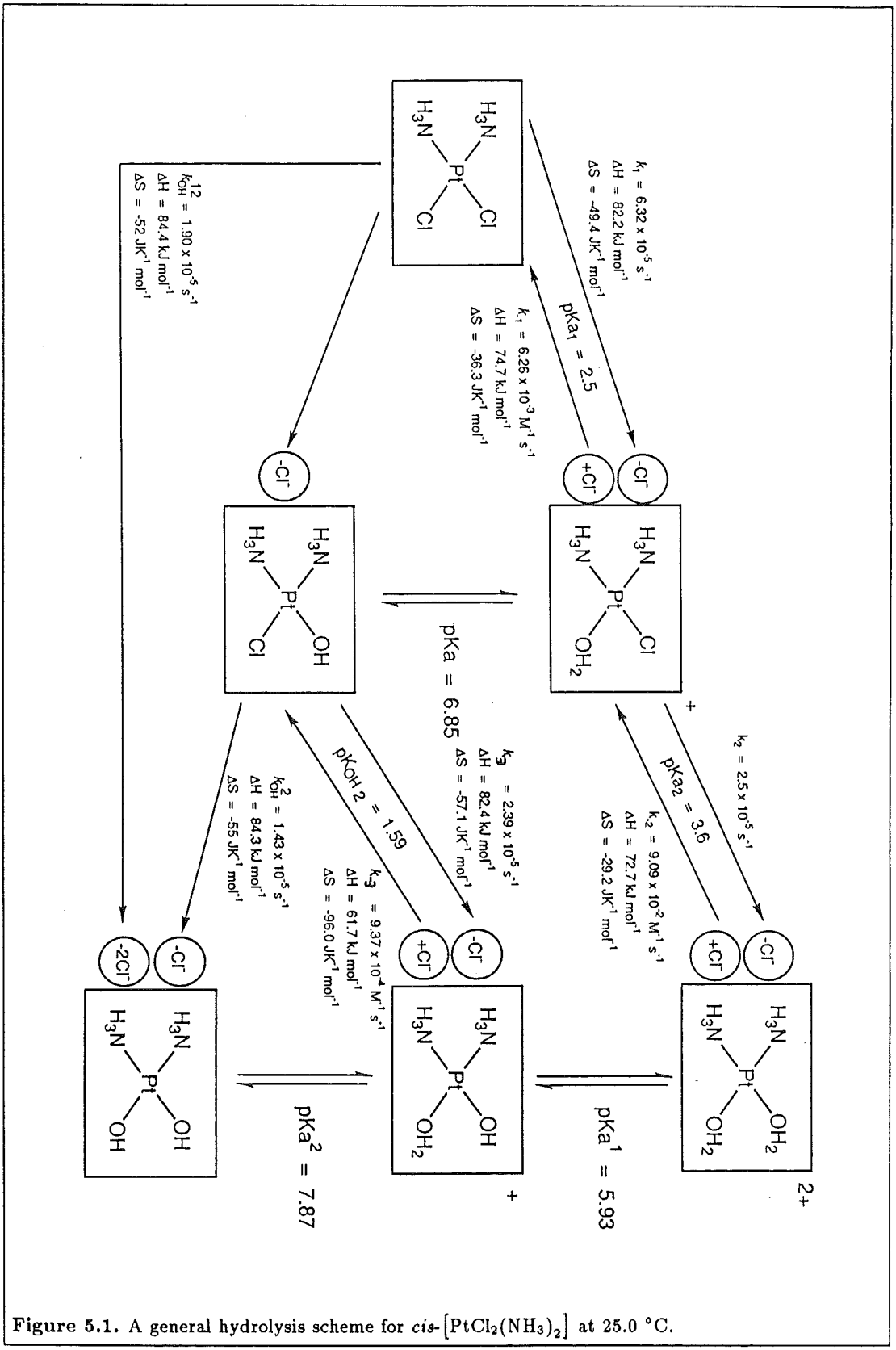

Figure 5.1. A general hydrolysis scheme for *cis*-$[PtCl_2(NH_3)_2]$ at 25.0 °C.

Table 5.1. Spectrophotometrically determined rate constants for the forward (k_3) and reverse (k_{-3}) reactions associated with the hydrolysis of *cis*-$[PtCl(OH)(NH_3)_2]$ (Equation 5.5) at pH = 7.4 (μ = 1.0 M).

Temperature (°C)	[K]	$10^4 k_3$ (s^{-1})	$10^4 k_3$ (calc.) [a] (s^{-1})	$10^4 k_{obs}$ [b] (s^{-1})	$10^3 k_{-3}$ (M^{-1} s^{-1})	$10^3 k_{-3}$ (calc.) [c] (M^{-1} s^{-1})
25.0	[298.2]		0.239			0.937
35.2	[308.4]	0.749±0.042	0.741	4.39±0.86	2.20	2.21
		0.730±0.170				
40.2	[313.4]	1.23±0.20	1.26	6.67±0.67	3.39	3.29
		1.29±0.34				
		1.25±0.29				
45.2	[318.4]	2.14±0.32	2.10	9.25±0.67	4.63	4.84
		2.07±0.38				
		2.12±0.81				
49.7	[322.9]	3.24±0.32	3.28	13.9±0.64	6.94	6.79
		3.27±0.58				

[a]Calculated from the activation parameters: $k_3 = 2.39 \times 10^{-5}$ s^{-1} at 25 °C, $\Delta H^{\neq} = 82.4 \pm 0.8$ kJ mol^{-1}, $\Delta S^{\neq} = -57 \pm 2$ J K^{-1} mol^{-1}.
[b]$[Cl^-] = 0.2$ M; k_{-3} is calculated using Equation 5.1.
[c]Calculated from the activation parameters: $k_{-3} = 9.37 \times 10^{-4}$ M^{-1} s^{-1} at 25 °C, $\Delta H^{\neq} = 61.7 \pm 3.2$ kJ mol^{-1}, $\Delta S^{\neq} = -96 \pm 6$ J K^{-1} mol^{-1}.

cis-$[Pt(OH)_2(NH_3)_2]$ will also form, but *cis*-$[Pt(NH_3)_2(OH_2)_2]^{2+}$ is most unlikely to form (the pK_a for the *cis*-$[Pt(NH_3)_2(OH_2)_2]^{2+}$ – *cis*-$[Pt(OH)(NH_3)_2(OH_2)]^+$ equilibrium is 5.93 [151]).

The forward reaction is characterised by isosbestic points in the repeat-scan absorbance spectra at 271 and 323 nm and the first-order rate constants, $k_3(s^{-1})$, were calculated from the absorbance versus time data (Table 5.1). At the end of the reaction, the reactant solution was made 0.2 M in chloride ions by the addition of a calculated amount of solid NaCl. As this reverse reaction proceeded, a constant pH of 7.4 was maintained by the manual addition of $HClO_4$ solution. Initially, an isosbestic point at 271 nm was observed but this shifted to 282 nm in the later stages of the reaction indicating that the reverse of Equation 1.1 was taking place via the *cis*-$[PtCl(NH_3)_2(OH_2)]^+$ present at pH = 7.4. Therefore the absorbance versus time data for this anation reaction (k_{-3}, M^{-1} s^{-1}) were monitored at 282 nm and these were used to calculate pseudo-first-order rate constants (k_{obs}, s^{-1}) which in turn, using Equation 5.1 gave values for the second-order rate constant k_{-3} (M^{-1} s^{-1}) (Table 5.1).

Knowledge of the rate constants k_3 and k_{-3} permitted the calculation of the equilibrium constant K_3 using Equation 5.3. Combining the temperature dependence expressions for $k_{-3} = 1.625 \times 10^8 \exp\left(\frac{-64.15 \times 10^3}{RT}\right)$ and $k_3 = 1.747 \times 10^{10} \exp\left(\frac{-84.85 \times 10^3}{RT}\right)$ (both at μ = 1.0 M, $NaClO_4$) with values of PZ and E_a for both k_3 and k_{-3} (obtained in the manner described in Chapter 2) from the Arrhenius equation (Equation 2.3), gave the temperature dependence of the equilibrium constant K_3 (Table 5.2) in the

Table 5.2. Forward (k_3) and reverse (k_{-3}) rate constants, and equilibrium constants (K_3) for the hydrolysis of *cis*-$[PtCl(OH)(NH_3)_2]$ (Equation 5.5) at pH = 7.4 (μ = 1.0 M).

Temperature (°C)	[K]	$10^5 k_3$ [a] (s^{-1})	$10^4 k_{-3}$ [b] ($M^{-1}\ s^{-1}$)	$10^3 K_3$ [c d]
10.0	[283.2]	0.392	2.39	16.4
15.0	[288.2]	0.732	3.84	19.1
20.0	[293.2]	1.34	6.05	22.2
25.0	[298.2]	2.40	9.41	25.5
30.0	[303.2]	4.22	14.4	29.3
35.0	[308.2]	7.28	21.8	33.4
40.0	[313.2]	12.4	32.5	38.1
45.0	[318.2]	20.6	47.9	43.0
50.0	[323.2]	33.9	69.6	48.7

[a]Calculated from the expression: $k_3 = 1.747 \times 10^{10} \exp\left(\frac{-84.85\times10^3}{RT}\right)$

[b]Calculated from the expression: $k_{-3} = 1.625 \times 10^{8} \exp\left(\frac{-64.15\times10^3}{RT}\right)$

[c]Calculated from Equation 5.8

[d]The variation of K_3 with temperature indicates that the forward reaction is endothermic with $\Delta H^{\ddagger}_{298.2}$ = 20.7 kJ mol^{-1}. Other thermodynamic parameters associated with the forward reaction are $\Delta G^{\ddagger}_{298.2}$ = 9.10 kJ mol^{-1} and $\Delta S^{\ddagger}_{298.2}$ = 39 J K^{-1} mol^{-1}.

form shown below (Equation 5.8). This expression is obtained, as in Chapter 2, by using the Arrhenius expressions for k_3 and k_{-3} and substituting them into Equation 5.3, that is

$$K_3 = \frac{k_3}{k_{-3}} = \frac{1.747 \times 10^{10} \exp\left(\frac{-84.85\times10^3}{RT}\right)}{1.625 \times 10^{8} \exp\left(\frac{-64.15\times10^3}{RT}\right)} \tag{5.6}$$

which gives

$$K_3 = 107.51 \exp\left(\frac{-20.7 \times 10^3}{RT}\right) \tag{5.7}$$

or

$$\ln K_3 = 4.676 - \frac{20.7 \times 10^3}{RT} \tag{5.8}$$

At 25 °C, $K_3 = 2.55 \times 10^{-2}$ for Equation 5.5 (where X = OH^-) whereas for Equation 1.1, $K_1 = 1.01 \times 10^{-2}$ (where X = Cl^-). The major difference between the reactions shown in Equations 5.5 and 1.1 appears in the pre-exponential function of the Arrhenius expression (Equation 2.3) for the reverse (anation) reaction, that is, $k_{-1} = 2.104 \times 10^{11} \exp\left(\frac{-77.21\times10^3}{RT}\right)$ and $k_{-3} = 1.625 \times 10^{8} \exp\left(\frac{-64.15\times10^3}{RT}\right)$.

Using the van't Hoff equation (Equation 2.13) and Equations 2.14 and 2.15 (Chapter 2), for the forward reaction (k_3) values of $\Delta H^{\ddagger}_{298.2}$ = 20.7 kJ mol^{-1}, $\Delta G^{\ddagger}_{298.2}$ =

9.10 kJ mol^{-1} and $\Delta S^{\ominus}_{298.2}$ = 39 J K^{-1} mol^{-1}. The positive value obtained for $\Delta G^{\ominus}_{298.2}$ and the positive (endothermic) value for $\Delta H^{\ominus}_{298.2}$ means that the forward reaction (Equation 5.5) is not spontaneous but for the reverse reaction (k_{-3}) a negative value for $\Delta G^{\ominus}_{298.2}$ = −9.10 kJ mol^{-1} (calculated using $K_3' = 1/K_3$) and a negative (exothermic) value for $\Delta H^{\ominus}_{298.2}$ = −20.70 kJ mol^{-1} shows that this reaction is the spontaneous process. That is there is a natural tendency for the reaction to proceed from the *cis*-$[Pt(OH)(NH_3)_2(OH_2)]^+$ plus Cl^- to the *cis*-$[PtCl(OH)(NH_3)_2]$. Also for the reverse reaction $\Delta S^{\ominus}_{298.2}$ = −39 J K^{-1} mol^{-1}. The corresponding data for the forward reaction associated with K_1 (Equation 1.1) are $\Delta H^{\ominus}_{298.2}$ = 7.52 kJ mol^{-1}, $\Delta G^{\ominus}_{298.2}$ = 11.4 kJ mol^{-1} and $\Delta S^{\ominus}_{298.2}$ = −13 J K^{-1} mol^{-1} (Chapter 2). These are similar to the values obtained for the forward reaction associated with K_3.

The rate of chloride anation of *cis*-$[Pt(OH)(NH_3)_2(OH_2)]^+$ was also measured spectrophotometrically by the addition of chloride ions in the form of solid NaCl to solutions of *cis*-$[Pt(OH)_2(NH_3)_2]$ adjusted to pH = 7.8 using $HClO_4$. This pH was chosen since it was determined that this was approximately the pH at which the greatest amount of *cis*-$[Pt(OH)(NH_3)_2(OH_2)]^+$ formed. Under these conditions, coordinated water is replaced by a chloride ion and the final product, at high chloride ion concentration is mainly the *cis*-$[PtCl_2(NH_3)_2]$ species. At either pH = 7.8 or 7.4 with very high chloride ion concentrations, the reaction products would be a mixture of *cis*-$[PtCl(OH)(NH_3)_2]$ and *cis*-$[PtCl(NH_3)_2(OH_2)]^+$, and then the *cis*-$[PtCl(NH_3)_2(OH_2)]^+$ would anate to give the *cis*-$[PtCl_2(NH_3)_2]$. To reestablish the equilibrium, the *cis*-$[PtCl(OH)(NH_3)_2]$ would react to give more *cis*-$[PtCl(NH_3)_2(OH_2)]^+$ which would then also anate to give more of the *cis*-$[PtCl_2(NH_3)_2]$. The amount of chloride ion present would determine how much of the *cis*-$[PtCl(OH)(NH_3)_2]$ and *cis*-$[PtCl_2(NH_3)_2]$ species were present in the final product mixture. Lower chloride ion concentrations would mean that far more of the *cis*-$[PtCl(OH)(NH_3)_2]$ was present.

As the reaction proceeded, an isosbestic point was formed at 271 nm which later shifted to 282 nm which is consistent with formation of the *cis*-$[PtCl_2(NH_3)_2]$. Constant pH was maintained by the manual addition of $HClO_4$. From absorbance versus time data collected at 282 nm, pseudo-first-order rate constants (k_{obs}, s^{-1}) (Table 5.3) were calculated and hence values of k_{-3} (M^{-1} s^{-1}) were calculated using Equation 5.2 (Table 5.3). Close agreement between $k_{-3} = 9.40 \times 10^{-4}$ M^{-1} s^{-1} at pH = 7.4, and $k_{-3} = 12.70 \times 10^{-4}$ M^{-1} s^{-1} at pH = 7.8 (both at 25 °C) is not to be expected since the concentration of *cis*-$[Pt(OH)(NH_3)_2(OH_2)]^+$ is pH dependent and the product distribution would be difficult to compare. However, closer agreement between the activation parameters for both systems (Tables 5.4) should have been obtained and it is thus unknown why this discrepancy exists.

The anation of *cis*-$[PtCl(NH_3)_2(OH_2)]^+$ by sodium hydrogen malonate (NaHmal) has also been investigated. Mixing solutions of NaHmal and *cis*-$[PtCl(NH_3)_2(OH_2)]^+$

Table 5.3. Spectrophotometrically determined rate constants for the chloride anation reaction of *cis*-$[Pt(OH)(NH_3)_2(OH_2)]^+$ at pH = 7.8 (μ = 1.0 M).

Temperature (°C)	[K]	$[Cl^-]$ (M)	$10^4 k_{obs}$ (s^{-1})	$10^3 k_{-3}$ [a] ($M^{-1}\ s^{-1}$)	$10^3 k_{-3}$ (calc.) [b] ($M^{-1}\ s^{-1}$)
20.3	[293.5]	0.60	6.05±0.69	1.01±0.11	0.968
25.0	[298.2]				1.27
25.4	[298.6]	0.20	2.62±0.31	1.31±0.15	1.30
		0.30	3.80±0.71	1.27±0.27	
		0.40	5.22±0.68	1.31±0.17	
		0.50	6.29±0.78	1.26±0.16	
		0.80	9.80±0.67	1.23±0.08	
30.3	[303.5]	0.40	7.04±0.45	1.76±0.11	1.72
		0.60	10.5±1.3	1.74±0.21	

[a] k_{-3}calculated using Equation 5.2
[b] Calculated from the activation parameters: at 25 °C, $k_{-3} = 12.7\times10^{-4}\ M^{-1}\ s^{-1}$, $\Delta H^{\neq} = 39.5\pm3.1$ kJ mol^{-1}, $\Delta S^{\neq} = -168 \pm 6$ J K^{-1} mol^{-1}.

at pH = 4.3 (the 'natural' buffered pH of NaHmal) resulted initially in an absorbance change in the repeat-scan spectra in the range 235 to 260 nm. No distinct isosbestic points were observed for this part of the reaction, and the absorbance in the region 270 to 330 nm hardly changed (Figure 5.2). This initial reaction was found to be independent of the concentration of NaHmal and the absorbance changes were monitored at 245 nm to give pseudo-first-order rate constants (k_{obs}, s^{-1}) (Table 5.5). Plots of k_{obs} versus NaHmal concentration were linear (Figure 5.3) but there was no systematic temperature trend for the intercepts of the plots with the y-axis.

Equation 5.4 is obeyed by this initial reaction. For square planar complexes, for example, those formed by the d^8 system of platinum(II), for reactions such as

$$MA_3X^{n+} + Nu^- \xrightarrow{H_2O} MA_3Nu^{n+} + X^- \tag{5.9}$$

or, more specifically

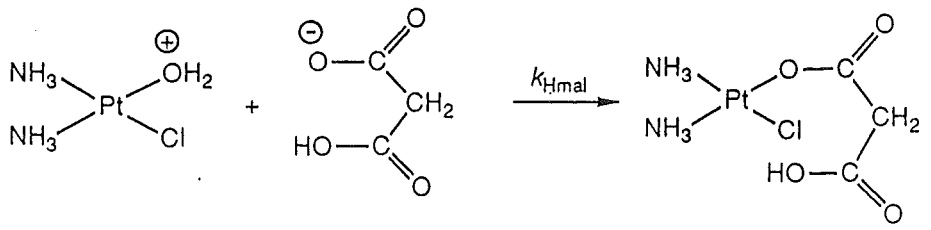

(5.10)

the kinetics are described by a two-term rate law which has the form [125]

$$\text{rate} = k_2[cis\text{-}[PtCl(NH_3)_2(OH_2)]^+] + k_{Hmal}[cis\text{-}[PtCl(NH_3)_2(OH_2)]^+][Hmal^-] \tag{5.11}$$

The composite nature of the rate law implies that such a reaction proceeds via two parallel routes, a solvent path

Table 5.4. Kinetic parameters for the reactions of some square planar platinum(II) complexes in various aqueous media at 25.0 °C.

Chloride Release					
Complex/Reference	Solvent	$10^5 k$ (s^{-1})	$\Delta H^{\neq}$ kJ mol^{-1}	$\Delta S^{\neq}$ J K^{-1} mol^{-1}	
$PtCl_4^{-2}$					
[36]	H_2O	3.9			
$PtCl_3(NH_3)_2$					
[36]	H_2O	5.6			
cis-$[PtCl_2(NH_3)_2]$					
Chapter 2	1.0 *M* $HClO_4$	6.32	82.2	-49	
[78]	H_2O	2.5	82.3	-59	
Chapter 3	0.1 *M* NaOH[a]	1.90	84.4	-52	
trans-$[PtCl_2(NH_3)_2]$					
[109]	0.01 *M* HNO_3	6.62	75.2	-84	
[36]	H_2O	9.8			
cis-$[PtCl(OH)(NH_3)_2]$					
Chapter 5	pH = 7.4	2.39	82.4±0.8	-57±2	
$[PtCl_2(NH_2CH_2CH_2NH_2)]$					
[109]	0.01 *M* HNO_3	5.2	92	-18	
[140]	H_2O	3.4			
cis-$[PtCl(NH_3)_2(OH_2)]^+$					
Chapter 3	1.0 *M* $HClO_4$	2.5			
$PtCl(en)(OH_2)^+$					
[140]	H_2O	4.4			

Anation						
Complex/Reference	Nu [b]	Ionic Strength (*M*)	pH	$10^4 k_{Nu}$ (M^{-1} s^{-1})	$\Delta H^{\neq}$ kJ mol^{-1}	$\Delta S^{\neq}$ J K^{-1} mol^{-1}
cis-$[PtCl(NH_3)_2(OH_2)]^+$						
Chapter 2	Cl^-	1.0	< 1	62.6	77.2	-36
Chapter 5	$Hmal^-$	1.0	4.3	9.90	74.8	-52
Chapter 5	gly	1.0	7.4	2.75	62.7	-103
cis-$[Pt(OH)(NH_3)_2(OH_2)]^+$						
Chapter 5	Cl^-	1.0	7.4	9.37	61.7±3.2	-96±6
Chapter 5			7.8	12.7	39.5±3.1	-168±6
$PtCl(en)(OH_2)^+$						
[36]	Cl^-	0.318	≤ 1	154	73.1	-33
trans – $PtCl(NH_3)_2(OH_2)^+$						
[109]	Cl^-	< 0.1	2	4630	70.2	-25

[a]Both chloride ligands lost.
[b]Nucleophile

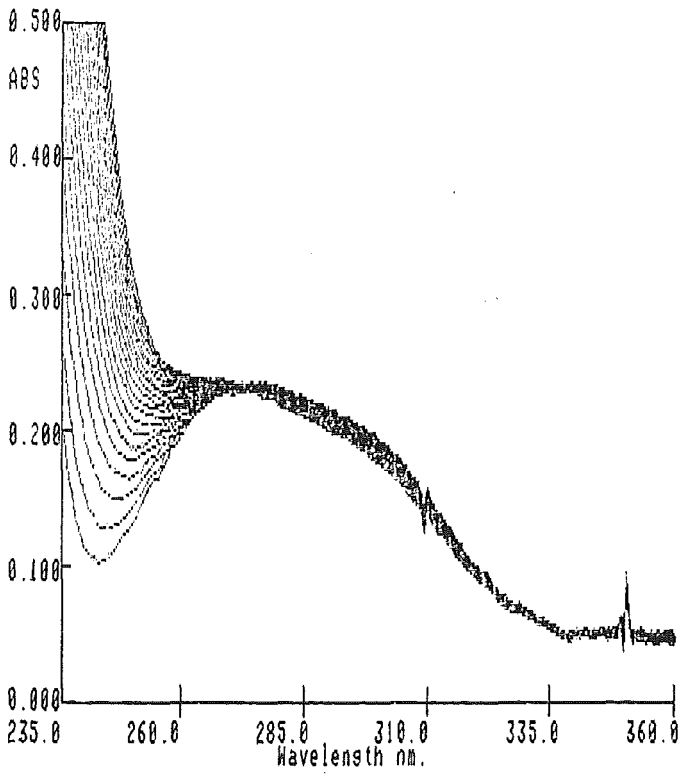

Figure 5.2. Spectrophotometric scans (2 minute intervals) for the first part of the anation reaction of *cis*-$[PtCl(NH_3)_2(OH_2)]^+$ by NaHmal at 45.1 °C and pH = 4.3 ($\mu = 1.0$ *M*) (Equation 5.10). The absorbance at 245 nm increases with time.

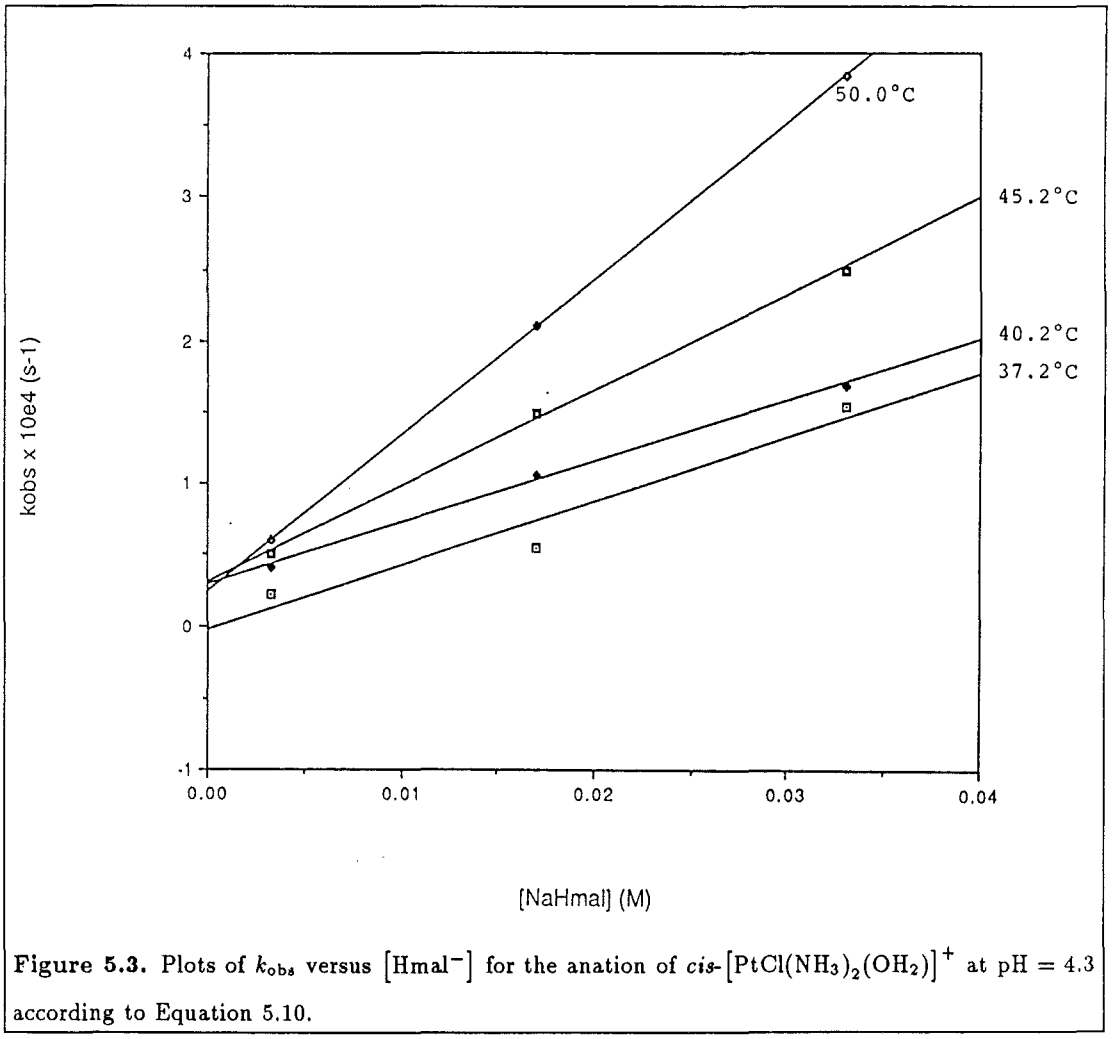

Figure 5.3. Plots of k_{obs} versus $[Hmal^-]$ for the anation of *cis*-$[PtCl(NH_3)_2(OH_2)]^+$ at pH = 4.3 according to Equation 5.10.

Table 5.5. Spectrophotometrically determined rate constants (k_{Hmal}, M^{-1} s^{-1}) for the reaction of *cis*-$[PtCl(NH_3)_2(OH_2)]^+$ with sodium hydrogen malonate (pH = 4.3; μ = 1.0 M, $NaClO_4$).

Temperature		[NaHmal] [a]	$10^4 k_{obs}$	$10^3 k_{Hmal}$ [b]	$10^3 k_{Hmal}$ [c] (calc.)	$10^4 k_{cycl}$	$10^4 k_{cycl}$ [d] (calc.)
(°C)	[K]	(mM)	(s^{-1})	(M^{-1} s^{-1})	(M^{-1} s^{-1})	(s^{-1})	(s^{-1})
37.3	[310.5]	33	1.54±0.20	3.19	3.37	0.408±0.058	0.444
		17	0.544±0.017			0.482±0.065	
		3.3	0.222±0.02			0.441±0.053	
40.2	[313.4]	33	1.69±0.11	4.82	4.49	0.620±0.11	0.616
		17	1.05±0.09			0.603±0.096	
		3.3	0.409±0.029			0.604±0.10	
45.2	[318.4]	33	2.50±0.10	7.19	7.16	1.17±0.11	1.07
						1.01±0.11	
						0.955±0.055	
		17	1.48±0.03			1.01±0.08	
		3.3	0.504±0.052			1.10±0.31	
50.0	[323.2]	33	3.84±0.18	10.82	11.04	2.09±0.45	1.79
						1.71±0.34	
		17	2.10±0.06			1.85±0.5	
		3.3	0.599±0.023			1.61±0.065	

[a] Calculated from the weight of Na_2mal used.
[b] Calculated from the slopes of plots of k_{obs} versus [$Hmal^-$] (Figure 5.3).
[c] Calculated from the activation parameters: at 25 °C, $k_{Hmal} = 9.9 \times 10^{-4}$ M^{-1} s^{-1}, $\Delta H^{\neq} = 74.8 \pm 6$ kJ mol^{-1}, $\Delta S^{\neq} = -52 \pm 12$ J K^{-1} mol^{-1}.
[d] Calculated from the activation parameters: at 25 °C, $k_{cycl} = 1.03 \times 10^{-5}$ s^{-1}, $\Delta H^{\neq} = 88.9 \pm 4$ kJ mol^{-1}, $\Delta S^{\neq} = -42 \pm 8$ J K^{-1} mol^{-1}.

$$cis\text{-}[PtCl(NH_3)_2(OH_2)]^+ + H_2O \overset{\text{slow},k_2}{\rightleftharpoons} cis\text{-}[Pt(NH_3)_2(OH_2)_2]^{2+} + Cl^- \quad (5.12)$$

$$cis\text{-}[Pt(NH_3)_2(OH_2)_2]^{2+} + Hmal^- \overset{\text{fast}}{\rightarrow} cis\text{-}[Pt(Hmal)(NH_3)_2(OH_2)]^+ + H_2O \quad (5.13)$$

and a direct displacement of a ligand (water) by an incoming nucleophile ($Hmal^-$)

$$cis\text{-}[PtCl(NH_3)_2(OH_2)]^+ + Hmal^- \overset{\text{slow}k_{Hmal}}{\rightleftharpoons} [PtCl(Hmal)(NH_3)_2(OH_2)] \quad (5.14)$$

$$[PtCl(Hmal)(NH_3)_2(OH_2)] \rightarrow cis - [PtCl(Hmal)(NH_3)_2] + H_2O \quad (5.15)$$

There are valid reasons for believing that both routes involve associative processes. Two pieces of evidence are that variation of the charge of the platinum(II) complex has only a slight effect on the rate, and that an increase in stearic hindrance in the complex is accompanied by a decrease in reactivity [37,125] (Table 3.10).

If the rates of a reaction conform to the expression in Equation 5.11, then, under conditions of excess nucleophile (Nu) concentration, the observed first-order rate constant can be defined as in Equation 5.4, where Nu = $Hmal^-$, that is

$$k_{obs} = k_0 + k_{Hmal}[Hmal^-] \quad (5.16)$$

When k_{obs} is plotted against the concentration of NaHmal used, the slopes of the lines yield k_{Hmal} (M^{-1} s^{-1}) (Figure 5.3). For this particular reaction it would be expected that the intercept k_0, which corresponds to k_2 in Equation 1.2, would be approximately equal to zero as the background chloride release (Equation 1.2) has an unfavourable equilibrium constant (Figure 5.1) (Chapter 3). There will however be a small contribution to the overall reaction from this path but the data are not accurate enough to produce sensible values for the intercepts. The values for the more accurately determined slopes (k_{Hmal}, M^{-1} s^{-1}) are presented in Table 5.5.

As the reaction proceeded beyond this initial stage, a second phase developed, independent of the concentration of NaHmal used, and a sharp isosbestic point at 267 nm formed, with a decrease in the absorbance of the *cis*-$[PtCl(NH_3)_2(OR)]^+$ chromophore in the region 270 to 320 nm (Figure 5.4). The absorbance versus time data for this second reaction were monitored at 290 nm. It is believed that this second process involves the cyclisation of the platinum(II)-Hmal species, that is

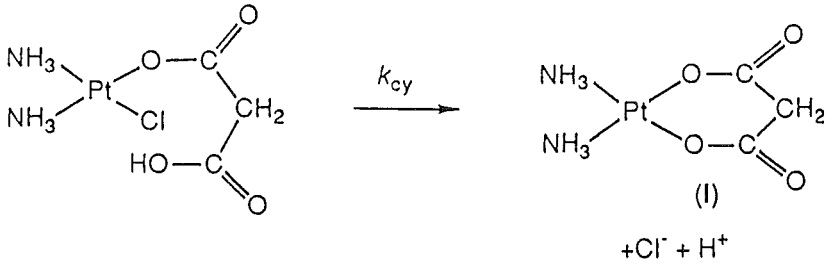

(5.17)

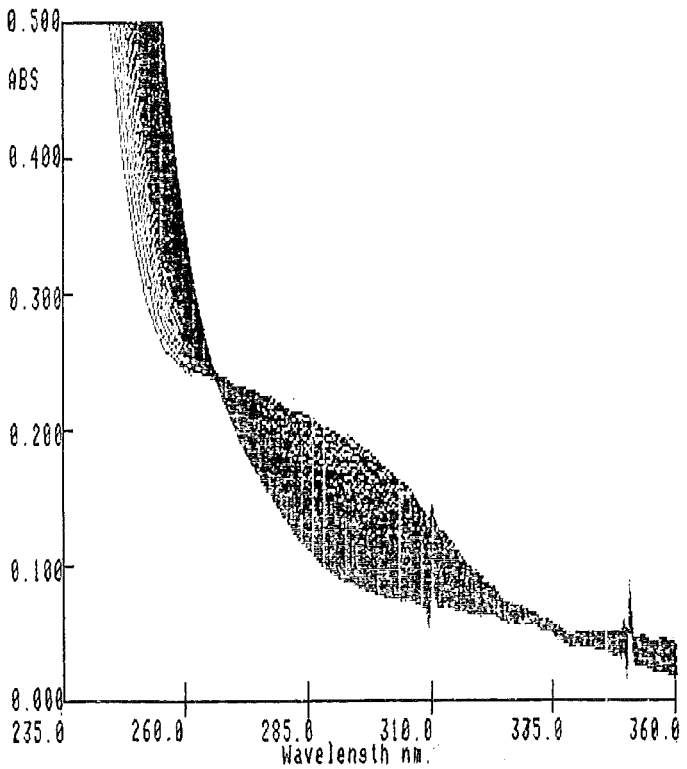

Figure 5.4. Spectrophotometric scans (5 minute intervals) for the second part of the anation reaction of *cis*-$[PtCl(NH_3)_2(OH_2)]^+$ by NaHmal at 45.1 °C and pH = 4.3 (μ = 1.0 *M*) (Equation 5.17). The absorbance at 300 nm decreases with time.

The rate constants (k_{cycl}, s^{-1}) obtained for this process are shown in Table 5.5. Previous investigations have shown that the species (I) can be synthesised in good yield from *cis*-DDP in aqueous DMF containing NaHmal [168].

Glycine is one of 20 amino acids commonly found in proteins [169], and is important for protein synthesis. It is a neutral amino acid and is one of the 'non-essential' amino acids, so called because it can be synthesised by the body and does not have to be obtained from dietary sources. It can react as either an acid or a base, depending on the circumstances. Amino acids contain both acidic and basic groups in the same molecule and for this reason they can undergo an intramolecular acid-base reaction and exist primarily as the bipolar ion or Zwitterion as shown below for glycine.

$$H_2\ddot{N}—CH_2—COOH \rightleftharpoons H_3N^+—CH_2—COO^- \qquad (5.18)$$

The reaction of *cis*-$[PtCl(NH_3)_2(OH_2)]^+$ with glycine was carried out at pH = 7.4, with the pH adjusted using 0.1 *M*NaOH. Very little subsequent pH adjustment was required as the reaction proceeded, due to the self-buffering nature of the glycine. The spectrophotometric changes associated with the reaction showed a well-defined isosbestic point at 275 nm (Figure 5.5). The final UV spectrum of the reaction was featureless with the absorbance increasing uniformly and continuously from 360 down

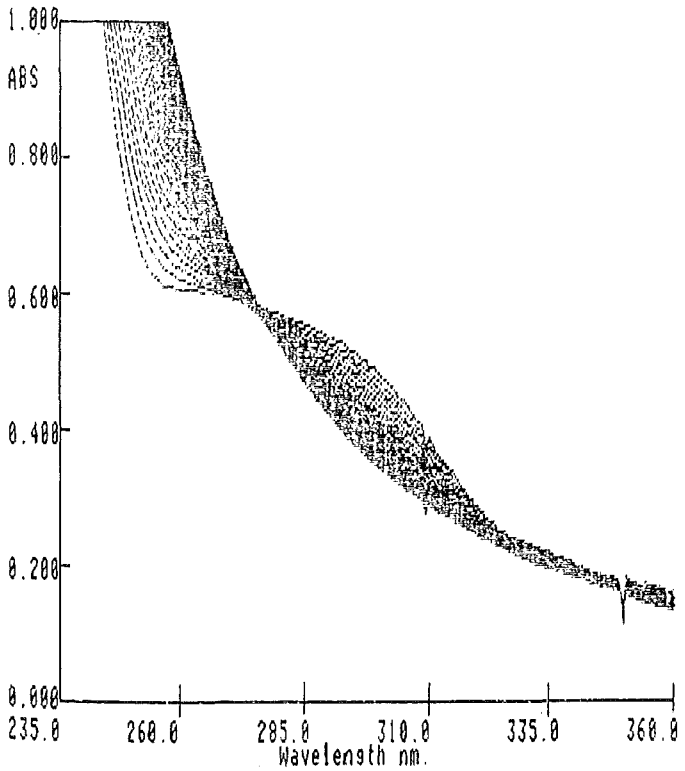

Figure 5.5. Spectrophotometric scans (5 minute intervals, 45.3 °C) for the anation reaction of *cis*-$[PtCl(NH_3)_2(OH_2)]^+$ with glycine at pH = 7.4 (μ = 1.0 *M*, $NaClO_4$) (Equation 5.20).

to 235 nm. The absorbance versus time data were collected at 304 and 245 nm and used to calculate the pseudo-first-order rate constants (k_{obs}, s^{-1}) (Table 5.6).

This reaction also obeyed Equation 5.4, thus k_{obs} was plotted against the glycine concentrations used (Figure 5.6). For this system, Equation 5.4 can be written

$$k_{obs} = k^2_{OH} + k_{gly}[\text{glycine}] \tag{5.19}$$

These plots were linear at the three temperatures that the reactions were carried out at. The slopes of the lines yielded values for k_{gly}. At pH = 7.4, it is believed that two competing reactions are occurring.

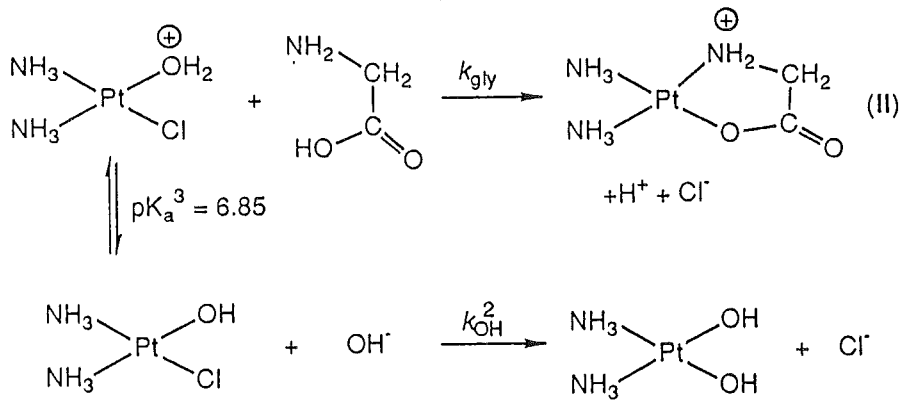

(5.20)

Table 5.6. Spectrophotometrically determined rate constants (k_{gly}, M^{-1} s^{-1}) for the reaction of *cis*-$[PtCl(NH_3)_2(OH_2)]^+$ with glycine (pH = 7.4; μ = 1.0 M, $NaClO_4$).

Temperature (°C)	[K]	[glycine] (M)	$10^4 k_{obs}$ (s^{-1})	$10^4 k_{gly}$ [a] (M^{-1} s^{-1})	$10^4 k_{gly}$ (calc.) [b] (M^{-1} s^{-1})	$10^5 k^2_{OH}$ [c] (s^{-1})	$10^5 k^2_{OH}$ [d] (s^{-1})
25.0	[298.2]				2.75		
35.2	[308.4]	0.1	1.12±0.21	6.69	6.57	4.71	4.37
			1.15±0.31				
		0.05	0.827±0.07				
			0.804±0.13				
		0.01	0.528±0.03				
			0.536±0.04				
40.2	[313.4]	0.1	1.96±0.46	9.48	9.85	9.71	7.54
			1.90±0.33				
		0.05	1.50±0.32				
			1.34±0.43				
		0.01	1.04±0.29				
			1.12±0.20				
45.3	[318.5]	0.1	3.39±0.55	15.0	14.7	17.7	12.1
			3.18±0.55				
		0.05	2.50±0.54				
			2.48±0.39				
		0.01	2.00±0.37				
			1.88±0.49				

[a] Estimated from the slope of plots of k_{obs} versus [glycine] (Figure 5.6).
[b] Calculated from the activation parameters: $\Delta H^{\neq}$ = 62.7 ± 5 kJ mol^{-1}, $\Delta S^{\neq}$ = −103 ± 10 J K^{-1} mol^{-1}.
[c] Estimated from the intercepts of the plots of k_{obs} versus [glycine] (Figure 5.6).
[d] Extrapolated from the k^2_{OH} data obtained independently and more reliably from the hydrolysis of *cis*-$[PtCl(OH)(NH_3)_2]$ in 0.1 M NaOH (Chapter 3).

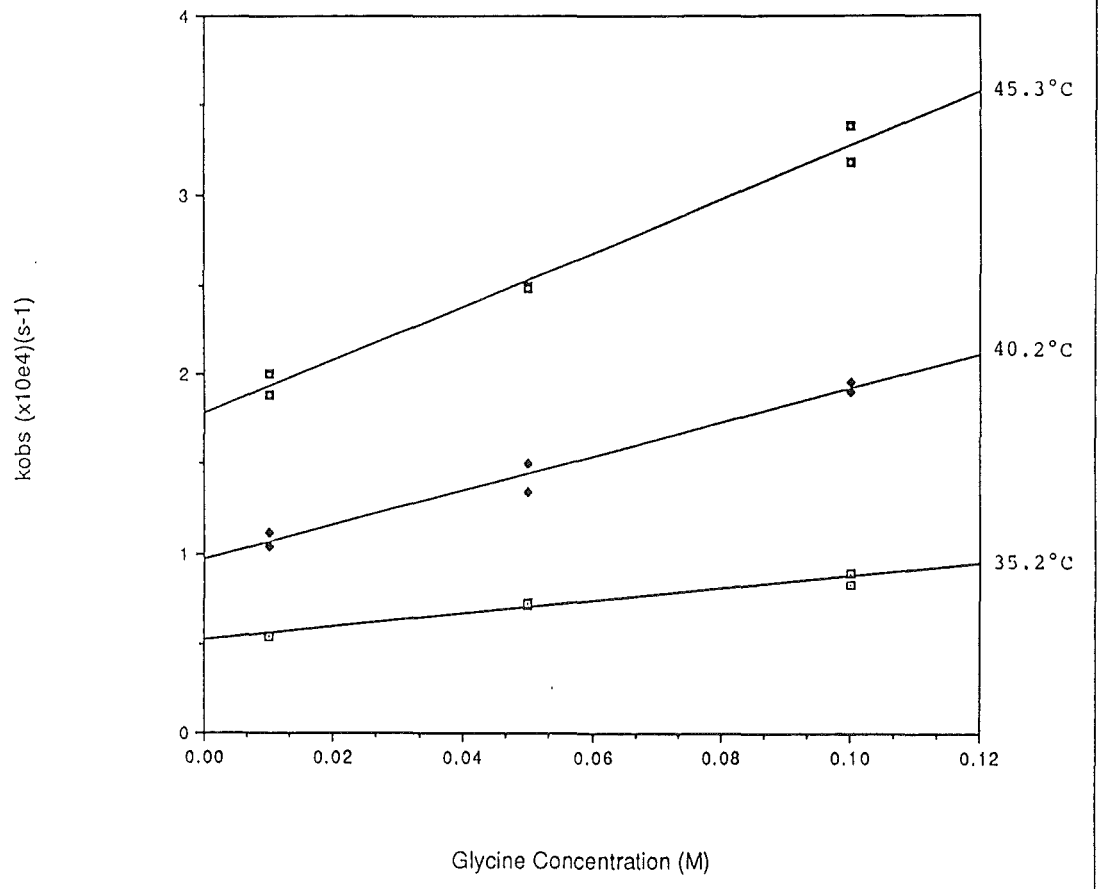

Figure 5.6. Plots of k_{obs} versus [glycine] for the anation of *cis*-$[PtCl(NH_3)_2(OH_2)]^+$ at pH = 7.4.

At this pH there will be both the *cis*-$[PtCl(NH_3)_2(OH_2)]^+$ and *cis*-$[PtCl(OH)(NH_3)_2]$ species present as well as the glycine nucleophile and hydroxide ions, therefore it seems reasonable to suppose that these two reactions are occurring. Evidence for this is provided by values obtained (k^2_{OH}) from the intercepts of the plots of k_{obs} versus glycine concentration with the y-axis. These values of k^2_{OH} (Table 5.6) so obtained are in agreement with those values obtained previously and independently of this experiment (Table 3.3).

Saudek and co-workers have investigated the reaction between *cis*-DDP and glycine at pH = 7.3 [170,171]. Using ^1H and ^{13}C NMR spectroscopy as a probe, the products of the reaction were determined to be mainly the species (II), with a trace of *cis*-$Pt(NH_2)_2(NH_2CO_2H)_2$, with the ratio of these two products to each other depending on the pH that the reaction was carried out at. The crystal structure of (II) has also recently been reported [172].

5.4 Conclusions.

It is thus possible to speculate further on the possible fate of hydrolysis products of *cis*-DDP under physiological conditions, as biological fluids contain ligands with both NH_2 (as amino acids) and carboxylate sites as potential donor groups. After hydrolysis of the *cis*-DDP in the cell plasma (where the chloride ion concentration is approximately 4 mM and the pH = 7.4), there is sufficient *cis*-$[PtCl(NH_3)_2(OH_2)]^+$ present at equilibrium, approximately 30% [159] (Chapter 4), to provide a reasonable concentration of labile platinum(II) species. This is in contrast to the remaining 60% *cis*-$[PtCl(OH)(NH_3)_2]$ which must be classed as inert with respect to anation. However, the inert *cis*-$[PtCl(OH)(NH_3)_2]$ can provide a mobile but unreactive source of labile *cis*-$[PtCl(NH_3)_2(OH_2)]^+$ since, as the *cis*-$[PtCl(NH_3)_2(OH_2)]^+$ is removed from the system by anation, *cis*-$[PtCl(OH)(NH_3)_2]$ will shift to the *cis*-$[PtCl(NH_3)_2(OH_2)]^+$ form to maintain the equilibrium concentrations, as determined by the $pK_a = 6.85$ [151].

Of the anating ligands investigated so far, the anionic systems such as chloride ion or the hydrogen malonate ion have been far more effective than the zwitterionic glycine, with a relative order of reactivity of 23 (chloride ion): 4 (hydrogen malonate ion): 1 (glycine) respectively (Table 5.4). The activation parameters for these reactions are similar therefore comparison of rate constants is a valid procedure. This order of reactivity is perhaps fortunate as otherwise protein material would compete unfavourably with the labile platinum(II) species for the binding sites in DNA.

CHAPTER 6

THE METAL ION ASSISTED AQUATION OF *cis*-DICHLORODIAMMINEPLATINUM(II) AND THE CRYSTAL STRUCTURE OF $[cis\text{-}[PtCl_2(NH_3)_2](HgCl_2)_3]_n$.

6.1 Introduction.

Under acid conditions, the rate of loss of the first chloro group from *cis*-DDP to give the *cis*-$[PtCl(NH_3)_2(OH_2)]^+$ species (k_1; Equation 1.1) has a half-life of approximately three hours at 25 °C, independent of the ionic strength or hydrogen ion concentration (Chapter 2). Loss of the second chloro group to give the *cis*-$[Pt(NH_3)_2(OH_2)_2]^{2+}$ species does not occur under these conditions due to the unfavourable equilibrium constant (K_2) associated with Equation 1.2, although a value for the rate constant k_2 for this process has been obtained indirectly from values of k_{-2} and K_2 determined in Chapter 3.

A chemical procedure used to accelerate chloride release from relatively inert metal chloro complexes is to add a metal ion, M^{n+}, which forms a strong M—Cl bond, for example, Hg^{2+}, Tl^{3+} or Pb^{2+}, or which precipitates an insoluble MCl_x salt, for example, Ag^+ or Hg_2^{2+}. Attempts to measure the rate of the Hg^{2+}-assisted aquation of *cis*-DDP using spectrophotometric techniques were initially thwarted by the high UV absorbance (345 to 230 nm) of solutions of Hg^{2+} in HNO_3 or $HClO_4$, but it was found that $HgCl_2$ or PbO dissolved in $HClO_4$ were sufficiently transparent in this region to enable kinetic measurements to be made. Thus rate constants for the $HgCl_2$-assisted and Pb^{2+}-assisted aquation reactions of *cis*-$[PtCl_2(NH_3)_2]$ were obtained.

Thus, in this Chapter, the rate constants and activation parameters for the metal ion assisted hydrolysis or aquation of *cis*-DDP using $HgCl_2$ and Pb^{2+} ions were determined. The effects of other metal ions not only on the acid hydrolysis reaction of *cis*-DDP but also on its base hydrolysis reaction were also investigated. An additional feature of this work was that crystals of the reaction product were obtained from the $HgCl_2$-assisted aquation of *cis*-DDP and the X-ray crystallographic data for structure are also presented in this Chapter.

6.2 Experimental.

6.2.1 Measurement of Rate Constants.

Solutions of $HgCl_2$ (22.1 to 36.8 mM) in various $HClO_4$ / $NaClO_4$ media were prepared from weighed amounts of the solid and allowed to reach thermal equilibrium in a temperature controlled water bath. A small sample (5 to 8 mg) of *cis*-DDP was dissolved in a few drops of DMF in a 1.00 cm quartz spectrophotometer cell and this solution was allowed to reach thermal equilibrium in the temperature controlled cell compartment of the spectrophotometer. The appropriate $HgCl_2$ / $HClO_4$ / $NaClO_4$ solution (2.5 to 3.0 ml) was then added and, after mixing, the absorbance versus time data were collected at 300 nm (and also at 285 and 310 nm if the time-scale of the reaction permitted) at appropriate time intervals (Figure 6.1). The reactions were monitored for six to eight half-lives and, as the initial $HgCl_2$ concentration was always greater than ten times that of the initial *cis*-DDP concentrations, pseudo-first-order rate constants (k_{obs}, s^{-1}) could be calculated (Table 6.5). Second-order rate constants (k_{Hg}, M^{-1} s^{-1}) (Table 6.5) were obtained from the expression

$$k_{Hg} = k_{obs}[HgCl_2]^{-1} \tag{6.1}$$

Plots of k_{obs} versus the $HgCl_2$ concentrations used were obtained (Figure 6.2) and, using Equation 5.4 (Chapter 5), $k_0 = 0$ and calculated values for $k_{Nu} = k_{Hg}$ were obtained from the slopes of these plots.

The solutions of Pb^{2+} in $HClO_4$ were prepared by dissolving the appropriate weight of PbOin 1.0 $M$$HClO_4$. Small samples of *cis*-DDP ($\sim$ 5 mg) were dissolved in the thermally equilibrated Pb^{2+} solution in a 1.00 cm spectrophotometer cell and absorbance versus time data were collected at 300 and 260 nm while the spectrophotometer was operating in the repeat scan mode between 350 and 250 nm (Figure 6.6). The pseudo-first-order rate constants (k_{obs}, s^{-1}) obtained (Table 6.10) were plotted against the concentrations of Pb^{2+} used (Figure 6.7), and, following Equation 5.4, values for $k_0 = k_1$ (s^{-1}) (Equation 1.1) and the second-order rate constant $k_{Nu} = k_{Pb}$ (M^{-1} s^{-1}) were calculated from the least squares intercepts and slopes of these plots (Table 6.11).

6.2.2 Formation and Structure of $[cis\text{-}[PtCl_2(NH_3)_2](HgCl_2)_3]_n$.

To a solution of 0.03 M $HgCl_2$ in 0.01 M $HClO_4$ (20 ml) was added 20 mg of *cis*-DDP. The mixture was heated at about 60 °C for approximately two hours and then allowed to cool slowly to room temperature in the dark. Pale yellow needles, suitable for single crystal X-ray analysis, deposited over the next 48 hours. The following structural analysis was performed by Miss Huo Wen and Dr W. T. Robinson.

Intensity data for a small, elongated, rod-like crystal (0.10 x 0.12 x 0.48 mm) were collected with a Nicolet R3m four-circle diffractometer at -125 °C. Graphite monochro-

Table 6.1. Crystal Data.

Complex	$[cis\text{-}[PtCl_2(NH_3)_2](HgCl_2)_3]_n$	Transmission factors	0.331, 0.192
Molecular formula	$H_6N_2Cl_8PtHg_3$	Scan mode	ω
Formula weight	1114.53	Octants	0, 0, -l; h, k, l
Space group	monoclinic, C2/c	$2\theta_{max}$ (°)	60 °
a (Å)	18.532(5)	Reflections measured	2179
b (Å)	6.506(2)	Reflections used	1653
c (Å)	12.492(4)	Parameters refined	61
β (°)	98.76(3)	Weighting (g $\times 10^3$)	5.55
V (Å^3)	1485.5(8)	R	0.0591
Z	4	R_W	0.0630
D_{calc} (g/cc)	4.98		
Temperature (°C)	-125		
F(000)	1859.27		
Abs. correction (cm^{-1})	418.21		

Table 6.2. Anisotropic thermal parameters (Å$^2 \times 10^3$) for $[cis\text{-}[PtCl_2(NH_3)_2](HgCl_2)_3]_n$. [a]

Atom	U_{11}	U_{22}	U_{33}	U_{23}	U_{13}	U_{12}
Hg(1)	5(1)	15(1)	10(1)	4(1)	1(1)	-4(1)
Pt(1)	2(1)	10(1)	3(1)	0	1(1)	0
Hg(2)	4(1)	15(1)	15(1)	2(1)	2(1)	-4(1)
Cl(1)	10(2)	9(2)	14(2)	-0(2)	6(1)	-3(2)
Cl(2)	8(2)	14(2)	20(2)	4(2)	4(1)	-2(2)
Cl(3)	10(2)	21(2)	20(2)	3(2)	4(2)	-9(2)
Cl(4)	4(2)	17(2)	8(2)	-3(2)	1(1)	1(1)

[a]The anisotropic temperature factor exponent takes the form: $-2\pi^2\left(h^2a^{*2}U_{11} + \cdots + 2hka^*b^*U_{12}\right)$.

mated MoK_α radiation (0.71069 Å) was used, with fixed ω scans. Cell parameters were determined by least squares refinement of 25 accurately centered reflections. During the data collection, the intensities of three standard reflections were monitored at regular intervals and these indicated no significant crystal decomposition. The collected intensities were corrected for Lorentz, polarisation and absorption effects (both automatically and from crystal indexing) (Table 6.1).

The structure was solved by conventional Patterson and Fourier methods and refined by blocked cascade least-squares procedures. The Pt and Hg atoms were distinguished on the basis of chemical reasoning, and all atoms heavier than nitrogen were refined with anisotropic thermal parameters (Tables 6.2 and 6.3). In the last cycles of refinement, the appropriate N—H hydrogen atoms were included in their calculated positions. All calculations were performed on a DG300 computer using the SHELXTL suite of programs [173] and Table 6.4 lists the non-hydrogen atom coordinates.

Table 6.3. Hydrogen atom coordinates ($\times 10^4$) and isotropic thermal parameters for $\left[cis\text{-}\left[PtCl_2(NH_3)_2\right](HgCl_2)_3\right]_n$.

Atom	x	y	z	U
H(1a)	1230	2968	2198	14
H(1b)	871	5473	2945	14
H(1c)	610	5471	1689	14

Table 6.4. Non-hydrogen atom coordinates ($\times 10^4$) for $\left[cis\text{-}\left[PtCl_2(NH_3)_2\right](HgCl_2)_3\right]_n$.

Atom	x	y	z
Hg(1)	0	0	0
Pt(1)	0	2398(2)	2500
Hg(2)	1996(1)	149(1)	-792(1)
Cl(1)	-639(2)	-2911(7)	345(3)
Cl(2)	1503(2)	-2672(7)	-58(4)
Cl(3)	2548(3)	2852(8)	-1537(4)
N(1)	784(9)	4629(26)	2307(14)
Cl(4)	851(2)	-78(7)	2252(4)

6.3 Results and Discussion.

Removal of certain coordinated ligands from complexes is enhanced considerably by the addition of some labile metal ions [174]. The rates of aquation of various transition metal complexes have been found to be accelerated to various degrees by different metal ions of 'hard', 'intermediate' and 'soft' types. The leaving groups or atoms include halides, alkyl groups and carboxylates among others. Most studies of such 'assisted' hydrolysis reactions have almost solely concerned cobalt(III) or chromium(III) complexes and there is very little data available on such assisted reactions of platinum(II) complexes [175,176,177].

For halogeno complexes such as *cis*-DDP, the rate of hydrolysis is considerably enhanced by the addition of halide abstractors such as Hg^{2+}, Tl^{3+} or Ag^{+} to the acidic solution [122]. Technically these metal ions are not catalysts as the initial and final states of the added reagent (*cis*-DDP) are different although the term is occasionally used in the literature, but 'assisted' is more correct. Depending on the conditions used, during the course of an assisted hydrolysis reaction, the assisting metal ion may find itself distributed in various forms. For example, during the course of an Hg^{2+}-assisted aquation of a chloro complex (RCl) in nitrate media, Hg^{2+}, $HgCl^{+}$, $HgCl(NO_3)$, R–$ClHg^{2+}$, R–$ClHgCl^{+}$ *etc.* all might be present [174]. Hydrolysed species such as $Hg(OH)^{+}$ are present in most cases since, generally, the pH of the media used is much lower than the pK_h (where K_h is the hydrolysis constant of the metal ion [37]). In the case of the Zn^{2+}-assisted base hydrolysis of *cis*-DDP however, the species $[Zn(OH)_4]^{2-}$ would be present.

Most kinetic studies in this area [174] involve either Hg^{2+} or Tl^{3+} as the metal ion

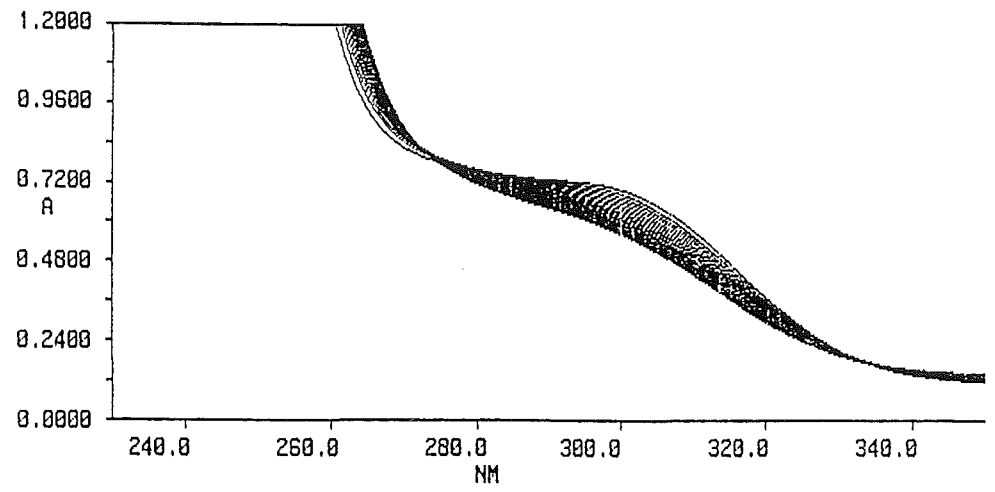

Figure 6.1. Spectrophotometric scans for the metal ion assisted aquation of *cis*-$[PtCl_2(NH_3)_2]$ ($\sim 2 \times 10^{-3}$ *M*) using $HgCl_2$ (0.022 *M*) dissolved in 0.1 *M* $HClO_4$ at room temperature. The decrease in absorbance corresponds to a repeat scan every 600 s.

assisting halide release [122] because the formation of a precipitate limits the methods available to monitor the reaction and heterogeneous systems are often subject to complicating surface effects. Nevertheless, the addition of stoichiometric quantities of Ag^+ to *cis*-DDP, followed by filtration of the AgCl, is the standard synthetic route to produce *cis*-$[PtCl(NH_3)_2(OH_2)]^+$ or *cis*-$[Pt(NH_3)_2(OH_2)_2]^{2+}$ in solution [178].

The spectrophotometric changes that take place on mixing solutions of $HgCl_2$ in $HClO_4$ / $NaClO_4$ with *cis*-DDP in DMF are shown in Figure 6.1. Although for most of the data obtained the *cis*-DDP was dissolved in DMF prior to the addition of the $HgCl_2$ / $HClO_4$ / $NaClO_4$ solution, experiments without DMF gave entirely similar results. Satisfactory isosbestic points were maintained at 275 and 335 nm, indicating a monophasic reaction, and the final absorbance spectra corresponded to that expected for *cis*-$[Pt(NH_3)_2(OH_2)_2]^{2+}$ dissolved in $HgCl_2$ / $HClO_4$ / $NaClO_4$ solutions. It is thus believed that the reaction under investigation here corresponded to Equations 6.2 and 6.3, with both chloride ligands on the *cis*-DDP being displaced simultaneously.

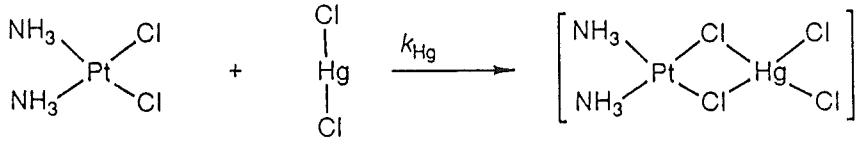

(6.2)

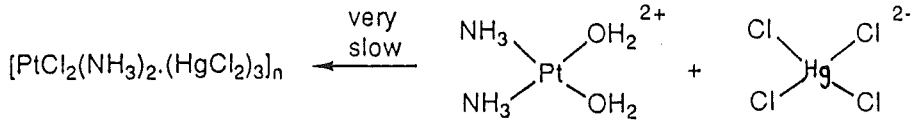

(6.3)

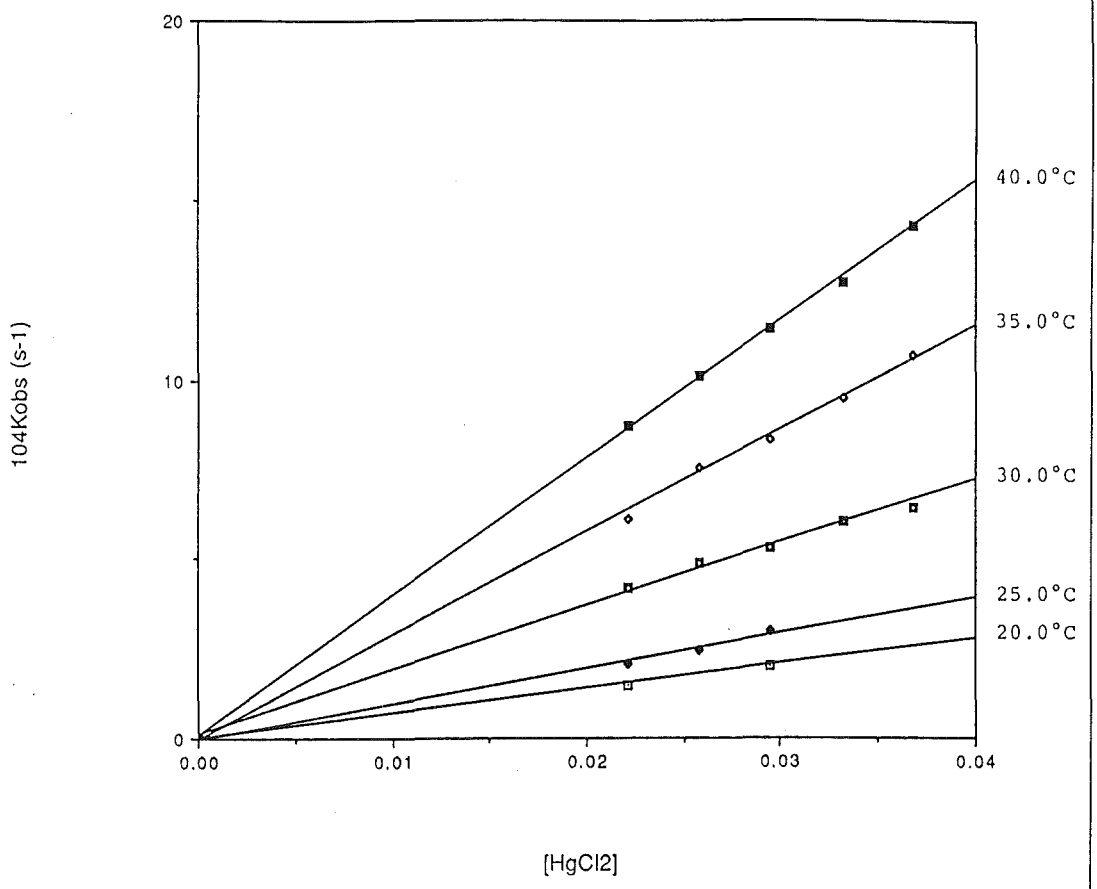

Figure 6.2. Plots of k_{obs} versus $[HgCl_2]$ for the metal ion assisted aquation of *cis*-$[PtCl_2(NH_3)_2]$ ($\mu = 1.0$ *M*).

This conclusion is also supported by the kinetic analysis, since excellent linear plots of k_{obs} versus the initial $HgCl_2$ concentrations used were obtained over a 20 °C temperature range, with the intercepts of the plots at the origin (Figure 6.2). One drawback was that only a limited range of initial $HgCl_2$ concentrations could be used as the lowest end (0.02 *M*) was constrained by the initial concentration of *cis*-DDP required and used for these experiments, and at the upper end, high concentrations of $HgCl_2$ (initial $HgCl_2$ concentrations above 0.04 *M*) resulted in the rapid formation of a precipitate. The reaction rate was found to be independent of hydrogen ion concentration (0.01 to 1.0 *M*) and ionic strength (0.01 to 1.0 *M*) (Table 6.5) and activation parameters of $\Delta H^{\neq} = 67.9$ kJ mol^{-1} and $\Delta S^{\neq} = -55.0$ J K^{-1} mol^{-1} were calculated from the variation of k_{Hg} with temperature.

Although $HgCl_2$ is regarded as a rather poor chloride abstractor [122,174], addition of this reagent to dissolved *cis*-DDP most definitely facilitates chloride release. For example, addition of 22.1 m*M* $HgCl_2$ to 2 m*M* *cis*-DDP reduces the half-life for acid hydrolysis from three hours to one hour at 25 °C but significantly different products are formed. Very few $HgCl_2$-assisted halide release reactions have been reported [174],

Table 6.5. Spectrophotometrically determined rate constants (k_{Hg}) for the metal ion assisted aquation of *cis*-$[PtCl_2(NH_3)_2]$ using $HgCl_2$ ($\mu = 1.0\ M$; $HClO_4$, $NaClO_4$). [a]

$[HgCl_2]_i$ (mM)	Temperature (°C)	[K]	$10^4 k_{obs}$ (s^{-1})	$10^2 k_{Hg}$ [b] ($M^{-1}\ s^{-1}$)	$10^2 k_{Hg}$ (calc.) ($M^{-1}\ s^{-1}$)	
22.1	20.0	[293.2]	1.47(2)	0.665(1)	0.675 [c]	0.662 [d]
29.5			2.00(3)	0.678(1)		
22.1	25.0	[298.2]	2.05(2)	0.928(1)	0.978	1.07
25.8			2.42(1)	0.938(1)		
29.5			2.98(8)	1.01(1)		
22.1	30.0	[303.3]	4.15(13)	1.88(6)	1.77	1.71
25.8			4.83(2)	1.87(1)		
29.5			5.25(10)	1.78(3)		
33.2			6.00(9)	1.81(3)		
36.8			6.41(4)	1.74(1)		
22.1	35.0	[308.2]	6.09(8)	2.76(4)	2.89	2.70
25.8			7.51(26)	2.91(10)		
29.5			8.33(9)	2.82(3)		
			7.04(4) [e]	2.39(1)		
			8.33(29) [f]	2.82(10)		
			9.67(25) [g]	3.28(9)		
33.2			9.51(5)	2.87(2)		
36.8			10.7(12)	2.91(3)		
22.1	40.0	[313.2]	8.73(1)	3.95(1)	3.87	4.18
25.8			10.1(1)	3.92(1)		
29.5			11.5(10)	3.89(3)		
33.2			12.7(19)	3.84(6)		
36.8			14.3(17)	3.89(5)		

[a] Numbers in parentheses are the uncertainty (standard deviation) in the last digit(s) from > 20 data points for each kinetic run.

[b] Determined using Equation 6.1

[c] Calculated from a linear least-squares analysis of plots of $[HgCl_2]_i$ versus k_{obs}.

[d] Calculated from the activation parameters obtained for k_{Hg} *viz*, $\Delta H^{\neq} = 67.9 \pm 2$ kJ mol^{-1} and $\Delta S^{\neq} = -55.0 \pm 4$ J K^{-1} mol^{-1}

[e] $[HClO_4] = 0.01\ M$; $[NaClO_4] = 0.99\ M$; $\mu = 1.0\ M$.

[f] $[HClO_4] = 0.1\ M$; $[NaClO_4] = 0.9\ M$; $\mu = 1.0\ M$.

[g] $[HClO_4] = 1.0\ M$; $\mu = 1.0\ M$.

although the reactions shown in Equations 6.4 and 6.5 have been studied spectrophotometrically

$$Pt(X)(gly)(NH_3) + Hg^{2+} \xrightarrow{k_f} Pt(gly)(NH_3)(XHg)^{2+} \quad (6.4)$$

$$Pt(gly)(NH_3)(XHg)^{2+} \xrightarrow{k_d} Pt(gly)(NH_3)(H_2O)^{+} + HgX^{+} \quad (6.5)$$

A well defined adduct has been characterised and its rate of formation (k_f) and decomposition measured [175,176,177]. Although probably fortuitous rather than meaningful, the rate of adduct formation ($k_f = 2 \times 10^{-2}\ M^{-1}\ s^{-1}$ at 25 °C) for $PtCl(NH_3)(gly)$ is of a similar magnitude to the $HgCl_2$-assisted chloride release from *cis*-DDP ($k_{Hg} = 1 \times 10^{-2}\ M^{-1}\ s^{-1}$ at 25 °C).

The concept of simultaneous release of both chloro ligands via a cyclic binuclear intermediate of the type shown in Equation 6.2 is not new and similar adducts have been proposed for the Hg^{2+}-assisted chloride ion release from some *cis*-$Co(L_4)Cl_2^{+}$ complexes [179,180,181]. Indeed, the structure of the binuclear complex *cis*-$[Rh(en)_2Cl_2]Cl.HgCl_2$ clearly shows the formation of a μ-dichloro bridged system [182]. Also, there are analagous structures reported for square planar, four coordinate metal systems which exhibit the metal-μ-dichloromercury(II) bridge system [183,184]. It must be noted, however, that the end product $[PtCl_2(NH_3)_2.(HgCl_2)_3]_n$ from the reaction between *cis*-DDP and $HgCl_2$ contains only platinum-μ-monochloromercury(II) bridges.

Crystals of the product $[PtCl_2(NH_3)_2.(HgCl_2)_3]_n$ deposit if the contents of the spectrophotometric cell (in the absence of DMF) are allowed to cool overnight. The single crystal X-ray structural analysis shows these to have a polymeric structure (Figure 6.3 and 6.5), similar to those reported for $[Et_4N]_2Hg_2PtCl_8$ and $[Et_4N]_2Hg_3PtCl_{10}$ [184]. In $[cis\text{-}[PtCl_2(NH_3)_2](HgCl_2)_3]_n$, the *cis*-$[PtCl_2(NH_3)_2]$ units are linked into chains by bridging of the chloro ligands through a $HgCl_2$ molecule lying on a special position (Cl(4)—Hg(1) = 3.004(4) Å). The chloro ligand bound to the platinum is also linked (Cl(4)—Hg(2) = 2.979(4) Å) to a second $HgCl_2$ molecule, whose next closest Hg...Cl interaction is at 3.25 Å, from an equivalent $HgCl_2$ molecule in another chain (Figure 6.4). Thus the chloro ligands bound to the platinum(II) are weakly linked to two $HgCl_2$ molecules.

Bond lengths and angles within the *cis*-DDP molecule are similar to those found in isolated *cis*-DDP [13] and its DMF adduct [185] (Table 6.6). The short Hg—Cldistances and the Cl—Hg—Cl angles in both the chain (Hg(1)) and terminal (Hg(2)) $HgCl_2$ molecules are similar to those found in isolated $HgCl_2$ or some of its weaker adducts (Table 6.7). The bridging Hg—Cl distances, for example, Pt—Cl(4)...Hg(1) (3.004(4) Å) in the chain or Pt—Cl(4)...Hg(2) (2.979(4) Å) for the terminal Hg atoms, are well within the sum of the Hg...Cl Van der Waals radii of 3.25 Å. Other bond lengths and bond angles are listed in Tables 6.8 and 6.9.

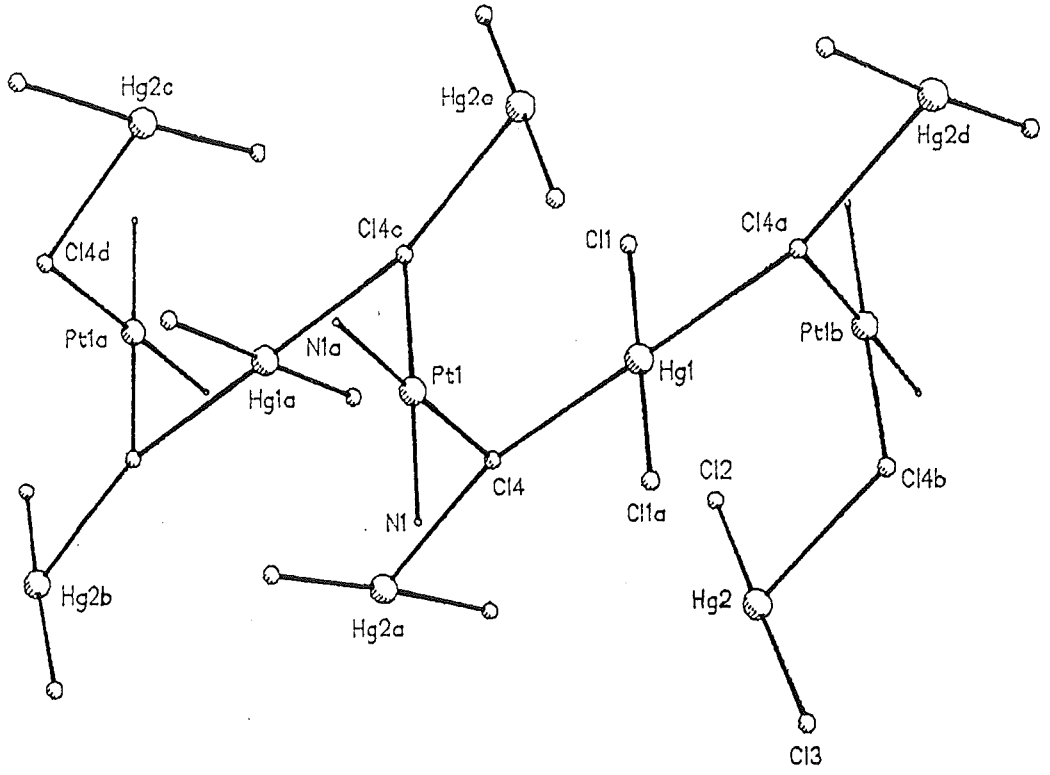

Figure 6.3. A view of the $\left[cis\text{-}\left[PtCl_2(NH_3)_2\right](HgCl_2)_3\right]_n$ chain showing the atom numbering system adopted.

Table 6.6. Bond lengths and bond angles in $cis\text{-}\left[PtCl_2(NH_3)_2\right]$ and its adducts. [a]

Complex	Pt—Cl (Å)	Pt—N (Å)	Cl—Pt—Cl (°)	N—Pt—N (°)
$cis\text{-}\left[PtCl_2(NH_3)_2\right]$ [b]	2.33(1) × 2	2.01(1) × 2	91.9(3)	87(1.5)
$cis\text{-}\left[PtCl_2(NH_3)_2\right]$.DMF [c]	2.315(7) 2.306(7)	2.00(2) 2.08(2)	92.4(3)	91.0(7)
$\left[cis\text{-}\left[PtCl_2(NH_3)_2\right](HgCl_2)_3\right]_n$ [d]	2.307(5) 2.308(5)	2.093(17) × 2	91.5(2)	92.2(1.0)

[a] See also [186] for the structure of $cis\text{-}\left[PtCl_2(NH_3)_2\right]$.DMA. $(18-\text{Crown}-6)_{1/2}$.
[b] Reference [13]
[c] Reference [185]
[d] Chapter 6

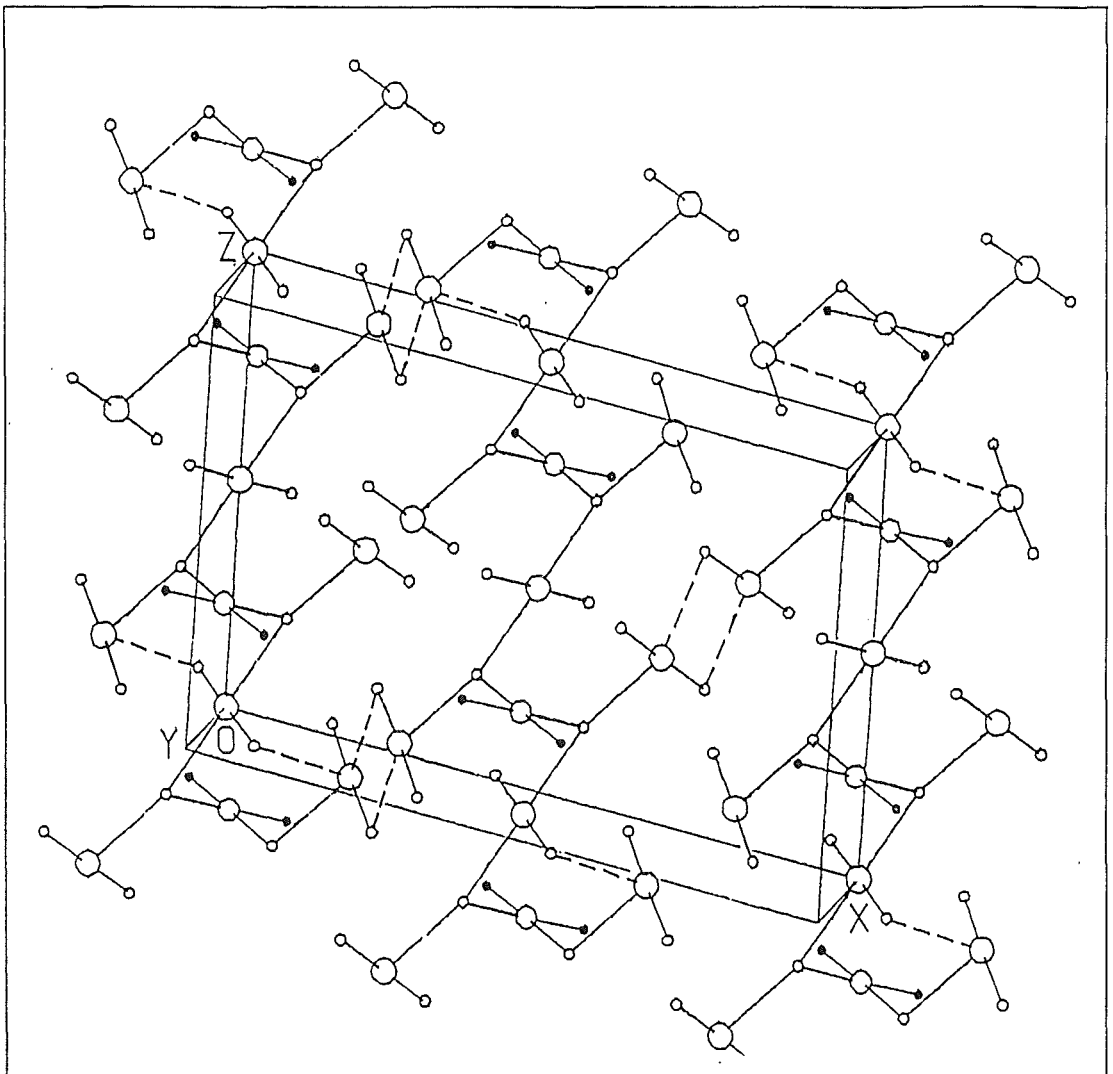

Figure 6.4. A packing diagram for $\left[cis\text{-}\left[PtCl_2(NH_3)_2\right](HgCl_2)_3\right]_n$.

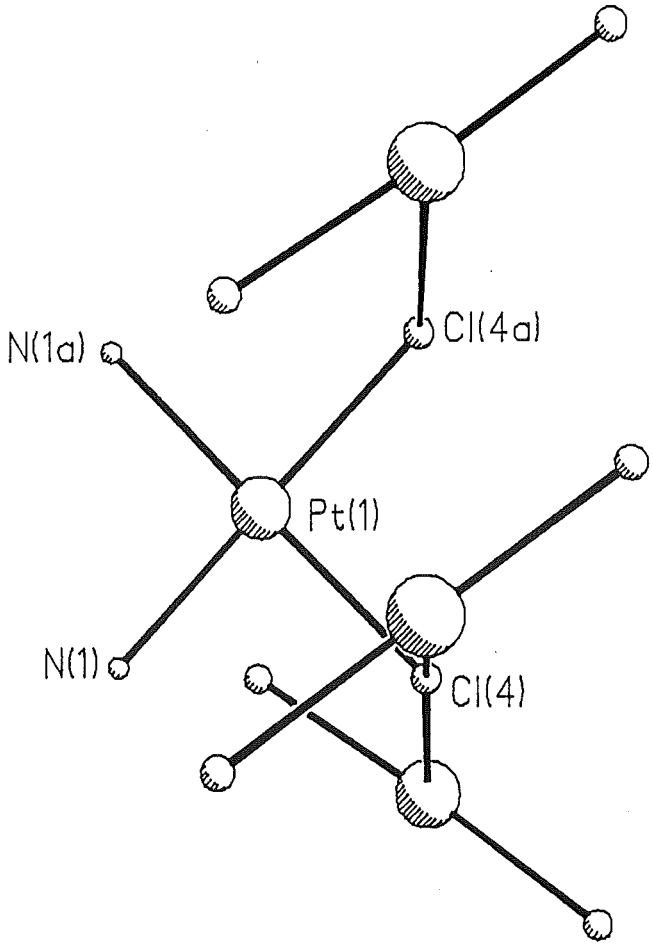

Figure 6.5. A view of the $\left[cis\text{-}\left[PtCl_2(NH_3)_2\right](HgCl_2)_3\right]_n$ unit.

Table 6.7. Bond lengths and angles in $HgCl_2$ and some adducts.

Compound	Hg—Cl (Å)	Hg...Cl (Å)	Cl—Hg—Cl (°)	Reference
$HgCl_2$ (cryst.)	2.284(12) 2.301(14)	3.37	178.9(5)	[187]
$HgCl_2$ (gas)	2.252(5) × 2		180(16)	[188]
$HgCl_2$ (encapsulated)	2.327(7) 2.304(7)		172.7(2)	[189]
$[H_4TTF][HgCl_2]_3$	2.309(5) × 2	2.989(6) × 2 3.235(5) × 2	180	[190]
$[DMSO]_2[HgCl_2]_3$	2.306(6) × 2	3.004(5) × 2 3.081(6) × 2	180	[191,192]
$HgCl_2$ ("chain")	2.308(5) × 2	3.004(4) × 2	180	Chapter 6
$HgCl_2$ ("terminal")	2.301(5) 2.300(5)	2.979(4)	176.6(2)	Chapter 6

Table 6.8. Bond lengths (Å) in $\left[cis\text{-}\left[PtCl_2(NH_3)_2\right](HgCl_2)_3\right]_n$.

Hg(1)—Cl(1)	2.308(5)	Hg(1)—Cl(4)	3.004(4)
Hg(1)—Cl(1A)	2.308(5)	Hg(1)—Cl(4A)	3.004(4)
Pt(1)—N(1)	2.093(17)	Pt(1)—Cl(4)	2.307(5)
Pt(1)—N(1A)	2.093(17)	Pt(1)—Cl(4C)	2.308(5)
Hg(2)—Cl(2)	2.301(5)	Hg(2)—Cl(3)	2.300(5)
Hg(2)—Cl(4B)	2.979(4)		
Cl(4)—Hg(2A)	2.979(4)		

Table 6.9. Bond angles (°) for $\left[cis\text{-}\left[PtCl_2(NH_3)_2\right](HgCl_2)_3\right]_n$.

Cl(1)—Hg(1)—Cl(1A)	180.0(1)
Cl(1)—Hg(1)—Cl(4A)	88.7(1)
Cl(1A)—Hg(1)—Cl(4A)	91.3(1)
N(1)—Pt(1)—N(1A)	92.2(10)
N(1)—Pt(1)—Cl(4C)	178.8(4)
N(1A)—Pt(1)—Cl(4C)	88.2(5)
Cl(2)—Hg(2)—Cl(4B)	92.1(1)
Hg(1)—Cl(4)—Pt(1)	80.9(1)
Pt(1)—Cl(4)—Hg(2A)	108.5(2)
Cl(1)—Hg(1)—Cl(4)	91.3(1)
Cl(4)—Hg(1)—Cl(1A)	88.7(1)
Cl(4)—Hg(1)—Cl(4A)	180.0(1)
N(1)—Pt(1)—Cl(4)	88.2(5)
Cl(4)—Pt(1)—N(1A)	178.8(4)
Cl(4)—Pt(1)—Cl(4C)	91.5(2)
Cl(2)—Hg(2)—Cl(3)	176.6(2)
Cl(3)—Hg(2)—Cl(4B)	89.2(1)
Hg(1)—Cl(4)—Hg(2A)	166.5(2)

During investigation of the Pb^{2+}-assisted chloride release from *cis*-DDP, it was found that solutions of PbO dissolved in $HClO_4$ were not completely transparent in the 250 to 350 nm region and as the concentration of Pb^{2+} increased, an increasingly dominant absorbance also developed (Figure 6.6). As a consequence, at high concentrations of Pb^{2+}, the initial absorption spectrum of *cis*-DDP dissolved in this medium was considerably distorted from that observed in $HClO_4$ alone (Figure 2.1). However, at all Pb^{2+} concentrations the maximum at 300 nm was maintained and, as the reaction proceeded, this peak decreased in intensity. As the Pb^{2+} concentration was increased, this initial minimum became less well defined and at a Pb^{2+} concentration of 0.1 *M* it was no longer discernable. The absorbance of the final product, *cis*-$[PtCl(NH_3)_2(OH_2)]^+$ was also distorted as the Pb^{2+} concentration increased. At low concentrations of Pb^{2+}, only the 263 nm maximum observed in $HClO_4$ was observed, but by increasing the Pb^{2+} concentration, the 240 nm minimum was slowly enveloped in the background continuum. At low Pb^{2+} concentrations, the reaction also proceeded with an isosbestic point at 282 nm, identical in position to the aquation in the absence of Pb^{2+}, but as the Pb^{2+} concentration increased, this point also became less distinct (at 0.1 *M* Pb^{2+}) and was lost completely at Pb^{2+} concentrations greater than or equal to 0.12 *M*.

As is shown in Table 6.10, the rate of hydrolysis was increased in the presence of Pb^{2+} ions, and the Pb^{2+} dependence is described by Equation 5.4, in the form

$$k_{obs} = k_1 + k_{Pb}\left[Pb^{2+}\right] \tag{6.6}$$

Plots of Pb^{2+} concentration versus k_{obs} were found to be linear (Figure 6.7) and the

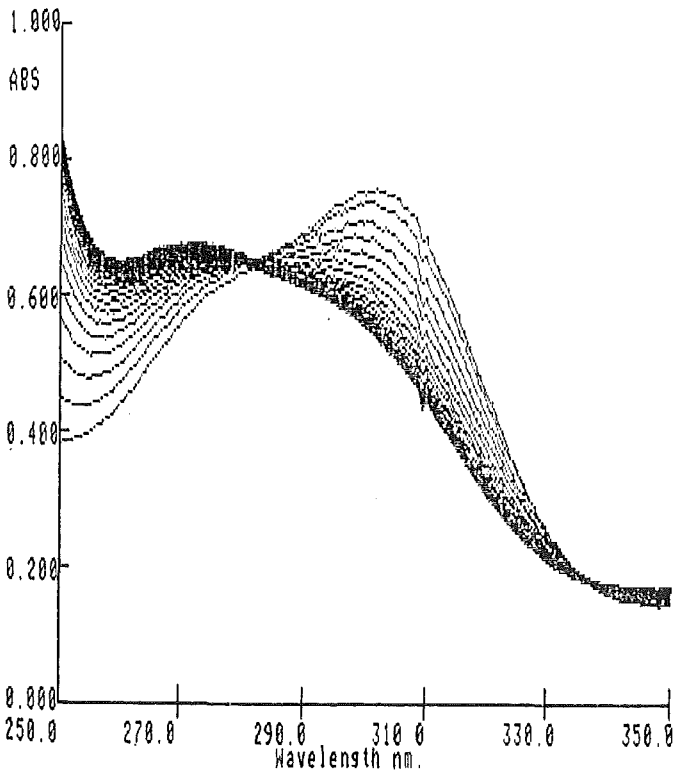

Figure 6.6. Spectrophotometric scans (5 minute intervals) for the metal ion assisted aquation of *cis*-$[PtCl_2(NH_3)_2]$ using Pb^{2+} ions at 45.2 °C (μ = 1.0 *M*, $HClO_4$). The absorbance at 300 nm decreases with time and increases with time at 265 nm.

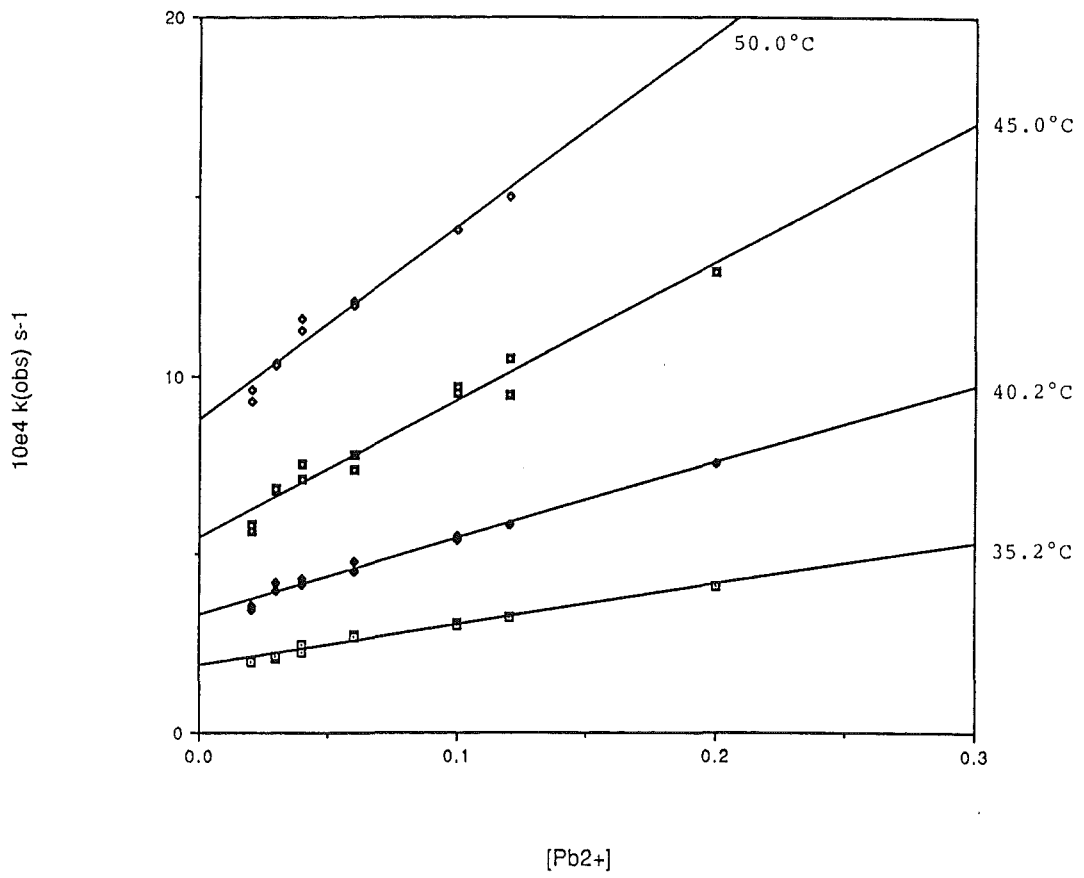

Figure 6.7. Plots of k_{obs} versus $[Pb^{2+}]$ for the metal ion assisted aquation of *cis*-$[PtCl_2(NH_3)_2]$ ($\mu = 1.0$ *M*).

slopes of these plots yielded values for k_{Pb} (M^{-1} s^{-1}) and the intercepts of the plots with the y-axis gave values equal to k_1 (s^{-1}) (Table 6.11), the rate of aquation in the absence of Pb^{2+} ions (Table 2.1). The acceleratory influence of Pb^{2+} is not large, with a rate increase of only about 2.3 observed in a 0.2 *M* Pb^{2+}, 0.58 *M* $HClO_4$ solution, relative to 1.0 *M* $HClO_4$, which suggests only a weak Pt—Cl...Pb interaction. The activation energies for the two processes (aquation with ($E_a = 88 \pm 8$ kJ mol^{-1}) and without ($E_a = 85 \pm 2$ kJ mol^{-1}) Pb^{2+} ions) were found to agree within experimental error and the only driving force for the Pb^{2+}-assisted reaction appears to be a slight increase in the activation entropy. This thus reinforces previous observations that Pb^{2+} is not a particularly effective metal ion for chloride abstraction [193,194,195].

Rates of these metal ion assisted hydrolysis reactions exhibit dependence on the metal ion concentration in either of the two following general forms.

$$k_{obs} = k[M^{n+}] \tag{6.7}$$

where a plot of k_{obs} versus the concentration of M^{n+} (where M^{n+} is the metal ion assisting the hydrolysis) is linear, and

Table 6.10. Spectrophotometrically determined observed rate constants (k_{obs}, s^{-1}) for the Pb^{2+}-assisted aquation of *cis*-$[PtCl_2(NH_3)_2]$ ($\mu = 1.0$ *M*, $HClO_4$).

$[Pb^{2+}]$ (*M*)	35.2 °C [308.4 K]	40.2 °C [313.4 K]	45.0 °C [318.2 K]	50.0 °C [323.2 K]
0.02	2.01±0.33	3.42±0.33	5.62±0.50	9.60±0.80
	2.01±0.24	3.53±0.52	5.81±0.69	9.29±0.42
0.03	2.12±0.36	4.21±0.75	6.78±1.2	10.4±0.6
	2.14±0.45	3.96±0.64	6.82±1.5	10.3±0.6
0.04	2.24±0.29	4.32±0.60	7.51±0.75	11.6±0.8
	2.48±0.32	4.16±0.45	7.07±0.82	11.3±0.7
0.06	2.73±0.42	4.76±0.20	7.79±0.49	12.1±0.6
	2.68±0.58	4.50±0.62	7.35±0.54	12.0±0.8
0.10	3.04±0.30	5.38±0.56	9.69±0.94	14.1±0.6
	3.02±0.88	5.49±0.43	9.54±1.2	
0.12	3.24±0.39	5.79±0.49	10.5±0.5	15.0±0.2
			9.46±0.5	
0.20	4.11±0.48		12.9±0.6	

Table 6.11. Calculated rate constants (k_{Pb}) for the Pb^{2+}-assisted aquation of *cis*-$[PtCl_2(NH_3)_2]$ ($\mu = 1.0$ *M*).

T °C	[K]	$10^3 k_{Pb}$ [a] (M^{-1} s^{-1})	$10^3 k_{Pb}$ (calc.) [b] (M^{-1} s^{-1})	$10^5 k_1$ [c] (s^{-1})	$10^5 k_1$ [d] (s^{-1})
25.0	[298.2]		0.372		
35.2	[308.4]	1.15	1.20	1.88	1.74
40.2	[313.4]	2.12	2.08	3.30	3.33
45.0	[318.2]	3.84	3.46	5.44	5.47
50.0	[323.2]	5.36	5.79	8.78	8.81

[a] Least-squares slopes of the plots of k_{obs} versus $[Pb^{2+}]$.

[b] Calculated from the activation parameters: $\Delta H^{\neq} = 85.5 \pm 7$ kJ mol^{-1}, $\Delta S^{\neq} = -24 \pm 14$ J K^{-1} mol^{-1}.

[c] Least-squares intercepts of the plots of k_{obs} versus $[Pb^{2+}]$ with the y-axis.

[d] Independently determined rate constants (k_1, s^{-1}) (Table 2.1) for the thermal aquation of *cis*-$[PtCl_2(NH_3)_2]$ in 1.0 *M* $HClO_4$.

$$k_{obs} = \frac{A[M^{n+}]}{1 + B[M^{n+}]} \tag{6.8}$$

where a plot of $1/k_{obs}$ versus $1/[M^{n+}]$ is linear. Dependence of the type shown in Equation 6.7, which is exhibited by both the $HgCl_2$- and Pb^{2+}-assisted hydrolysis reactions (Figures 6.2 and 6.7), might arise from a one-step attack by the metal ion, M^{n+}, at a suitable site on the leaving ligand, L, in the complex R—L, that is, S_E2 attack at M^{n+} (Equation 6.9).

$$RL + M^{n+} \xrightarrow{k} [\text{activated complex}]^{\neq} \xrightarrow{\text{fast}} \text{products} \tag{6.9}$$

The following expression (Equation 6.10) [174] can be used to describe the Pb^{2+}-assisted hydrolysis of *cis*-DDP, but not the $HgCl_2$-assisted reaction.

$$\text{Rate} = \sum_{n=0}^{n=3} k_{Pb}[PbCl_n^{n-}][cis\text{-DDP}] \tag{6.10}$$

This expression for the assisted pathway of these reactions only applies to the Pb^{2+} reaction system as only one chloride is being removed from the *cis*-DDP to give the *cis*-$[PtCl(NH_3)_2(OH_2)]^+$, whereas $HgCl_2$ removes both chlorides simultaneously to give *cis*-$[Pt(NH_3)_2(OH_2)_2]^{2+}$ and $HgCl_4^{2-}$ (which then combine to give the crystalline product). For the Pb^{2+}-assisted system, there is an intermediate step of the reaction where one Pb^{2+} is bound to one of the chloro groups on the *cis*-$[PtCl_2(NH_3)_2]$. Then this Pb^{2+} leaves with the chloride attached to it, to give $PbCl^+$ and *cis*-$[PtCl(NH_3)_2(OH_2)]^+$. As soon as some $PbCl^+$ forms, there is the possibility of another pathway in this reaction, where the $PbCl^+$ reacts further with the *cis*-$[PtCl_2(NH_3)_2]$, removing another chloride to give $PbCl_2$ and *cis*-$[PtCl(NH_3)_2(OH_2)]^+$. However, the concentration of $PbCl^+$ available to react after the first step is limited to being, at the maximum, the same as the concentration of *cis*-DDP present, which is only approximately 10^{-3} *M*. Since the total concentration of Pb^{2+} present at the beginning of the reaction is at least ten times that of the *cis*-DDP concentration, it seems unlikely that this second pathway will contribute much to the overall rate. Also, there is no real electrostatic effect or driving force for this second pathway. Thus, for $PbCl_n^{n-}$, from Equation 6.10, $n = 0$. In the case of $HgCl_2$-assisted hydrolysis reactions, there was loss of both chloro groups from the *cis*-DDP giving *cis*-$[Pt(NH_3)_2(OH_2)_2]^{2+}$ and $HgCl_4^{2-}$ which together formed the crystalline product $[cis\text{-}[PtCl_2(NH_3)_2](HgCl_2)_3]_n$.

Other metal ions were investigated in order to determine what effect they may have had on the hydrolysis of *cis*-DDP. Small amounts of solid *cis*-DDP were added to solutions of 0.3 *M* metal ion in $HClO_4$ (μ = 1.0 *M*) inside a 1.00 cm quartz cell, thermally equilibrated in the temperature controlled cell compartment of the spectrophotometer. Absorbance versus time data for the subsequent reaction were collected at 304, 260 and 236 nm. From this data, first-order rate constants, k_1 (s^{-1}), were calculated and the

Table 6.12. Spectrophotometrically determined rate constants (k_1, s^{-1}) for the metal ion assisted aquation of *cis*-$[PtCl_2(NH_3)_2]$ using a variety of metal ions ($\mu = 1.0$ *M*, $HClO_4$).

Temperature (°C)	[K]	$[M^{n+}]$ (*M*)	$10^4 k_1$ [a] (s^{-1})
37.6	[310.8]	0.3 *M* Ca^{2+}	2.28±0.67
37.9	[311.1]	0.3 *M* Ca^{2+}	2.52±0.47
37.8	[311.0]	0.3 *M* Mg^{2+}	2.83±0.21
38.1	[311.3]	0.3 *M* Zn^{2+}	2.72±0.32
38.0	[311.2]	0.3 *M* Cu^{2+}	3.03±0.15

[a]Rate constant is the average of three values, obtained at 304, 260 and 236 nm.

Table 6.13. Spectrophotometrically determined rate constants (k_{OH}^{12}, s^{-1}) obtained for the Zn^{2+}-assisted base hydrolysis of *cis*-$[PtCl_2(NH_3)_2]$.

Temperature (°C)	[K]	$[Zn^{2+}]$ (*M*)	$10^4 k_{OH}^{12}$ [a] (s^{-1})
45.2	[318.4]	0.02	2.40±0.28
44.8	[318.0]	0.03	2.66±0.11
45.2	[318.4]	0.06	2.53±0.05
45.2	[318.4]	0.08	2.60±0.01
45.3	[318.5]	0.10	2.67±0.10

[a]Rate constant is the average of two values, obtained at 300 and 245 nm.

values obtained are presented in Table 6.12. All of these 'metal ion assisted' reactions were carried out at approximately the same temperature and compared with the values obtained for k_1 in $HClO_4$ solution (Table 2.1, Chapter 2). However, it was found that the rate of aquation of *cis*-DDP in 1.0 *M* was not increased by the addition of Cu^{2+}, Zn^{2+}, Ca^{2+} or Mg^{2+} ions and these are the metal ions most likely to be encountered *in vivo* rather than Hg^{2+}, $HgCl_2$ or Pb^{2+}. Therefore it seems unlikely that metal ions are playing any role in accelerating the rate of hydrolysis of *cis*-DDP *in vivo*, although the possibility that the rate of base hydrolysis (a more likely hydrolysis route at physiological pH) could be accelerated by the presence of metal ions also needed to be explored.

The possibility of metal ion assisted base hydrolysis of *cis*-DDP was investigated using solutions of $ZnCl_2$ dissolved in NaOH. At physiological pH, hydroxide ions are present so it was also thought that investigation of the effect of metal ions on the rate of base hydrolysis of *cis*-DDP could be interesting. One possible metal ion to try that might have had an effect on base hydrolysis *in vivo* was Zn^{2+}. Solutions of various concentrations of Zn^{2+} (0.02 to 0.1 *M*) in 1.0 *M* NaOH were prepared and small samples of *cis*-DDPdissolved in the chosen Zn^{2+} / NaOH solution thermally equilibrated in a 1.00 cm quartz cell in the temperature controlled cell compartment of the spectrophotometer. The subsequent reaction was monitored between 345 and 225

nm with absorbance versus time data collected at 300 and 245 nm. First-order rate constants were calculated from this data and the results are presented in Table 6.13. However, by comparing these rate constants with those obtained in NaOH / $NaClO_4$ solutions (μ = 1.0 M) (Tables 3.1 and 3.2, Chapter 3), it can be seen that the rate of hydrolysis in 1.0 M NaOH was not changed in the presence of Zn^{2+} in the concentration range 0.02 to 0.08 M.

6.4 Conclusions.

The aquation of *cis*-DDP in acidic media was found to be accelerated by the presence of $HgCl_2$ or Pb^{2+} ions. Addition of *cis*-DDP to a solution of $HgCl_2$ reduced the half-life for the aquation reaction to one third of what it was previously without the presence of the halide abstractor. However, the final products for this reaction were *cis*-$[PtCl(NH_3)_2(OH_2)]^+$ and $HgCl_4^{2-}$ which combined to give crystals of [*cis*-$[PtCl_2(NH_3)_2](HgCl_2)_3]_n$ after a period of time. The structure of one of these crystals was determined using X-ray crystallography, its main feature being the platinum-μ-monochloromercury(II) bridges. The presence of Pb^{2+} ions also accelerated the aquation of *cis*-DDP under acid conditions although the products for this reaction were believed to be *cis*-$[PtCl(NH_3)_2(OH_2)]^+$ and $PbCl^+$ and the acceleratory effect was not large.

Under physiological conditions (pH = 7.4 [91]), since base hydrolysis is likely to be an important reaction pathway for *cis*-DDP (Chapter 3), it was thought that metal ion assisted aquation may play some role in accelerating the base hydrolysis reaction. Since Zn^{2+} ions are present *in vivo*, it was believed that these may have been the most likely ions to have an effect, but no acceleratory effect on the rate of base hydrolysis could be found. Other metal ions that are present *in vivo* were tested for their possible acceleratory effect on the rate of acid hydrolysis of *cis*-DDP but none could be found. Thus it seems unlikely that the biologically important metal ions present under physiological conditions have any acceleratory role for the hydrolysis processes of *cis*-DDP *in vivo*.

CHAPTER 7

MISCELLANEOUS REACTIONS OF *cis*-$[PtCl_2(NH_3)_2]$.

7.1 Introduction.

In this Chapter are reported the results of three different areas of work on *cis*-DDP and its relatives *cis*-$[PtBr_2(NH_3)_2]$ and *cis*-$[PtBr(NH_3)_2(OH_2)]^+$, which did not fit into the work reported in the previous six Chapters.

The first area investigated was the bromide anation of *cis*-$[PtBr(NH_3)_2(OH_2)]^+$ (k_{-1}^{Br}, M^{-1} s^{-1}). As a consequence of this work, the rate constants for the forward reaction, the hydrolysis (k_1^{Br}, s^{-1}) of *cis*-$[PtBr_2(NH_3)_2]$, were also obtained (Equation 7.3). The second area concerned a preliminary investigation of the reaction of *cis*-$[PtCl_2(NH_3)_2]$ with *ortho*-phenylenediamine, a macromolecular carrier that might have possible therapeutic use [196]. Finally, the third area investigated was the hydrolysis of *cis*-$[PtCl_2(NH_3)_2]$ in mixed aqueous solvents. That is, the acid hydrolysis of *cis*-DDP was investigated in a series of solutions containing varying ratios of ethylene glycol and 0.1 M $HClO_4$, in order to determine what effect a non-aqueous solvent might have on the hydrolysis of *cis*-DDP. Rate constants obtained for these reactions, along with possible interpretations, are presented in this Chapter.

7.2 Experimental.

7.2.1 The Kinetics of the Anation of *cis*-$[PtBr(NH_3)_2(OH_2)]^+$.

A solution of 3.33×10^{-3} M *cis*-DDP (50 mg) in 0.01 M NaOH (50 ml) was prepared and allowed to hydrolyse for four to five hours at approximately 50 °C and then left overnight at room temperature to finally give *cis*-$[Pt(OH)_2(NH_3)_2]$. The released chloride ions were removed from this solution by slurrying it with approximately 0.5 g of AgO and leaving it for about an hour. The solution was then filtered into another clean vessel and a few drops of this solution tested for the presence of chloride ions using a solution of $AgNO_3$ / HNO_3.

A series of solutions of NaBr (0.1 to 0.5 M) in $HClO_4$ (μ = 1.0 M) were also prepared. The separate test-tube arms of the Y-shaped rapid mixing device were filled, respectively, with 2.0 ml of the *cis*-$[Pt(OH)_2(NH_3)_2]$ solution (minus chloride

ions) and with 1.0 ml of the appropriate NaBr / $HClO_4$ solution. The solutions in the mixing device were then thermally equilibrated in a temperature controlled water bath. Once equilibrated, a 1.00 cm quartz spectrophotometer cell was filled with the two solutions mixing rapidly (as in Chapter 2). The temperature of the cells inside the cell compartment of the spectrophotometer was controlled by the use of a water-cooled, jacketed cell holder connected to a pump/heater-unit in the water bath.

On mixing the two solutions together, the species *cis*-$[PtBr(NH_3)_2(OH_2)]^+$ was formed instantaneously and the subsequent reaction, monitored spectrophotometrically between 380 and 250 nm (Figure 7.1), involved the anation of *cis*-$[PtBr(NH_3)_2(OH_2)]^+$ to give *cis*-$[PtBr_2(NH_3)_2]$. Absorbance versus time data were collected at 318 and 260 nm and these gave pseudo-first-order rate constants (k_{obs}, s^{-1}) (Table 7.1). These values of k_{obs} were plotted versus [NaBr] (Figure 7.2) with the plots obeying the expression

$$k_{obs} = k_1^{Br} + k_{-1}^{Br}[Br^-] \tag{7.1}$$

where the slopes of the lines yielded values for k_{-1}^{Br} (M^{-1} s^{-1}) (Table 7.1) and the intercepts values for the rate constant for the forward reaction, k_1^{Br} (s^{-1}) (Equations 7.3) (Table 7.1).

7.2.2 Reaction of *cis*-$[PtCl_2(NH_3)_2]$ with *ortho*-Phenylenediamine.

Prior to each experiment, a fresh solution of *cis*-$[PtCl_2(NH_3)_2]$ (0.0012, 0.0031 or 0.0050 g) dissolved in distilled water (250 ml) was prepared. Stock solutions of *ortho*-phenylenediamine (OPDA) (0.10 to 0.30 g) in DMF (250 ml) were also prepared. These OPDA solutions had a tendency to decompose to a dark brown colour in daylight after a short period of time so all flasks containing these solutions were wrapped in aluminium foil.

Using the Y-shaped rapid mixing device, 2.0 ml of the *cis*-$[PtCl_2(NH_3)_2]$ / H_2O solution were placed in one arm of the device and 1.0 ml of the OPDA in the other. These were then left to equilibrate thermally in a temperature controlled water bath. Once equilibrated, the two solutions were rapidly mixed while being poured into the 1.00 cm spectrophotometric cell (as in Chapter 2). The temperature of the cells inside the cell compartment was controlled by means of the heated cell-block.

The subsequent reaction was monitored between 800 and 400 nm (Figure 7.3) with absorbance versus time data collected at 704 and 440 nm, to give pseudo-first-order rate constants (k_{IN}, s^{-1}) for the 'induction period' of the reaction (monitored at 440 nm) and k_{obs} (s^{-1}) for the reaction that occurs after this period (monitored at 704 nm) (Table 7.3).

7.2.3 The Hydrolysis of *cis*-$[PtCl_2(NH_3)_2]$ in Ethylene Glycol Solvent.

A series of solutions (100 ml) containing varying percentages (by volume) of ethylene glycol and 0.1 *M* $HClO_4$ were prepared, ranging from 5% ethylene glycol plus 95% 0.1 *M* $HClO_4$, to 75% ethylene glycol plus 25% 0.1 *M* $HClO_4$. A small amount of solid *cis*-DDP ($\sim$ 3 mg) was dissolved in 3.0 to 3.5 ml of the appropriate ethylene glycol/$HClO_4$ solution inside the 1.00 cm quartz spectrophotometer cell, inside the temperature controlled cell compartment of the spectrophotometer. On dissolution of the *cis*-DDP, the repeat scanning mode of the spectrophotometer was activated with the reaction monitored between 345 and 220 nm. Absorbance versus time data were collected at 300 and 245 nm and this data gave values for the pseudo-first-order rate constants k_s (s^{-1}) (Table 7.4). These values of k_s were plotted versus the percentages of ethylene glycol (Figure 7.4) with the plots obeying the expression

$$k_{obs} = k_1 + k_{EtG}[\ EtGlyc\ ] \tag{7.2}$$

where the slopes of the lines yielded values for k_{EtG} ($M^{-1}\ s^{-1}$) (Table 7.4) and the intercepts with the y-axis values for k_1, the rate constant for the first acid hydrolysis step of *cis*-DDP in $HClO_4$ (Tables 7.4 and 2.1).

7.3 Results and Discussion.

7.3.1 The Kinetics of the Anation of *cis*-$[PtBr(NH_3)_2(OH_2)]^+$.

In terms of the requirements stated in Chapter 1 for anti-cancer activity to be exhibited in square planar platinum(II) complexes, *cis*-$[PtBr_2(NH_3)_2]$ should be almost the same as *cis*-$[PtCl_2(NH_3)_2]$ if the pair are considered only in terms of their leaving groups, since the chloride and bromide ligands are both considered to be of intermediate leaving ability. The compound *cis*-$[PtBr_2(NH_3)_2]$ has been tested for anti-tumour activity and although it was found to have good activity when tested against standard tumours, difficulty with its low solubility and hence the high size of dose required for an effect, with a correspondingly high level of toxicity, have precluded its use clinically as an anti-cancer drug [31].

The *cis*-$[PtBr(NH_3)_2(OH_2)]^+$ species was prepared from *cis*-DDP via the species *cis*-$[Pt(OH)_2(NH_3)_2]$. Removal of the chloride ions released in the irreversible base hydrolysis of *cis*-DDP (Chapter 3) meant that the *cis*-$[Pt(NH_3)_2(OH_2)_2]^{2+}$ species formed immediately on addition of $HClO_4$ and anation to the *cis*-$[PtBr(NH_3)_2(OH_2)]^+$ (k_{-2}^{Br}) was very rapid since the bromide ions were the only anating ligands present. However, the bromide anation of the *cis*-$[PtBr(NH_3)_2(OH_2)]^+$ species (k_{-1}^{Br}) (Equation 7.3) was slower (as was the case with the *cis*-$[PtCl_2(NH_3)_2]$ system) and thus the rate of anation of *cis*-$[PtBr(NH_3)_2(OH_2)]^+$ to give *cis*-$[PtBr_2(NH_3)_2]$ could be measured.

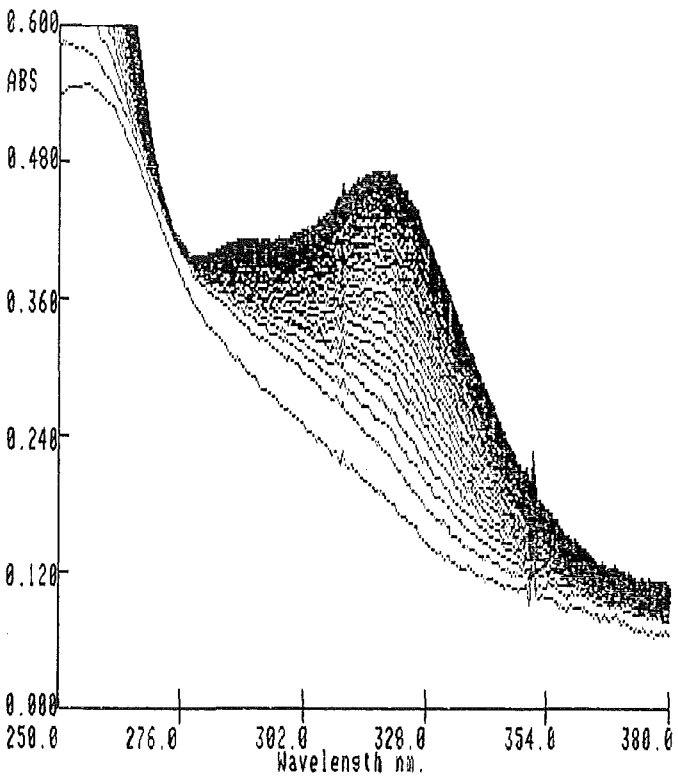

Figure 7.1. Spectrophotometric scans (2 minute intervals) for the bromide anation reaction of *cis*-$[PtBr(NH_3)_2(OH_2)]^+$ at 14.9 °C (μ = 1.0 M, $HClO_4$). No isosbestic points were observed and the absorbance at 318 nm increases with time.

$$cis\text{-}[PtBr_2(NH_3)_2] \underset{k_{-1}^{Br}}{\overset{k_1^{Br}}{\rightleftharpoons}} cis\text{-}[PtBr(NH_3)_2(OH_2)]^+ + Br^- \qquad (7.3)$$

The UV absorption spectra for the anation reaction changed reasonably quickly with time. The absorbance increased at 318 nm and the shape of the final spectrum of the reaction products, with its maximum at approximately 318 nm and a shoulder at about 293 nm agreed with the UV spectrum of the *cis*-$[PtBr_2(NH_3)_2]$ obtained by Gano *et al.* [197]. The overall shape was similar to that of the spectrum of *cis*-$[PtCl_2(NH_3)_2]$. No isosbestic points for the anation reaction were observed (Figure 7.1).

Pseudo-first-order rate constants (k_{obs}, s^{-1}) were obtained from the absorbance versus time data obtained at 318 and 260 nm (Table 7.1) and these were used to calculate the second-order rate constants k_{-1}^{Br} (M^{-1} s^{-1}) by plotting k_{obs} versus the concentrations of NaBr used (Figure 7.2), with the lines obeying Equation 7.1. The slopes of the plots gave values for k_{-1}^{Br} and the intercepts of these plots with the y-axis gave values for k_1^{Br} (s^{-1}), the rate constants for the forward reaction (Equation 7.3, Table 7.1). The variation of k_{-1}^{Br} and k_1^{Br} with temperature meant that the activation parameters associated with both the forward and reverse reactions could be calculated in the same manner as in Chapter 2.

Table 7.1. Spectrophotometrically determined rate constants for the bromide anation reaction of *cis*-$[PtBr(NH_3)_2(OH_2)]^+$ (k_{-1}^{Br}, M^{-1} s^{-1}) and the hydrolysis of *cis*-$[PtBr_2(NH_3)_2]$ (k_1^{Br}, s^{-1}) ($\mu = 1.0$ M, $HClO_4$) (Equation 7.3).

Temperature (°C)	[K]	[NaBr] (M)	$10^4 k_{obs}$ [a] (s^{-1})	$10^3 k_{-1}^{Br}$ [b] (M^{-1} s^{-1})	$10^3 k_{-1}^{Br}$ [c] (M^{-1} s^{-1})	$10^4 k_1^{Br}$ [d] (s^{-1})	$10^4 k_1^{Br}$ [e] (s^{-1})
12.5	[285.7]	0.10	4.64±0.48	5.51	5.23	2.03	2.02
			4.43±1.15				
		0.20	6.45±0.44				
			6.05±0.64				
		0.30	8.44±0.55				
			7.54±0.77				
		0.40	10.25±0.53				
			9.40±0.42				
		0.50	12.20±0.66				
			11.70±1.07				
15.0	[288.2]	0.10	5.44±0.44	6.24	6.94	2.26	2.43
		0.20	8.46±0.42				
			7.28±0.55				
		0.30	10.17±0.48				
			9.34±1.20				
		0.40	12.02±0.55				
			10.59±0.45				
		0.50	14.99±0.87				
			13.40±0.58				
20.0	[293.2]	0.10	8.13±0.65	12.72	12.04	3.80	3.49
		0.20	11.76±1.10				
			10.89±1.01				
		0.30	17.34±0.65				
			16.40±0.95				
		0.40	21.20±0.78				
			19.63±0.87				
		0.50	25.01±0.76				
			24.22±1.07				
25.1	[298.3]	0.10	11.37±0.64	21.36	20.72	4.44	4.97
		0.20	18.58±0.77				
			18.14±0.58				
		0.30	24.93±0.29				
			23.56±0.88				
		0.40	33.07±0.90				
			32.22±0.32				
		0.50	39.55±0.99				
			39.98±0.61				
30.1	[303.2]	0.10	18.44±0.86	33.58	34.66	7.50	6.96
			17.57±0.75				
		0.20	29.32±0.55				
			29.33±1.57				
		0.30	39.79±2.31				
			39.02±2.52				
		0.40	52.53±1.23				
			51.32±3.22				

[a] Calculated from the absorbance versus time data obtained at 318 and 260 nm using Equation 2.2.
[b] Calculated from a least-squares analysis of the slopes of the plots of k_{obs} versus [NaBr] (Figure 7.2).
[c] Calculated from the activation parameters: $\Delta H^{\neq} = 74.9 \pm 4$ kJ mol^{-1}, $\Delta S^{\neq} = -26 \pm 8$ J K^{-1} mol^{-1}.
[d] Estimated from the intercepts of the plots of k_{obs} versus [NaBr] with the y-axis (Figure 7.2).
[e] Calculated from the activation parameters: $\Delta H^{\neq} = 48.1 \pm 3$ kJ mol^{-1}, $\Delta S^{\neq} = -147 \pm 6$ J K^{-1} mol^{-1}.

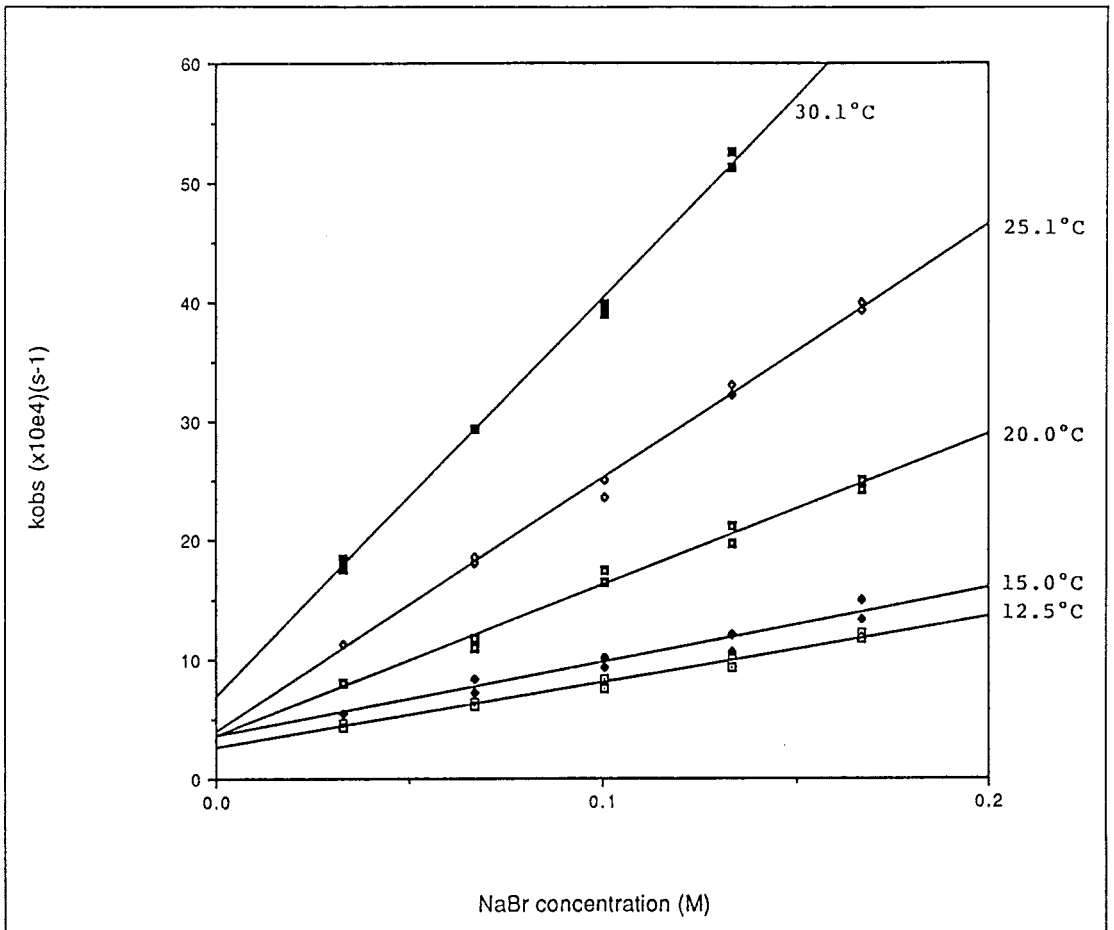

Figure 7.2. Plots of k_{obs} versus [NaBr] for the bromide anation reaction of *cis*-$[PtBr(NH_3)_2(OH_2)]^+$.

While the values obtained for the activation energy and entropy for k_{-1}^{Br} were satisfactory this was not the case for E_a and $\Delta S^{\neq}$ for k_1^{Br}. The activation energy $E_a = 50.5 \pm 3$ kJ mol^{-1} seems too low while the activation entropy $\Delta S^{\neq} = -147 \pm 6$ J K^{-1} mol^{-1} seems too high. The method used for obtaining values of k_1^{Br} from the intercepts of the lines plotted is not such a good method as measuring k_1^{Br} directly by hydrolysing *cis*-$[PtBr_2(NH_3)_2]$, but *cis*-$[PtBr_2(NH_3)_2]$ has a very low solubility in water, probably less than 5 mM, which thus makes direct measurement difficult [197]. Gano *et al.* obtained, at 25 °C, values of $k_1^{Br} = 3.2 \times 10^{-5}$ s^{-1} (compared to a value of $k_1^{Br} = 4.94 \times 10^{-4}$ s^{-1} obtained here) and $k_{-1}^{Br} = 3.3 \times 10^{-2}$ M^{-1} s^{-1} (compared to $k_{-1}^{Br} = 2.05 \times 10^{-2}$ M^{-1} s^{-1}). There is reasonable agreement between the values of k_{-1}^{Br} but not between the values of k_1^{Br}.

However, comparison of the rates of hydrolysis $PtCl_4^{2-}$ and $PtBr_4^{2-}$ and anation of their hydrolysis products measured by Elding, showed that the rate constants for the hydrolysis and anation reactions of $PtBr_4^{2-}$ and its hydrolysis products, the bromoaquo and the diaquo species, were invariably higher than those for the analagous reactions of $PtCl_4^{2-}$, of the order of 3 to 44 times faster [198,199,200,201,202,203,204]. Therefore, comparison of the values for k_1^{Br} at 25 °C obtained here and by Gano *et al.* with the value of k_1 for Equation 1.1 ($k_1 = 6.32 \times 10^{-5}$ s^{-1}) shows that Gano's value is inconsistent with the trend observed by Elding. However, the value of k_1^{Br} obtained here did fit this trend. The problem with Gano's values seems to be caused by the experimental techniques used to obtain them. Comparison of the values of k_1 ($= 6.32 \times 10^{-5}$ s^{-1}) and k_{-1} ($= 6.26 \times 10^{-3}$ M^{-1} s^{-1}) for *cis*-DDP at 25 °C (Chapter 2), with k_1^{Br} ($= 4.94 \times 10^{-4}$ s^{-1}) and k_{-1} ($= 2.05 \times 10^{-2}$ M^{-1} s^{-1}) for *cis*-$[PtBr_2(NH_3)_2]$ (this Chapter) shows that the rate constants for the *cis*-$[PtBr_2(NH_3)_2]$ are higher than those of the *cis*-$[PtCl_2(NH_3)_2]$, which is consistent with Elding's work.

Knowledge of the rate constants for both the forward and reverse reactions of Equation 7.3 meant that the equilibrium constant K_1^{Br} could be calculated from the expression

$$K_1^{Br} = \frac{k_1^{Br}}{k_{-1}^{Br}} \tag{7.4}$$

The temperature dependence expressions for both k_1^{Br} and k_{-1}^{Br} were derived from the Arrhenius Equation (Equation 2.3) and from the computer calculated activation parameters for k_1^{Br} and k_{-1}^{Br} (see Chapter 2 for method of calculation). The activation energies, E_a, and values for PZ were obtained for both rate constants and these values inserted into Equation 2.3 to give the above temperature dependence expressions for k_1^{Br} and k_{-1}^{Br}. Combination of the temperature dependence expressions for $k_1^{Br} = 3.537 \times 10^5 \exp\left(\frac{-50.55 \times 10^3}{RT}\right)$ and $k_{-1}^{Br} = 7.393 \times 10^{11} \exp\left(\frac{-77.39 \times 10^3}{RT}\right)$ (both at $\mu = 1.0$ M) gave the temperature dependence of the equilibrium constant K_1^{Br} in the form

Table 7.2. Forward (k_1^{Br}) and reverse (k_{-1}^{Br}) rate constants and equilibrium constants (K_1^{Br}) for the first step in the acid hydrolysis of *cis*-$[PtBr_2(NH_3)_2]$ ($\mu = 1.0\ M$, $HClO_4$).

Temperature (°C)	[K]	$10^4 k_1^{Br}$ [a] (s^{-1})	$10^2 k_{-1}^{Br}$ [b] ($M^{-1}\ s^{-1}$)	$10^2 K_1^{Br}$ [c,d]
10.0	[283.2]	1.68	0.39	4.31
15.0	[288.2]	2.43	0.70	3.47
20.0	[293.2]	3.49	1.21	2.88
25.0	[298.2]	4.94	2.05	2.41
30.0	[303.2]	6.91	3.43	2.02
35.0	[308.2]	9.57	5.65	1.69
40.0	[313.2]	13.11	9.15	1.43
45.0	[318.2]	17.79	14.60	1.22
50.0	[323.2]	23.91	22.95	1.04

[a]Calculated from the expression $k_1^{Br} = 3.537 \times 10^5 \exp\left(\frac{-50.55\times10^3}{RT}\right)$ (Table 7.1).

[b]Calculated from the expression $k_{-1}^{Br} = 7.393 \times 10^{11} \exp\left(\frac{-77.39\times10^3}{RT}\right)$ (Table 7.1).

[c]Calculated from Equation 7.4 which is equivalent to Equation 7.5.

[d]The variation of values of K_1^{Br} with temperature indicates that the forward reaction is exothermic and from [c], $\Delta H^{\ddagger}_{298.2} = -26.91$ kJ mol^{-1}. Other thermodynamic parameters associated with the forward reaction are $\Delta G^{\ddagger}_{298.2} = 9.24$ kJ mol^{-1} and $\Delta S^{\ddagger}_{298.2} = -121$ J K^{-1} mol^{-1}.

$$\ln K_1^{Br} = \frac{26.84 \times 10^3}{RT} - 14.55 \qquad (7.5)$$

Hence values for k_1^{Br} and k_{-1}^{Br} were calculated over a range of temperatures and values of K_1^{Br} could also be calculated (Table 7.2). A comparison of K_1 ($= 1.01 \times 10^{-2}$) for *cis*-$[PtCl_2(NH_3)_2]$ and K_1^{Br} ($= 2.41 \times 10^{-2}$) for *cis*-$[PtBr_2(NH_3)_2]$ shows that the equilibrium constant for Equation 7.3 is larger than that for the corresponding chloro system.

The enthalpy of the reaction, $\Delta H^{\ddagger}_m$, was calculated using Equation 2.15 by plotting $\ln K_1^{Br}$ versus 1/T. The variation of K_1^{Br} with temperature indicated that the forward reaction (Equation 7.3) was exothermic and $\Delta H^{\ddagger}_{298.2} = -26.91$ kJ mol^{-1}. The equilibrium constant K_1^{Br} becomes smaller as the temperature increases (Table 7.2) therefore the equilibrium shifts towards the reactants (*cis*-$[PtBr_2(NH_3)_2]$ and H_2O) since, for an exothermic reaction, a rise in temperature favours the reactants [120]. However, since the rate constants obtained for the forward reaction (k_1^{Br}, s^{-1}) and hence its activation parameters were not thought to be very good, this caused some distortion in the calculated values of k_1^{Br} (Table 7.2) and hence in the values of K_1^{Br} and $\Delta H^{\ddagger}_{298.2}$. It is thought that $\Delta H^{\ddagger}_{298.2}$ should probably be more positive.

Other thermodynamic parameters associated with Equation 7.3 were calculated using Equations 2.14 and 2.15. A positive value of $\Delta G^{\ddagger}_{298.2} = 9.24$ kJ mol^{-1} was obtained for the forward reaction indicating that the reaction in this direction is not spontaneous, that is, it has a natural tendency to move towards the reactants *cis*-$[PtBr_2(NH_3)_2]$ and H_2O. This is interesting since a negative (exothermic) value for $\Delta H^{\ddagger}_{298.2}$ is combined

with a positive (non-spontaneous) value for $\Delta G^{\ominus}_{298.2}$ and the exothermic reaction is usually the spontaneous process [131], or looked at from an alternative point of view, the reverse reaction (k_{-1}^{Br}) is endothermic ($\Delta H^{\ominus}_{298.2} = 26.91$ kJ mol^{-1}) yet is the spontaneous process ($\Delta G^{\ominus}_{298.2} = -9.24$ kJ mol^{-1}). It is thought that this effect is caused by the poor k_1^{Br} values. When $\Delta G^{\ominus}_m$ is strongly positive, the equilibrium lies over to the left in favour of the reactants and the yield of product will be very small [120]. The less positive $\Delta G^{\ominus}_m$ is, the further towards the products the equilibrium will lie.

The negative value for $\Delta G^{\ominus}_{298.2}$ for the reverse reaction (calculated using $K_1^{Br'} = 1/K_1^{Br}$) indicated that this was the spontaneous process, as was the case for the anation reaction of *cis*-$[PtCl(NH_3)_2(OH_2)]^+$ (Chapter 2). The entropies for both the forward and reverse reactions were calculated using Equation 2.15. For the forward reaction $\Delta S^{\ominus}_{298.2} = -121$ J K^{-1} mol^{-1}. Using Equation 2.15 rearranged to give

$$-\frac{\Delta G^{\ominus}_m}{T} = -\frac{\Delta H^{\ominus}_m}{T} + \Delta S^{\ominus}_m \qquad (7.6)$$

when the reaction is exothermic, $-\Delta H^{\ominus}_m/T$ represents a positive change in the entropy of the surroundings and is a driving force for the reaction going from left to right. However, if the temperature is raised $-\Delta H^{\ominus}_m/T$ gets smaller and so the increasing entropy of the surroundings is a less potent driving force and the equilibrium lies far less to the right [120]. For the reverse reaction (k_{-1}^{Br}) $\Delta S^{\ominus}_{298.2} = 121$ J K^{-1} mol^{-1}.

7.3.2 Reaction of *cis*-$[PtCl_2(NH_3)_2]$ with *ortho*-Phenylenediammine.

Work was done recently by Schechter *et al.* on soluble polymers as possible macromolecular carriers of *cis*-DDP [196]. Their work was on an aspect of research concerning chemotherapy and the development of means to suppress the toxicity of existing anti-cancer drugs such as *cis*-DDP, without impairing their therapeutic activity. One possible approach was to use the drug in combination with high molecular weight carrier molecules such as *ortho*-phenylenediamine (OPDA). These macromolecularised drug derivatives were expected to increase the efficacy of the drug through more effective distribution, retardation of chemical or metabolic degradation and maintenance of prolonged non-toxic levels of the drug in the body due to its slow release. Due to its two chloro leaving groups, *cis*-DDP was thought to be highly suitable for use in such carrier systems as it can form complexes of varying degrees of stability with a variety of reactive groups, on the loss of one or both chloride ligands [196].

During their investigation, Schechter *et al.* found that the OPDA interacted with *cis*-DDP to form a light blue complex. Since they reported that the reaction took 10 minutes at 100 °C to complete, that is, to develop the blue colour, it was felt that a preliminary investigation of the kinetics of the reaction could be worth looking at and the results of this investigation are reported in this Chapter. Golla *et al.* had also investigated the reaction of platinum(II) and platinum(IV) complexes with OPDA [205],

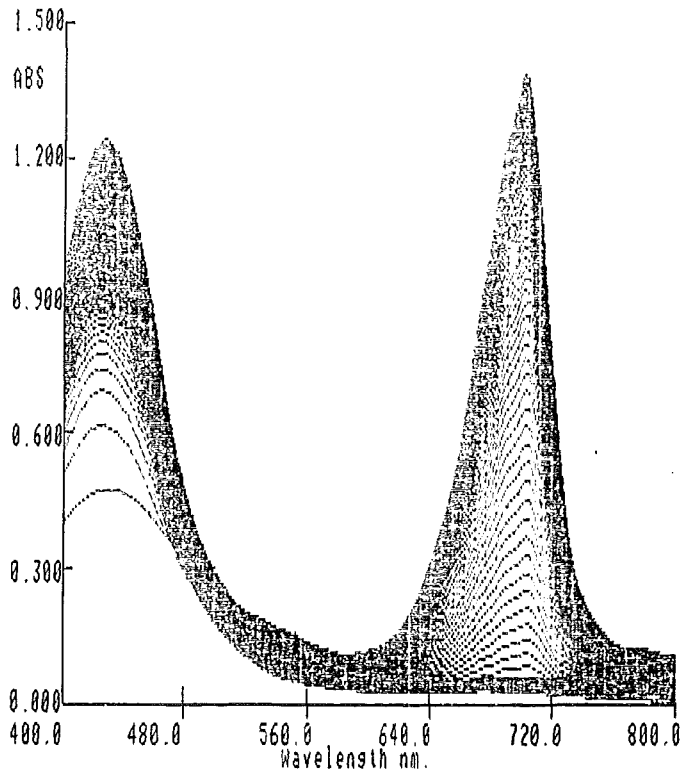

Figure 7.3. Spectrophotometric scans (5 minute intervals) for the reaction of *cis*-$[PtCl_2(NH_3)_2]$ with *ortho*-phenylenediamine at 45.0 °C. The absorbances at 440 nm (induction period) and 704 nm increase with time.

and had determined that the final product of the reaction had an absorption maximum at approximately 704 nm. From this preliminary kinetic investigation of the reaction of *cis*-DDP with OPDA, a few interesting features of the reaction not mentioned by either Golla or Schechter were found. The major feature noticed was the presence of what was believed to be an induction period at the beginning of the reaction. During this period, the absorbance increased with time at about 440 nm for a number of cycles with little or no change in absorbance in the remainder of the range of wavelengths scanned (Figure 7.3). After a period of time had elapsed, the absorbance at 704 nm would then start to increase with little or no subsequent increase in absorbance at 440 nm.

According to Golla *et al.* [205], the absorption maximum at 430 to 440 nm was due to oxidation of some of the OPDA with a yellow colour formed due to the oxidation products. The OPDA reagent itself has little absorption in the 600 to 800 nm region. The absorption maximum at about 704 nm was said to be characteristic of the platinum(II)-OPDA complex. It was also claimed by Golla *et al.* that when platinum(IV) reacted with the OPDA, the OPDA was oxidised while the platinum(IV) was reduced to platinum(II), followed by formation of the blue complex, $Pt(OPDA)_2$. For the reaction of OPDA with Platinum(II), this redox process did not occur and the same

blue complex was formed as a final product. However, the results of the investigation presented in this Chapter showed that this oxidation process of OPDA still occured when platinum(II) was used. It is thus likely that whatever process was occurring in the induction period involved the OPDA but not the platinum(II).

It was thought that oxygen may have been playing a part in the reaction, therefore three experiments were conducted, all three using 0.30 g of OPDA (0.0111 M) in 250 ml of DMF and 0.0052 g of *cis*-DDP (6.93×10^{-5} M) in 250 ml of (a) normal distilled water, (b) pre-boiled distilled water (to remove some of the oxygen) and (c) de-oxygenated distilled water (boiled and then cooled with N_2 bubbled through it), all at 45 °C. The reaction of *cis*-DDP dissolved in normal distilled water behaved as it had done when carried out previously, with an induction period (increasing absorbance at 440 nm) and after this, an increase in absorbance at 704 nm. When the partially and totally deoxygenated distilled water were used, the reaction behaved in the same manner as it had done in normal distilled water. The only difference was the extent of the reaction. The absorption maxima at 704 nm obtained for the reactions using partially and totally deoxygenated distilled water were far smaller than that obtained in normal distilled water. However, no real importance can be attached to this result as it was found during the course of prior experimental work that this smaller than expected absorbance maximum at 704 nm occurred randomly throughout the experiments done with each of the OPDA in DMF solutions and there did not appear to be any systematic trend in its occurrence. The height of the absorption maximum at 440 nm was also found to vary from experiment to experiment. The induction periods for all three reactions above were found to be the same, within experimental error. Therefore it appears that oxygen plays little or no role in the reaction.

Pseudo-first-order rate constants were obtained for both the reaction at 704 nm (k_{obs}, s^{-1}) and at 440 nm (k_{IN}, s^{-1}) (Table 7.3). At 440 nm the rate constants obtained (k_{IN}) were found to be independent of both the concentrations of OPDA and *cis*-DDP. One experiment was also done without the presence of any *cis*-DDP or distilled water, in order to see what, if anything, happened to the OPDA in DMF. It was observed that an increase in absorbance again occurred at 440 nm in the same manner as before but there was no subsequent increase in absorbance at 704 nm after the induction period. The pseudo-first-order rate constant for this reaction was found to be the same as those calculated at the same temperature and wavelength when *cis*-DDP in distilled water was used, that is, the process that occurs in this induction period will take place whether platinum(II) is present or not and at the same rate.

It is thus postulated that this induction period involved a redox reaction of OPDA. Initially it was thought that while some of the OPDA was being oxidised, the oxygen was being reduced, yet removal of as much oxygen as possible did not appear to effect the duration or extent of the induction period. There is the possibility that the OPDA

Table 7.3. Spectrophotometrically determined rate constants (k_{obs}) obtained for the reaction of *cis*-$[PtCl_2(NH_3)_2]$ in *ortho*-phenylenediamine/DMF.

Temperature (°C)	[K]	10^3[OPDA] [a] (M)	10^5[*cis*-$[PtCl_2(NH_3)_2]$] [b] (M)	$10^4 k_{obs}$ (s^{-1})	$10^4 k_{IN}$ (s^{-1})
37.0	[310.2]	3.70	1.07	0.726±0.124	9.61±0.28
37.2	[310.4]	3.70	2.75	0.699±0.099	9.27±0.56
37.2	[310.4]	3.70	2.75	0.738±0.134	9.66±0.07
37.2	[310.4]	3.70	4.53	0.697±0.092	9.67±0.51
40.3	[313.5]	3.70	1.07	0.833±0.129	10.88±0.35
40.5	[313.7]	3.70	1.07	0.853±0.041	10.52±1.02
40.2	[313.4]	3.70	2.75	0.826±0.121	10.67±0.09
40.4	[313.6]	3.70	2.75	0.831±0.134	10.61±0.49
40.3	[313.5]	3.70	4.53	0.873±0.103	10.72±0.50
40.3	[313.5]	3.70	4.53	0.804±0.133	10.64±0.33
45.0	[318.2]	3.70	1.07	1.37±0.06	
45.3	[318.5]	3.70	1.07	1.37±0.06	12.72±0.15
45.0	[318.2]	3.70	2.75	1.40±0.39	
45.2	[318.4]	3.70	2.75	1.66±0.38	12.05±1.18
45.2	[318.4]	3.70	2.75	1.62±0.33	12.54±0.04
45.1	[318.3]	3.70	4.53	1.49±0.45	12.26±0.70
45.2	[318.4]	3.70	4.53		12.36±0.62
45.2	[318.4]	3.08	2.75	1.41±0.37	12.36±1.22
45.1	[318.3]	3.08	2.75	1.35±0.33	12.75±0.66
45.2	[318.4]	2.47	2.75	1.66±0.22	
45.0	[318.2]	2.47	2.75	1.42±0.92	12.54±0.48
45.2	[318.4]	1.85	2.75	1.56±0.28	
45.1	[318.3]	1.23	2.75	1.43±0.27	12.21±0.13
50.1	[323.3]	2.47	2.75	2.80±0.36	14.50±0.52
50.1	[323.3]	2.47	2.75	2.47±0.24	14.97±0.53
50.3	[323.5]	3.70	1.07	2.63±0.68	
50.1	[323.3]	3.70	2.75	2.43±0.35	
50.1	[323.3]	3.70	2.75	2.47±0.50	
50.1	[323.3]	3.70	4.53	2.33±0.45	

[a] Concentration after dilution with *cis*-$[PtCl_2(NH_3)_2]$ / H_2O solution.
[b] Concentration after dilution by OPDA/DMF solution.

could be reducing the oxygen present in the spectrophotometer cell but this seems unlikely since the induction period is not effected. Another possibility exists and this is that OPDA is undergoing an internal redox reaction as it is known to do, along with 2,2'-diaminobiphenyl and aniline [206].

7.3.3 The Hydrolysis of *cis*-$[PtCl_2(NH_3)_2]$ in Ethylene Glycol Solvent.

An initial investigation into the effects of a non-aqueous solvent ethylene glycol (ethanediol, $CH_2(OH)CH_2OH$) on the acid hydrolysis of *cis*-DDP was made. Solutions were prepared containing the varying percentages of ethylene glycol and 0.1 M $HClO_4$ outlined in the experimental section of this Chapter. The pseudo-first-order rate constants (k_s, s^{-1}) obtained were plotted against the percentage of ethylene glycol solvent present (Figure 7.4) and the slopes of the lines gave values for the second-order rate constant k_{EtG} (M^{-1} s^{-1}) (Table 7.4). When no ethylene glycol was present, the reaction that took place was solely the acid hydrolysis of *cis*-DDP in 0.1 M $HClO_4$ (k_1, s^{-1}). The values for $k_1$obtained by experiment in Chapter 2 (Table 2.1) were used as the zero values for Figure 7.4 and the values of k_1 obtained from the intercepts of the plots with the y-axis (Table 7.4) were in agreement with the values of k_1 obtained previously, as were the activation parameters (Tables 2.7 and 7.4). However, uncertainty still exists as to what is the nature of the reaction that the second-order rate constant k_{EtG} applies to. Possibilities will be discussed later on in this section.

In general, the solvent can influence both the rate and mechanism of a reaction [207]. Sometimes the solvent alters the rate without influencing the mechanism, but a change in the mechanism without a change in the rate would only be coincidental. A solvent can change a rate without changing the mechanism by changing the force between reacting particles and hence altering the readiness with which they approach each other. Such a phenomenon is illustrated by the effect of the dielectric constant (ϵ) on electrostatic forces among reacting particles. The solvent may change the rate of diffusion of particles by its viscosity effect and hence alter the frequency of collisions between reactant types, and in this way alter the rate of diffusion controlled reactions. For a given medium, the magnitude of its dielectric constant increases with temperature [208]. The dielectric constant (ϵ) of a medium is defined in terms of the equation

$$F = \frac{q_1 q_2}{C \epsilon r^2} \tag{7.7}$$

where F is the force of attraction acting on each of the two charges q_1 and q_2, r is the distance between the two charges and C is a constant. The dielectric constant of a vacuum is unity. From Equation 7.7, the force of attraction between two charged particles in a solute decreases as the dielectric constant increases. However, the reactions of *cis*-DDP are not electrostatically influenced (Table 3.10).

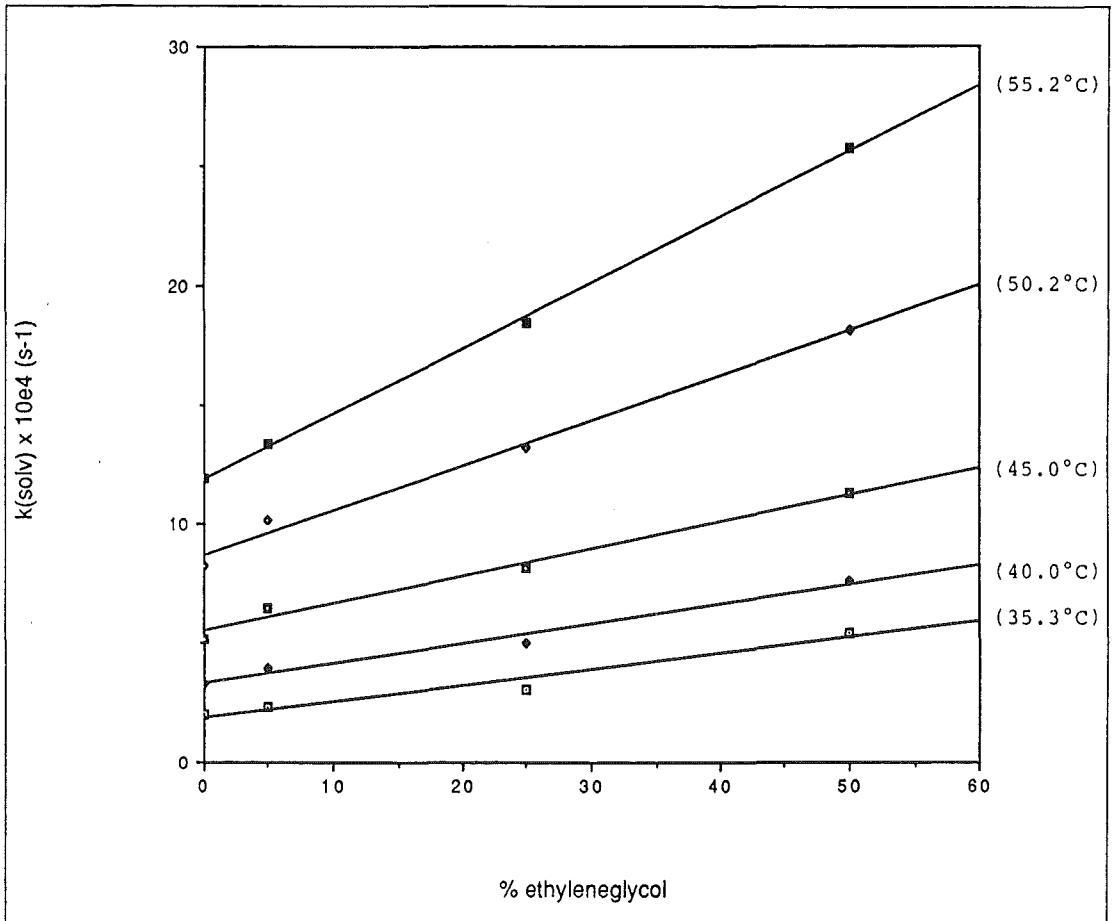

Figure 7.4. Plots of k_s versus percentage of ethylene glycol solvent for the hydrolysis of *cis*-$[PtCl_2(NH_3)_2]$ in ethylene glycol and 0.1 *M* $HClO_4$.

Table 7.4. Spectrophotometrically determined rate constants (k_{EtG}) for the hydrolysis reaction of *cis*-$[PtCl_2(NH_3)_2]$ in ethylene glycol and 0.1 *M* $HClO_4$.

Temperature		% ethylene [a]	$10^4 k_s$	k_{EtG} [b]	k_{EtG} [c] (calc.)	$10^4 k_1$ [d]	$10^4 k_1$ [e] (calc.)
(°C)	[K]	glycol	(s^{-1})	(M^{-1} s^{-1})	(M^{-1} s^{-1})	(s^{-1})	(s^{-1})
35.3	[308.5]	0	2.20 ± 0.67	0.066	0.061	1.88	2.03
		5	2.31 ± 0.04				
		25	3.04 ± 0.40				
		50	5.42 ± 0.33				
40.0	[313.2]	0	3.12 ± 0.20	0.083	0.087	3.29	3.16
		5	3.96 ± 0.11				
		25	4.96 ± 0.26				
		50	7.62 ± 0.40				
45.0	[318.2]	0	5.21 ± 0.30	0.115	0.127	5.46	5.10
		5	6.44 ± 0.64				
		25	8.16 ± 0.31				
		50	11.27 ± 0.11				
50.2	[323.4]	0	9.54 ± 0.63	0.189	0.185	8.66	8.24
		5	10.18 ± 0.68				
		25	13.20 ± 0.37				
		50	18.13 ± 0.13				
55.2	[328.4]	0	12.40 ± 0.20	0.274	0.264	11.88	12.89
		5	13.39 ± 0.08				
		25	18.46 ± 0.18				
		50	25.73 ± 2.21				

[a] Values for the rate constants k_1 in 100% 0.1 *M* $HClO_4$ (no ethylene glycol) are obtained from Table 2.1.

[b] Calculated from the slopes of plots of k_s versus percentage of ethylene glycol (Figure 7.4).

[c] Calculated from the activation parameters: $\Delta H^{\neq} = 60 \pm 4$ kJ mol^{-1}, $\Delta S^{\neq} = -75 \pm 8$ J K^{-1} mol^{-1}.

[d] Estimated from the intercepts of the plots of k_s versus percentage of ethylene glycol with the y-axis (Figure 7.4).

[e] Calculated from the activation parameters: $\Delta H^{\neq} = 77 \pm 5$ kJ mol^{-1}, $\Delta S^{\neq} = -68 \pm 10$ J K^{-1} mol^{-1}.

Table 7.5. Pearson's determination of the effects of various solvents on the chloride exchange reaction of *trans*-$[PtCl_2(py)]$ at 25 °C (Equation 7.8) [a]

Solvents in which exchange proceeds via the solvent path	$10^5 k_s$ (s^{-1})	Solvents in which exchange proceeds via the reagent path	k_{Cl^-} (M^{-1} s^{-1})
DMSO	38	CCl_4	10^4
H_2O	3.5	C_6H_6	10^2
$MeNO_2$	3.2	*m*-cresol	10^{-1}
EtOH	1.4	*t*-C_4H_9OH	10^{-2}
n-C_3H_7OH	0.42	$EtOAc^-$	10^{-2}
		$CH_{32}CO$	10^{-2}
		DMF	10^{-3}

[a] All data from reference [209].

Little or no work exists in the literature on the reactions of platinum(II) in mixed solvents. However, the rate of chloride exchange of *trans*-$[PtCl_2(py)]$ (Equation 7.8) in a variety of solvents was investigated [209].

$$trans\text{-}[PtCl_2(py)] +^* Cl^- \rightarrow trans\text{-}[Pt^*Cl_2(py)] + Cl^- \qquad (7.8)$$

In aqueous solution, the rate of this reaction was virtually independent of the chloride ion concentration and the exchange proceeded almost completely through the solvent path, k_s (the solvent binds to the platinum(II) in a slow step (k_s) and is then quickly displaced by the nucleophile $^*Cl^-$ [125]).

Behaviour similar to this was observed when the same reaction was conducted in the solvents dimethyl sulphoxide (DMSO), nitromethane ($MeNO_2$), ethanol and 1-propanol. The results showed that the solvent effect on the value of k_s was in the order DMSO > H_2O, $MeNO_2$ > R-OH (Table 7.5). There was no parallel between the dielectric constant or general solvating properties of the solvent and the rate of exchange. Water should be more effective than the alcohols and the alcohols more effective than the nitromethane, but nitromethane can form π-bonds with the filled d_{yz} or d_{xz} orbitals of the platinum, stabilising the transition state and permitting displacement of the chloride ion.

Contrasting behaviour was displayed by a number of solvents which, possessing poor coordinating power towards platinum(II), contributed little to the k_s path and the chloride ion exchange proceeded principally through the reagent dependent path k_y (the intermediate species in this path has both the incoming nucleophile $^*Cl^-$ and the leaving group Cl^- bound to the platinum(II) centre simultaneously, before the Cl^- leaves and the product containing the labelled chloride ion forms [125]). In this class of solvents, the order of reactivity was carbon tetrachloride > benzene > *m*-cresol > *t*-butanol > ethyl acetate > acteone > dimethylformamide (DMF) (Table 7.5).

Thus from Pearson's work there were shown to be two classes of solvents: those

Table 7.6. Summary of the rate data obtained by Sundquist *et al.* for the hydrolysis of *cis*-$[PtCl_2(NH_3)_2]$ in dimethyl sulphoxide ([210]).

Temperature (°C)	[K]	Solvent	$10^4 k_s$ (s^{-1})	Reference
26	[299.2]	DMSO	0.63	[210] [a] [b]
33	[306.2]	DMSO	1.35	[210]
37	[310.2]	DMSO	2.00	[210]
40	[313.2]	DMSO	2.88	[210]
49	[322.2]	DMSO	6.60	[210]
23	[296.2]	DMSO	0.44	[210] [c] [d]
30	[303.2]	DMSO	0.93	[210]
37	[310.2]	DMSO	1.87	[210]
46	[319.2]	DMSO	4.41	[210]

[a] Obtained from ^{195}Pt spectroscopy.
[b] Activation parameters are: $\Delta H^{\neq} = 82.8$ kJ mol^{-1} and $\Delta S^{\neq} = -48.5$ J K^{-1} mol^{-1}.
[c] Obtained from UV-visible spectroscopy with the reaction monitored at 276 nm.
[d] Activation parameters are: $\Delta H^{\neq} = 79$ kJ mol^{-1} and $\Delta S^{\neq} = -60.6$ J K^{-1} mol^{-1}.

that would coordinate to the platinum(II) centre, such as DMSO and water, and those that did not, such as DMF and carbon tetrachloride. For the specific case of the reactions of *cis*-DDP in mixed and pure solvents, the comparison between behaviour in coordinating and non-coordinating solvents can also be made. The systems that can be looked at are *cis*-DDP in ethylene glycol / 0.1 *M* $HClO_4$ (this Chapter) , DMSO ([210] and this Chapter), H_2O and $HClO_4$ (Chapter 2), DMF ([211] and this Chapter) and DMF/water mixtures. The rate data obtained is summarised in Tables 2.1, 7.4 and 7.6).

For the reaction of *cis*-DDP with DMSO, the kinetics were determined by Sundquist *et al.* in pure DMSO, in order to highlight the dangers of using DMSO to dissolve *cis*-DDP for experimental work [210]. For *cis*-DDP the rates of reaction in DMSO were comparable to, although slightly slower than, those obtained in 0.1 *M* $HClO_4$ (Table 2.1 and Chapter 2), but different products were formed in each case. The DMSO substituted for a single chloro ligand and coordinated to the platinum(II) to form *cis* – $[Pt(NH_3)_2(DMSO)Cl]Cl$, whereas for the reaction in $HClO_4$, the species *cis*-$[PtCl(NH_3)_2(OH_2)]^+$ plus a chloride ion were formed.

Qualitative rate data from UV spectra of the reaction of *cis*-DDP with DMSO also showed the rate at a particular temperature to be comparable with that in $HClO_4$ although the UV spectra for the *cis*-DDP / DMSO reaction looked quite different. A peak at 307 nm was evident at the beginning of the reaction in pure DMSO which decreased as the reaction proceeded, while another much larger peak developed at about 265 nm (Figure 7.5). When a 50:50 (by volume) mixture of DMSO and 0.01 *M* $HClO_4$ was used, the rate of the overall reaction appeared to be faster than the rates in either pure DMSO or in 0.1 *M* $HClO_4$ and the UV spectra of this reaction differed

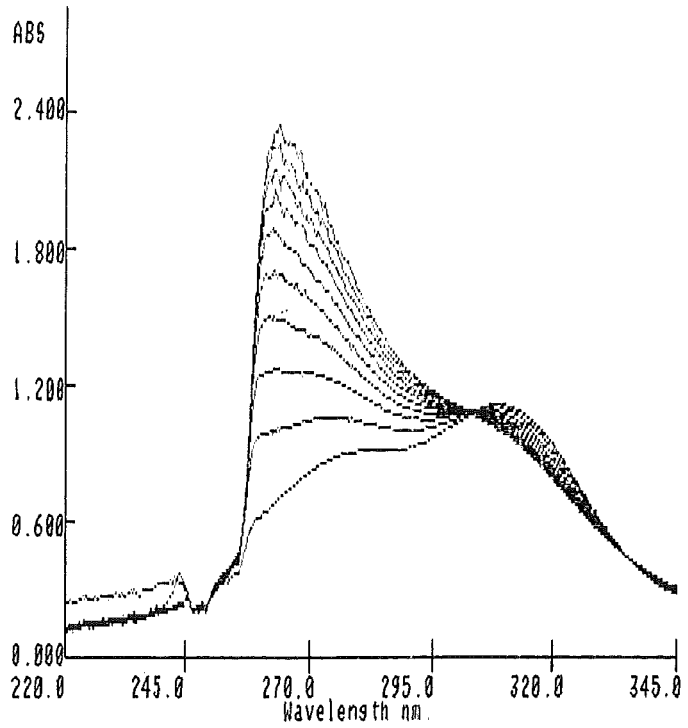

Figure 7.5. Spectrophotometric scans (3 minute intervals) for the reaction of *cis*-$[PtCl_2(NH_3)_2]$ in dimethyl sulphoxide (DMSO) at 50.6 °C. The absorbance at 315 nm decreases with time, and the absorbance at 265 nm increases.

from those of the reaction in DMSO only. In DMSO / $HClO_4$ there was little or no absorption maximum observed at 307 nm and the absorption maximum was shifted to 250 nm. The observation that the rate of reaction was faster in the DMSO / $HClO_4$ mixture agrees with the expected effect of increasing the percentage of water present in the DMSO solvent, where for the general S_N2 reaction (Equation 7.9), an increase in the percentage of water present will increase the rate of reaction [207]. However, the rate in 0.1 *M* $HClO_4$ was expected to be the fastest, which it did not appear to be although it was difficult to determine accurately how fast the reaction of *cis*-DDP in the 50:50 DMSO / $HClO_4$ mixture was going. A possible explanation will be discussed later in this section.

$$RX + Y \rightarrow \overset{\delta+}{Y} \cdots R \cdots \overset{\delta-}{X} \rightarrow RY^+ + X^- \tag{7.9}$$

The repeat-scan UV spectra for the reaction of *cis*-DDP in DMF only, showed that little or no reaction occurred even at high temperatures, but when a 50:50 mixture of DMF / 0.1 *M* $HClO_4$ was used a reaction did occur, although it was considerably slower than the hydrolysis of *cis*-DDP in $HClO_4$ only and the final product of the reaction appeared to be the *cis*-$[PtCl(NH_3)_2(OH_2)]^+$ species. Again the rate of the reaction in DMF was increased from virtually zero by increasing the percentage of water present [207], although DMF is not thought to coordinate here.

The reaction of *cis*-DDP in the ethylene glycol / 0.1 *M* $HClO_4$ solvent mixtures differed from the reactions in *cis*-DDP and DMF or DMSO. The rate constants obtained with the 5% ethylene glycol / 95% 0.1 *M* $HClO_4$ were similar to those obtained for *cis*-DDP in 0.1 *M* $HClO_4$ (Table 7.4) and the sets of UV spectra for both reactions were very similar. As the percentage of ethylene glycol in the reaction solutions was increased, the rate constants for the reactions also increased and the UV spectra looked less and less like that of *cis*-DDP in $HClO_4$ only (Figure 2.1).

One possible explanation of these results in the ethylene glycol / $HClO_4$ system, and indeed the reactions in DMSO, DMSO / $HClO_4$, DMF and DMF / $HClO_4$, is to look at the reaction from the aspect of the water involved and its nature. The present understanding of the nature of liquid water is still very elementary with active research currently underway [212]. Water molecules are effectively 'tetrahedral' since each H_2O molecule has two O–H bonds and two lone pairs of electrons which can be used in hydrogen bonding. Liquid water can be described using the following equation

$$H_2O_{bulk} \rightleftharpoons OH_{free} + LP_{free} \tag{7.10}$$

where 'bulk' refers to four-bonded molecules and OH_{free} and LP_{free} each refer to three-bonded molecules, LP standing for a lone pair of electrons (Figure 7.6). For pure water the concentrations of these species must be equal [212].

Arguments for the chemical reactivity of water hinge on two concepts. Firstly, that water reacts preferentially via OH_{free} and LP_{free} units rather than via fully hydrogen bonded molecules and secondly, that these units act independently of the compounds added to change their concentrations. For instance, if DMSO is added to water, LP_{free} units are generated that are in no way connected to the DMSO and which are the active centres [212]. Looked at from another point of view, when an aprotic solvent such as DMSO is added to the water, there is a rapid decrease in the amount of OH_{free} present. Experimental evidence for this is presented by Symons [212]. Generation of more LP_{free} on addition of DMSO to water therefore increases the rate of reaction, and the same argument can be used for DMF. It is postulated that the DMSO or DMF can reduce the amount of OH_{free} present in the bulk water by hydrogen bonding between the oxygen on the DMSO or DMF and the hydrogen of a water molecule (an OH_{free} unit).

For S_N2 reactions, a typical mechanism for the reactions of platinum(II) complexes [208], both OH_{free} and LP_{free} units are required so the dependence on the concentration of the added cosolvent B should be less marked than in the case of a reaction with an S_N1 mechanism, such as the hydrolysis of *t*-butylchloride. The S_N2 reaction mechanism can be illustrated by the general reaction shown in Equation 7.9. In water, RX molecules are generally monosolvated [213], and 'attack' by a second OH_{free} unit is rate-determining. Added basic cosolvents (B) scavenge the OH_{free} and retard the

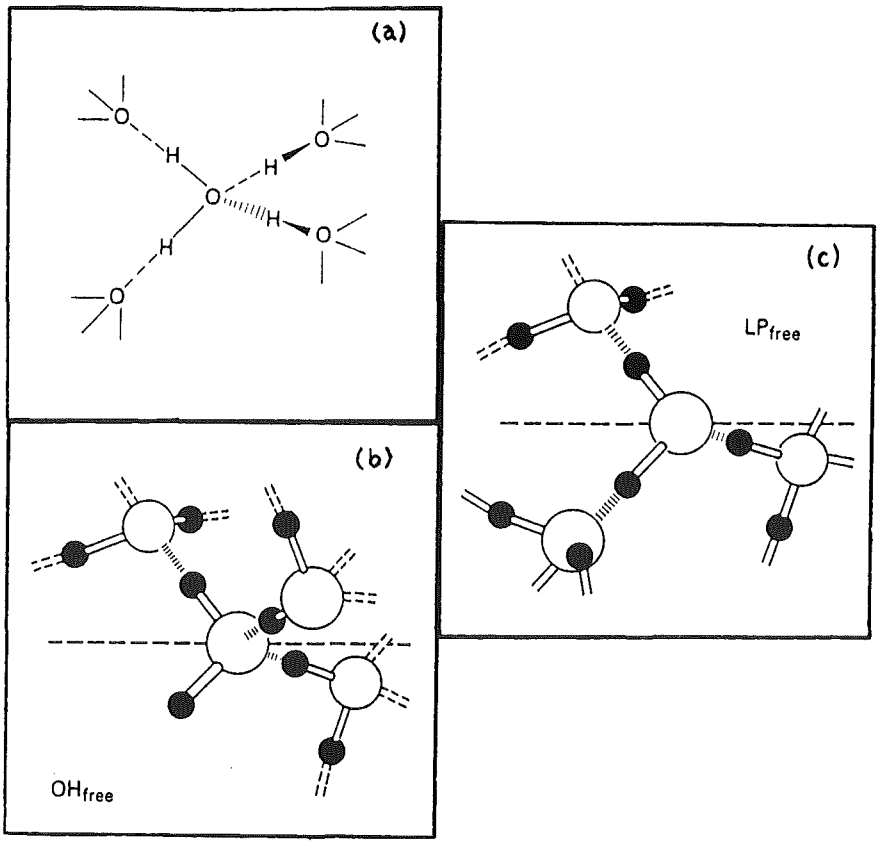

Figure 7.6. Symons' model of the nature of water.

(a) Tetrahedral coordination for water molecules in ice;

(b) OH_{free} units;

(c) LP_{free} units [212]

reaction so that the rate is a function of the solvation number of the solvent B rather than of its base strength. This fits in with the observation that for an S_N2 reaction of this type (Equation 7.9) where increasing the percentage of water present increases the reaction rate. Therefore for *cis*-DDP and DMSO, the reaction of *cis*-DDP in pure DMSO should be slower than that in DMSO / $HClO_4$. Whether the reaction in 0.1 M $HClO_4$ should be slower or faster than in DMSO / $HClO_4$ mixtures is uncertain using Symons' arguments, but it is possible that the presence of DMSO generates even more LP_{free} units than would be present in $HClO_4$ only so that the reaction in the solvent mixture would be faster than that in pure $HClO_4$, which is what was observed.

Thus, the concentrations of OH_{free} or LP_{free} in water can be changed by the addition of a solvent to the system which will remove or decrease the concentration of one of the species, hence increasing or decreasing the reaction rate. For the ethylene glycol / $HClO_4$ system, the rate of reaction of *cis*-DDP increases as the percentage of ethylene glycol present increases, which is the reverse of the above trend. Symons also presented the idea that the hydrogen bond between a chloro group and the OH group of an alcohol ($R-OH$) was strong, and as the number of OH groups on the alcohol increased so the strength of this hydrogen bond decreased [212]. Therefore a possible explanation for the behaviour of the ethylene glycol / $HClO_4$ system is that there is a hydrogen bond between a chloro group of the *cis*-$[PtCl_2(NH_3)_2]$ and the OH group of the ethylene glycol and, even though the strength of this hydrogen bonding may be smaller due to the presence of two OH groups instead of one, this bonding may still be strong enough to facilitate the departure of the chloro group, increasing the rate of reaction. The greater the percentage of ethylene glycol present, the faster the reaction goes.

The possibility also exists that, since ethylene glycol has two OH groups, both are hydrogen bonded to the *cis* chloro groups of the *cis*-$[PtCl_2(NH_3)_2]$. There is also some evidence to show that the ethylene glycol acts as a bidentate chelate towards metal ions [37] and recently an ethylene glycol complex of platinum(II) was reported and its crystal structure determined [214]. The complex, $[S-(R^*,R^*)]-[Pt(HO(CH_2)_2OH)(1,2-C_6H_4(PMePh)_2)](O_3SCF_3)_2$, has both alcohol groups of the ethylene glycol bound to the platinum(II).

7.4 Conclusions.

The rate constants k_{-1}^{Br} and k_1^{Br} for the anation reaction of *cis*-$[PtBr(NH_3)_2(OH_2)]^+$ and the hydrolysis of *cis*-$[PtBr_2(NH_3)_2]$ (Equation 7.3) were obtained, and the equilibrium constant K_1^{Br} calculated. Values of k_1^{Br} were obtained from the intercepts of plots of k_{obs} for the anation reaction of *cis*-$[PtBr(NH_3)_2(OH_2)]^+$ versus bromide ion concentration with the y-axis. Although this method did not give very satisfactory values for k_1^{Br}, the very low solubility of *cis*-$[PtBr_2(NH_3)_2]$ in aqueous solutions would have made it diffcult to measure k_1^{Br} directly in the same manner as k_1 for *cis*-$[PtCl_2(NH_3)_2]$ was

measured (Chapter 2).

A preliminary investigation into the reaction of *cis*-DDP with *ortho*-phenylenediamine, a possible macromolecular carrier of *cis*-DDP, found the presence of an induction period at the beginning of the reaction which still occurred when oxygen was removed from the reaction system and even when the *cis*-DDP itself was omitted. It is thus thought that this induction period is due to oxidation of the *ortho*-phenylenediamine - possibly an internal redox reaction, something which *ortho*-phenylenediamine is known to undergo. The subsequent reaction is thought to be due to the binding of *cis*-DDP to the *ortho*-phenylenediamine or its redox reaction products.

The third area investigated to some extent was the effect of non-aqueous solvents and mixtures of aqueous and non-aqueous solvents on the hydrolysis of *cis*-DDP. Some work on the solvents DMSO, DMSO / $HClO_4$, DMF and DMF / $HClO_4$ had been carried out in the literature as well as for the work presented in this thesis, but the reaction of *cis*-DDP in the ethylene glycol / $HClO_4$ mixture used here did not behave as these other solvents and solvent mixtures had as the reaction got faster as the percentage of ethylene glycol present increased. A possible explanation of these reactions with *cis*-DDP was based on Symons' theories about the nature of liquid water and the effects of adding solvents to the water. Hence, this was used to attempt to explain the behaviour of the ethylene glycol / $HClO_4$ system.

CHAPTER 8

CONCLUSIONS AND FUTURE WORK.

In the Introduction to this thesis (Chapter 1), a summary of the current information on *cis*-$[PtCl_2(NH_3)_2]$, its history, use, nature and interactions with DNA was given. Due to the high level of activity of *cis*-DDP as an anti-cancer drug and the fact that it has a high rate of cure [28], many investigations of the chemistry of *cis*-DDP have been made in order to try and understand how and why it is so effective and thus how the knowledge can be used to further improve the performance of it and other related anti-cancer drugs *in vivo*.

At the beginning of this work, a fundamental decision was made to investigate the reactions of *cis*-DDP under stringent reaction conditions where the nature of the products could be controlled, and not to attempt to reproduce physiological conditions to any great extent. Thus the data obtained under the reaction conditions used was specific but essentially unrelated to the physiological situation. However, it was thought to be more useful to extrapolate the specific data to the biological situation than to attempt to interpret unspecific results from reactions done under physiological conditions where there are a large number of variables involved.

The hydrolysis of *cis*-DDP has been extensively studied in a variety of media and the problems involved with the use of water, nitric acid or buffer systems as reaction media were outlined in Chapter 1. For this thesis it was decided to investigate the acid hydrolysis of *cis*-DDP (Equation 1.1) in $HClO_4$ media over a range of temperatures to give the rate constants k_1 (s^{-1}). The value referred to most commonly in the literature for this reaction at 25 °C $k_1 = 2.5 \times 10^{-5}$ s^{-1} [78] was determined in water which was 0.318 M in Na_2SO_4. The values of k_1 obtained from the work presented in this thesis, in $HClO_4$ media with ionic strength controlled by the addition of $NaClO_4$ (Table 2.1), at the same temperatures were found to be approximately 2.5 times larger ($k_1 = 6.32 \times 10^{-5}$ s^{-1} at 25 °C and $\mu = 1.0$ M, $HClO_4$) than the many literature values (Table 1.1). This was thought to be due to the removal of the influence of the *cis*-$[PtCl(OH)(NH_3)_2]$ species on the rate of reaction by having acidic reaction conditions. The rate constants k_1 were found to be independent of ionic strength and hydrogen ion concentration.

For the anation reaction of *cis*-$[PtCl(NH_3)_2(OH_2)]^+$ (Equation 1.1; k_{-1}, M^{-1} s^{-1}),

the *cis*-$[PtCl(NH_3)_2(OH_2)]^+$ species was isolated in chloride ion free $HClO_4$ using anion exchange chromatography, a useful yet seldom used method. From the literature it seems most common to use stoichiometric amounts of Ag^+ ions to remove one or both of the chloride ions present. On addition of small amounts of chloride ion to the *cis*-$[PtCl(NH_3)_2(OH_2)]^+$, pseudo-first-order rate constants (k_{obs}, s^{-1}) were obtained and thus values for the second-order rate constants (k_{-1}, M^{-1} s^{-1}) were calculated (Table 2.4). Values of k_{-1} reported in the literature (Table 2.5) were comparable to the value obtained from this work at 25 °C ($k_{-1} = 6.26 \times 10^{-3}$ M^{-1} s^{-1}).

The equilibrium constant K_1 for Equation 1.1 at 25 °C was calculated as $K_1 = 1.01 \times 10^{-2}$. Using this equilibrium constant, it was determined that the forward reaction largely proceeded to completion (greater than 90%) and from the thermodynamic parameters obtained from K_1 and its variation with temperature (Table 2.6), the reverse anation reaction (k_{-1}, M^{-1} s^{-1}) was found to be the spontaneous process in Equation 1.1. At 25 °C, the value of K_1 obtained from this work was found to be about 2.5 to three times larger than values reported in the literature (Table 2.5). Since K_1 was calculated using Equation 2.11 and values of k_{-1} reported in the literature are very similar to those reported here [130], the difference in K_1 values is thus due to the higher values obtained for k_1 from this work.

The values of k_1, k_{-1} and K_1 obtained hence enable a comparison to be made between the equilibrium constants K_1 for *cis*-$[PtCl_2(NH_3)_2]$ and *trans*-$[PtCl_2(NH_3)_2]$ hydrolysing under acid conditions to give their respective chloro(aquo) species. At 30 °C, for *cis*-DDP $K_1 = 1.06 \times 10^{-2}$ ($\mu = 1.0$ M, $HClO_4$) whereas for *trans*-DDP $K_1 = 2.46 \times 10^{-4}$ ($\mu = 0.1$ M, $NaNO_3$) [109]. Reasons as to why *cis*-DDP is a more effective anti-cancer drug than *trans*-DDP have tended to centre on structural differences between the two compounds, in particular their arrangements of ligands, but when their equilibrium constants for the same reaction are examined, a major difference can be seen. If the level of anti-cancer activity displayed by a compound is a function of how much reactive aquo species can get to the DNA, the *cis*-DDP has an advantage over *trans*-DDP since its equilibrium in water lies to greater than 90% towards the *cis*-$[PtCl(NH_3)_2(OH_2)]^+$ whereas the percentage of *trans*-$[PtCl(NH_3)_2(OH_2)]^+$ present would not be nearly so great due to its smaller equilibrium constant. At 25 °C $[PtCl_2(NH_2CH_2CH_2NH_2)]$ also has a much smaller equilibrium constant ($K_1 = 2.19 \times 10^{-3}$, $\mu = 0.318$ M, $NaClO_4$ [140]) than *cis*-DDP. However, a general statement that the level of anti-cancer activity reflects the size of the equilibrium constant K_1 of a compound cannot yet be made as not enough platinum(II) complexes have had their hydrolysis and anation rates measured and hence their equilibrium constants calculated.

The effect of ionic strength on the anation reaction of the *cis*-$[PtCl(NH_3)_2(OH_2)]^+$ was not investigated here and no work on it exists in the literature, although the effect of ionic strength on the anation reaction of *trans*-$[PtCl(NH_3)_2(OH_2)]^+$ has been

investigated and it was found that the rate decreased with increasing ionic strength [109]. For both *cis*-DDP and *trans*-DDP it has been shown that the ionic strength does not effect the rate of the forward (hydrolysis) reaction (Chapter 2; [109]), but if the anation reaction is affected, the equilibrium constant for the overall process will vary according to what the ionic strength conditions for the reverse (anation) reaction are. The previous comparison made between the equilibrium constants K_1 for the hydrolysis reactions of *cis*-DDP and *trans*-DDP is therefore not a good one as the ionic strengths associated with each of the values of K_1 are different. Thus K_1 could vary considerably *in vivo* depending on the ionic strength of the blood stream or the cell interior.

The Bronsted Equation (Equation 8.1) [215] predicts that a plot of $\log_{10}k$ (where k is the rate constant of the reaction) versus the square root of the ionic strength should be a straight line.

$$\log_{10}k_{-1} = B + 1.018 z_A z_B \sqrt{\mu} \tag{8.1}$$

where B is the constant $\log_{10}(kT/h)K$. For an aqueous solution at 25 °C, the slope is nearly equal to $z_A z_B$, the product of the ionic charges. Three special cases can occur [215]. Firstly, if z_A and z_B have the same sign, $z_A z_B$ is positive and the rate constant increases increasing ionic strength. Secondly, if z_A and z_B have different signs, $z_A z_B$ is negative and the rate constant decreases with increasing ionic strength (as is the case for *trans*-$[PtCl(NH_3)_2(OH_2)]^+$ and also should be the case for *cis*-$[PtCl(NH_3)_2(OH_2)]^+$). Finally, if one of the reactants is uncharged, $z_A z_B$ is zero and the rate constant is independent of the ionic strength (which is the case for the hydrolysis reactions of both the *cis*-DDP and the *trans*-DDP). Thus the ionic strength should have an influence on the rate of the anation reaction of *cis*-$[PtCl(NH_3)_2(OH_2)]^+$ and this effect should be investigated in future work.

Another important area is to look at the measure of lability of the coordinated water molecule in the complexes *cis*-$[PtCl(NH_3)_2(OH_2)]^+$, *trans*-$[PtCl(NH_3)_2(OH_2)]^+$ and *cis*-$\left[PtCl(en)(OH_2)^+\right]$ to see if the degree of lability is different for each complex. The rate of chloride anation of each of these aquo complexes can be examined to find the differences. At 30 °C, the order of reactivity is *trans*-$[PtCl(NH_3)_2(OH_2)]^+$ ($k_{-1} = 0.452$ M^{-1} s^{-1}, $\mu = 0.1$ M [109]) > *cis*-$[PtCl(NH_3)_2(OH_2)]^+$ ($k_{-1} = 0.0105$ M^{-1} s^{-1}, $\mu = 0.1$ M (Chapter 2, Table 2.4)) > *cis*-$\left[PtCl(en)(OH_2)^+\right]$ ($k_{-1} = 2.53 \times 10^{-2}$ M^{-1} s^{-1}, $\mu = 0.318$ M [140]).

However, a definite comparison cannot be made since, due to the effect of ionic strength on the anation reactions, for a proper comparison, all three reactions at 30 °C should be carried out at the same ionic strength, which they were not. The other assumption made is that the activation energies for all three reactions are similar, and for *trans*-$[PtCl(NH_3)_2(OH_2)]^+$, $E_a = 75.31$ kJ mol^{-1} [109], for *cis*-$[PtCl(NH_3)_2(OH_2)]^+$, $E_a = 77.2$ kJ mol^{-1} (Chapter 2) and for *cis*-$\left[PtCl(en)(OH_2)^+\right]$, $E_a = 73$ kJ mol^{-1}

[140]. The rate of anation of the three aquo complexes may thus give an indication of how the water molecule in each of the complexes would behave at a DNA binding site *in vivo*. The pK_a of the water molecule in these chloro(aquo) complexes also appears to vary from complex to complex, since different ligands are attached to each platinum(II) complex. A measure of the pK_a of the *cis*-$[PtCl(NH_3)_2(OH_2)]^+$ species is 6.85 [151], whereas for the *trans*-$[PtCl(NH_3)_2(OH_2)]^+$ species, from Jensen's work, the pK_a is estimated as 5.85 [216]. Thus it would appear that chemical reactivity as well as structural features are factors in determining the efficacy of an anti-cancer drug.

In Chapter 3, in order to measure k_{-2} (Equation 1.2) the rate constants for the base hydrolysis of *cis*-DDP (Tables 3.1 and 3.2) over a range of temperatures were measured (provide access to the *cis*-$[PtCl(NH_3)_2(OH_2)]^+$ – *cis*-$[Pt(NH_3)_2(OH_2)_2]^{2+}$ reaction system). By generating the *cis*-$[Pt(OH)_2(NH_3)_2]$ species, and then simultaneously acidifying it and adding a known amount of chloride ions, k_{obs} for the anation reaction of *cis*-$[Pt(NH_3)_2(OH_2)_2]^{2+}$ can be measured and then values for k_{-2} calculated (Table 3.9). Calculation of the equilibrium constant $K_2 = 2.7 \times 10^{-4}$ for Equation 1.2 from molar absorptivity coefficients (Table 3.6) meant that the rate constant k_2 for the forward reaction was calculated (Table 3.7). At 25 °C, the value obtained for $k_{-2} = 9.1 \times 10^{-2}\ M^{-1}\ s^{-1}$ agreed with that obtained in the literature [130] as did the value of $k_2 = 2.5 \times 10^{-5}\ s^{-1}$ with the literature value [139].

There are a number of studies that have used the species *cis*-$[Pt(NH_3)_2(OH_2)_2]^{2+}$ as the starting material, particularly studies on the interactions of the hydrolysis products of *cis*-DDP with DNA [40,141,142,143,144,146,151,165,166]. Since the equilibrium constant K_2 for Equation 1.2 is small, calculation of the concentrations of the hydrolysis products of *cis*-DDP present at equilibrium (Table 3.8) showed how little of the *cis*-$[Pt(NH_3)_2(OH_2)_2]^{2+}$ species was present. Thus, for the purposes of attempting to recreate the reactions occurring *in vivo*, there seems little point in using the *cis*-$[Pt(NH_3)_2(OH_2)_2]^{2+}$ species as a starting point since it is unlikely to be present under physiological conditions.

The generally accepted model of how *cis*-DDP behaves *in vivo* was based on hydrolysis reaction data obtained in the pH region 0 to 6.5, with the *cis*-DDP remaining unhydrolysed in the blood plasma, passing through the cell membrane and then hydrolysing to give the *cis*-$[PtCl(NH_3)_2(OH_2)]^+$ or *cis*-$[Pt(NH_3)_2(OH_2)_2]^{2+}$ species [26,30]. However, it has already been shown in the work presented in this thesis that some of the previously generally accepted rate and equilibrium constants were incorrect and while it was accepted that hydroxo species such as *cis*-$[Pt(OH)(NH_3)_2(OH_2)]^+$ existed at physiological pH inside the cell [97], the possible reactions in the blood plasma at pH 7.4 were never usually mentioned. This was probably due to the fact that it appeared to be unknown in the literature that the base hydrolysis of *cis*-DDP could take place in the presence of 0.1 *M* NaCl (Chapter 3). The change in chloride ion concentration

from the blood plasma ($\sim$ 103 mM [97]) to the interior of the cell ($\sim$ 4 mM [97]) is supposed to delay hydrolysis of the *cis*-DDP until it crosses the cell membrane into the cell itself. This would be the case if blood plasma was acidic and had a pH somewhere between 0 and 6.5, but this is not so. The most important factor is the physiological pH of 7.4 that exists *in vivo* [91], although pH gradients can exist within a cell itself [48]. It is this physiological pH of 7.4 that will determine which platinum(II) species are present *in vivo.*

Since it has been established in Chapter 3 that base hydrolysis of *cis*-DDP will occur irrespective of the concentration of chloride ion present, and at pH 7.4 pure acid hydrolysis will not be occurring, it is thus immediately obvious that the situation will not be as simple as that in Rosenberg's model [30], although the likelihood of hydroxo species present inside the cell at physiological pH was commented on. The pH-stat was found to be the best method to use in investigating the hydrolysis of *cis*-DDP between the two extremes of pH, particularly since a number of buffers were found to readily coordinate to the platinum(II), thereby changing the nature of the reaction. The use of buffers in the literature to investigate reactions of *cis*-DDP and its hydrolysis products under conditions approximating those found *in vivo*, seems quite common and this may have distorted some of the results. It is thus felt that the use of buffers for this purpose should be tempered with caution. This uncertainty does not occur with a pH-stat and the pH of the reaction can be closely monitored and controlled. In the future, further investigation of the buffer systems should be made, using NaCl or a far more dilute solution of HCl than was used here, to reverse the reaction of the *cis*-DDP in the buffer soluion, which might give a better indication of whether the buffer had coordinated to the hydrolysis products.

Rate data for the hydrolysis reactions of *cis*-DDP over a range of pH were measured using the technique of the pH-stat and spectrophotometer in combination (Table 4.1). These results showed that at pH greater than 9, complete base hydrolysis took place and at pH less than 5, the reaction was predominantly acid hydrolysis. As the pH increased, the initially monophasic reaction (acid hydrolysis) became biphasic between pH 5 and 7, and then at a pH of 7.2 and above, the reaction again became mainly monophasic with base hydrolysis dominating (Chapter 4). The *cis*-DDP hydrolyses in the pH region 5.5 to 7.2 to give the *cis*-$[PtCl(NH_3)_2(OH_2)]^+$ and *cis*-$[PtCl(OH)(NH_3)_2]$ species in a fixed ratio that depends on the pK_a value for the *cis*-$[PtCl(NH_3)_2(OH_2)]^+$–*cis*-$[PtCl(OH)(NH_3)_2]$ equilibrium and the set pH. The concentration of the *cis*-$[PtCl(OH)(NH_3)_2]$ species present is reduced by hydrolysis to the *cis*-$[Pt(OH)(NH_3)_2(OH_2)]^+$ which also has the effect of diminishing the concentration of *cis*-$[PtCl(NH_3)_2(OH_2)]^+$ (since the equilibrium ratio must be maintained). Increasing the set pH to the region 7.2 to 8.4 means that the *cis*-$[Pt(OH)(NH_3)_2(OH_2)]^+$–*cis*-$[Pt(OH)_2(NH_3)_2]$ equilibrium dominates more. Thus, at pH 7.4 it would appear

that the presence of all the species *cis*-$[PtCl(NH_3)_2(OH_2)]^+$, *cis*-$[Pt(NH_3)_2(OH_2)_2]^{2+}$, *cis*-$[PtCl(OH)(NH_3)_2]$, *cis*-$[Pt(OH)(NH_3)_2(OH_2)]^+$and *cis*-$[Pt(OH)_2(NH_3)_2]$ is possible.

At pH 7.5, T = 25 °C, an initial chloride ion concentration of 0.10 M and a total platinum(II) concentration of 1×10^{-3} M, approximating the physiological conditions found in blood plasma and using the values of K_1 and K_2 determined in Chapters 2 and 3 and the pK_a values determined recently by Appleton *et al.* [151], it was calculated (Appendix C) that the predominant species present would be the *cis*-$[PtCl_2(NH_3)_2]$ at 68%, the *cis*-$[PtCl(NH_3)_2(OH_2)]^+$ at 7% and the *cis*-$[PtCl(OH)(NH_3)_2]$ at 24%. The *cis*-$[Pt(OH)_2(NH_3)_2]$, *cis*-$[Pt(OH)(NH_3)_2(OH_2)]^+$ and *cis*-$[Pt(NH_3)_2(OH_2)_2]^{2+}$ species accounted for approximately 1% total. These results agreed to a certain extent with those calculated by LeRoy *et al.* but they used the older literature values for the equilibrium constants K_1 and K_2 and also older pK_a values [159].

Recalculating the distribution of species at the intracellular chloride ion concentration of $\sim$ 4 mM was also possible using this method (Appendix C) and LeRoy *et al.* calculated that *cis*-$[PtCl_2(NH_3)_2]$ was present at about 31%, *cis*-$[PtCl(NH_3)_2(OH_2)]^+$ at about 28%, *cis*-$[PtCl(OH)(NH_3)_2]$ at about 32% and *cis*-$[Pt(OH)(NH_3)_2(OH_2)]^+$ at about 7%. The *cis*-$[Pt(NH_3)_2(OH_2)_2]^{2+}$ and *cis*-$[Pt(OH)_2(NH_3)_2]$ species were present at approximately 1% each. Investigations into the calculation of distribution of platinum(II) species in the intracellular environment (Appendix C) were in general agreement with that estimated by LeRoy *et al.*. The distribution calculated by Martin was also in general agreement. Roos also gave an equilibrium *cis*-DDP hydrolysis product distribution in blood plasma in the literature, which consists of 89% *cis*-$[PtCl_2(NH_3)_2]$, 11% *cis*-$[PtCl(NH_3)_2(OH_2)]^+$ and 0.09% *cis*-$[Pt(NH_3)_2(OH_2)_2]^{2+}$, but this does not agree with these results and no indication was given by Roos of how this particular distribution was arrived at [162]. These calculations based on the results presented in this thesis (K_1 and K_2 values) thus provided further confirmation of the belief that the *cis*-$[Pt(NH_3)_2(OH_2)_2]^{2+}$ species is one of the least likely platinum(II) species to be attacked by DNA donor atoms at physiological pH, whereas the *cis*-$[PtCl(NH_3)_2(OH_2)]^+$ and, to a lesser extent, the *cis*-$[Pt(OH)(NH_3)_2(OH_2)]^+$ seem to be the most likely.

In Chapter 5, the kinetics of the anation reaction of *cis*-$[Pt(OH)(NH_3)_2(OH_2)]^+$ at pH 7.4 were studied. This was an extension of the work done under physiological conditions as, having determined that the two aquo species *cis*-$[PtCl(NH_3)_2(OH_2)]^+$ and *cis*-$[Pt(OH)(NH_3)_2(OH_2)]^+$ were the most likely species to bind to DNA under these conditions, kinetic data for the *cis*-$[Pt(OH)(NH_3)_2(OH_2)]^+$ species (Equation 5.5) was required to complete the reaction scheme for *cis*-DDP shown in Figure 5.1. The reaction of *cis*-$[PtCl(NH_3)_2(OH_2)]^+$ with the amino acid glycine was also investigated and rate constants measured, but the reaction was found to be slow in comparison to the anation of the *cis*-$[PtCl(NH_3)_2(OH_2)]^+$ by chloride ions (Chapter 2) or by NaHmal

which was also investigated. This tends to indicate that proteins or protein material consisting of amino acids such as glycine were unlikely to compete to any great extent with the DNA in binding to the *cis*-$[PtCl(NH_3)_2(OH_2)]^+$ species and this also provides further evidence that the DNA is the most likely target of the labile platinum(II) species inside the cell.

Investigations were also made into the possible acceleratory effect that some metal ions were thought to possibly have on both the acid and base hydrolysis of *cis*-DDP, with particular emphasis on some metal ions which are present *in vivo*. The metal ions Ca^{2+}, Mg^{2+}, Zn^{2+} and Cu^{2+} were tested initially with the acid hydrolysis of *cis*-DDP but were found to have no effect on the rate of hydrolysis (Table 6.12). It was found that the ions Hg^{2+} and Pb^{2+} both had an acceleratory effect on the rate of hydrolysis but since neither ion exists naturally *in vivo* and are unlikely to be administered to a patient, the work mainly contributed to present knowledge on metal ion assisted reactions of platinum(II) complexes, on which very little data was available. Crystals of the product, $[cis\text{-}[PtCl_2(NH_3)_2](HgCl_2)_3]_n$, from the reaction between the *cis*-DDP and the $HgCl_2$ were obtained and their X-ray crystal structure determined (Chapter 6). An initial investigation of the effect of metal ions on the base hydrolysis of *cis*-DDP was also made but only one metal ion, Zn^{2+}, was investigated and it was found to have no effect also (Table 6.13). Future work should perhaps investigate more metal ions and their possible effects on the base hydrolysis of *cis*-DDP.

The compound *cis*-$[PtBr_2(NH_3)_2]$, while showing good anti-tumour activity [31], is not very soluble in aqueous solutions and this, combined with its high level of toxicity, has precluded its use as an anti-cancer drug. Nevertheless, the kinetics of the anation reaction of *cis*-$[PtBr(NH_3)_2(OH_2)]^+$ and hence the hydrolysis reaction of *cis*-$[PtBr_2(NH_3)_2]$ (Equation 7.3) were determined (Chapter 7). Possible further work on this system could involve the determination of the rate of loss of a bromo ligand in the second step of the acid hydrolysis reaction (*cis*-$[PtBr(NH_3)_2(OH_2)]^+$ to *cis*-$[Pt(NH_3)_2(OH_2)_2]^{2+}$ plus bromide ions) and possibly also the anation reaction of the *cis*-$[Pt(NH_3)_2(OH_2)_2]^{2+}$ to the *cis*-$[PtBr(NH_3)_2(OH_2)]^+$, although this reaction might be too fast to measure its rate constants. Base hydrolysis might also be a possibility but here again, the low solubility of the *cis*-$[PtBr_2(NH_3)_2]$ in aqueous solutions would probably cause experimental problems.

The reaction of *cis*-DDP with *ortho*-phenylenediamine (OPDA), a possible macromolecular drug carrier [196,205], was investigated in a preliminary manner. An induction period to the reaction between *cis*-DDP and OPDA was found to occur, even when no *cis*-DDP was present and also when no little or no oxygen was present. This induction period did not appear to be observed and was not commented on in the literature studies of this reaction. It is thought that the induction period is due to some internal redox process, which is something OPDA is known to undergo. Further experimen-

tation in this field could involve attempting to reverse the reaction of *cis*-DDP with OPDA by, for example, the addition of chloride ions, or the product of the reaction could be monitored under the physiological pH of 7.4 to determine whether there is any reversibility or change, using the pH-stat and spectrophotometer in combination. To be of use as a macromolecular carrier of the *cis*-DDP, the OPDA must get an aquo species of the platinum(II) to the DNA binding sites and since the OPDA is thought to be bound to the sites where the chloro ligands were, under physiological conditions, some reversibility to the reaction must exist. However, there is also the possibility that the *cis*-DDP/OPDA reaction product itself is anti-tumour active.

The hydrolysis of *cis*-DDP in mixtures of aqueous and non-aqueous solvents was investigated in order to determine the effect of various solvents on the rate of hydrolysis. Since one of the solvents investigated was ethylene glycol, it was noticed that this solvent bore a resemblence to lipid-like substances present *in vivo*, for example, simple lipids such as cholesterol which contain -OH groups [169]. It is thus possible that the reaction of *cis*-DDP would give insight to any possible reactions with lipid-like substances *in vivo*. The rate of reaction of *cis*-DDP in the ethylene glycol / $HClO_4$ solvent mixtures was found to increase as the percentage of ethylene glycol increased, a phenomenon which contradicted the expected trend in rate constants predicted knowing the nature of the reactants [207], trends which the other solvent mixtures investigated obeyed. A possible explanation put forward by Symons [212] for the behaviour of the reaction in the ethylene glycol solvent mixtures was the nature of the water present, and this could also be used to explain the behaviour of the other solvent mixtures investigated. Further investigation of this reaction in the future, using a different range of ratios of ethylene glycol to 0.1 M $HClO_4$, could prove to be interesting, and since crystal structures of ethylene glycol complexes with platinum(II) species are known, obtaining crystals from the reaction products of ethylene glycol with *cis*-DDP could also be attempted.

Of the first generation platinum anti-cancer drugs, *cis*-DDP was the most effective and it is still used widely. However, its toxicity and unpleasant side effects, coupled with a desire for more effective, less toxic drugs with a wide spectrum of activity, has meant that further research into second and even third generation platinum anti-cancer drugs has continued. The structures of some of the newer clinically important anti-tumour platinum complexes are given in Figure 8.1. The analogue syntheses were guided by the set of empirical structure - activity relationships outlined in Chapter 1. These relationships reduced the number of possible complexes to be synthesized to a manageable number [22]. However, a wide range of platinum structures are now known which violate these empirical relationships [22], for example, *cis*-$[PtCl(NH_3)_2(py)]^+$, where py is a substituted pyridine ligand, purine or pyrimidine [217]. Nevertheless, the basic structure based on the *cis*-$[Pt(amine)_2]$ unit does give the most active species,

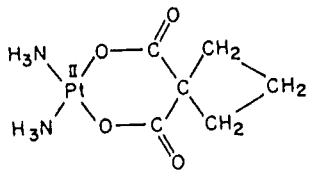

Carboplatin (*cis*-diammine(1,1-cyclobutanedicarboxylato)platinum(II))

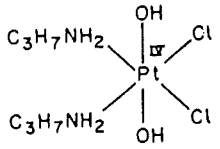

Iproplatin (*cis*-dichloro-*trans*-dihydroxybis(isopropylamine)platinum(IV))

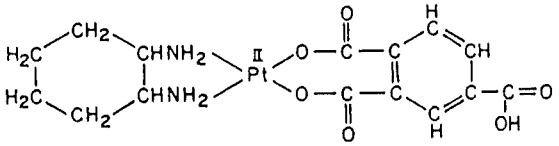

DACCP (4′-carboxyphthalato(1,2-diaminocyclohexane)platinum(II))

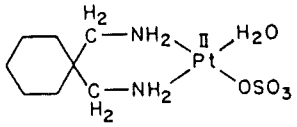

Spiroplatin (aquo-1,1-bis(aminomethyl)cyclohexanesulphatoplatinum(II))

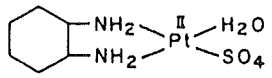

Sulphato(1,2-diaminocyclohexane)platinum(II)

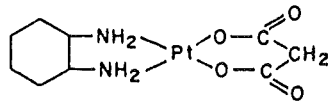

Malonato(1,2-diaminocyclohexane)platinum(II)

Figure 8.1. Structures of more recent clinically important anti-tumour platinum complexes.

and indeed, few closely related second generation analogues have demonstrated greater activity than *cis*-$[PtCl_2(NH_3)_2]$ in a range of murine tumours.

It is now acknowledged in the literature that the reactive platinum species in cell cytoplasm will be a combination of species with aquo and hydroxo ligands and that the physiological pH of 7.4 means that platinum(II) species other than *cis*-$[PtCl_2(NH_3)_2]$ on its own will exist in blood plasma, although prior to this thesis, calculations of species distribution were based on old or inaccurate equilibrium constants and pK_a values [22,159]. The idea was thus formed that it is a hydrolysis step at pH 7.4 that gives an active aquo species (such as *cis*-$[PtCl(NH_3)_2(OH_2)]^+$ or *cis*-$[Pt(OH)(NH_3)_2(OH_2)]^+$) at the DNA binding site, which is required for a platinum drug to be anti-tumour active

(unless enzyme activation is required). This in turn raises the question of how important are the equilibrium constants for the hydrolysis reactions. Not enough kinetic data is available on all the platinum(II) (or platinum(IV)) compounds that are anti-tumour active or on those that are not active (for the purpose of comparison), to make any conclusions possible. Future work needs to be done on collecting these data in order to compare and identify any trends.

From a biological point of view also, there is much that is still a mystery about the behaviour of *cis*-DDP *in vivo*. For example, why is *cis*-DDP active against such a narrow range of types of cancer (mainly testicular and ovarian) and why do one in ten cancer patients being treated with *cis*-DDP not respond at all to treatment. It is still unknown whether *cis*-DDP or its hydrolysis products diffuse or are carried accross cell membranes, and there is still much speculation about what happens inside the cell. Although DNA is thought to be the principle target, reactions can take place with biomolecules other than DNA present, for example, amino acids (such as glycine) or molecules containing sulphur groups [22].

Some progress has thus been made in this thesis in attempting to quantify and understand some of the solution chemistry of the anti-cancer drug *cis*-$[PtCl_2(NH_3)_2]$, and to extrapolate this data to the physiological situation. Although there is still work to be done on the chemistry of *cis*-$[PtCl_2(NH_3)_2]$ in solution and under physiological conditions, the second and third generation platinum anti-tumour compounds also require kinetic investigation of their simple solution chemistry, from which a better understanding of the mechanism of action of all these complexes *in vivo* will be obtained.

APPENDIX A

CONSTANTS, UNITS, SYMBOLS AND ABBREVIATIONS.

A.1 Constants.

Gas constant, R = 8.31441 J K^{-1} mol^{-1}
Planck's constant, h = 6.62618×10^{-34} J s
Avogadro's constant, N = 6.022169×10^{23} mol^{-1}

A.2 Units.

mg = 10^{-3}g or 10^{-6}kg
nm = 10^{-9} m
M = mol l^{-1} or mol dm^{-3}
K = 273.2 + °C
ml = 10^{-3} l
m*M* = 10^{-3} mol l^{-1}
cm = 10^{-2} m
kJ = 10^{3} J
J = N m
N = kg m s^{-2}
kg = 10^{3} g
M^{-1} s^{-1} = mol^{-1} l s^{-1}
l = $10^{-3}m^3$ or 1 dm^3
cm^3 = $10^{-6}m^3$
g/cc = g ml^{-1}
mm = 10^{-3} m
Å = 10^{-10} m

A.3 Symbols and Abbreviations.

UV = ultraviolet
± = plus or minus
≃ = approximately equal to

[ ]	= concentration of (unless enclosing a reference or a temperature in °K)
λ	= wavelength (nm)
$\exp(x)$	= e^x
k_x, k_x^m	= rate constant
K_x, K_x^m	= equilibrium constant
calc.	= calculated
μ	= ionic strength, = $1/2\Sigma c_i z_i^2$
c	= concentration (M)
l	= path length (cm)
z	= ionic charge
A	= absorbance
A_0	= absorbance at time $t = 0$
A_∞	= absorbance at time $t = \infty$
A_t	= absorbance at time = t
t	= time (s)
∞	= infinity
ϵ	= molar absorptivity coefficient (M cm^{-1})
E_a	= activation energy (kJ mol^{-1})
Z	= collision rate between reactant molecules
P	= probability factor
T	= absolute temperature (degrees Kelvin)
$\Delta G^{\neq}$	= free energy of activation (kJ mol^{-1})
$\Delta H^{\neq}$	= enthalpy of activation (kJ mol^{-1})
$\Delta S^{\neq}$	= entropy of activation (J K^{-1} mol^{-1})
$\Delta V^{\neq}$	= volume of activation (cm^3 mol^{-1})
$\Delta G_m^\ominus$	= free energy (kJ mol^{-1})
$\Delta H_m^\ominus$	= enthalpy (kJ mol^{-1})
$\Delta S_m^\ominus$	= entropy (J K^{-1} mol^{-1})
m	= temperature (degrees Kelvin)
pH	= $-\log_{10}[H]^+$
pK_a	= $-\log_{10}[K]_a$
$A_e(\lambda)$	= absorbance of an equilibrium mixture at any wavelength, λ
$\epsilon_{CA}(\lambda)$	= molar absorptivity of the *cis*-$[PtCl(NH_3)_2(OH_2)]^+$ species at any λ
$\epsilon_{DA}(\lambda)$	= molar absorptivity of the *cis*-$[Pt(NH_3)_2(OH_2)_2]^{2+}$ species at any λ
c_{CA}	= equilibrium concentration *cis*-$[PtCl(NH_3)_2(OH_2)]^+$
c_{DA}	= equilibrium concentration of *cis*-$[Pt(NH_3)_2(OH_2)_2]^{2+}$
$[Pt]_t$	= the total concentration of platinum(II) species
$[Cl^-]_e$	= the equilibrium concentration of chloride ions
Nu, Y	= general nucleophile

M^{n+} = general metal ion
A = general amino ligand
X, L = general leaving group
R = general group
A, B = general constants
V = volume (cm^3)
D_{calc} = calculated density (g/cc)
Z = the number of molecules in a unit cell
F(0,0,0) = the structure factor at $h, k, l = 0$
$2\theta_{max}$ = the maximum degrees for data collection
R, R_w = refinement factors
U_{xy} = anisotropic thermal parameters (where x, $y = 1, 2, 3$)
U = isotropic thermal parameters
K_h = the hydrolysis constant of a metal ion
$[Cl_2]$ = the total platinum(II) concentration present, [*cis*-$[PtCl_2(NH_3)_2]$]
$[Cl(OH_2)^+]$ = [*cis*-$[PtCl(NH_3)_2(OH_2)]^+$]
$[(OH_2)_2^{2+}]$ = [*cis*-$[Pt(NH_3)_2(OH_2)_2]^{2+}$]
[Cl(OH)] = [*cis*-$[PtCl(OH)(NH_3)_2]$]
$[(OH)_2]$ = [*cis*-$[Pt(OH)_2(NH_3)_2]$]
$[OH(OH_2)^+]$ = [*cis*-$[Pt(OH)(NH_3)_2(OH_2)]^+$]
$[H^+]_0$ = the total hydrogen ion concentration
$[Cl^-]_0$ = the total chloride ion concentration
∞ = infinity
s = seconds
Σ = the sum of
z_A, z_B = ionic charges
F = the force of attraction acting between two charges
q_1, q_2 = two charges
r = the distance between two charges
ϵ = the dielectric constant
C = a constant
ln = $\log_e$
log = $\log_{10}$

A.4 Abbreviations for Ligands and Chemicals.

cis-DDP = *cis*-$[PtCl_2(NH_3)_2]$
trans-DDP = *trans*-$[PtCl_2(NH_3)_2]$
en = $NH_2CH_2CH_2NH_2$

d(pGpG) = an oligodeoxynucleotide, deoxy(phosphate-guanine-phosphate-guanine)
d(pApG) = an oligodeoxynucleotide, deoxy(phosphate-adenine-phosphate-guanine)
HTF = trfluoroacetic acid, CF_3CO_2H
HAc = acetic acid, CH_3CO_2H
HTS = *p*-toluenesulphonic acid, $CH_3C_6H_4SO_3H$
DMF = dimethylformamide, $HCON[CH_3]_2$
DMSO = dimethylsulphoxide, $(CH_3)_2SO$
EtGlyc = ethylene glycol, $CH_2(OH)CH_2(OH)$
BICINE = N,N-bis(2-hydroxyethyl)glycine
MES = 2(N-morpholino)ethanesulphonic acid
HEPES = N-2-hydroxyethylpiperazine-N'-2-ethanesulphonic acid
TRIS = tris(hydroxymethyl)aminomethane
OPDA = *ortho*-phenylenediamine, $C_6H_4(NH_2)_2$
R,R-chxn = (R,R)-1,2-diaminocyclohexane, $C_6H_{10}(NH_2)_2$
NaHmal = sodium hydrogen malonate, $NaO_2CCH_2CO_2H$
gly, glyc = glycine, $NH_2CH_2CO_2H$
H_4TTF = tetrahydrotetrathiafulvalene
DMA = N,N-dimethylacetamide, $CH_3CON(CH_3)_2$
Et_4N = tetraethylamine, $(CH_3CH_2)N$
Me = methyl group, CH_3-
Et = ethyl group, CH_3CH_2-
picdien = 1,9-bis(2-pyridyl)2,5,8-triazanonane
picditn = 1,11-bis(2-pyridyl)2,6,10-triazaundecane
$MeNO_2$ = nitromethane

APPENDIX B

CALCULATION OF EQUILIBRIUM CONCENTRATIONS

For the first step of the acid hydrolysis of *cis*-$[PtCl_2(NH_3)_2]$ shown below,

$$\underset{a-x}{\textit{cis}\text{-}[PtCl_2(NH_3)_2]} + H_2O \rightleftharpoons \underset{x}{\textit{cis}\text{-}[PtCl(NH_3)_2(OH_2)]^+} + \underset{x}{Cl^-} \tag{B.1}$$

the calculated equilibrium constant $K_1 = 1.01 \times 10^{-2}$ at 25 °C (Chapter 2), for this reaction can be written as

$$K_1 = \frac{[\textit{cis}\text{-}[PtCl(NH_3)_2(OH_2)]^+][Cl^-]}{[\textit{cis}\text{-}[PtCl_2(NH_3)_2]]} \tag{B.2}$$

It is assumed that the concentration of chloride ions, $[Cl^-]$, is equal to the concentration of *cis*-$[PtCl(NH_3)_2(OH_2)]^+$, therefore Equation B.2 can be written as

$$K_1 = \frac{[Cl^-]^2}{[\textit{cis}\text{-}[PtCl_2(NH_3)_2]]} \tag{B.3}$$

Using x and $a - x$ to represent respectively, the concentrations of the chloride ions and the *cis*-$[PtCl_2(NH_3)_2]$ (Equation B.1), Equation B.3 can be rewritten further to give

$$K_1 = \frac{x^2}{a - x} \tag{B.4}$$

where a is the total concentration of *cis*-$[PtCl_2(NH_3)_2]$ present. This equation can be expanded to

$$x^2 + K_1 x - K_1 a = 0 \tag{B.5}$$

which is a quadratic function in the form

$$lx^2 + mx + n = 0 \tag{B.6}$$

and can be solved [157] using

$$x = \frac{-m \pm \sqrt{m^2 - 4ln}}{2l} \tag{B.7}$$

which, for Equation B.5 is written as

$$x = \frac{-K_1 \pm \sqrt{{K_1}^2 + 4K_1 a}}{2} \tag{B.8}$$

For this calculation, as an example, the total concentration of *cis*-$[PtCl_2(NH_3)_2]$, a = 100 mM or 0.1 M (Table 2.2). Substituting this value into Equation B.8 gives

$$x = \frac{-1.01 \times 10^{-2} \pm \sqrt{1.02 \times 10^{-4} + 4.04 \times 10^{-3}}}{2} \tag{B.9}$$

and thus $x = 0.027$ M or 27 mM. Using this value in Equation B.4 gives

$$1.01 \times 10^{-2} = \frac{(0.027)^2}{[cis\text{-}[PtCl_2(NH_3)_2]]} \tag{B.10}$$

and therefore, at equilibrium, the concentration of *cis*-$[PtCl_2(NH_3)_2]$ present is 0.073 M or 73 mM. This method of calculation was used for all the initial concentrations of *cis*-$[PtCl_2(NH_3)_2]$ shown in Table 2.2.

For the second step of the acid hydrolysis of *cis*-$[PtCl_2(NH_3)_2]$,

$$\underset{a-x}{cis\text{-}[PtCl(NH_3)_2(OH_2)]^+} + H_2O \rightleftharpoons \underset{x}{cis\text{-}[Pt(NH_3)_2(OH_2)_2]^{2+}} + \underset{x}{Cl^-} \tag{B.11}$$

the calculated equilibrium constant $K_2 = 2.70 \times 10^{-4}$ at 25 °C (Chapter 3), for this reaction can also be written as

$$K_2 = \frac{[cis\text{-}[Pt(NH_3)_2(OH_2)_2]^{2+}][Cl^-]}{[cis\text{-}[PtCl(NH_3)_2(OH_2)]^+]} \tag{B.12}$$

It is assumed that the concentration of chloride ions, $[Cl^-]$, is equal to the concentration of *cis*-$[Pt(NH_3)_2(OH_2)_2]^{2+}$, and x and $a - x$ are used to represent the concentrations of the chloride ions and the *cis*-$[Pt(NH_3)_2(OH_2)_2]^{2+}$ respectively (Equation B.11), therefore Equation B.12 can be rewritten as

$$K_2 = \frac{[Cl^-]^2}{[cis\text{-}[PtCl(NH_3)_2(OH_2)]^+]} \tag{B.13}$$

or

$$K_2 = \frac{x^2}{a - x} \tag{B.14}$$

Expansion of Equation B.13 gives

$$x^2 + K_2 x - K_2 a = 0 \tag{B.15}$$

which is a quadratic function of the form shown in Equation B.6 and can be solved using Equation B.7 as

$$x = \frac{-K_2 \pm \sqrt{{K_2}^2 + 4K_2a}}{2} \tag{B.16}$$

For this example, the total initial concentration of *cis*-$[PtCl(NH_3)_2(OH_2)]^+$, a = 100 mM or 0.1 M. Substituting this value into Equation B.16 gives

$$x = \frac{-2.70 \times 10^{-4} \pm \sqrt{7.29 \times 10^{-8} + 1.08 \times 10^{-4}}}{2} \tag{B.17}$$

and thus x = 0.005 M or 95 mM. Using this value in Equation B.14 gives

$$2.70 \times 10^{-4} = \frac{(0.005)^2}{[cis\text{-}[PtCl(NH_3)_2(OH_2)]^+]} \tag{B.18}$$

and therefore, at equilibrium, the concentration of *cis*-$[PtCl(NH_3)_2(OH_2)]^+$ present is 0.095 M or 95 mM. This method of calculation was used for all the initial concentrations of *cis*-$[PtCl(NH_3)_2(OH_2)]^+$ shown in Table 3.8 and the rest of the calculations are done in the same way as above.

APPENDIX C

CALCULATION OF CONCENTRATIONS OF PLATINUM(II) SPECIES UNDER PHYSIOLOGICAL CONDITIONS.

Using LeRoy's method [159], but with more modern estimates for the equilibrium constants ($K_1 = 1.13 \times 10^{-2}$ M at 35 °C (Chapter 2) and $K_2 = 2.7 \times 10^{-4}$ M at 25 °C (Chapter 3)) and pK_a values (for *cis*-$[PtCl(NH_3)_2(OH_2)]^+$ – *cis*-$[PtCl(OH)(NH_3)_2]$ $pK_3 = 6.85$ [151], for *cis*-$[Pt(NH_3)_2(OH_2)_2]^{2+}$ – *cis*-$[Pt(OH)(NH_3)_2(OH_2)]^+$ $pK_4 = 5.93$ [151]) and for *cis*-$[Pt(OH)_2(NH_3)_2]$ – *cis*-$[Pt(OH)(NH_3)_2(OH_2)]^+$ $pK_5 = 7.87$ [151]), the concentration and hence the percentage of each platinum(II) species present at equilibrium could be calculated. The following method was used. These equations used are taken from LeRoy's paper [159].

$$K_1 = \frac{[Cl(OH_2)^+][Cl^-]}{[Cl_2]} \tag{C.1}$$

$$= [Cl(OH_2)^+] \times \frac{[Cl^-]_0 + [Cl(OH_2)^+] + [Cl(OH)] + 2([(OH_2)_2^{2+}] + [OH(OH_2)^+] + [(OH)_2])}{[Cl_2]_0 - [Cl(OH_2)^+] - [(OH_2)_2^{2+}] - [Cl(OH)] - [OH(OH_2)^+] - [(OH)_2]}$$

$$K_2 = \frac{[(OH_2)_2^{2+}][Cl^-]}{[Cl(OH_2)^+]} \tag{C.2}$$

$$= [(OH_2)_2^{2+}] \times \frac{[Cl^-]_0 + [Cl(OH_2)^+] + [Cl(OH)] + 2([(OH_2)_2^{2+}] + [OH(OH_2)^+] + [(OH)_2])}{[Cl(OH_2)^+]}$$

$$K_3 = \frac{[Cl(OH)][H^+]_0}{[Cl(OH_2)^+]} \tag{C.3}$$

$$K_4 = \frac{[OH(OH_2)^+][H^+]_0}{[(OH_2)_2^{2+}]} \tag{C.4}$$

$$K_5 = \frac{[(OH)_2][H^+]_0}{[OH(OH_2)^+]} \tag{C.5}$$

where $[Cl_2]_0$ = [*cis*-$[PtCl_2(NH_3)_2]$] or the total platinum(II) species concentration present; $[Cl(OH_2)^+]$ = the concentration of the *cis*-$[PtCl(NH_3)_2(OH_2)]^+$; $[(OH_2)_2^{2+}]$ = the concentration of the *cis*-$[Pt(NH_3)_2(OH_2)_2]^{2+}$; [Cl(OH)] = the concentration of the *cis*-$[PtCl(OH)(NH_3)_2]$; $[(OH)_2]$ = the concentration of the *cis*-$[Pt(OH)_2(NH_3)_2]$; $[OH(OH_2)^+]$ = the concentration of the *cis*-$[Pt(OH)(NH_3)_2(OH_2)]^+$; $[Cl^-]_0$ = the total

chloride ion concentration present and $[H^+]_0 = [H^+]$, the total hydrogen ion concentration present.

Using the expressions [131],

$$pH = -\log_{10}[H^+] \tag{C.6}$$

and

$$pK_a = -\log_{10} K_a \tag{C.7}$$

and the values for the pK_a's [151] (see above) and pH = 7.5, we obtain $K_3 = 1.413 \times 10^{-7}$, $K_4 = 1.175 \times 10^{-6}$, $K_5 = 1.349 \times 10^{-8}$ and $[H^+]_0 = 3.162 \times 10^{-8}\ M$. These values can be substituted into Equations C.3 to C.5 to give the relationships

$$4.47 = \frac{[Cl(OH)]}{[Cl(OH_2)^+]} \tag{C.8}$$

$$37.16 = \frac{[OH(OH_2)^+]}{[(OH_2)_2^{2+}]} \tag{C.9}$$

$$0.43 = \frac{[(OH)_2]}{[OH(OH_2)^+]} \tag{C.10}$$

These can then be rewritten as, from Equation C.8

$$[Cl(OH)] = 4.47[Cl(OH_2)^+] \tag{C.11}$$

from Equation C.9,

$$[OH(OH_2)^+] = 37.16[(OH_2)_2^{2+}] \tag{C.12}$$

and from Equations C.9 and C.10

$$[(OH)_2] = 0.43[OH(OH_2)^+] = 15.98[(OH_2)_2^{2+}] \tag{C.13}$$

Also known are values for the chloride ion concentration present $[Cl^-]_0 = 0.10\ M$ (the approximate chloride ion concentration present in blood plasma [48,97,92]), the total concentration of *cis*-DDP used $[Cl_2]_0 = 1 \times 10^{-3}\ M$ and the temperature T = 37 °C.

The above relationships and known concentrations can thus be substituted into Equations C.1 and C.2 to give

$$\begin{aligned} K_1 &= [Cl(OH_2)^+] \times \frac{0.10 + 5.47[Cl(OH_2)^+] + 108.28[(OH_2)_2^{2+}]}{1 \times 10^{-3} - 5.47[Cl(OH_2)^+] - 54.14[(OH_2)_2^{2+}]} \\ &= 1.13 \times 10^{-2} \end{aligned} \tag{C.14}$$

and

$$K_2 = [(OH_2)_2^{2+}] \times \frac{0.10 + 5.47[Cl(OH_2)^+] + 108.28[(OH_2)_2^{2+}]}{[Cl(OH_2)^+]}$$
$$= 2.70 \times 10^{-4} \quad (C.15)$$

Both Equations C.14 and C.15 are written in terms of only two variables, $[Cl(OH_2)^+]$ and $[(OH_2)_2^{2+}]$. To simplify things further, the $[Cl(OH_2)^+]$ will be written henceforth as x and the $[(OH_2)_2^{2+}]$ as y. Thus we have

$$K_1 = 1.13 \times 10^{-2}(1.0 \times 10^{-3} - 5.47x - 54.14y) = x(0.10 + 5.47x + 108.28y) \quad (C.16)$$

and

$$K_2 = 2.70 \times 10^{-4}x = y(0.10 + 5.47x + 108.28y) \quad (C.17)$$

Further expansion of these two Equations gives

$$1.13 \times 10^{-5} = 0.16x + 5.47x^2 + 108.28xy + 0.61y \quad (C.18)$$

and

$$0 = -2.70 \times 10^{-4}x + 0.10y + 5.47xy + 108.28y^2 \quad (C.19)$$

Before any attempt can be made to solve these two equations, they must be simplified even further. The xy terms are removed by multiplying Equation C.18 by 5.47 and by multiplying Equation C.19 by 108.28, and then subtracting Equation C.19 from Equation C.18. This gives us

$$6.18 \times 10^{-5} = 0.91x + 29.92x^2 - 7.49y + 11724.56y^2 \quad (C.20)$$

At the particular pH and chloride ion concentration used, we assume that there is no *cis*-$[Pt(NH_3)_2(OH_2)_2]^{2+}$ present, that is $y = 0$, therefore we can write Equation C.20 as

$$29.92x^2 + 0.91x = 6.18 \times 10^{-5} \quad (C.21)$$

or as

$$29.92x^2 + 0.91x - 6.18 \times 10^{-5} = 0 \quad (C.22)$$

which is a quadratic function, of the form

$$ax^2 + bx + c = 0 \quad (C.23)$$

and this can be solved for x using [157]

$$x = \frac{-b \pm \sqrt{b^2 - 4ac}}{2a} \tag{C.24}$$

Thus we obtain a value for x or [*cis*-$[PtCl(NH_3)_2(OH_2)]^+$] of 6.77×10^{-5} M. As a percentage of the total *cis*-DDP concentration, the *cis*-$[PtCl(NH_3)_2(OH_2)]^+$ species is present as approximately 7% of the equilibrium mixture. Using Equation C.8 we can substitute in this concentration, to get a concentration of [*cis*-$[PtCl(OH)(NH_3)_2]] = 3.03 \times 10^{-4}$ M or approximately 30% of the equilibrium mixture. The assumption that the *cis*-$[Pt(NH_3)_2(OH_2)_2]^{2+}$ species is not present at this particular chloride ion concentration and pH means that the species *cis*-$[Pt(OH)_2(NH_3)_2]$, *cis*-$[Pt(NH_3)_2(OH_2)_2]^{2+}$ and *cis*-$[Pt(OH)(NH_3)_2(OH_2)]^+$ are present at less than 1% of the equilibrium mixture. Hence the *cis*-$[PtCl_2(NH_3)_2]$ is present as approximately 63% of the equilibrium mixture.

Inside the cell where the chloride ion concentration drops to approximately 4mM, LeRoy *et al.* [159] calculated the composition of the equilibrium mixture to be 31% *cis*-$[PtCl_2(NH_3)_2]$, 28% *cis*-$[PtCl(NH_3)_2(OH_2)]^+$, 32% *cis*-$[PtCl(OH)(NH_3)_2]$ and 7% *cis*-$[Pt(OH)(NH_3)_2(OH_2)]^+$, with the *cis*-$[Pt(NH_3)_2(OH_2)_2]^{2+}$ present at less than 1%. In this case the calculation of the equilibrium concentrations was carried out by LeRoy *et al.* in the same manner as demonstrated above, although the calculation is further complicated in this case (intracellular environment) by not being able to assume that the concentration of the *cis*-$[Pt(NH_3)_2(OH_2)_2]^{2+}$ is zero. However, the values calculated by LeRoy *et al.* most likely accurately reflect the true distribution of platinum(II) species inside a cell.

APPENDIX D

PUBLICATIONS ASSOCIATED WITH THIS THESIS.

S.E. Miller and D.A. House. The Hydrolysis Products of *cis*-Dichlorodiammineplatinum(II). 1. The Kinetics of Formation and Anation of the *cis*-Diammine(aqua)-chloroplatinum(II) Cation in Acidic Aqueous Media. *Inorg. Chim. Acta.*, 161:131-137, 1989.

S.E. Miller and D.A. House. The Hydrolysis Products of *cis*-Dichlorodiammineplatinum(II). 2. The Kinetics of Formation and Anation of the *cis*-Diamminedi(aqua)-platinum Cation. *Inorg. Chim. Acta.*, 166:189-197, 1989.

S.E. Miller and D.A. House. The Hydrolysis Products of *cis*-Dichlorodiammineplatinum(II). 3. Hydrolysis Kinetics at Physiological pH. *Inorg. Chim. Acta.*, 173:53-60, 1990.

S.E. Miller, Huo Wen, D.A. House, and W.T. Robinson. The Hydrolysis Products of *cis*-Dichlorodiammineplatinum(II). 4. The Kinetics of the Reaction between *cis*-$[PtCl_2(NH_3)_2]$ and $HgCl_2$ and the Structure of $[cis\text{-}[PtCl_2(NH_3)_2](HgCl_2)_3]_n$. Submitted to *Inorg. Chim. Acta.*

S.E. Miller and D.A. House. The Hydrolysis Products of *cis*-Dichlorodiammineplatinum(II). 5. The Anation Kinetics of *cis*-$[PtX(NH_3)_2(OH_2)]^+$ X = (Cl^-, OH^-) with Glycine, Monohydrogen Malonate and Chloride. Submitted to *Inorg. Chim. Acta.*

REFERENCES

[1] M.J. Cleare. Transition Metal Complexes in Cancer Chemotherapy. *Coord. Chem. Rev.*, 12(4):349–405, 1974.

[2] B. Rosenberg, L. Van Camp, and T. Krigas. Inhibition of Cell Division in *Escherichia coli* by Electrolysis Products from a Platinum Electrode. *Nature*, 205(4972):698–699, 1965.

[3] B. Rosenberg, L. Van Camp, E.B. Grimley, and A.J. Thomson. The Inhibition of Growth or Cell Division in *Escherichia coli* by Different Ionic Species of Platinum(IV) Complexes. *J. Biol. Chem.*, 242(6):1347–1352, 1967.

[4] B. Rosenberg, E. Renshaw, L. Van Camp, J. Hartwick, and J. Drobnik. Platinum-Induced Filamentous Growth in *Escherichia coli*. *J. Bacteriol.*, 93(2):716–721, 1967.

[5] J.J. Roberts and A.J. Thomson. The Mechanism of Action of Antitumour Platinum Compounds. In W. E. Cohen, editor, *Prog. Nucl. Acid Res. Mol. Biol. Vol. 22.*, pages 71–133, Academic Press, New York, 1979.

[6] A.J. Thomson, R.J.P. Williams, and S. Reslova. The Chemistry of Complexes Related to *cis*-$[Pt(NH_3)_2Cl_2]$. An Antitumour Drug. *Struct. Bond. (Berlin)*, 11:1–46, 1972.

[7] B. Rosenberg. Some Biological Effects of Platinum Compounds. New Agents for the Control of Tumours. *Platinum Met. Rev.*, 15(2):42–51, 1971.

[8] B. Rosenberg, L. Van Camp, J. E. Trosko, and V. H. Mansour. Platinum Compounds: A New Class of Potent Antitumour Agents. *Nature*, 222(5191):385–386, 1969.

[9] B. Rosenberg and L. Van Camp. The Successful Regression of Large Solid Sarcoma 180 Tumours by Platinum Compounds. *Cancer Res.*, 30(6):1799–1802, 1970.

[10] M. Peyrone. De l'Action de l'Ammoniaque sur le Protochlorure de Platine. *Annalen der Chemie und Pharmacie*, 51:1–29, 1844.

[11] M. Peyrone. De l'Action de l'Ammoniaque sur le Protochlorure de Platine. *Annalen der Chemie und Pharmacie*, 55:205–213, 1845.

[12] A. Werner. *New Ideas on Inorganic Chemistry.* Longmans, Green & Co., London, translated by E.P. Hedley from the second german edition, 1911.

[13] G.H.W. Milburn and M.R. Truter. The Crystal Structures of *cis-* and *trans-*Dichlorodiammineplatinum(II). *J. Chem. Soc. A*, (11):1609–1616, 1966.

[14] B. Rosenberg. Cisplatin: Its History and Possible Mechanisms of Action. In A. W. Prestayko, S. T. Crooke, and S. K. Carter, editors, *Cisplatin: Current Status and New Developments.*, chapter 2, pages 9–20, Academic Press, New York, 1980.

[15] D.J. Higby, H.J. Wallace (Jr), D. Albert, and J.F. Holland. Diamminodichloroplatinum in the Chemotherapy of Testicular Tumours. *The J. Urol.*, 112:100–104, 1974.

[16] C.F.J. Barnard. Platinum Anti-Cancer Agents – Twenty Years of Continuing Development. *Platinum Met. Rev.*, 33(4):162–167, 1989.

[17] E. Cvitkovic, J. Spaulding, V. Bethune, J. Martin, and W.F. Whitmore. Improvement of *cis*-Dichlorodiammineplatinum (NSC 119875): Therapeutic Index in an Animal Model. *Cancer (Philadelphia)*, 39(4):1357–1361, 1977.

[18] B. Rosenberg. Fundamental Studies with Cisplatin. *Cancer (Philadelphia)*, 55(10):2303–2315, 1985.

[19] R.J. Woodman, A.E. Sirica, M. Gang, I. Kline, and J.M. Venditti. The Enhanced Therapeutic Effect of *cis*-Platinum(II) Diamminedichloride against L1210 Leukemia when Combined with Cyclophosphamide or 1,2-bis(3,5-Dioxopiperazine-1-yl)propane or Several other Antitumour Agents. *Chemother.*, 18(3):169–183, 1973.

[20] L.H. Einhorn and J. Donohue. *Cis*-Diamminedichloroplatinum, Vinblastine,and Bleomycin Combination Chemotherapy in Disseminated Testicular Cancer. *Ann. Intern. Med.*, 87(3):296–298, 1977.

[21] C.F.J. Barnard, M.J. Cleare, and P.C. Hydes. Second Generation Anticancer Platinum Compounds. *Chemistry in Britain*, 22(11):1001–1004, 1986.

[22] N. Farrell. *Transition Metal Complexes as Drugs and Chemotherapeutic Agents.* Volume 11 of *Catalysis by Metal Complexes. Editors: R. Ugo and B.R. James.*, Kluwer Academic Publishers, Dordrecht, 1989.

[23] R.F. Borch and M. Markman. Biochemical Modulation of Cisplatin Toxicity. *Pharmacol. Ther.*, 41(1-2):371–380, 1989.

[24] C.P. Swainson, B.M. Colls, and B.M. Fitzharris. Cis-platinum and Distal Renal Tubule Toxicity. *The N.Z. Med. J.*, 98(779):375–378, 1985.

[25] J. Reedijk, A.M.J. Fichtinger-Schepman, A.T. van Oosterom, and P. van de Putte. Platinum Amine Coordination Compounds as Anti-Tumour Drugs. Molecular Aspects of the Mechanism of Action. *Struct. Bond. (Berlin)*, 67:53–89, 1987.

[26] S.E. Sherman and S.J. Lippard. Structural Aspects of Platinum Anticancer Drug Interactions with DNA. *Chem. Rev.*, 87(5):1153–1181, 1987.

[27] M. Jarman. The Development of Anticancer Drugs. *Chemistry in Britain*, 25(1):51–54, 1989.

[28] J. Reedijk. The Mechanism of Action of Platinum Anti-Tumour Drugs. *Pure Appl. Chem.*, 59(2):181–192, 1987.

[29] J.L. van der Veer and J. Reedijk. Investigating Antitumour Drug Mechanisms. *Chemistry in Britain*, 24(8):775–780, 1988.

[30] B. Rosenberg. Platinum Complexes for the Treatment of Cancer. *Interdiscipl. Sci. Rev.*, 3(2):134–147, 1978.

[31] M.J. Cleare and J.D. Hoeschele. Studies on the Antitumour Activity of Group VIII Transition Metal Complexes. Part I. Platinum(II) Complexes. *Bioinorg. Chem.*, 2(3):187–210, 1973.

[32] T.A. Connors, M. Jones, W.C.J. Ross, P.D. Braddock, A.R. Khokar, and M.L. Tobe. New Platinum Complexes with Anti-Tumour Activity. *Chem.-Biol. Interact.*, 5(6):415–424, 1972.

[33] M.J. Cleare, P.C. Hydes, B.W. Malerbi, and D.M. Watkins. Antitumour Platinum Complexes: Relationship Between Chemical Properties and Activity. *Biochimie*, 60(9):835–850, 1978.

[34] M.J. Cleare, P.C. Hydes, D.R. Hepburn, and B.W. Malerbi. Antitumour Platinum Complexes: Structure – Activity Relationships. In A. W. Prestayko, S. T. Crooke, and S. K. Carter, editors, *Cisplatin: Current Status and New Developments.*, chapter 9, pages 149–170, Academic Press, New York, 1980.

[35] F.K.V. Leh and W. Wolf. Platinum Complexes: A New Class of Antineoplastic Agents. *J. Pharm. Sci.*, 65(3):315–327, 1976.

[36] M.A. Tucker, C.B. Colvin, and D.S. Martin (Jr). Substitution Reactions of Trichloroammineplatinate(II) Ion and the *trans* Effect. *Inorg. Chem.*, 3(10):1373–1383, 1964.

[37] F. Basolo and R.G. Pearson. *Mechanisms of Inorganic Reactions.* J. Wiley and Sons, Inc., New York, second edition, 1967.

[38] M.L. Tobe and A.R. Khokar. Structure, Activity, Reactivity and Solubility Relationships of Platinum Diamine Complexes. *J. Clin. Hematol. Oncol.*, 7(1):114–137, 1977.

[39] M. Gullotti, G. Pacchoni, A. Pasini, and R. Ugo. Complexes of Platinum(II) with Chiral Diamines and Guanosine. Stereochemical Investigation Related to the Mechanism of Antitumour Activity of *cis*-Bis(amine)platinum(II) Type Complexes. *Inorg. Chem.*, 21(5):2006–2014, 1982.

[40] A.T.M. Marcelis, C. Erkelens, and J. Reedijk. The Interaction of Aquated Platinum(II) Compunds with Purine Mononucleotides. *Inorg. Chim. Acta*, 91(2):129–135, 1984.

[41] D.F. Long and A.J. Repta. Cisplatin: Chemistry, Distribution and Biotransformation. *Biopharm. Drug Dispos.*, 2(1):1–16, 1981.

[42] R.J. Speer, H. Ridgway, L.M. Hall, D.P. Stewart, K.E. Howe, D.Z. Lieberman, A.D. Newman, and J.M. Hill. Coordination Complexes of Platinum as Antitumour Agents. *Cancer Chemother. Rep.*, 59(3):629–641, 1975.

[43] P.D. Braddock, T.A. Connors, M. Jones, A.R. Khokhar, D.H. Melzack, and M.L. Tobe. Structure and Activity Relationships of Platinum Complexes with Anti-Tumour Activity. *Chem.-Biol. Interact.*, 11(3):145–161, 1975.

[44] C.B. Colvin, R.G. Grunther, L.D. Hunter, J.A. McLean, M.A. Tucker, and D.S. Martin. Kinetics of Ammonation of the Chloro – Ammine Series of Platinum(II) Complexes. *Inorg. Chim. Acta*, 2(4):487–489, 1968.

[45] E. Reed, R.F. Ozols, R. Tarone, S.H. Yuspa, and M.C. Poirier. Platinum - DNA Adducts in Leucocyte DNA Correlate with Disease Response in Ovarian Cancer Patients Receiving Platinum-Based Chemotherapy. *Proc. Natl. Acad. Sci. U.S.A.*, 84(14):5024–5028, 1987.

[46] R. Bernards and A.J. Van Der Eb. Adenovirus: Transformation and Oncogenicity. *Biochem. Biophys. Acta*, 783(3):187–204, 1984.

[47] A.T.M. Marcelis and J. Reedijk. Binding of Platinum Compounds to Nucleic Acids with respect to the Anti-Tumour Activity of *Cis*-Diamminedichloroplatinum(II) and Derivatives. *Rec. Trav. Chim. Pays-Bas.*, 102(3):121–129, 1983.

[48] B. Lippert. Platinum Nucleobase Chemistry. In S. J. Lippard, editor, *Progress in Inorganic Chemistry. Vol 37.*, chapter 1, pages 1–97, John Wiley and Sons, New York, 1989.

[49] D.E. Thurston and A.S. Thompson. The Molecular Recognition of DNA. *Chemistry in Britain*, 26(8):767–772, 1990.

[50] M. Howe-Grant and S.J. Lippard. Aqueous Platinum(II) Chemistry; Binding to Biological Molecules. In H. Sigel, editor, *Metal Ions in Biological Systems, Vol. 11.*, chapter 2, pages 63–125, Marcel Dekker, Inc., New York, 1980.

[51] R.N. Bose, R.D. Cornelius, and R.E. Viola. Kinetics and Mechanism of Platinum(II) - Promoted Hydrolysis of Inorganic Polyphosphates. *Inorg. Chem.*, 24(24):3989–3996, 1985.

[52] T.G. Appleton, J.R. Hall, D.W. Neale, and S.F. Ralph. ^{195}Pt Chemical Shifts and Pt–Pt Coupling Constants for Sulfato- and Phosphato- Bridged Platinum(II) Dimeric Cations. *Inorg. Chim. Acta*, 77(4):L149–L151, 1983.

[53] R.B. Martin and Y.H. Mariam. Interactions Between Metal Ions and Nucleic Bases, Nucleosides, and Nucleotides in Solution. In H. Sigel, editor, *Metal Ions in Biological Systems, Vol. 8. (Nucleotides and Derivatives:- Their Ligating Ambivalency).*, chapter 2, pages 57–124, Marcel Dekker, Inc., New York, 1979.

[54] L.G. Marzilli and T.J. Kristenmacher. Stereoselectivity in the Binding of Transition Metal - Chelate Complexes to Nucleic Acid Constituents: Bonding and Non-Bonding Effects. *Acc. Chem. Res.*, 10(4):146–152, 1977.

[55] A.M.J. Fichtinger-Schepman, J.L. van der Veer, J.H.J. den Hartog, P.H.M. Lohman, and J. Reedijk. Adducts of the Antitumour Drug *cis*-Diamminedichloroplatinum(II) with DNA: Formation, Identification and Quantitation. *Biochem.*, 24(3):707–713, 1985.

[56] A.M.J. Fichtinger-Schepman, J.L. van der Veer, P.H.M. Lohman, and J. Reedijk. A Simple Method for the Inactivation of Monofunctionally DNA-Bound *cis*-Diamminedichloroplatinum(II). *J. Inorg. Biochem.*, 21(2):103–112, 1984.

[57] A. Eastman. Characterisation of the Adducts Produced in DNA by *cis*-Diamminedichloroplatinum (II) and *cis*-Dichloro(ethylenediamine)platinum(II). *Biochem.*, 22(16):3927–3933, 1983.

[58] A. Eastman. Interstrand Cross-Links and Sequence Specificity in the Reaction of *cis*-Dichloro(ethylenediamine)platinum(II) with DNA. *Biochem.*, 24(19):5027–5032, 1985.

[59] N.P. Johnson, A.M. Mazard, J. Escalier, and J.P. Macquet. Mechanism of the Reaction Between *cis*-$[PtCl_2(NH_3)_2]$ and DNA *in vitro*. *J. Am. Chem. Soc.*, 107(22):6376–6380, 1985.

[60] R.O. Rahn. Chromatographic Analysis of the Adducts Formed in DNA Complexed with *cis*-Diamminedichloroplatinum(II). *J. Inorg. Biochem.*, 21(4):311–321, 1984.

[61] R. Olinski and Z. Walter. Isolation of the Products Resulting from the Reaction of *cis*- and *trans*- Diaminedichloroplatinum(II) with DNA and Chromatin on the Dowex 50 W Column. *Z. Naturforsch.*, 39C(11–12):1057–1062, 1984.

[62] A.L. Pinto and S.J. Lippard. Sequence - Dependent Termination of *in vitro* DNA Synthesis by *cis*- and *trans*- Diamminedichloroplatinum(II). *Proc. Natl. Acad. Sci. U.S.A.*, 82(14):4616–4619, 1985.

[63] A.C.M. Plooy, A.M.J. Fichtinger-Schepman, H.H. Schutte, M. van Dijk, and P.H.M. Lohman. The Quantitative Detection of Various Pt-DNA-Adducts in Chinese Hamster Ovary Cells Treated with Cisplatin: Application of Immunochemical Techniques. *Carcinogenesis*, 6(4):561–566, 1985.

[64] S.E. Sherman, D. Gibson, A.H.-J. Wang, and S.J. Lippard. X-Ray Structure of the Major Adduct of the Anticancer Drug Cisplatin with DNA: *cis* – $[Pt(NH_3)_2d(pGpG)]$. *Science*, 203(4724):412–417, 1985.

[65] S.E. Sherman, D. Gibson, A.H.-J. Wang, and S.J. Lippard. Crystal and Molecular Structure of *cis* – $[Pt(NH_3)_2d(pGpG)]$, the Principal Adduct Formed by *cis*-Diamminedichloroplatinum(II) with DNA. *J. Am. Chem. Soc.*, 110(22):7368–7381, 1988.

[66] G.L. Cohen, W.R. Bauer, J.K. Barton, and S.J. Lippard. Binding of *cis*- and *trans*- Dichlorodiammineplatinum(II) to DNA: Evidence for Unwinding and Shortening of the Double helix. *Science*, 203(4384):1014–1016, 1978.

[67] P. Umapathy. The Chemical and Biochemical Consequences of the Binding of the Antitumour Drug Cisplatin and Other Platinum Group Metal Complexes to DNA. *Cancer Chemother. Rep.*, 95(2):129–181, 1989.

[68] B. Rosenberg. Introduction to Metal Complexes and the Treatment of Cancers. In S.J. Lippard, editor, *A. C. S. Symposium Series. Volume 140 (Inorganic Chemistry in Biology and Medicine).*, pages 141–146, American Chemical Society, Washington D.C., 1980.

[69] W.I. Sundquist and S.J. Lippard. The Coordination Chemistry of Platinum Anticancer Drugs and Related Compounds with DNA. *Coord. Chem. Rev.*, 100:293–322, 1990.

[70] J.L. van der Veer, G.J. Ligtvoet, H. van den Elst, and J. Reedijk. *trans*-Diamminedichloroplatinum(II) Can Chelate d(GpTpG) via Both Guanines in a Similar Fashion as the *cis* Isomer. *J. Am. Chem. Soc.*, 108(13):3860–3862, 1986.

[71] C.A. Lepre, K.G. Strothkamp, and S.J. Lippard. Synthesis and ^{1}H NMR Spectroscopic Characterisation of *trans*-[Pt(NH_3)$_2$ d(ApGpGpCpCpT)-N7-A(1),N7-G(3)]. *Biochem.*, 26(18):5651–5657, 1987.

[72] B. Lambert and J.-B. Le Pecq. Pharmacology of DNA Binding Drugs. In W. Guschlbauer and W. Saenger, editors, *DNA-Ligand Interactions. N.A.T.O. A.S.I. Series A: Life Sciences. Volume 137 (DNA - Ligand Interactions).*, pages 141–157, Plenum, New York, 1987.

[73] M. Wright, I. Lacorre-Arescaldino, J.-P. Macquet, and M. Daffé. Induction of Polyploid Nuclei in the Plasmodium of *Physarum Polycephalum* by Platinum Antitumor Compounds. *Cancer Res.*, 44(2):777–783, 1984.

[74] B. Lippert. Modelling Platinum-Nucleic Acids Interactions: Coordination Chemistry with Biological Aspects. *Gazzetta Chim. Ital.*, 118(3):153–165, 1988.

[75] H.C. Harder and B. Rosenberg. Inhibitory Effects of Anti-Tumour Platinum Compounds on DNA, RNA and Protein Syntheses in Mammalian Cells *in vitro*. *Int. J. Cancer*, 6(2):207–216, 1970.

[76] J.A. Howle and G.R. Gale. *Cis*-Dichlorodiammineplatinum(II) - Persistent and Selective Inhibition of Deoxyribonucleic Acid Synthesis *In Vivo*. *Biochem. Pharmacol.*, 19(10):2757–2762, 1970.

[77] F. Aprile and D.S. Martin. Chlorotriammineplatinum(II) Ion. Acid Hydrolysis and Isotopic Exchange of Chloride Ligand. *Inorg. Chem.*, 1(3):551–557, 1962.

[78] J.W. Reishus and D.S. Martin (Jr). *Cis*-Dichlorodiammineplatinum(II). Acid Hydrolysis and Isotopic Exchange of the Chloride Ligands. *J. Am. Chem. Soc.*, 83(2):2457–2462, 1961.

[79] R. Faggiani, B. Lippert, C.J.L. Lock, and B. Rosenberg. Hydroxo-Bridged Platinum(II) Complexes. 1. Di-μ-hydroxo-bis[diammineplatinum(II)]Nitrate, $[(NH_3)_2Pt(OH)_2Pt(NH_3)_2](NO_3)_2$. Crystalline Structure and Vibrational Spectra. *J. Am. Chem. Soc.*, 99(3):777–781, 1977.

[80] J.A. Stanko, L.S.Hollis, J.A. Schreifels, and J.D. Hoeschele. Hydroxide Bridged Complexes of Platinum. Crystal Structure, Infrared and X-Ray Photoelectron Spectra of Di-μ-hydroxobis(diammineplatinum(II)) Nitrate. *J. Clin. Hematol. Oncol.*, 7(1):138–168, 1977.

[81] B. Lippert, C.J.L. Lock, B. Rosenberg, and M. Zvagulis. Hydroxo-Bridged Platinum(II) Complexes. 4. Crystal Structure and Vibrational Spectra of Di-μ-hydroxo-bis[diammineplatinum(II)]Carbonate Dihydrate, $[(NH_3)_2Pt(OH)_2Pt(NH_3)_2](CO_3).2H_2O$. *Inorg. Chem.*, 17(11):2971–2975, 1978.

[82] B. Longato, G. Pilloni, G. Valle, and B. Corain. Synthesis and Solvolytic Behaviour of *cis*- (1,1'-Bis(diphenylphosphino)ferrocene)platinum(II) and palladium(II) Complexes. X-Ray Structure of Bis(μ-hydroxy)bis(1,1'-bis(diphenylphosphino) ferrocene)diplatinum(II) Tetrafluoroborate. *Inorg. Chem.*, 27(5):956–958, 1988.

[83] R. Faggiani, B. Lippert, C.J.L. Lock, and B. Rosenberg. Hydroxo-Bridged Platinum(II) Complexes. 2. Crystallographic Charcterisation and Vibrational Spectra of *cyclo*-Tri-μ-hydroxo-tris[*cis*-diammineplatinum(II)] Nitrate. *Inorg. Chem.*, 16(5):1192–1196, 1977.

[84] R. Faggiani, B. Lippert, C.J.L. Lock, and B. Rosenberg. Hydroxo-Bridged Platinum(II) Complexes. 3. Bis[*cyclo*-tri-μ-hydroxo-tris(*cis*-diammineplatinum-(II)] Trisulfate Hexahydrate. Crystallographic Characterisation and Vibrational Spectra. *Inorg. Chem.*, 17(7):1941–1945, 1978.

[85] J.-P. Macquet, S. Cros, and A.L. Beauchamp. Preparation and Crystal Structure of the Hydroxo-Bridged Complex Bis{*cyclo*-tri-μ-hydroxo-tris[(*trans*-1,2-diaminocyclohexane)-platinum(II)]} Trisulfate. *J. Inorg. Biochem.*, 25(3):197–206, 1985.

[86] F.D. Rochon, A. Morneau, and R. Melanson. Crystal Structure of a Hydroxo-Bridged Platinum(II) Tetramer, *cyclo*-Tetrakis(μ-hydroxo)tetrakis(ethylenediamine)platinum(II) Tetranitrate. *Inorg. Chem.*, 27(1):10–13, 1988.

[87] C.J. Boreham, J.A. Broomhead, and D.P. Fairlie. A ^{195}Pt and ^{15}N NMR Study of the Anticancer Drug, *cis*-Diamminedichloroplatinum(II), and Its Hydrolysis and Oligomerization Products. *Aust. J. Chem.*, 34:659–664, 1981.

[88] M. Chikuma and R.J. Pollock. The ^{195}Pt Chemical Shifts and ^{195}Pt–^{15}N Coupling Constants for *cis*-Diammineplatinum(II) Complexes. *J. Magn. Res.*, 47(2):324–327, 1982.

[89] C.A. Bignozzi, C. Bartocci, C. Chiorboli, and V. Carassiti. Dimerization Processes of *cis*-$[Pt(NH_3)_2(OH_2)_2]^{2+}$ in Aqueous Solution. *Inorg. Chim. Acta*, 70(1):87–90, 1983.

[90] T.G. Appleton, R.D. Berry, C.A. Davis, J.R. Hall, and H.A. Kimlin. Reactions of Platinum(II) Aquo Complexes. 1. Multinuclear (^{195}Pt, ^{15}N and ^{31}P) NMR

Study of Reactions Between the *cis*-Diamminediaquaplatinum(II) Cation and the Oxygen Donor Ligands Hydroxide, Perchlorate, Nitrate, Sulphate, Phosphate and Acetate. *Inorg. Chem.*, 23(22):3514–3521, 1984.

[91] D.D. Perrin and B. Dempsey. *Buffers for pH and Metal Ion Control.* Chapman and Hall, London, 1971.

[92] S.J. Lippard. Platinum Complexes: Probes of Polynucleotide Structure and Antitumour Drugs. *Acc. Chem. Res.*, 11(5):211–217, 1978.

[93] R.B. Martin. Hydrolytic Equilibria and N7 Versus N1 Binding in Purine Nucleosides of *Cis*-Diamminedichloroplatinum(II). – Palladium(II) as a Guide to Platinum(II) Reactions at Equilibrium. In S.J. Lippard, editor, *A. C. S. Symposium Series. Volume 209 (Platinum, Gold, Other Met. Chemother. Agents: Chem., Biochem.)*, pages 231–244, American Chemical Society, Washington D.C., 1983.

[94] F. Basolo, H.B. Gray, and R.G. Pearson. Mechanism of Substitution Reactions of Complex Ions. XVII. Rates of Reaction of Some Platinum(II) and Palladium(II) Complexes with Pyridine. *J. Am. Chem. Soc.*, 82(3):4200–4203, 1960.

[95] H.B. Gray and R.J. Olcott. Kinetics of the Reactions of Diethylenetriamineaquoplatinum(II) Ion with Different Ligands. *Inorg. Chem.*, 1(3):481–485, 1962.

[96] H.D.K. Drew, F.W. Pinkard, W. Wardlaw, and E.G. Cox. The Structure of the Isomeric Diamminoplatinous Chlorides. Discovery of a Third Isomeride. *J. Chem. Soc.*, 135(1):988–1004, 1932.

[97] B. Rosenberg. Platinum Complex - DNA Interactions and Anticancer Activity. *Biochem.*, 60(9):859–867, 1978.

[98] J.R. Perumareddi and A.W. Adamson. Photochemistry of Complex Ions. V. The Photochemistry of some Square Planar Platinum(II) Complexes. *J. Phys. Chem.*, 72(2):414–420, 1978.

[99] A.I. Stetsenko and L.B. Sel'derkhanova. Kinetics of Acid Hydrolysis of Certain Platinum(II) *cis* Non-Electrolytes. *Russ. J. Inorg. Chem.*, 26(1):164–168, 1981.

[100] J.E. Teggins, K.W. Lee, J.M. Baker, and E.D. Smith. Kinetics of the *cis*-Dichlorodiammineplatinum(II) - Oxalate Reaction in Aqueous Solution. *J. Coord. Chem*, 1(3):215–219, 1971.

[101] J.L. Butour, A.M. Mazard, and J.-P. Macquet. Kinetics of the Reaction of *cis*-Platinum Compounds with DNA *in vitro*. *Biochem. Biophys. Res. Comm.*, 133(1):347–353, 1985.

[102] R.N. Bose, R.D. Cornelius, and R.E. Viola. Phosphorus-31 NMR and Kinetic Studies of the Formation of Ortho-, Pyro- and Triphosphato Complexes of *cis*-Dichlorodiammineplatinum(II). *J. Am. Chem. Soc.*, 106(11):3336–3343, 1984.

[103] R.N. Bose, R.D. Cornelius, and R.E. Viola. Multinuclear NMR Studies and the Kinetics of Formation of Platinum(II) - Adenine Nucleotide Complexes. *J. Am. Chem. Soc.*, 108(15):4403–4408, 1986.

[104] C.M. Riley, L.A. Sternson, A.J. Repta, and S.A. Slyter. Reactivity of *cis*-Dichlorodiammineplatinum(II) (Cisplatin) Toward Selected Nucleophiles. *Polyhedron*, 1(2):201–202, 1982.

[105] C.M. Riley, L.A. Sternson, A.J. Repta, and R.W. Siegler. High-Performance Liquid Chromatography of Platinum Complexes on Solvent Generated Anion Exchangers. III. Application to the Analysis of Cisplatin in Urine Using Automated Column Switching. *J. Chromatogr.*, 229(2):373–386, 1982.

[106] A.A. Hincal, D.F. Long, and A.J. Repta. Cis-Platin Stability in Aqueous Parenteral Vehicles. *J. Parent. Drug Assoc.*, 33(3):107–116, 1979.

[107] R.F. Greene, D.C. Chatterji, P.K. Hiranaka, and J.F. Gallelli. Stability of Cisplatin in Aqueous Solution. *Am. J. Hosp. Pharm.*, 36(1):38–43, 1979.

[108] D. Banerjea, F. Basolo, and R.G. Pearson. Mechanism of Substitution Reactions of Complex Ions. XII. Reactions of some Platinum(II) Complexes with Various Reactants. *J. Am. Chem. Soc.*, 79(3):4055–4062, 1957.

[109] V.D. Panasyuk and N.F. Malashok. Kinetic Studies of the Acid Hydrolysis of Various Platinum(II) Complexes in Aqueous Solution. *Russ. J. Inorg. Chem.*, 13(10):1405–1408, 1968.

[110] P.C. Dedon and R.F. Borch. Characterisation of the Reactions of Platinum Antitumour Agents with Biologic and Non-Biologic Sulfur-Containing Nucleophiles. *Biochem. Pharmacol.*, 36(12):1955–1964, 1987.

[111] E. Segal and J.-B. Le Pecq. Role of Ligand Exchange Processes in the Reaction Kinetics of the Antitumour Drug *cis*-Diamminedichloroplatinum(II) with its Targets. *Cancer Res.*, 45(2):492–498, 1985.

[112] K.W. Lee and D.S. Martin. *Cis*-Dichlorodiammineplatinum(II). Aquation Equilibria and Isotopic Exchange of Chloride Ligands with Free Chloride and Tetrachloroplatinate. *Inorg. Chim. Acta*, 17(1):105–110, 1976.

[113] A.A. Grinberg and A.A. Korableva. Hydrolysis of Isomeric Diammine Complexes $[PtCl_2(NH_3)_2]$. *Russ. J. Inorg. Chem.*, 13(4):565–569, 1968.

[114] G. Bombieri, E. Forsellini, A. Del Pra, and M.L. Tobe. Crystal and Molecular Structure of Chloro[1,11-bis(2-pyridyl)2,6,10-triazaunadecane]- cobalt(III) Tetrachlorocobaltate(II) Hemihydrate, [Co(picditn)Cl]$CoCl_4.1/2H_2O$. *Inorg. Chim. Acta*, 40(1):71–77, 1980.

[115] B.J. Corden. Reaction of Platinum(II) Antitumour Agents with Sulfhydral Compounds and the Implications for Nephrotoxicity. *Inorg. Chim. Acta*, 137(1–2):125–130, 1987.

[116] Y. Kitamura and K. Ida. Pressure Effect on the Aquation Velocity of *cis*-$[PtCl_2(NH_3)_2]$ and $[PtCl_2(NH_2CH_2CH_2NH_2)]$. *Inorg. Chim. Acta*, 88(2):161–163, 1984.

[117] D.A. House. Kinetics of *mer* to *fac* Isomerisation in some Octahedral Cobalt(III) Complexes. *Inorg. Chim. Acta*, 30(2):281–287, 1978.

[118] A.J. Cunningham, D.A. House, and H.K.J. Powell. The Kinetics of the Base Hydrolysis of the Iodo and Nitrato Pentaaminecobalt(III) Ions. *J. Inorg. Nucl. Chem.*, 33(2):572–577, 1971.

[119] W.G. Jackson, G.A. Lawrence, P.A. Lay, and A.M. Sargeson. Base-Catalysed Linkage Isomerism. *J. Chem. Ed.*, 58(9):734–738, 1981.

[120] P.W. Atkins. *Physical Chemistry.* Oxford University Press, Oxford, 1982.

[121] A.A. Frost and R.G. Pearson. *Kinetics and Mechanism.* J. Wiley and Sons, Inc., New York, second edition edition, 1961.

[122] D.A. House. Stereochemistry and Reaction Rates of Anionopentaamine Complexes of Cobalt(III) and Chromium(III). *Cancer Chemother. Rep.*, 23(3):223–322, 1977.

[123] P.J.F. Griffiths and J.D.R. Thomas. *Calculations in Advanced Physical Chemistry.* Edward Arnold (Publishers) Ltd, London, second edition, 1971.

[124] C.F. Prutton and S.H. Maron. *Fundamental Principles of Physical Chemistry.* The Macmillan Company, New York, second (revised) edition, 1951.

[125] D. Benson. *Mechanisms of Inorganic Reactions in Solution - An Introduction. European Chemistry Series*, McGraw - Hill, London, 1968.

[126] W.M. Scovell and T. O'Connor. Interaction of Aquated $cis - [(NH_3)_2Pt(II)]$ with Nucleic Acid Constituents. 1. Ribonucleosides. *J. Am. Chem. Soc.*, 99(1):120–126, 1977.

[127] A. Bachmaier, G. Just, and E. Holler. *In Vitro* Competition Between Adenosine(5')tetraphosphato(5')adenosine and Deoxyribonucleic Acid in the Reaction with Diamminedichloroplatinum(II). *Eur. J. Biochem.*, 161(3):621–627, 1986.

[128] S. Murakami, K. Saito, A. Muromatsu, M. Moriyasu, A. Kato, and Y. Hashimoto. Studies on the Reactions of $PtCl_2$en, *cis*-$[Pt(NH_3)_2Cl_2]$ and their Aqua Species with Adenosine, Deoxyadenosine and Adenine Using Ion-pair HPLC. *Inorg. Chim. Acta*, 152(2):91–99, 1988.

[129] G.I. Brown. *Introduction to Physical Chemistry.* Longmans, Green & Co., London, 1964.

[130] L. Canovese, L. Cattalini, G. Chessa, and M.L. Tobe. Kinetics of the Displacement of Cyclobutane-1,1-dicarboxylate from Diammine(cyclobutane-1,1-dicarboxylato)platinum(II) in Aqueous Solution. *J. Chem. Soc. Dalton Trans.*, (8):2135–2140, 1988.

[131] D.E. Wilson. *Essential Ideas in Physical Chemistry.* Hodder & Stoughton, London, 1981.

[132] J.E. Teggins, J.A. McCann, and E.D. Smith. Kinetics of the *cis*-Dichlorodiammineplatinum(II) - Diethylenetriamine Reaction. *Inorg. Chem.*, 9(5):1294–1296, 1970.

[133] F. Basolo and R.G. Pearson. *Mechanisms of Inorganic Reactions.* J. Wiley and Sons, Inc., New York, first edition, 1958.

[134] F. Basolo and R.C. Johnson. *Coordination Chemistry.* Science Reviews, U.S.A., second edition, 1986.

[135] R.G. Pearson. Hard and Soft Acids and Bases. *J. Am. Chem. Soc.*, 85(3):3533–3539, 1963.

[136] R.G. Pearson. Hard and Soft Acids and Bases. *Chemistry in Britain*, 3(3):103–107, 1967.

[137] J.D. Hoeschele, T.A. Butler, J.A. Roberts, and C.E. Guyer. Analysis and Refinement of the Microscale Synthesis of the ^{195m}Pt-labeled Antitumour Drug, *cis*-Dichlorodiammineplatinum(II), *cis*-DDP. *Radiochim. Acta*, 31(1–2):27–36, 1982.

[138] C.A. Bignozzi, C. Bartocci, A. Maldotti, and V. Carassiti. Photochemistry of Dimeric and Trimeric Hydroxo - Bridged Diammine Platinum(II) Complexes in Aqueous Solution. *Inorg. Chim. Acta*, 62(2):187–191, 1982.

[139] N.P. Johnson, J.D. Hoeschele, and R.O. Rahn. Kinetic Analysis of the *in vitro* Binding of Radioactive *cis*- and *trans*- Dichlorodiammineplatinum(II) to DNA. *Chem.-Biol. Interact.*, 30(2):151–169, 1980.

[140] R. Coley and D.S. Martin. Kinetics and Equilibria for the Acid Hydrolysis of Dichloro(ethylenediamine)platinum(II). *Inorg. Chim. Acta*, 7(4):573–577, 1973.

[141] S. Eapen, M. Green, and I.M. Ismail. Kinetic Studies on the Diaqua Form of *cis*-Platin and Various Nucleobases. *J. Inorg. Biochem.*, 24(3):233–237, 1985.

[142] D.J. Evans, N.R. Ford, and M. Green. Kinetic and Thermodynamic Selectivity in the Reactions of the Diaqua Form of *cis*-Platin with 3'- and 5'-Guanosinemonophosphoric Acid. *Inorg. Chim. Acta*, 125(3):L39–L40, 1986.

[143] D.J. Evans, M. Green, and R. van Eldik. The Kinetics and Mechanism of the Reaction of 2'-Deoxy-5'-guanosinemonophosphoric Acid and the Diaqua Form of *cis*-Platin. *Inorg. Chim. Acta*, 128(1):27–29, 1987.

[144] B. Van Hemelryck, J.-P. Girault, C. Chottard, P. Valadon, A. Laoui, and J.-C. Chottard. Sequence - Dependent Platinum Chelation by Adenylyl(3'-5')guanosine and Guanylyl(3'-5')adenosine Reacting with *cis*-Diamminedichloroplatinum-(II) and Its Diaqua Derivative. *Inorg. Chem.*, 26(6):787–795, 1987.

[145] K. Ingaki, F.J. Dijt, E.L.M. Lempers, and J. Reedijk. Bulky Ligand Substituent Effect on the Reaction of 5'-GMP with Pt(1,3-diamine). Rotation of 5'-GMP About the Pt–N Bond and Kinetic Effects. *Inorg. Chem.*, 27(2):382–387, 1988.

[146] A. Laoui, J. Kozelka, and J.-C. Chottard. *cis*-Diamminediaquaplatinum(II) Selectivity for GpG: Influence of the Adjacent Base on the First Platination Step. *Inorg. Chem.*, 27(16):2751–2753, 1988.

[147] N. Goswami, L.L. Bennett-Slavin, and R.N. Bose. New Insights into the Mechanism of the *cis*-Platin - Guanosine 5'-Monophosphate Reaction. *J. Chem. Soc.*, (7):432–433, 1989.

[148] R.W. Hay, L.J. Porter, and P.J. Morris. The Basic Hydrolysis of Amino Acid Esters. *Aust. J. Chem.*, 19(7):1197–1205, 1966.

[149] D.A. House, P.R. Normal, and R.W. Hay. The Application of Secondary Deuterium Isotope Effects to Inorganic Reactions. The Meachanism of Base Hydrolysis of *cis*-$[CoCl(en)_2py]^{2+}$. *Inorg. Chim. Acta*, 45(2):L117–L119, 1980.

[150] R.W. Hay and P.L. Cropp. Kinetics of Base Hydrolysis of Chloropenta-ammines of the Type *cis*-$[Coen_2RNH_2Cl]^{2+}$ in Aqueous Solution at 25°. *J. Chem. Soc.*, A1(1):42–44, 1969.

[151] T.G. Appleton, J.W. Connor, J.R. Hall, and P.D. Prenzler. NMR Study of the Reactions of the *cis*-Diamminediaquaplatinum(II) Cation with Glutathione and Amino Acids Containing a Thiol Group. *Inorg. Chem.*, 28(11):2030–2037, 1989.

[152] A.A. El-Awady. Kinetics of the Acid and Base Hydrolysis of $\alpha\beta R$- and $\alpha\beta S$-Isothiocyanatotetraethylenepentaminecobalt(III) Cations. *J. Chem. Soc. Dalton Trans.*, (14):1463–1469, 1972.

[153] J. McKenzie and D.A. House. The Kinetics of Base Hydrolysis of some *cis*-Chlorobis(ethylenediamine)(pyridine)cobalt(III) Complexes. *J. Inorg. Nucl. Chem.*, 39(10):1843–1844, 1977.

[154] J.A. Broomhead, D.P. Fairlie, and M.W. Whitehouse. *cis*-Platinum(II) Amine Complexes: Some Structure - Activity Relationships for Immunosuppressive, Nephrotoxic and Gastrointestinal (Side) Effects in Rats. *Chem.-Biol. Interact.*, 31(1):113–132, 1980.

[155] S.K. Aggarwal, J.A. Broomhead, D.P. Fairlie, and M.W. Whitehouse. Platinum Drugs: Combined Anti-Lymphoproliferative and Nephrotoxicity Assay in Rats. *Cancer Chemother. Pharmacol*, 4(4):249–258, 1980.

[156] B. Rosenberg. Anticancer Activity of *cis*-Dichlorodiammineplatinum(II) and Some Relevant Chemistry. *Cancer Treat. Rep.*, 63(9-10):1433–1438, 1979.

[157] Eton. *Statistical and Math Tables.* Heinemann (N.Z.) Ltd., New Zealand, 1983.

[158] E.H. Earhart. Instability of *cis*-Dichlorodiammineplatinum(II) in Dextrose Solution. *Cancer Treat. Rep.*, 62(7):1105–1106, 1978.

[159] A.F. LeRoy, R.J. Lutz, R.L. Dedrick, C.L. Litterst, and A.M. Guarino. Pharmacokinetic Study of *cis*-Diamminedichloroplatinum(II) (DDP) in the Beagle Dog: Thermodynamic and Kinetic Behaviour of DDP in a Biologic Milieu. *Cancer Treat. Rep.*, 63(1):59–71, 1979.

[160] S.J. Lippard. Binding of a Platinum Antitumour Drug to Its Likely Biological Targets. In S. J. Lippard, editor, *A. C. S. Symposium Series. Volume 140 (Inorg. Chem. Biol. Med.)*, chapter 9, pages 147–156, American Chemical Society, Washington D.C., 1980.

[161] J.P. Macquet, J.L. Butour, and N.P. Johnson. Physicochemical and Structural Studies of the *In Vitro* Interactions Between Platinum(II) Compounds and DNA. In S. J. Lippard, editor, *A. C. S. Symposium Series. Volume 209 (Platinum, Gold, Other Met. Chemother. Agents: Chem., Biochem.)*, chapter 4, pages 75–100, American Chemical Society, Washington D.C., 1983.

[162] I.A.G. Roos. The Anti-Tumour Activity of Platinum Complexes. *Chemistry in Australia*, 47(11):435–439, 1980.

[163] J.H.J. den Hartog, H. van den Elst, and J. Reedijk. Coordination of 9-Methyladenine to *cis* – $[Pt(NH_3)_2]^{2+}$ and $[Pt(dien)]^{2+}$ as Studied by Proton NMR. *J. Inorg. Biochem.*, 21(1):83–92, 1984.

[164] H.H. Kohl, M.E. Friedman, P. Melius, E.C. Mora, and C.A. McAuliffe. Enhanced Inhibition of Both Cellular Protein Synthesis and Matate Dehydrogenase by Aged Aquoplatinum(II) Complexes. *Chem.-Biol. Interact.*, 24(2):209–215, 1979.

[165] S.J.S. Kerrison and P.J. Sadler. Coordination of Amides to *cis*-$[Pt(NH_3)_2(OH_2)_2]^{2+}$. *J. Chem. Soc. Chem. Comm.*, (2):61–62, 1981.

[166] M. Green and J.M. Miller. A Cyclic Nucleobase Phosphate: Fast Atom Bombardment Studies on a 1:1 Mixture of *cis*-$[Pt(OH)_2(NH_3)_2](CF_3SO_3)_2$ and Guanosine 5'-Monophosphoric Acid. *J. Chem. Soc. Chem. Comm.*, (24):1864–1865, 1987.

[167] A. Woollins and B. Rosenberg. High Performance Liquid Chromatography Studies on the Interaction of *cis*-$[Pt(NH_3)_2(OH_2)_2]^{2+}$ with Guanine and Methylated Guanines. *J. Inorg. Biochem.*, 20(1):23–27, 1984.

[168] A. Pasini and C. Caldirola. A New Synthetic Method for Diaminomalonatoplatinum Type Complexes and the Unexpected Behaviour of $[PtCl_2$(*trans*-dach)]. *Inorg. Chim. Acta*, 151(1):19–20, 1988.

[169] J. McMurray. *Organic Chemistry.* Brooks/Cole Publishing Company (Wadsworth Inc.), Monterey, California, 1984.

[170] H. Pivcová, V. Saudek, D. Nosková, and J. Drobník. The Reaction of Pt-Antitumour Drugs with Selected Nucleophiles. I. The Reaction of *cis*-$[Pt(NH_3)_2Cl_2]$ with Glycine. *J. Inorg. Biochem.*, 23(1):43–53, 1985.

[171] V. Saudek, H. Pivcová, D. Nosková, and J. Drobník. Reaction of Pt(II) Antitumour Drugs with Selected Nucleophiles. III. *cis*-$[Pt(NH_3)_2Cl_2]$ and Diamminemalonato-Pt(II) Complexes Compared in the Reaction with Glycine and L-Histidine. *J. Inorg. Biochem.*, 24(1):13–24, 1985.

[172] A. Iakovidis, N. Hadjiliadis, H. Schöllhorn, U. Thewalt, and G. Trötscher. Interaction of *cis*-$[PtCl_2(NH_3)_2]$ with Amino Acids. The Crystal Structure of *cis*-$[Pt(NH_3)_2$(gly)$](NO_3)$ *cis*-$[Pt(NH_3)_2$(ala)$](NO_3)$ and *cis*-$[Pt(NH_3)_2$(val)$](NO_3)$. *Inorg. Chim. Acta*, 164(2):221–229, 1989.

[173] G.M. Sheldrick. *SHELXTL User Manual.* Nicolet XRD Corp., Madison WI, revision 5 edition, 1986.

[174] R. Banerjee. Metal - Ion Catalysed Aquation of Transition Metal Complexes. *Cancer Chemother. Rep.*, 68:145–167, 1985.

[175] A.B. Venediktov and A.V. Belyaev. Formation of a Stable Intermediate in the Reaction of *trans*-Chloro(glycinato)ammineplatinum(II) with Mercury(II) Ions. *Izv. Sib. Otd. Akad. Nauk S.S.S.R., Ser. Khim. Nauk*, (1):46–50, 1974.

[176] A.B. Venediktov and A.V. Belyaev. Kinetics and Mechanism of Mercury(II) - Induced Aquation of *trans*-Chloroglycinodiammineplatinum(II). *Izv. Sib. Otd. Akad. Nauk S.S.S.R., Ser. Khim. Nauk*, (1):51–55, 1974.

[177] A.B. Venediktov and A.V. Belyaev. Kinetics and Mechanism of Mercury(II) - Induced Aquation of *trans*-Bromoglycinodiammineplatinum(II). *Izv. Sib. Otd. Akad. Nauk S.S.S.R., Ser. Khim. Nauk*, (3):67–72, 1975.

[178] J.Arpalahti and B. Lippert. Coordination of Aquated *cis*-Platinum(II) Diamines to Purine Nucleosides. Kinetics of Complex Formation. *Inorg. Chem.*, 29(1):104–110, 1990.

[179] C. Bifano and R.G. Linck. The Rates of some Mercury(II) - Catalysed Aquations of Chloroaminecobalt(III) Complexes. *Inorg. Chem.*, 7(5):908–914, 1968.

[180] J.H. Worrell. Kinetics and Stereochemistry of the Spontaneous and Mercury(II) - Catalysed Acid Hydrolysis for the Symmetrical *cis* Isomer of the Dichloro(1,8-diamino-3,6-dithiaoctane)cobalt(III) Cation. *Inorg. Chem.*, 14(7):1699–1705, 1975.

[181] J.H. Worrell and C.R. Fortune. Mercury(II) Bridged Intermediates in the Catalysed Aquation of Dichloro Complexes of Cobalt(III). *J. Inorg. Nucl. Chem.*, 33(10):3571–3574, 1971.

[182] N.V. Podberezskaya, A.V. Belyaev, and V.W. Balkin. Synthesis and Crystal Structure of the *cis*-(Dichlorobis(ethylenediamine)rhodium(III)) Chloride - Mercuric Chloride Adduct (*cis*-[$Rhen_2Cl_2$]$Cl.HgCl_2$). *Zh. Strukt. Khim.*, 22(6):32–36, 1981.

[183] R.W. Baker, M.J. Braithwaite, and R.S. Nyholm. Preparation and Properties of Some Mercury Halide - Platinum Compounds and Crystal Structure of *cd*-μ-Dichloro-*ab*-dichloro-*ef*- bis(dimethylphenylphosphine)mercury(II)- platinum(II). *J. Chem. Soc. Dalton Trans.*, (18):1924–1928, 1972.

[184] R.M. Barr, M. Goldstein, T.N.D. Hairs, N. McPartlin, and A.J. Markwell. Crystal and Molecular Structures of Novel Polynuclear Complex Halogeno-Anions Containing Mercury and Platinum or Palladium: $[Et_4N]_2Hg_2PtCl_8$,

$[Et_4N]_2Hg_3PtCl_{10}$ and $[Et_4N]_2Hg_3PdCl_{10}$. *J. Chem. Soc. Chem. Comm.*, (6):221–223, 1974.

[185] G. Raudaschl, B. Lippert, J.D. Hoeschele, H.E. Howard-Lock, C.J.L. Lock, and P. Pilon. Adduct Formation of *cis*-$(NH_3)_2PtX_2$ (X = Cl^-, I^-) with Formamides and the Crystal Structures of *cis* – $(NH_3)_2PtCl_2.(CH_3)_2NCHO$. Application for the Purification of the Antitumour Agent Cisplatin. *Inorg. Chim. Acta*, 106(3):141–149, 1985.

[186] D.R. Alston, J.F. Stoddart, and D.J. Williams. The Isolation and X-Ray Crystal Structure of an Adduct Formed Between 18-Crown-6 and Cisplatin. *J. Chem. Soc. Chem. Comm.*, (9):532–533, 1985.

[187] V. Subramarian and K. Seff. Mercuric Chloride, a Redetermination. *Acta Cryst.*, 36B(9):2132–2135, 1980.

[188] K. Kashiwabara, A. Konaka, and M. Kimura. Electron Diffraction Investigation of Gaseous Mercury(II) Chloride. *Bull. Chem. Soc. Japan*, 46(2):410–413, 1973.

[189] S. Akabori, H. Munegumi, Y. Habata, S. Sato, K. Kawazoe, C. Tamura, and M. Sato. Preparation of Polyoxa-1,*n*-dithia[*n*]- (1,1')ruthenocenophanes and the Structural Studies of their Metal Complexes. *Bull. Chem. Soc. Japan*, 58(8):2185–2191, 1985.

[190] M.D. Glick, W.H. Ilsley, and A.R. Siedle. Synthesis and Structure of a Tetrahydrotetrathiafulvalene - Mercuric Chloride Complex, $(H_4TTF)(HgCl_2)_3$. *Inorg. Chem.*, 20(11):3819–3822, 1981.

[191] P. Biscarini, L. Fusina, G. Nivellini, and G. Pelizzi. Three-Co-ordinate Mercury: Crystal Structure and Spectroscopic Properties of Trimethylsulphonium Trichloromercurate(II). *J. Chem. Soc. Dalton Trans.*, (7):664–668, 1977.

[192] P. Biscarini, L. Fusina, G. Nivellini, and G. Pelizzi. Crystal Structure and Spectroscopic Properties of Mercury(II) Halide Complexes. Part 3. The Di-*n*-butyl Sulphoxide - Mercury(II) Chloride (1/1) Adduct. *J. Chem. Soc. Dalton Trans.*, (4):1024–1027, 1981.

[193] R. Dyke and W.C.E. Higginson. Catalysis of the Elimination of Chloride Ion From Chloro(ethylenediaminetriacetatoacetate)cobalt(III) and Its Conjugate Acid by Metal Cations. *J. Chem. Soc. A*, (3):2788–2797, 1963.

[194] S.P. Tanner and W.C.E. Higginson. Catalysis by Metal Cations. Part II. A Further Study of the Elimination of Chloride Ion from Chloro(ethylenediaminetriacetatoacetate)- cobaltate(III) Catalysed by Metal Cations. *J. Chem. Soc. A*, (7):1164–1171, 1969.

[195] H.M. Comely and W.C.E. Higginson. Catalysis by Metal Ions. Part III. Kinetics of Elimination of Chloride Ion from *cis*-Chlorobis(ethylenediamine)glycinato-N-cobalt(III). *J. Chem. Soc. Dalton Trans.*, (22):2522–2525, 1972.

[196] B. Schechter, A. Neumann, A. Wilchek, and R. Arnon. Soluble Polymers as Carriers of *cis*-Platinum. *J. Controlled Release*, 10(1):75–87, 1989.

[197] D.R. Gano, G.F. Vandegrift, and D.S. Martin Jr. Isotopic Exchange of Bromide Ligands in Platinum(II) Complexes. *Cis*-Dibromodiammineplatinum(II). *Inorg. Chim. Acta*, 2(3):219–224, 1968.

[198] L.I. Elding and I. Leden. On the Stepwise Dissociation of the Tetrachloridoplatinate(II) Ion in Aqueous Solution. I. Equilibria at 25 °C. *Acta Chem. Scand.*, 20(3):706–715, 1966.

[199] L.I. Elding. The Stepwise Dissociation of the Tetrachloridoplatinate(II) Ion in Aqueous Solution. II. Kinetics of the First Step. *Acta Chem. Scand.*, 20(9):2559–2567, 1966.

[200] L.I. Elding. The Stepwise Dissociation of the Tetrachloroplatinate(II) Ion in Aqueous Solution. IV. The Chlorotriaquaplatinum(II) Ion. *Acta Chem. Scand.*, 24(4):1331–1340, 1970.

[201] L.I. Elding. The Stepwise Dissociation of the Tetrachloroplatinate(II) Ion in Aqueous Solution. V. Chloride Anations of the Chloro Aqua Complexes of Platinum(II). *Acta Chem. Scand.*, 24(4):1341–1354, 1970.

[202] L.I. Elding. The Stepwise Dissociation of the Tetrachloroplatinate(II) Ion in Aqueous Solution. VI. Rates of Formation and Equilibria of the Chloro Aqua Complexes of Platinum(II). *Acta Chem. Scand.*, 24(5):1527–1540, 1970.

[203] L.I. Elding. Acid Hydrolysis of Tetrabromoplatinate(II) and Bromide Anation of Tribromoaquaplatinate(II). *Acta Chem. Scand.*, 24(7):2546–2556, 1970.

[204] L.I. Elding. Equilibria, Rates of Formation and Bromide Anations of *cis*- and *trans*-Dibromodiaquaplatinum(II). *Acta Chem. Scand.*, 24(7):2557–2564, 1970.

[205] E.D. Golla and G.H. Ayres. Spectrophotometric Determination of Platinum with *o*-Phenylenediamine. *Talanta*, 20(3):199–210, 1973.

[206] D.A. House. Ammonia and Amines. In G. Wilkinson, editor, *Comprehensive Coordination Chemistry – The Synthesis, Reactions, Properties and Applications of Coordination Compounds. Volume 2. Ligands.*, chapter 13.1, pages 23–72, Pergamon Press, Oxford, 1987.

[207] E.S. Amis. *Solvent Effects on Reaction Rates and Mechanisms.* Academic Press, New York, 1966.

[208] T. Moeller. *Inorganic Chemistry - A Modern Introduction.* J. Wiley & Sons, New York, 1982.

[209] R.G. Pearson, H.B. Gray, and F. Basolo. Mechanism of Substitution Reactions of Complex Ions. XVI. Exchange Reactions of Platinum(II) Complexes in Various Solvents. *J. Am. Chem. Soc.*, 82(3):787–792, 1960.

[210] W.I. Sundquist, K.J.Ahmed, and L.S. Hollis S.J. Lippard. Solvolysis Reactions of *cis*- and *trans*- Diamminedichloroplatinum(II) in Dimethyl Sulfoxide. Structural Characterization and DNA Binding of *trans*-$[Pt(NH_3)_2(Me_2SO)Cl]^+$. *Inorg. Chem.*, 26(10):1524–1528, 1987.

[211] G. Raudaschl, B. Lippert, and J.D. Hoeschele. A Simple Procedure for Purifying the Antitumour Agent *cis*-$[PtCl_2(NH_3)_2]$ (Cisplatin). *Inorg. Chim. Acta*, 78(3):L43–L44, 1983.

[212] M.C. Symons. Liquid Water – The Story Unfolds. *Chemistry in Britain*, 25(5):491–494, 1989.

[213] M.C. Symons, N.G.M. Pay, and G. Eaton. Spectroscopic Evidence for Hydrogen-Bond Formation between Methanol and Halogenoalkanes. *J. Chem. Soc. Faraday Trans.,I*, 78(6):1841–1846, 1982.

[214] A.M. Appelt, V. Ariaratnam, P.A. Duckworth, A.C. Willis, and S.B. Wild. Alcohol Complexes of Platinum(II). In *XXVII International Conference on Coordination Chemistry, 2–7 July, Abstracts.*, page W100, Broadbeach, Queensland, Australia, 1989.

[215] W.J. Moore. *Physical Chemistry.* Longmans, Green & Co., London, second edition, 1956.

[216] K.A. Jensen. The Acid Strength of the Stereoisomeric Diaquodiammineplato Ions. *Zeit. Anorg. Allgem. Chemie*, 242:87–91, 1939.

[217] L.S. Hollis, A.R. Amundsen, and E.W. Stern. Chemical and Biological Properties of a New Series of *cis*-Diammineplatinum(II) Antitumour Agents Containing Three Nitrogen Donors: *cis*-$[Pt(NH_3)_2(\text{N-donor})Cl]^+$. *J. Med. Chem.*, 32(1):128–136, 1989.